A Large Ion Collider Experiment

QCD Matter: dense and hot
Overview of ALICE results

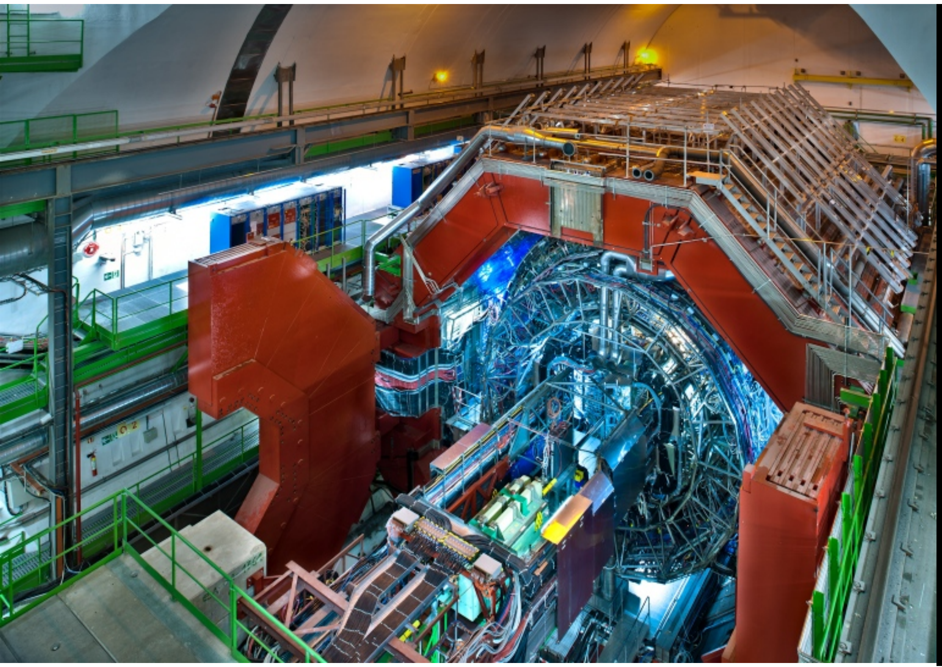
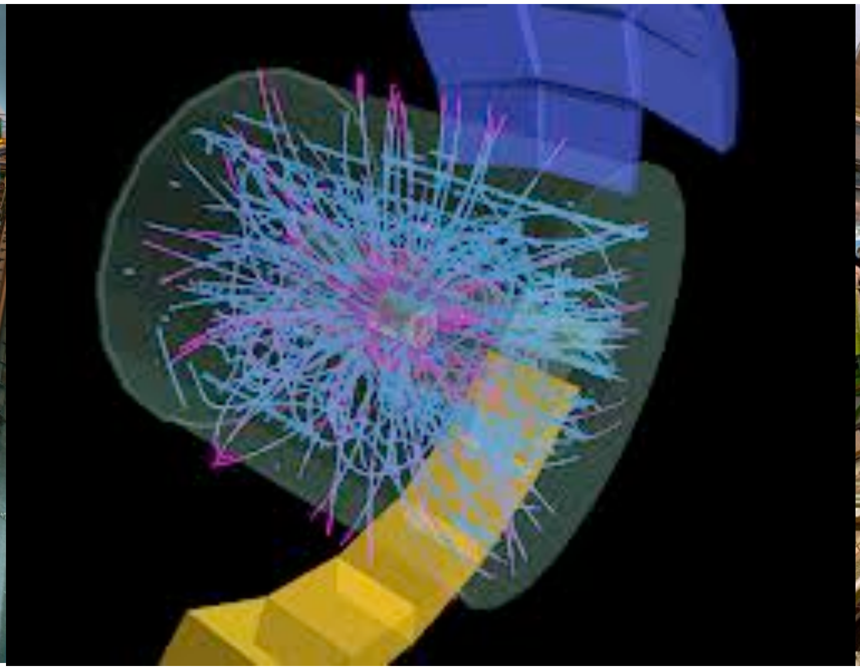


A. Kalweit, *CERN*
on behalf of the ALICE collaboration

Outline

- Introduction: ALICE and ultra-relativistic heavy-ion physics

- Highlights from LHC Run 1: November 2009 - March 2013
  - pp (0.9 TeV, 2.76 TeV, 7 TeV)
  - p-Pb (5.02 TeV)
  - Pb-Pb (2.76 TeV)

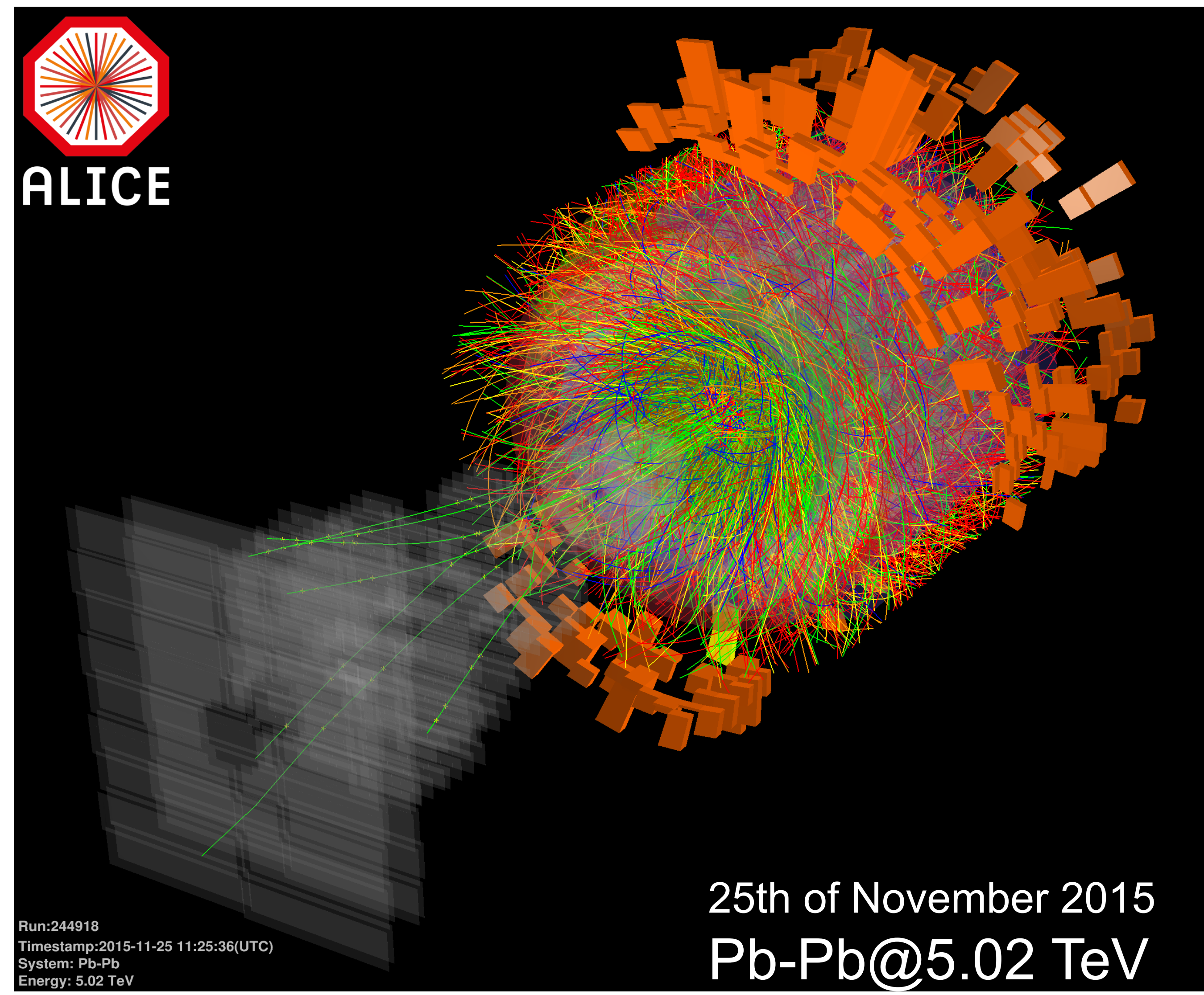

- First results from LHC Run 2: since March 2015
  - pp (5.02 TeV, 13 TeV)
  - Pb-Pb (5.02 TeV)

- A little outlook on LHC Run 3

Introduction

Large Hadron Collider

Large Hadron Collider

ALICE

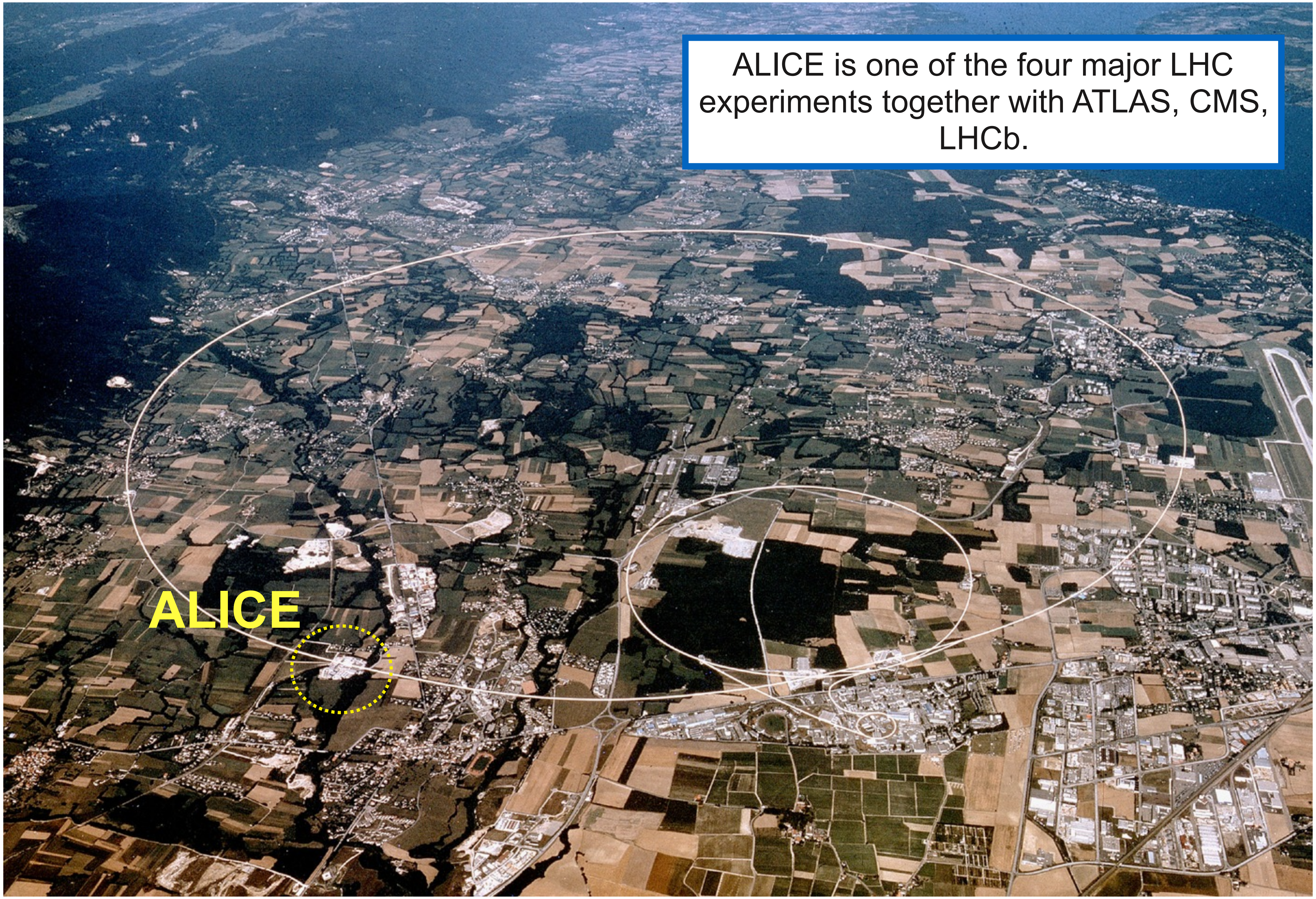

ALICE is one of the four major LHC experiments together with ATLAS, CMS, LHCb.

Large Hadron Collider

ALICE

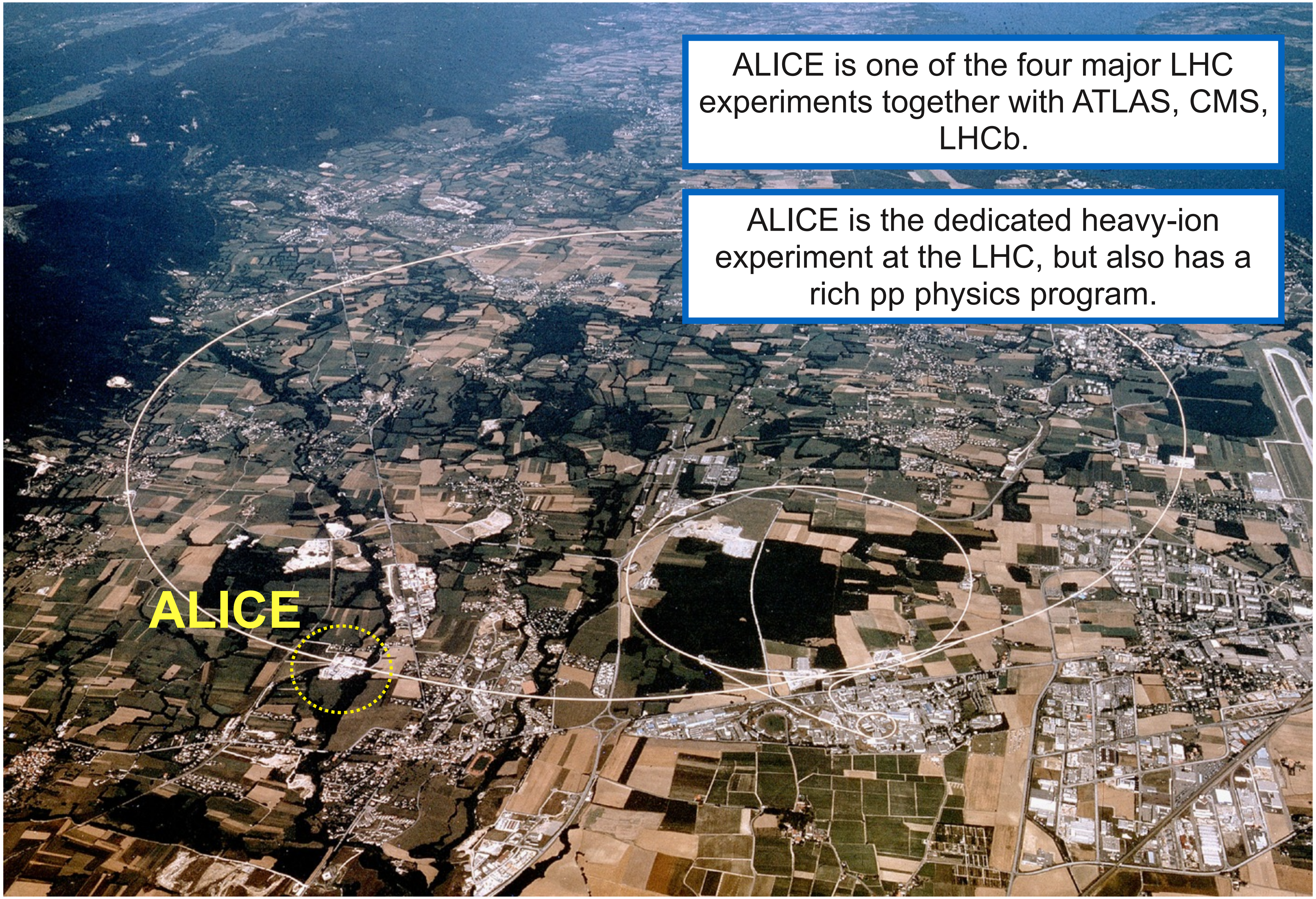

Large Hadron Collider

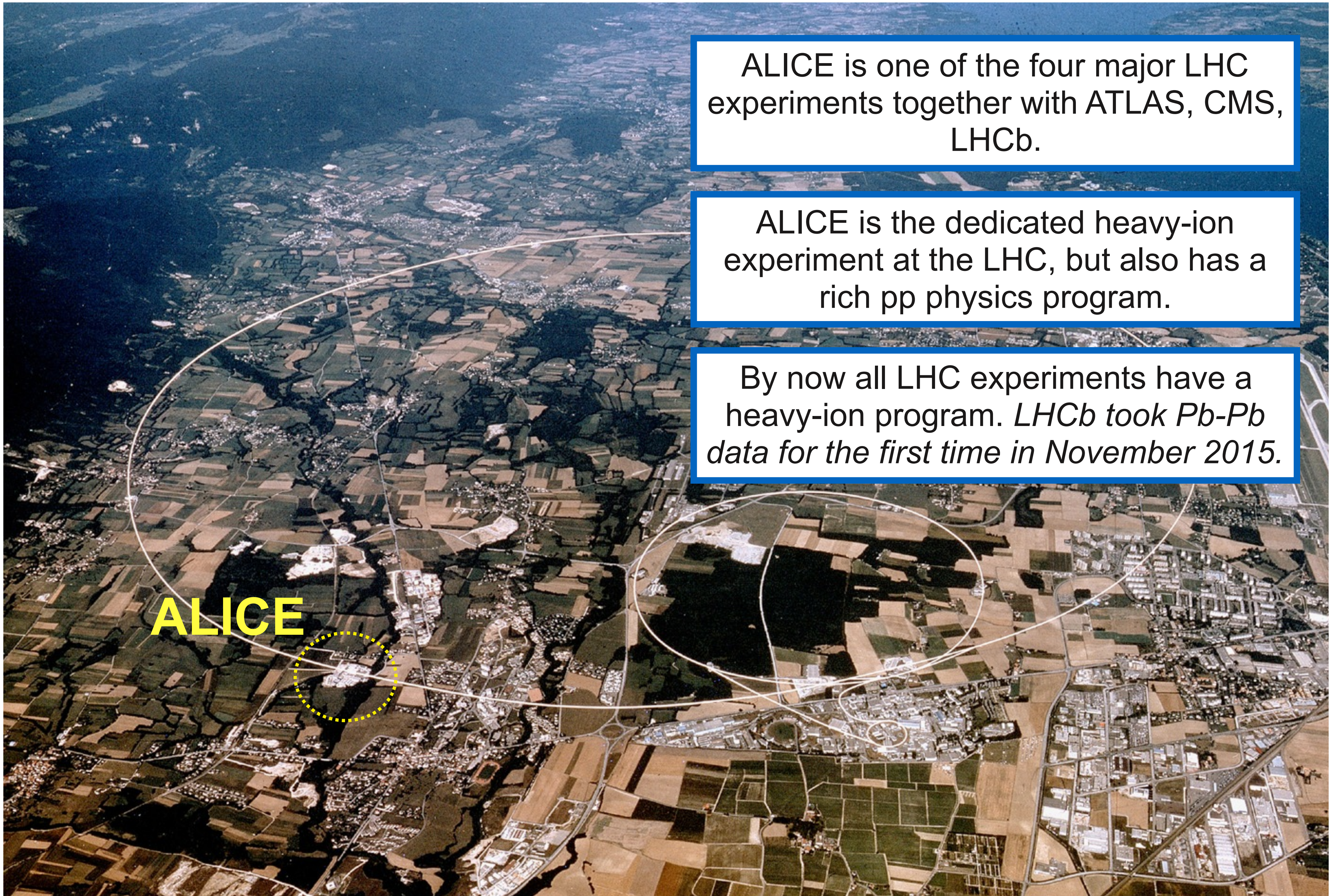

ALICE is one of the four major LHC experiments together with ATLAS, CMS, LHCb.

ALICE is the dedicated heavy-ion experiment at the LHC, but also has a rich pp physics program.

By now all LHC experiments have a heavy-ion program. *LHCb took Pb-Pb data for the first time in November 2015.*

Large Hadron Collider

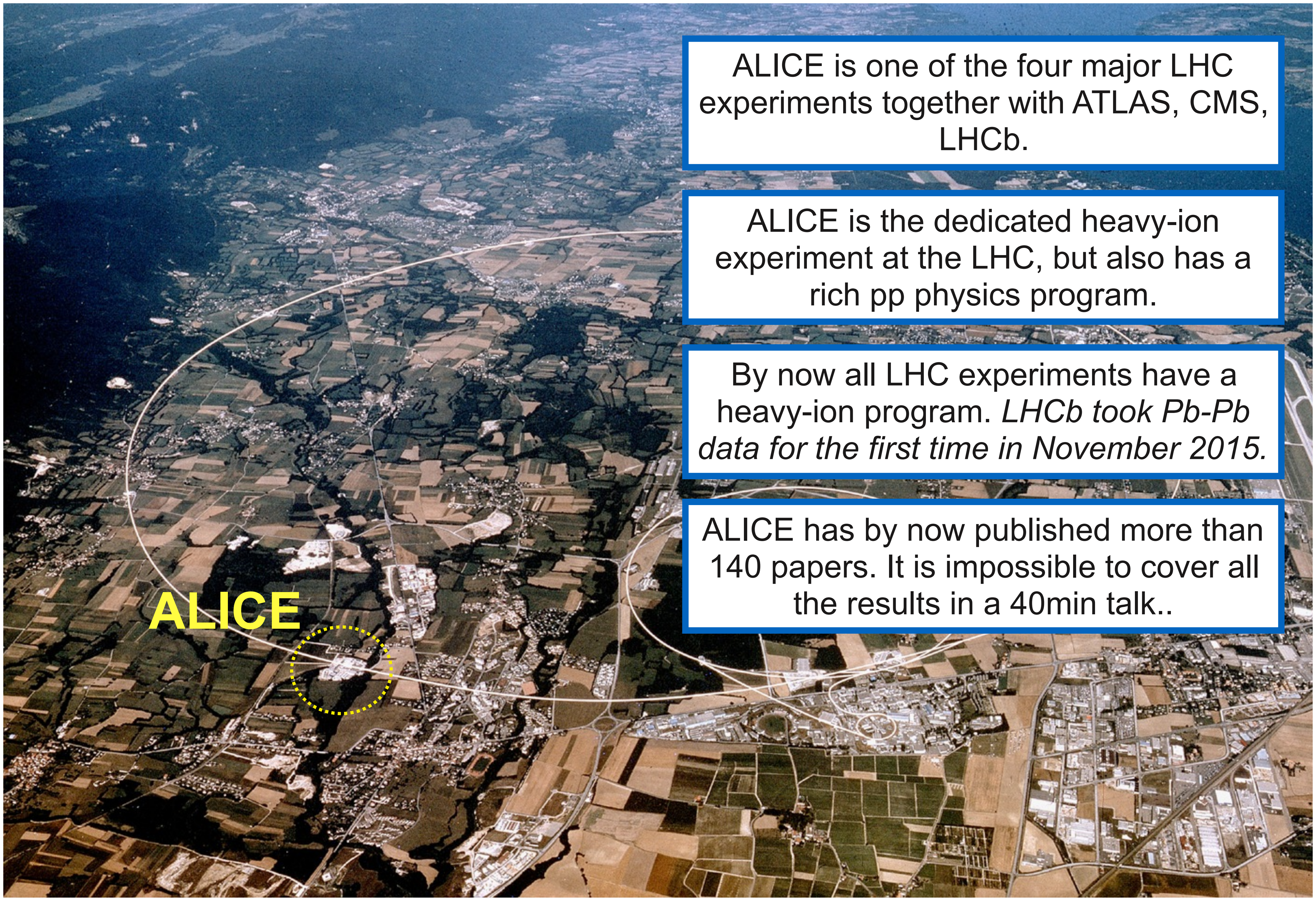

ALICE is one of the four major LHC experiments together with ATLAS, CMS, LHCb.

ALICE is the dedicated heavy-ion experiment at the LHC, but also has a rich pp physics program.

By now all LHC experiments have a heavy-ion program. *LHCb took Pb-Pb data for the first time in November 2015.*

ALICE has by now published more than 140 papers. It is impossible to cover all the results in a 40min talk..

A Large Ion Collider Experiment

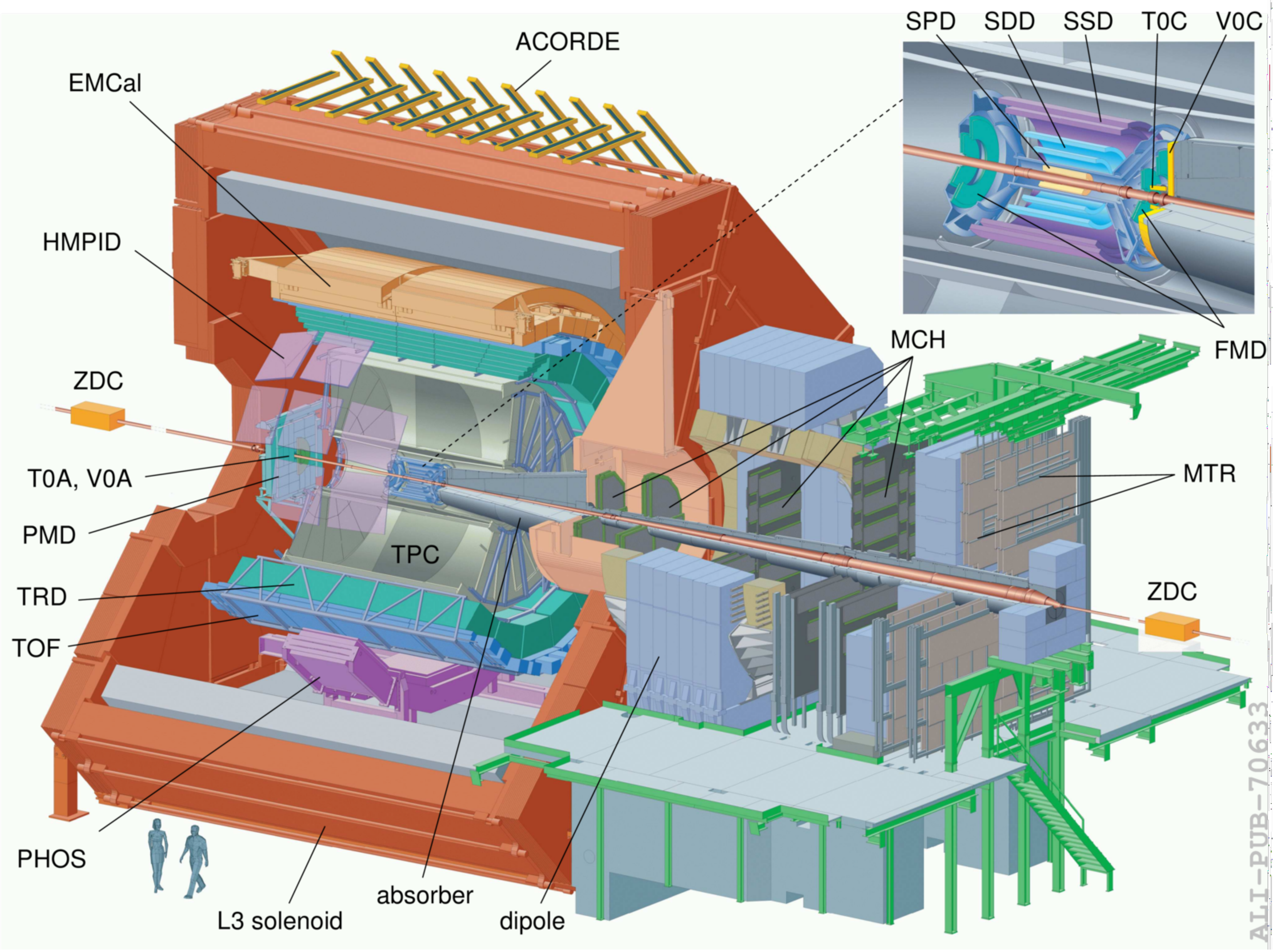

A Large Ion Collider Experiment

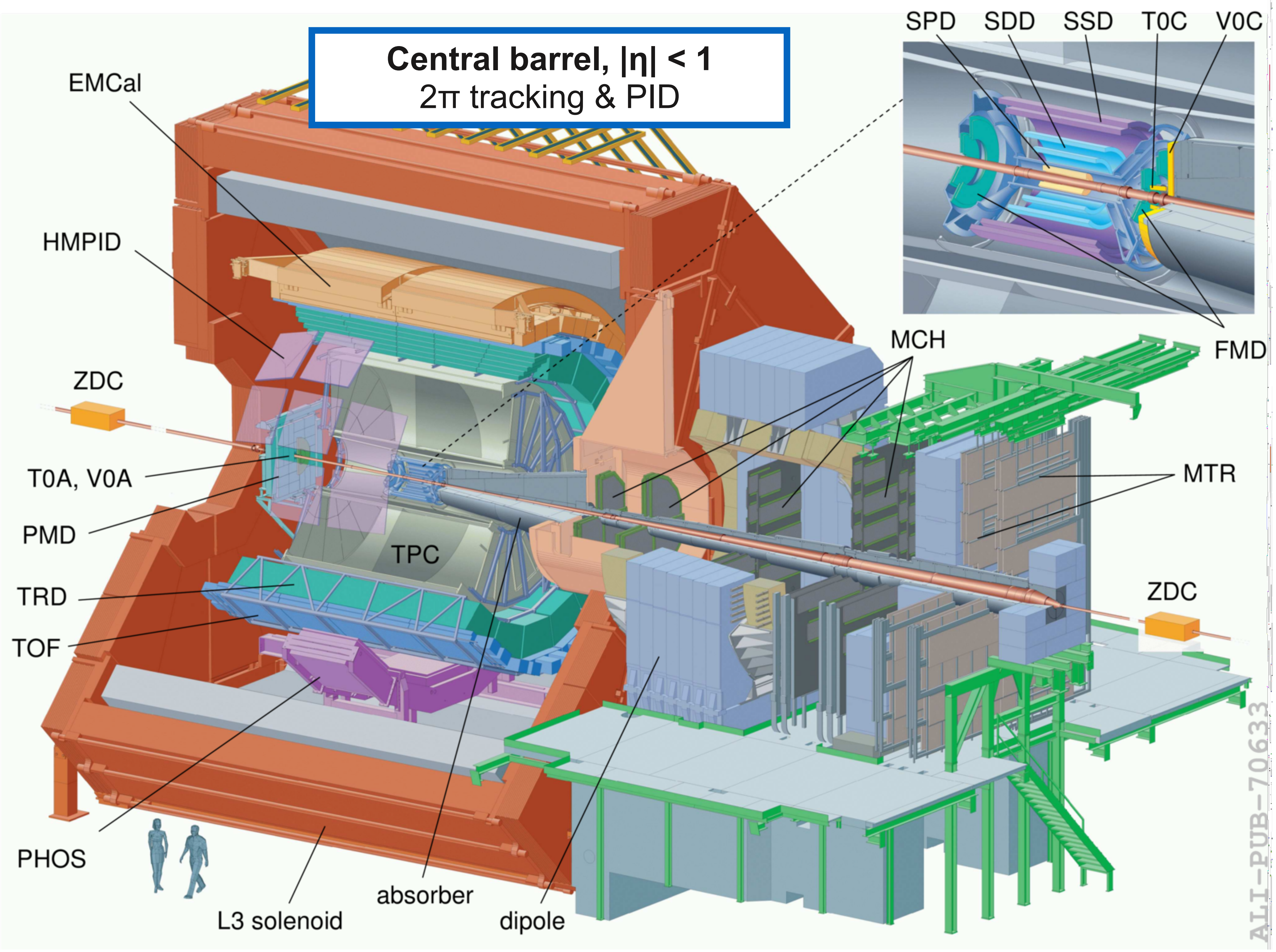

A Large Ion Collider Experiment

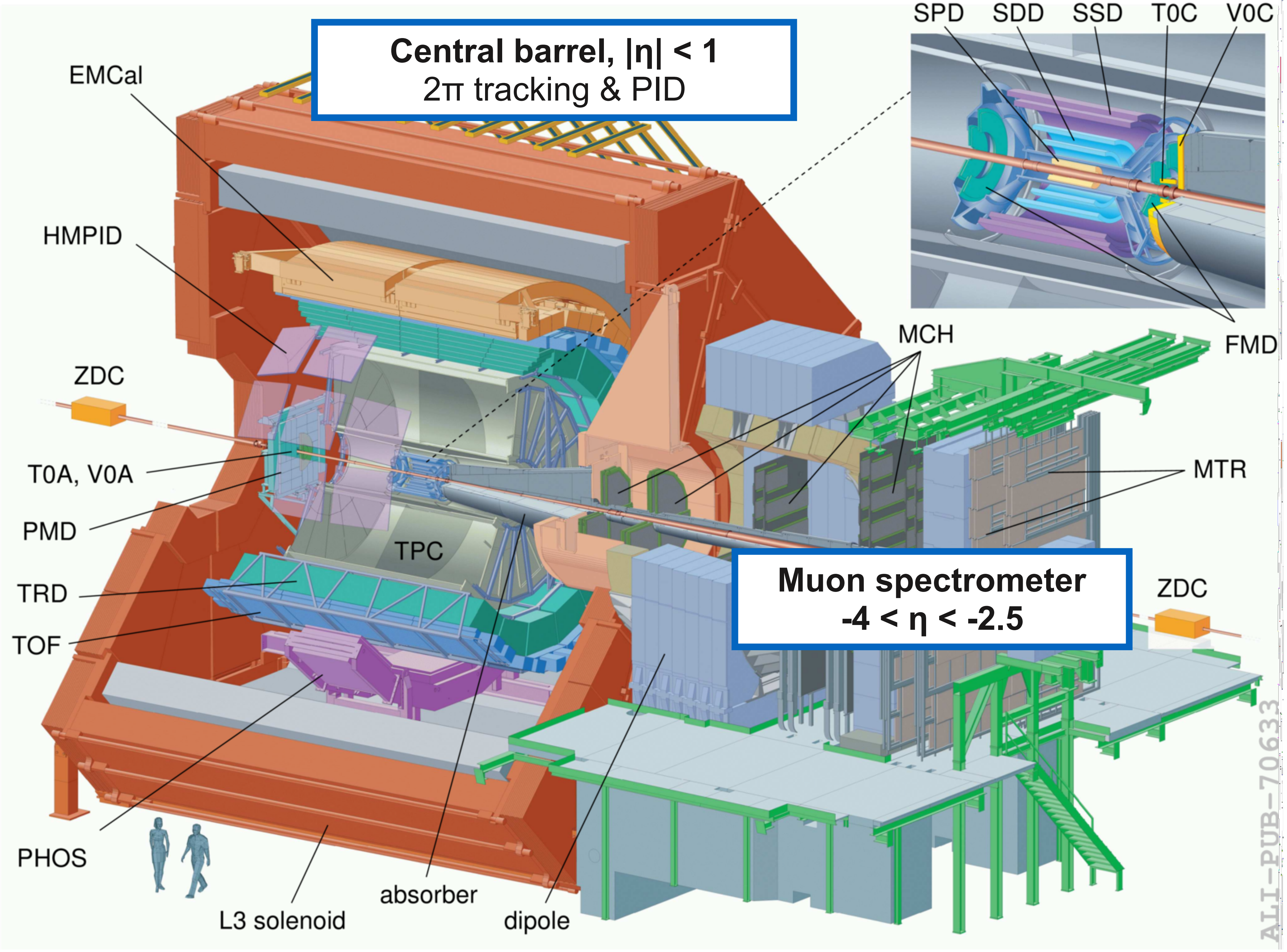

A Large Ion Collider Experiment

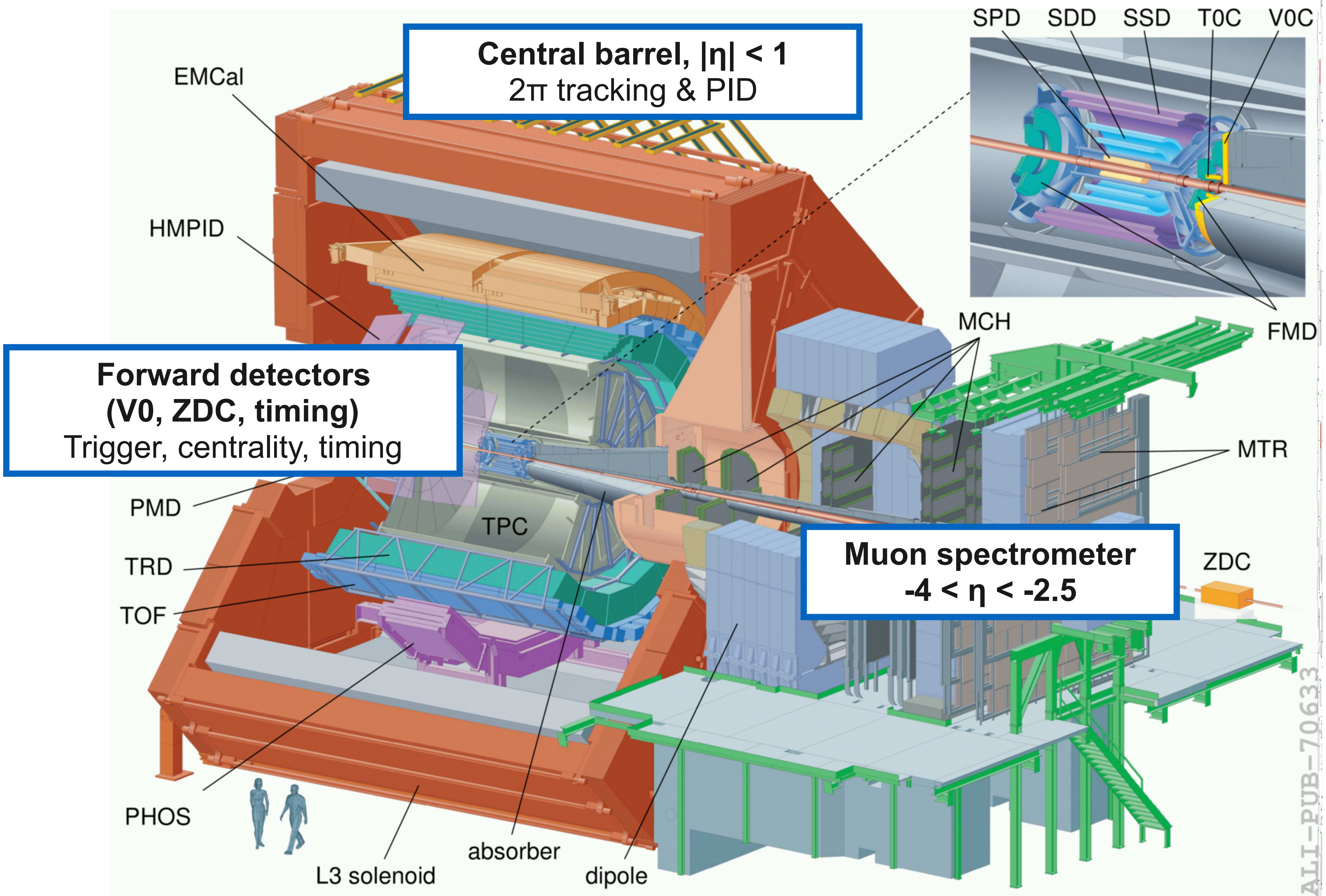

A Large Ion Collider Experiment

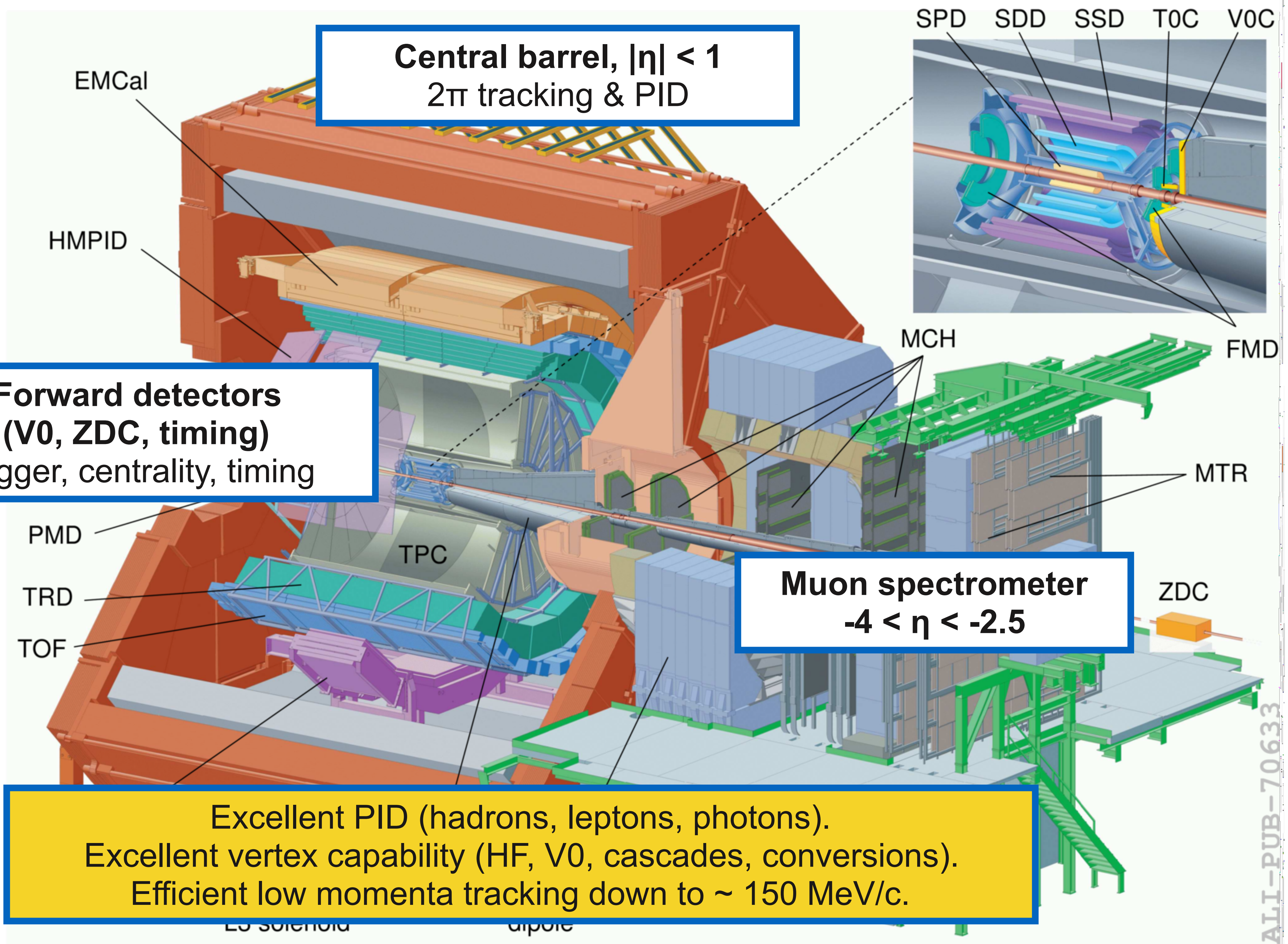

Central barrel, |η| < 1
2π tracking & PID

Forward detectors
(V0, ZDC, timing)
Trigger, centrality, timing

Muon spectrometer
-4 < η < -2.5

Excellent PID (hadrons, leptons, photons).
Excellent vertex capability (HF, V0, cascades, conversions).
Efficient low momenta tracking down to ~ 150 MeV/c.

Particle identification

ALICE

- ALICE has the strongest PID capabilities and exploits all main techniques: energy loss d*E*/dx, time of flight, Cherenkov radiation, transition radiation, calorimetry..

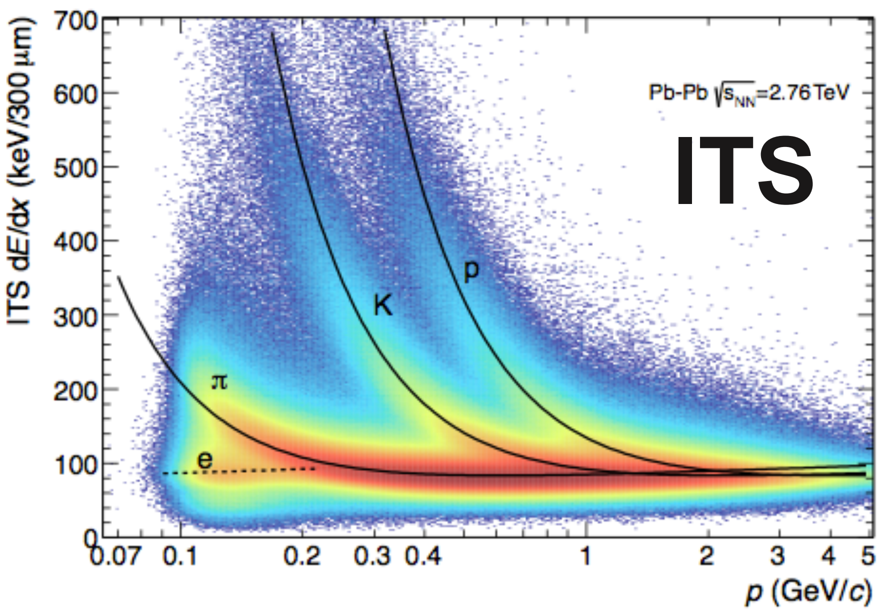

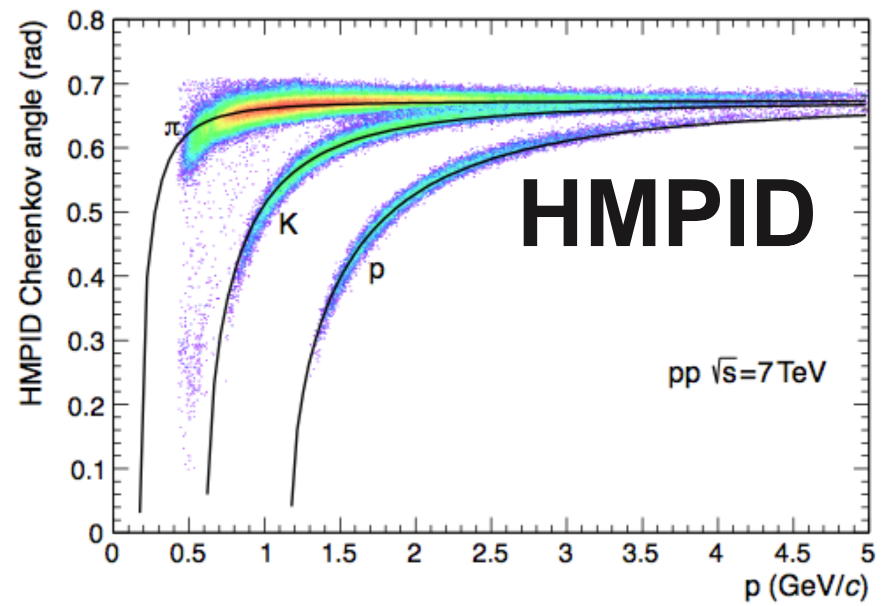

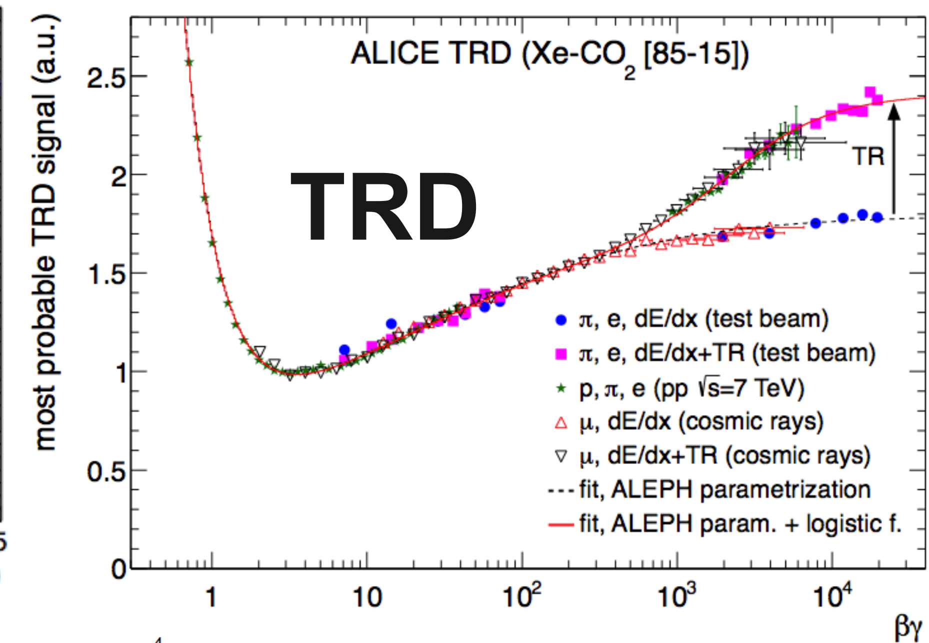

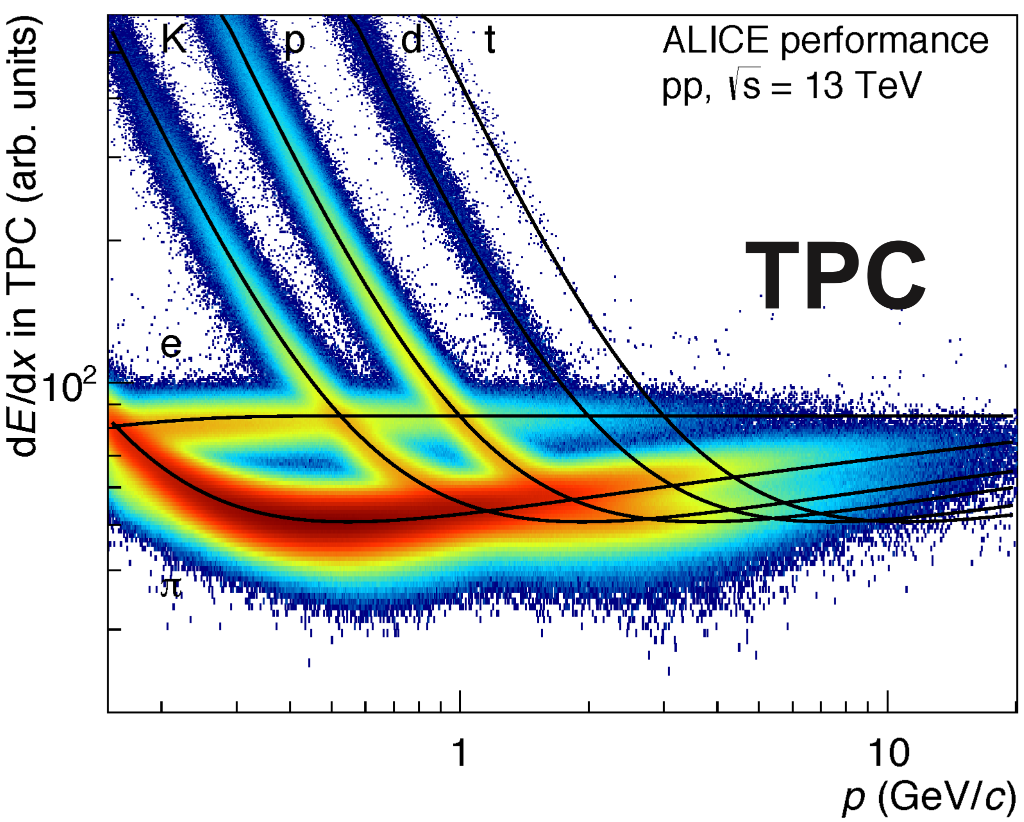

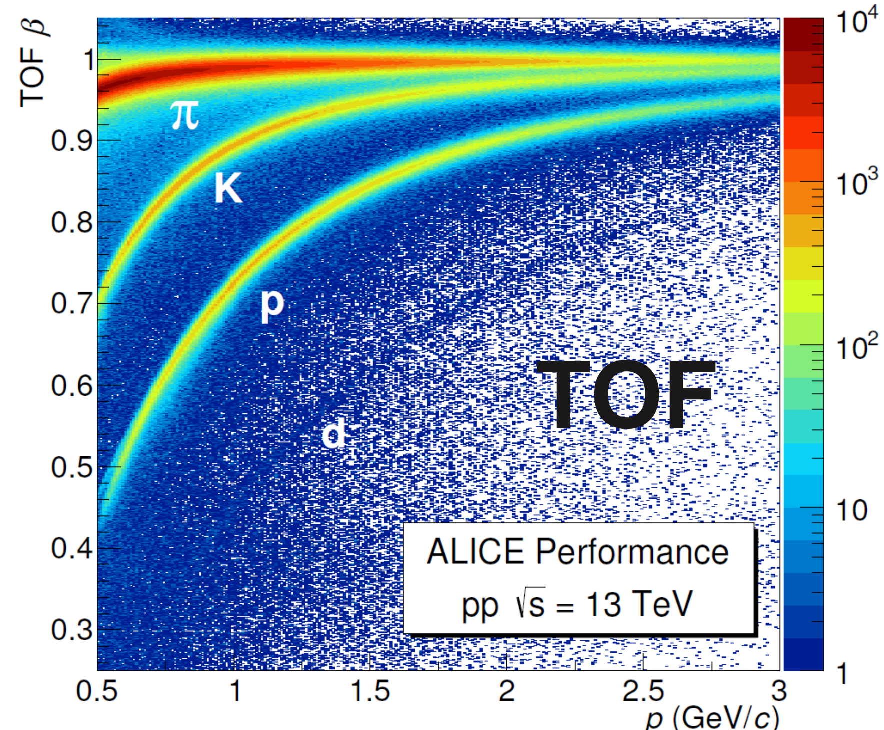

[JMP A29 (2014) 1430044]

Particle identification

- ALICE has the strongest PID capabilities and exploits all main techniques: energy loss d*E*/dx, time of flight, Cherenkov radiation, transition radiation, calorimetry..

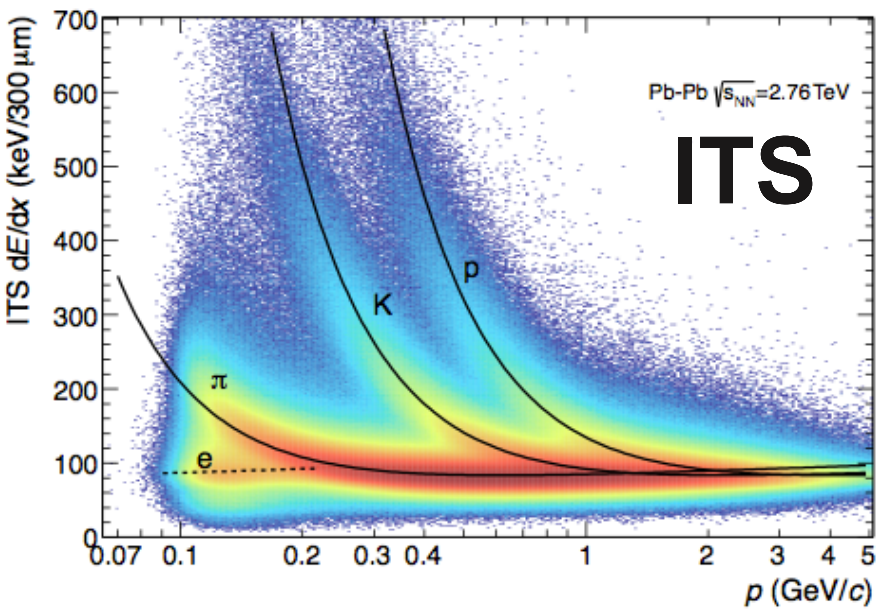

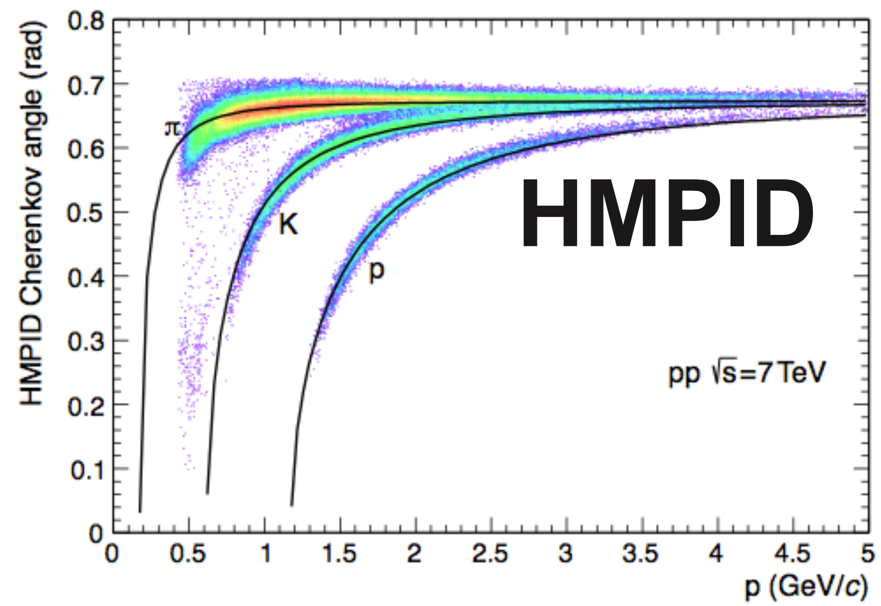

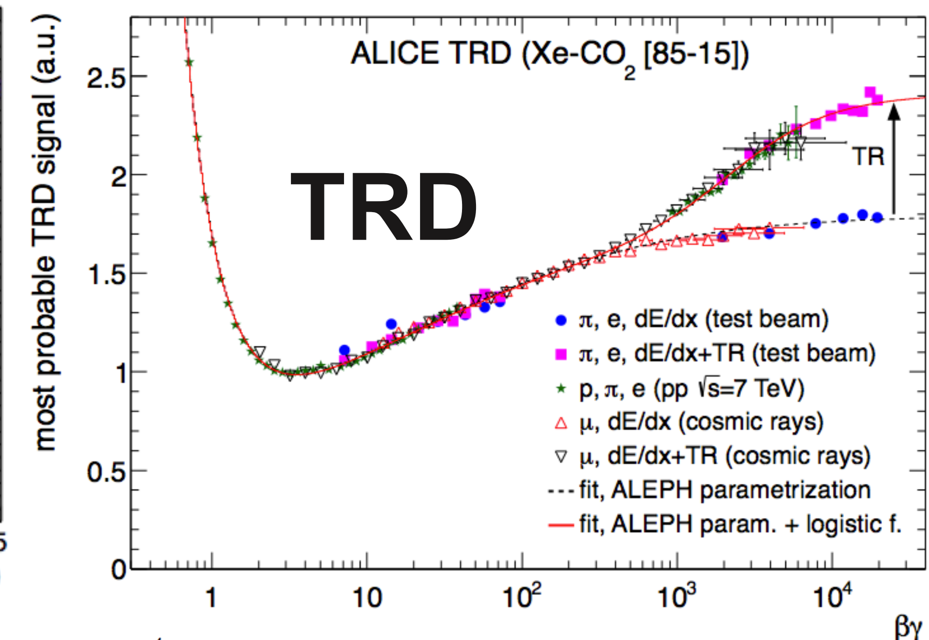

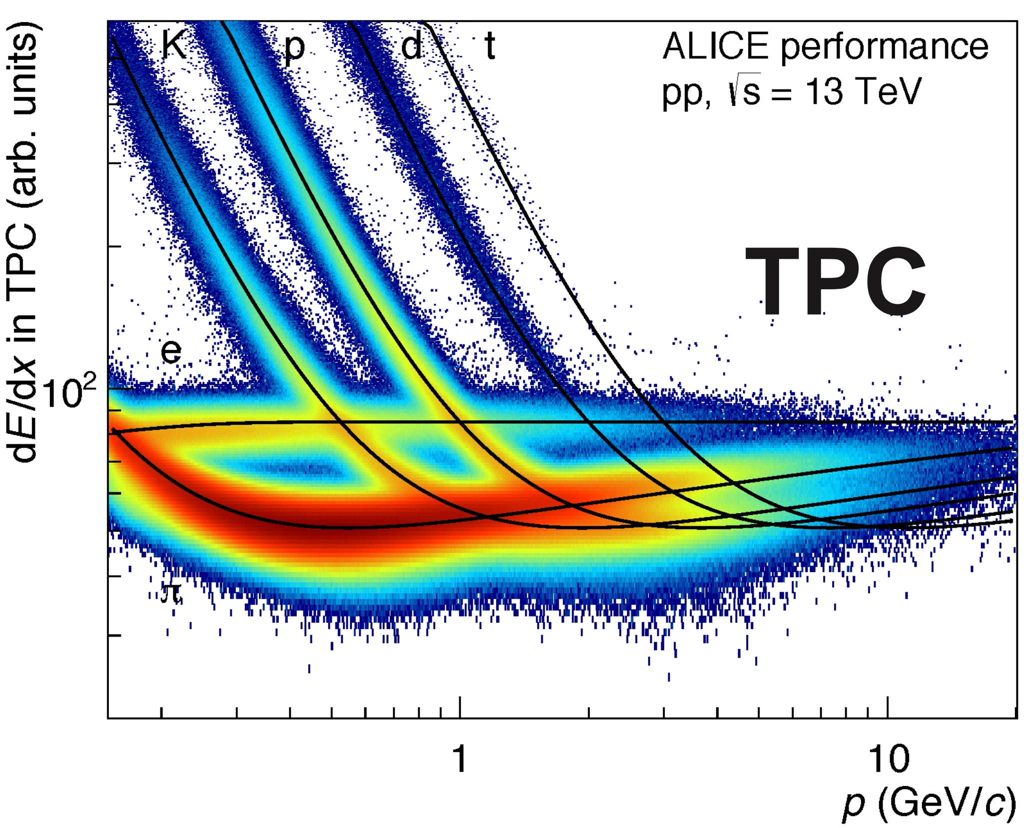

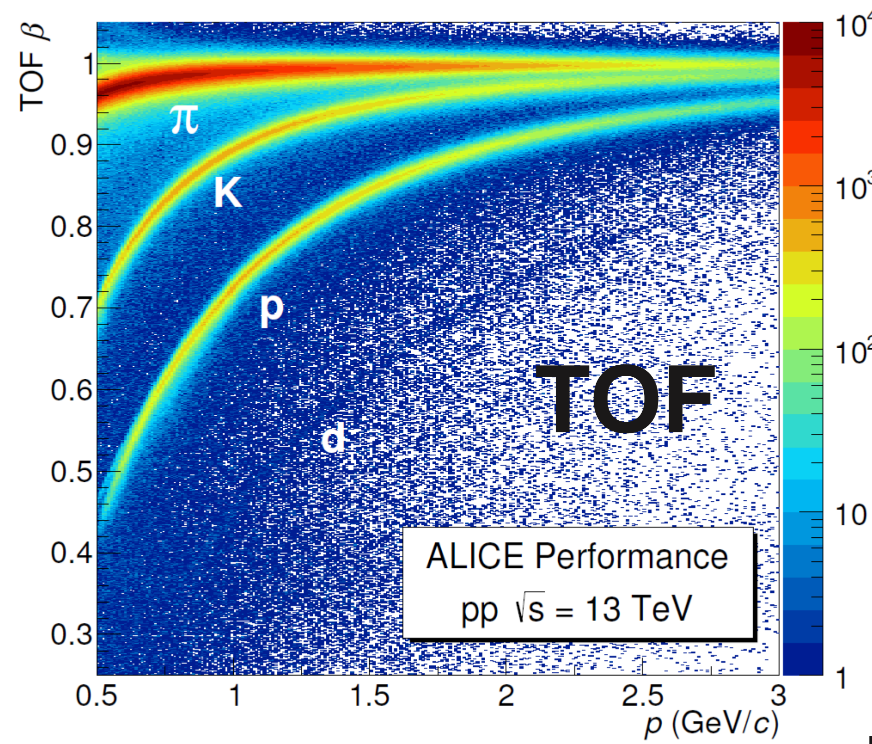

Very good data taking performance also in Run 2. ALICE continues to collect very high quality at the highest LHC energies.

[JMP A29 (2014) 1430044]

Global event observables

Charged particle multiplicity density (1)

- The very first step before one can do anything else: count particles..

pp, 13 TeV

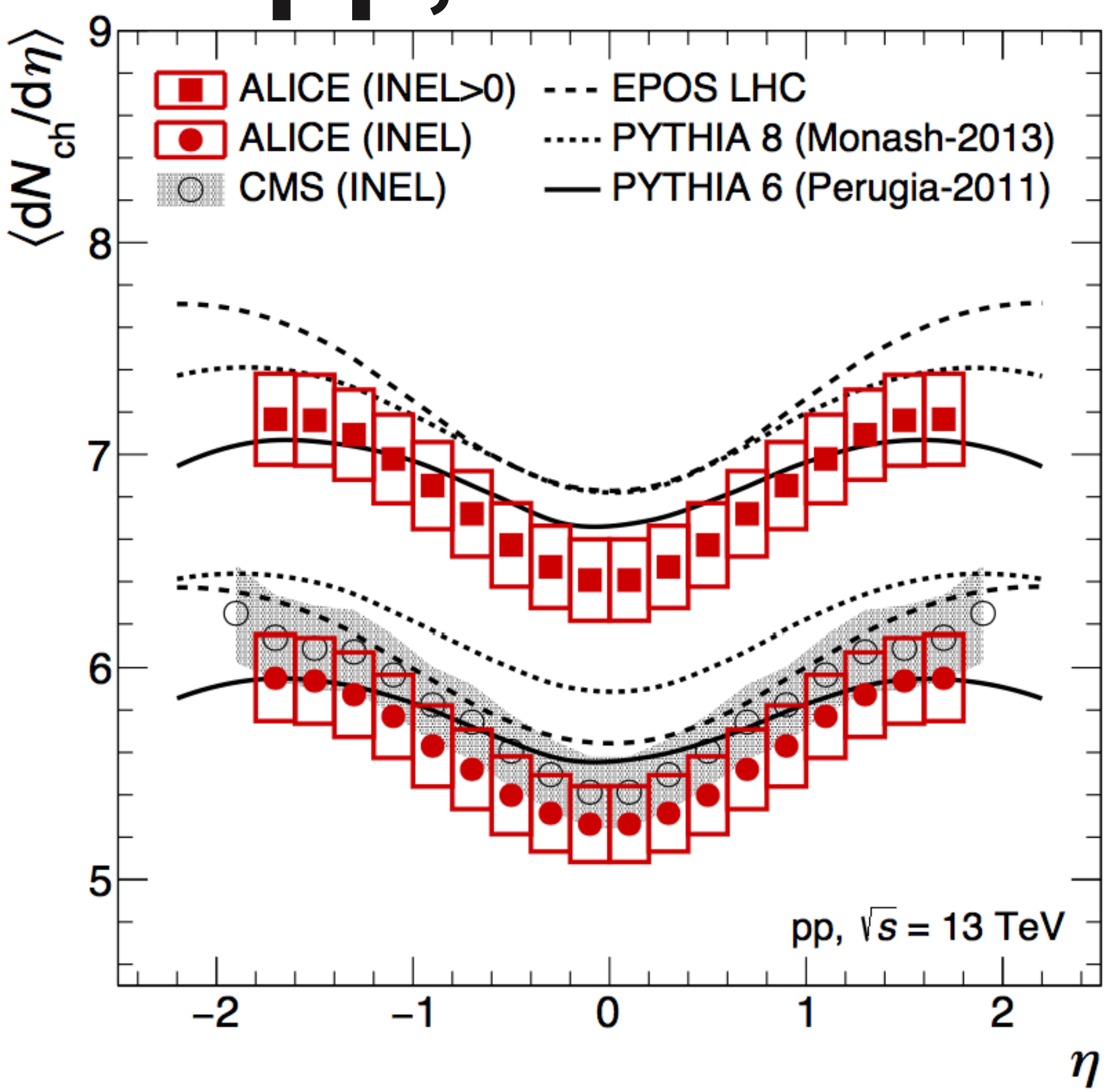

[arXiv:1509.08734]

Pb-Pb, 5.02 TeV

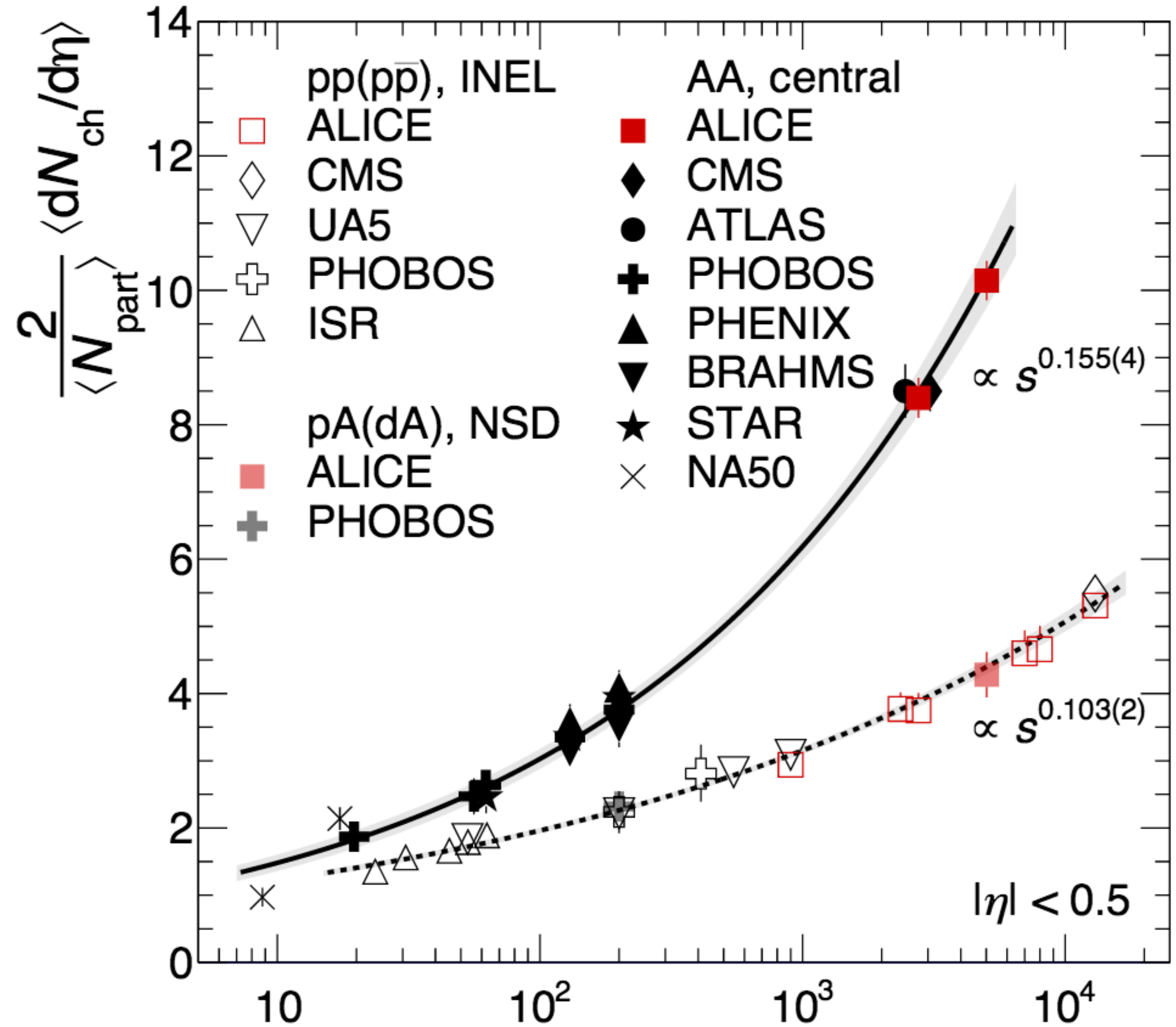

[arXiv:1512.06104]

Charged particle multiplicity density (2)

Pb-Pb, 2.76 TeV

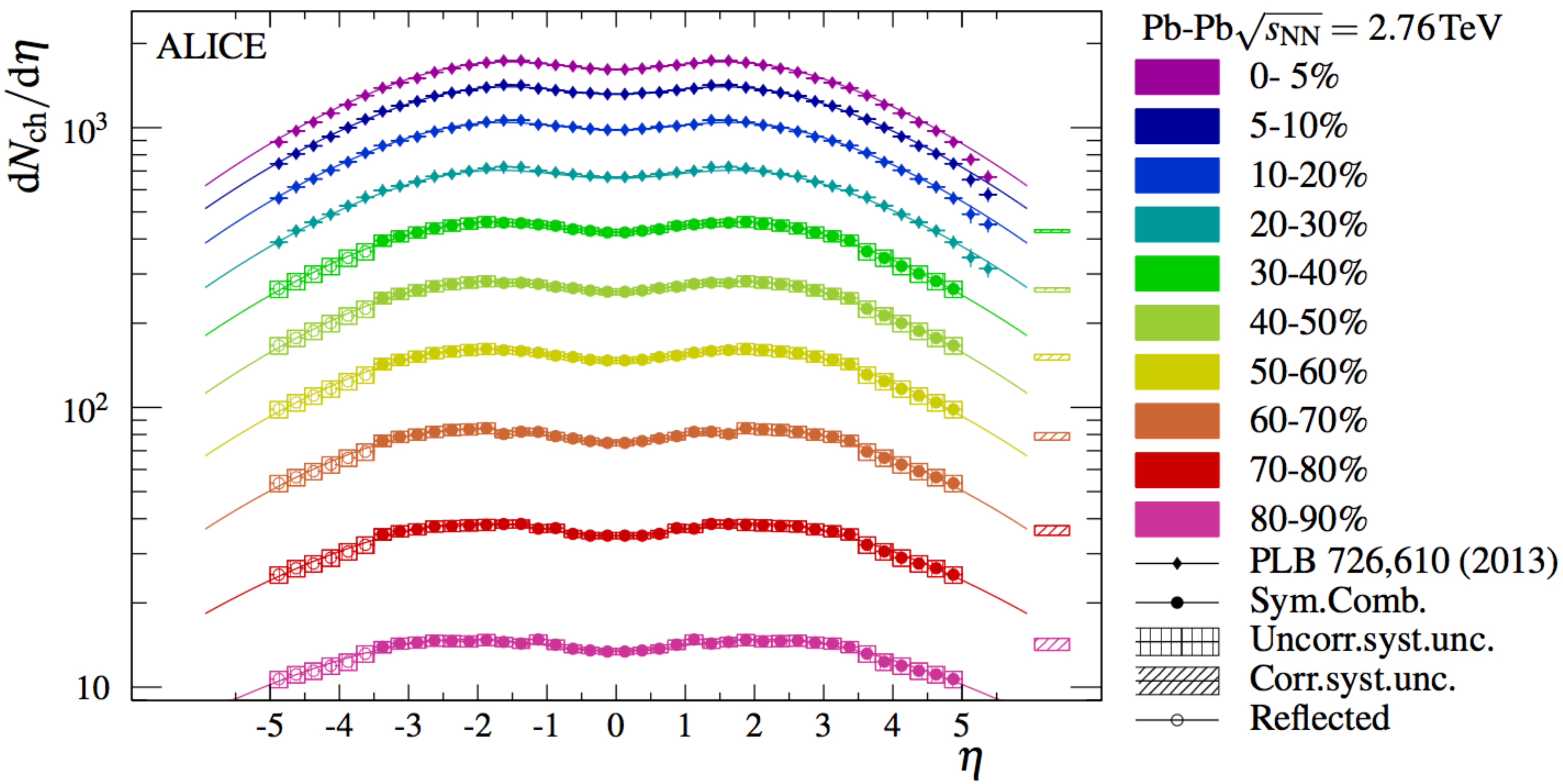

[arXiv:1509.07299]

Charged particle multiplicity density (2)

ALICE

Pb-Pb, 2.76 TeV

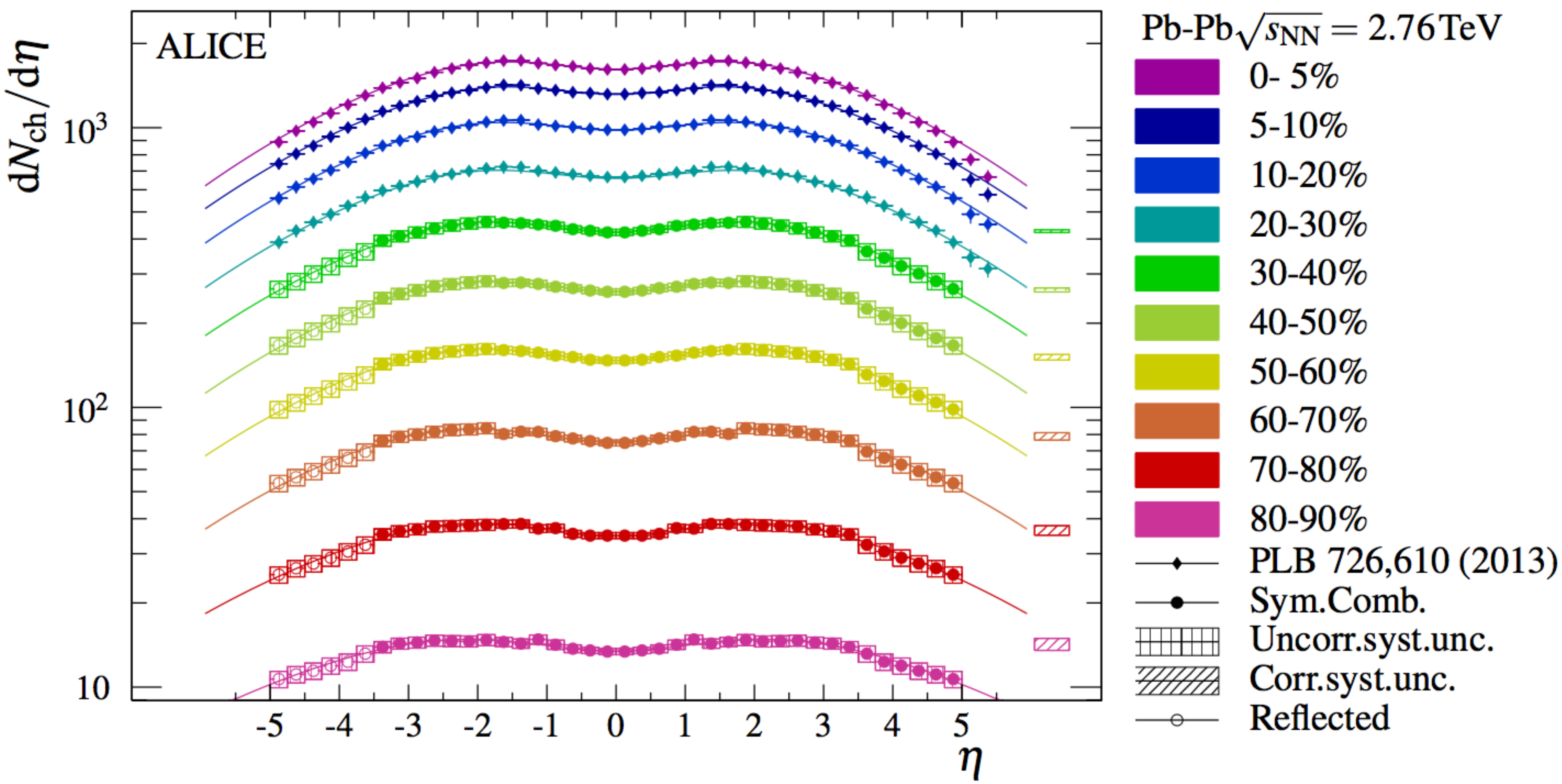

[arXiv:1509.07299]

In total, 17170 +/- 770 particles are produced in a central heavy-ion collision (integrated over the entire η-range) at 2.76 TeV.

Charged particle multiplicity density (2)

ALICE

Pb-Pb, 2.76 TeV

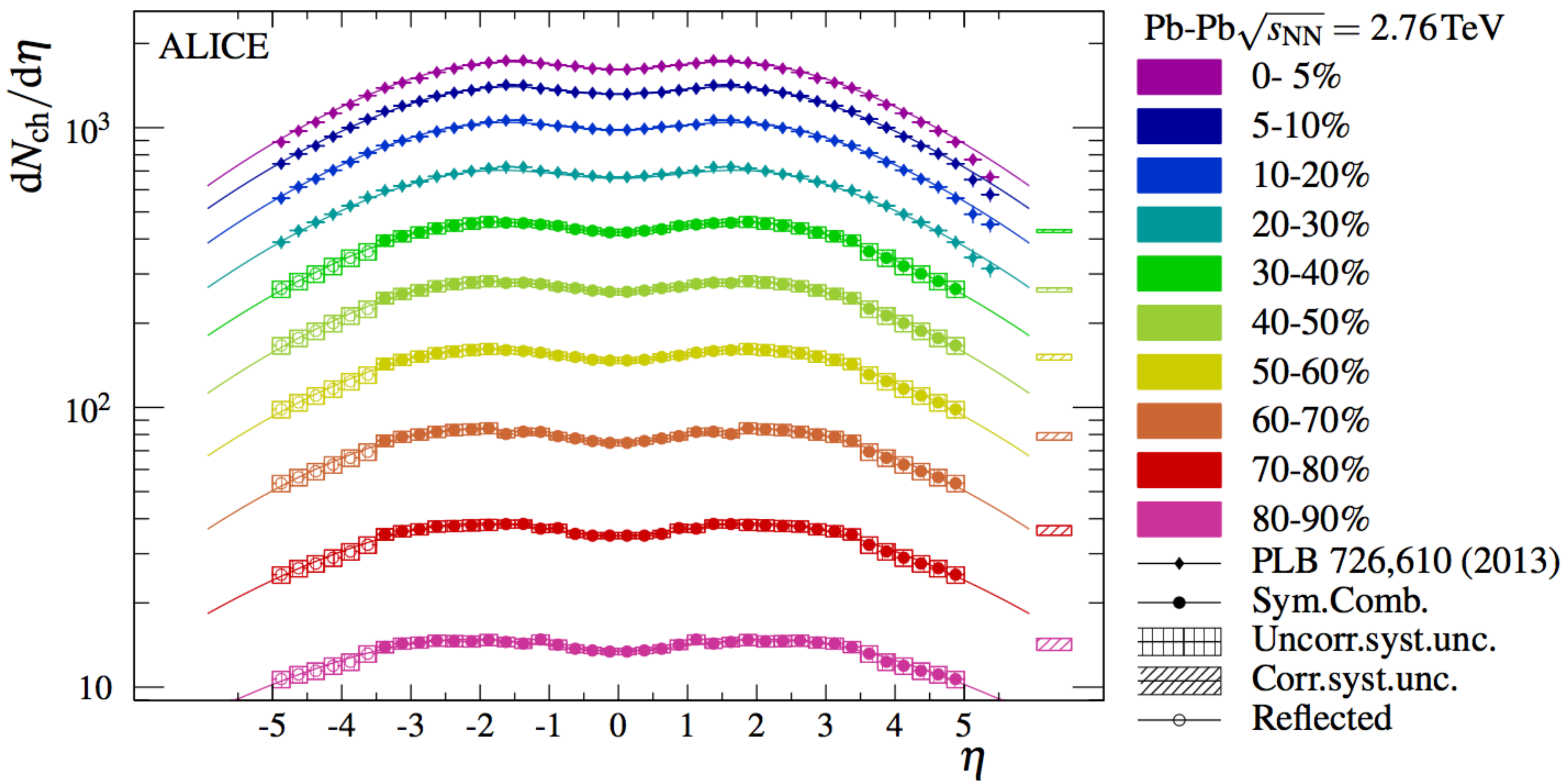

[arXiv:1509.07299]

In total, 17170 +/- 770 particles are produced in a central heavy-ion collision (integrated over the entire η-range) at 2.76 TeV.

In the central rapidity range, we can also identify them! We can count the number of pions, kaons, protons,..

Charged hadron p_T-Spectra

pp, 13 TeV

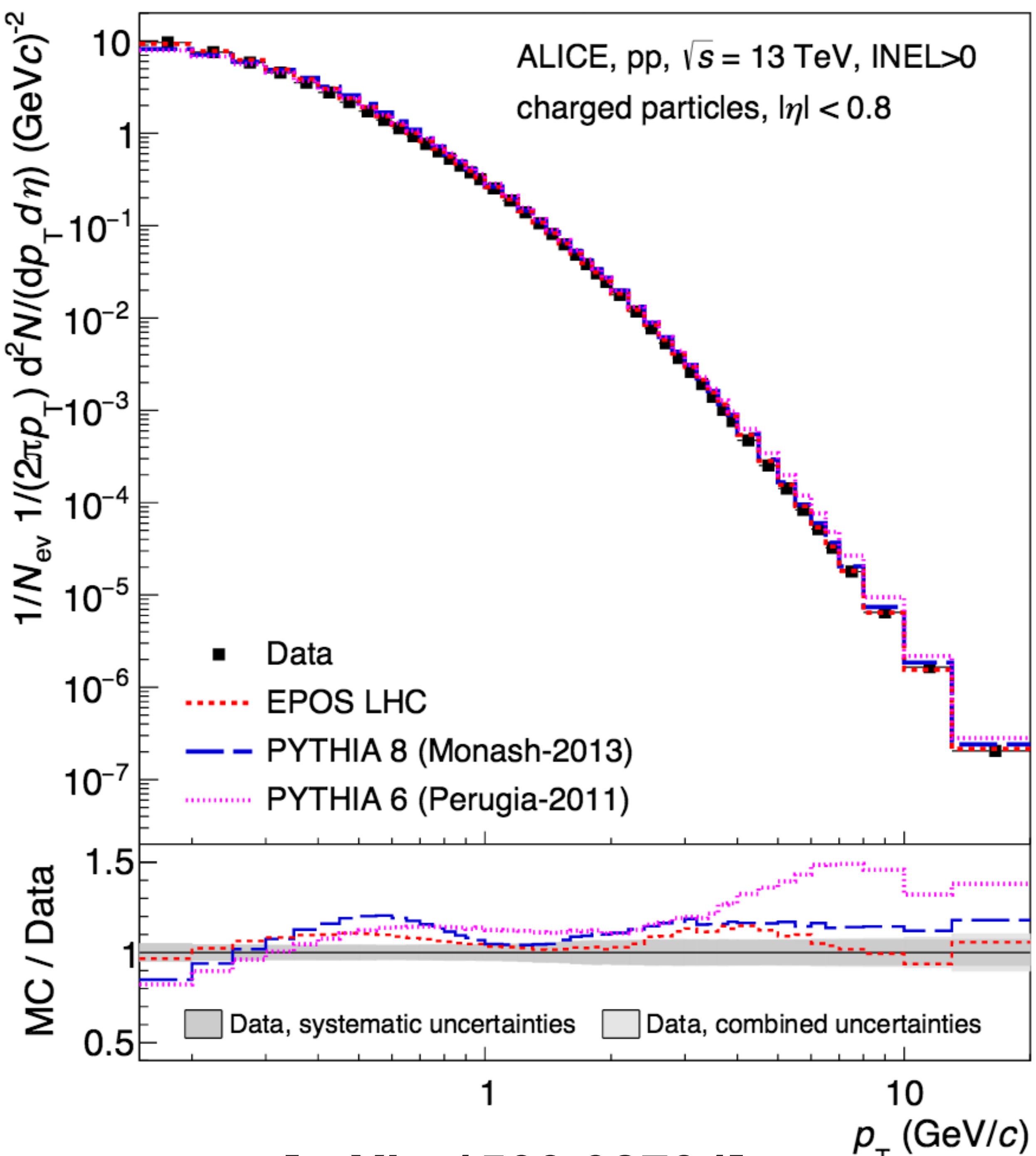

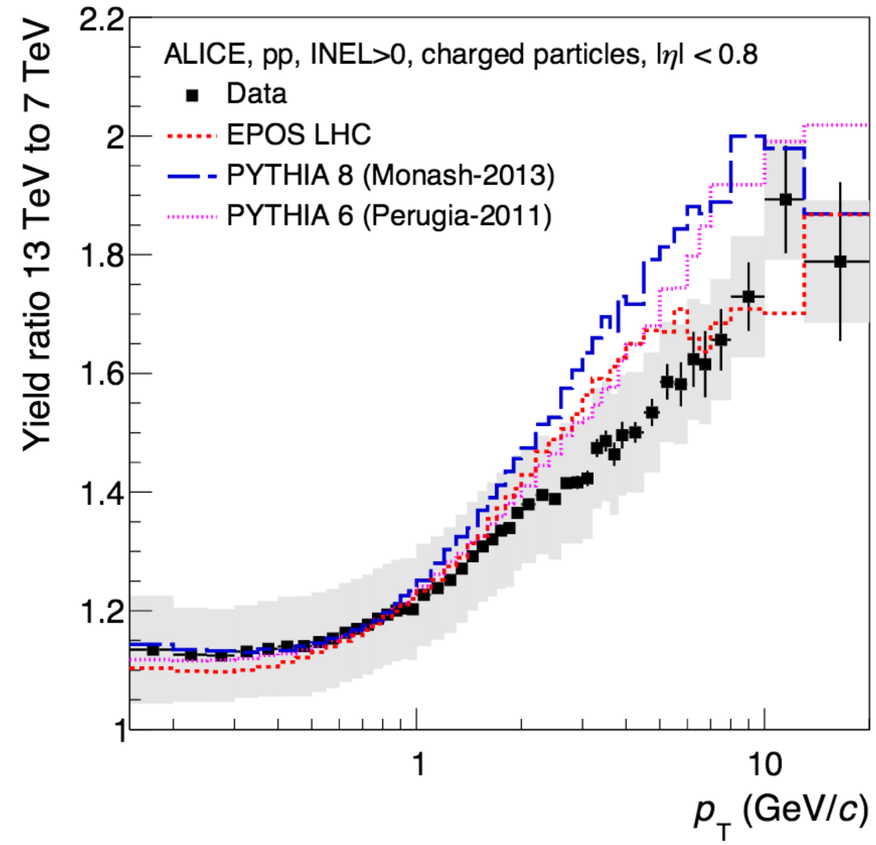

[arXiv:1509.08734]

Charged hadron p_T-Spectra

pp, 13 TeV

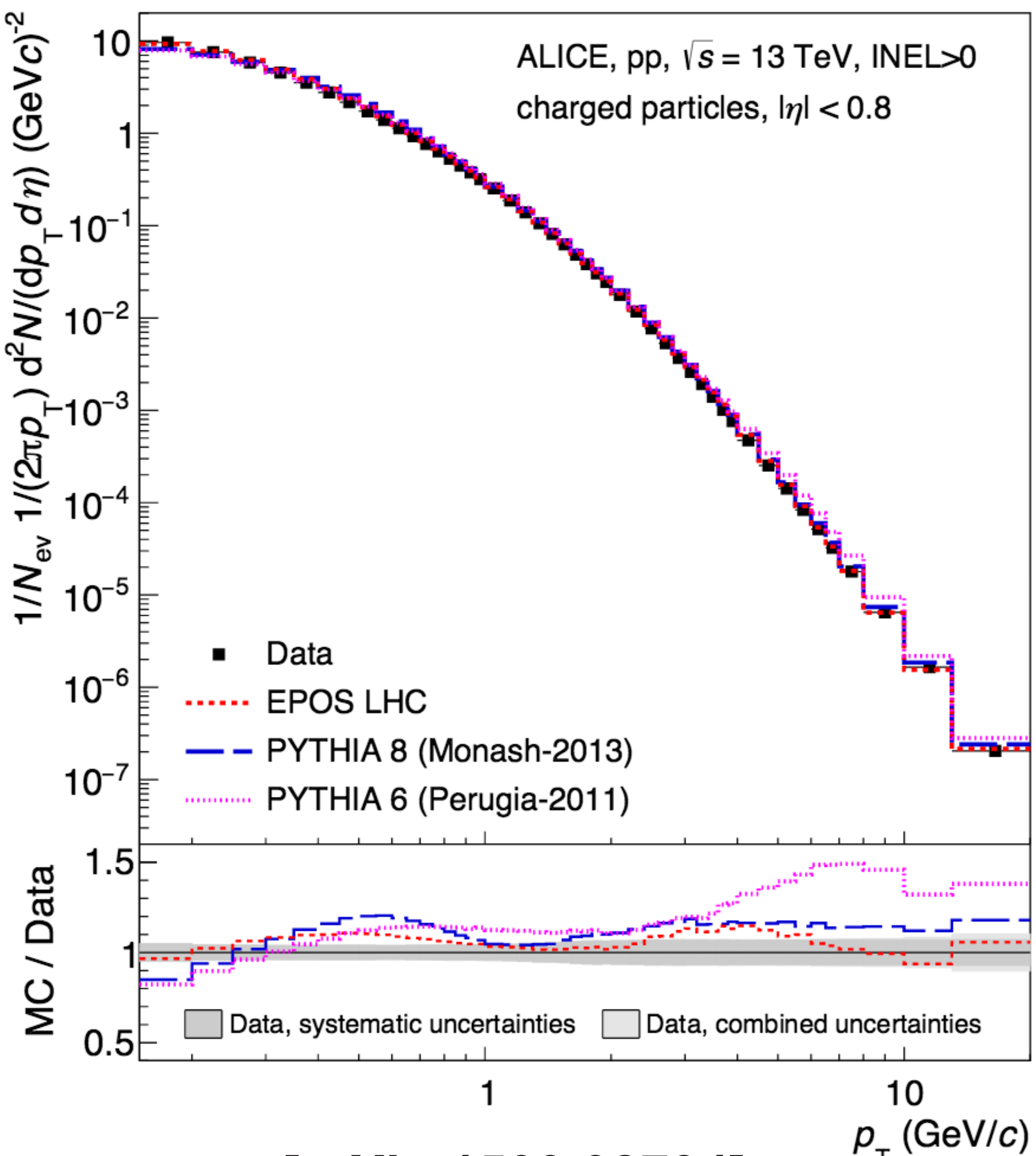

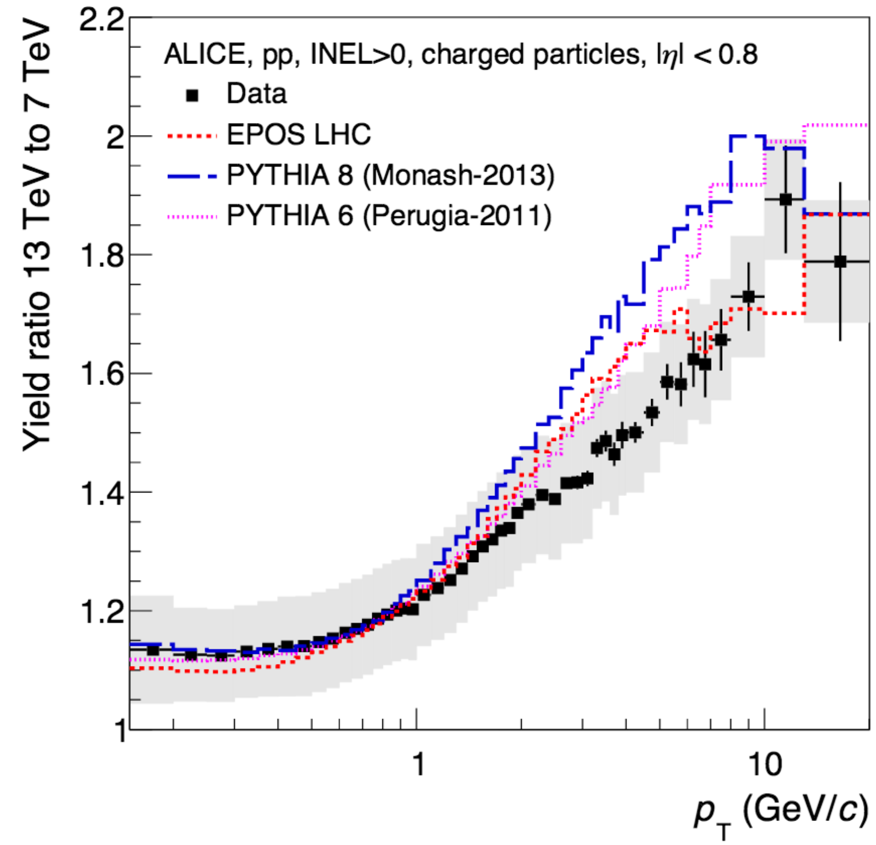

Spectra are significantly harder at 13 TeV than at 7 TeV. MC generators describe the spectra fairly well.

[arXiv:1509.08734]

Charged hadron p_T-Spectra

pp, 13 TeV

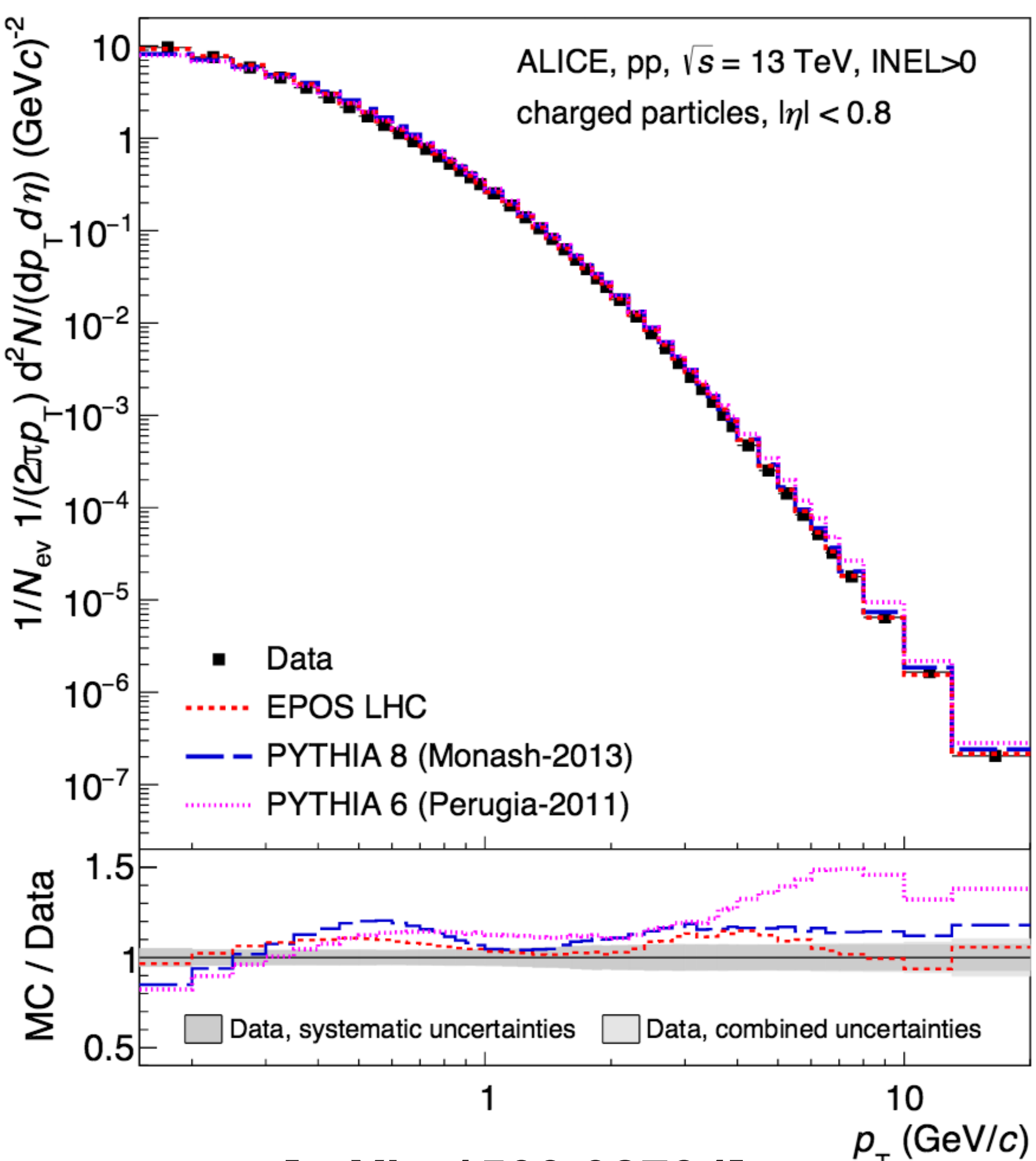

[arXiv:1509.08734]

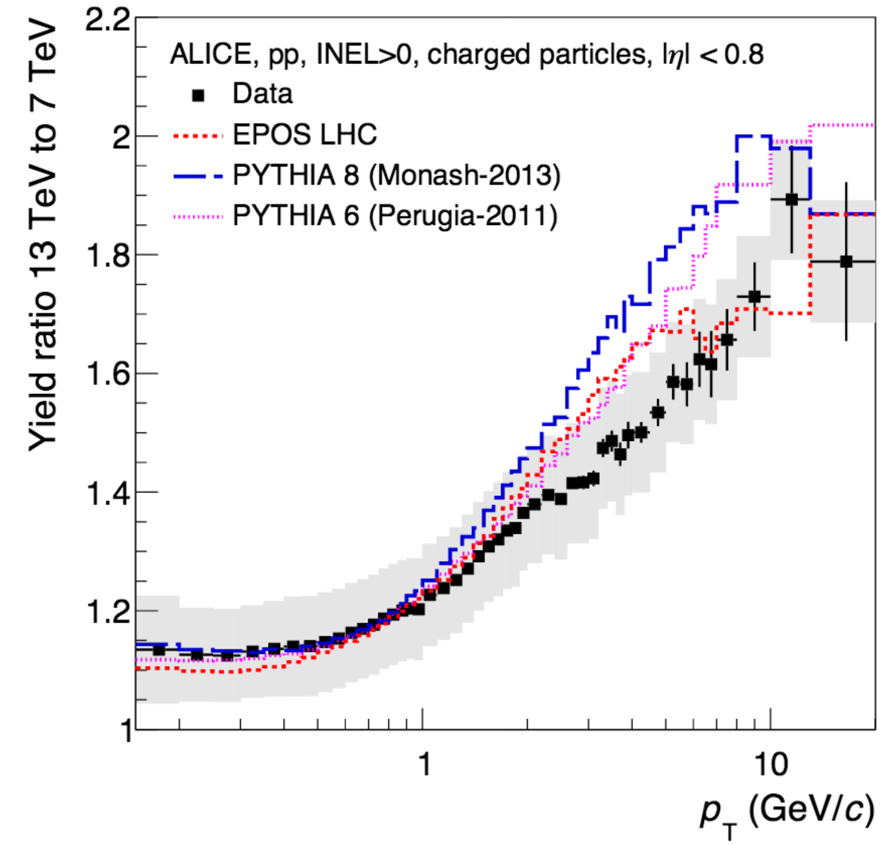

Spectra are significantly harder at 13 TeV than at 7 TeV. MC generators describe the spectra fairly well.

Still ≈98% of all particles are produced with $p_T < 2$ GeV/c.

Charged hadron p_T-Spectra

pp, 13 TeV

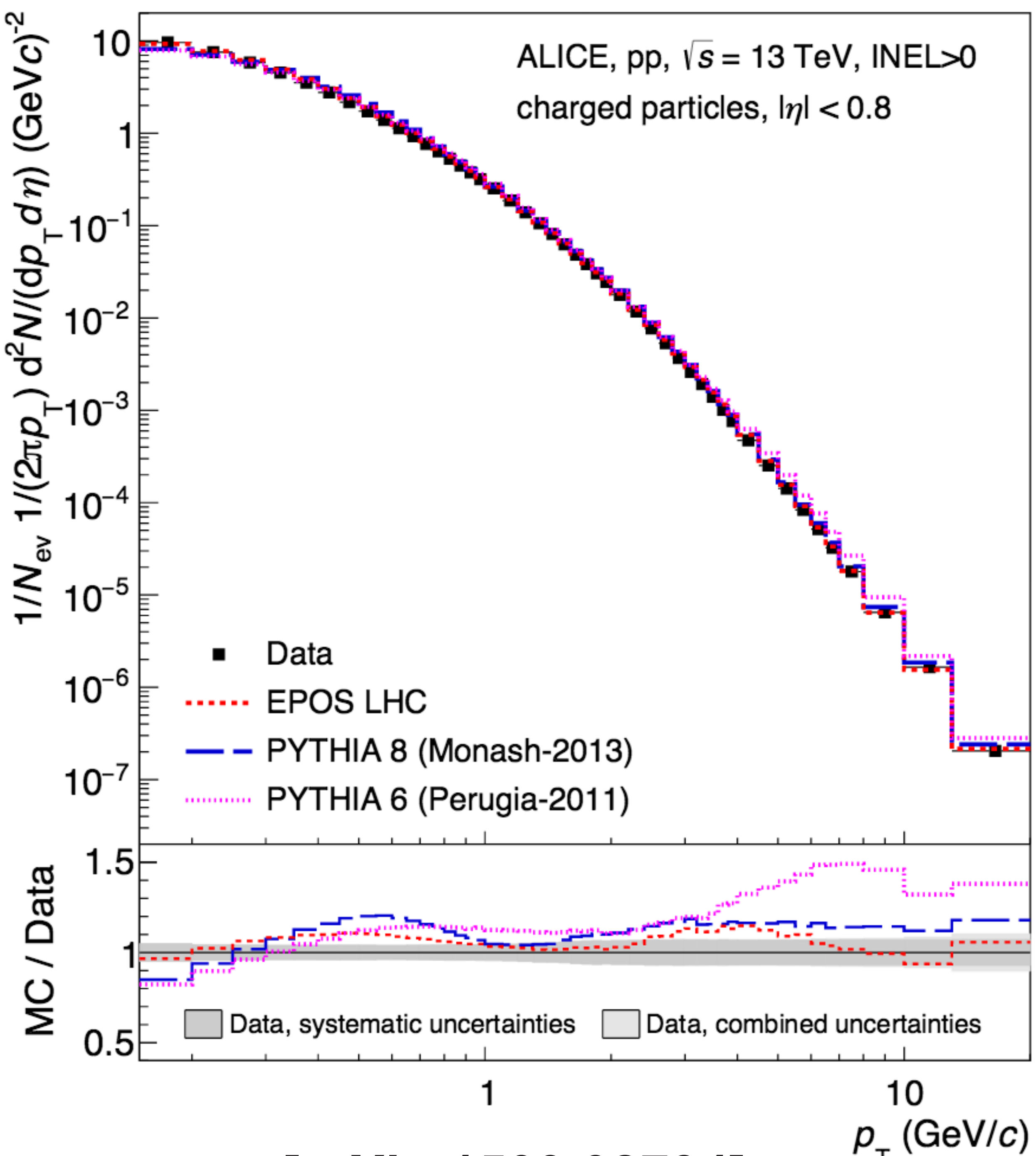

[arXiv:1509.08734]

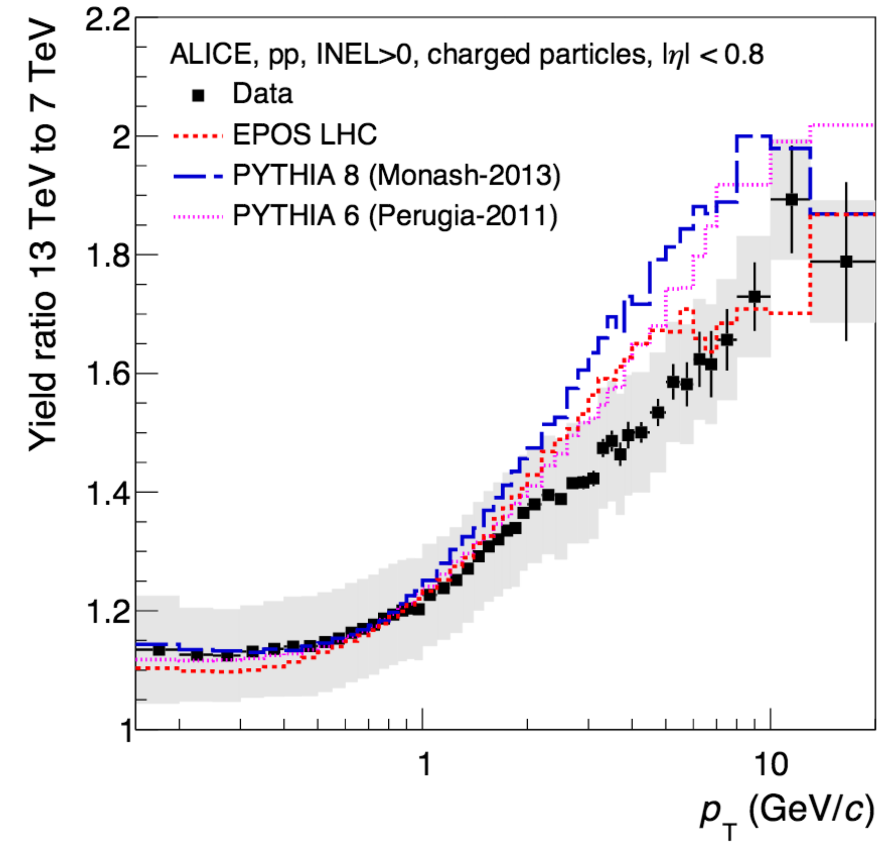

Spectra are significantly harder at 13 TeV than at 7 TeV. MC generators describe the spectra fairly well.

Still ≈98% of all particles are produced with p_T < 2 GeV/c.

≈ 80% of all particles are pions, ≈ 13% are kaons, and ≈ 4% are protons.

ALICE

A fireball in thermal equilibrium

- It is important to distinguish between
  - a *system of individual particles* and
  - a *medium* in which individual degrees of freedom do not matter anymore and we can apply thermodynamic concepts.

- Thermodynamic concepts are typically used for systems with 10^5-10^{23} particles in *local thermal equilibrium*.
  - central Pb-Pb collision 2.76 TeV (LHC): $dN_{ch}/d\eta \approx 1600$
  - high mult. p-Pb collision (LHC): $dN_{ch}/d\eta \approx 60$
  - pp collision 7 TeV (LHC): $dN_{ch}/d\eta \approx 6$

- Lifetime of the system must be long enough so that equilibrium can be established by several (simulations indicate 5-6) interactions between its constituents.

pp

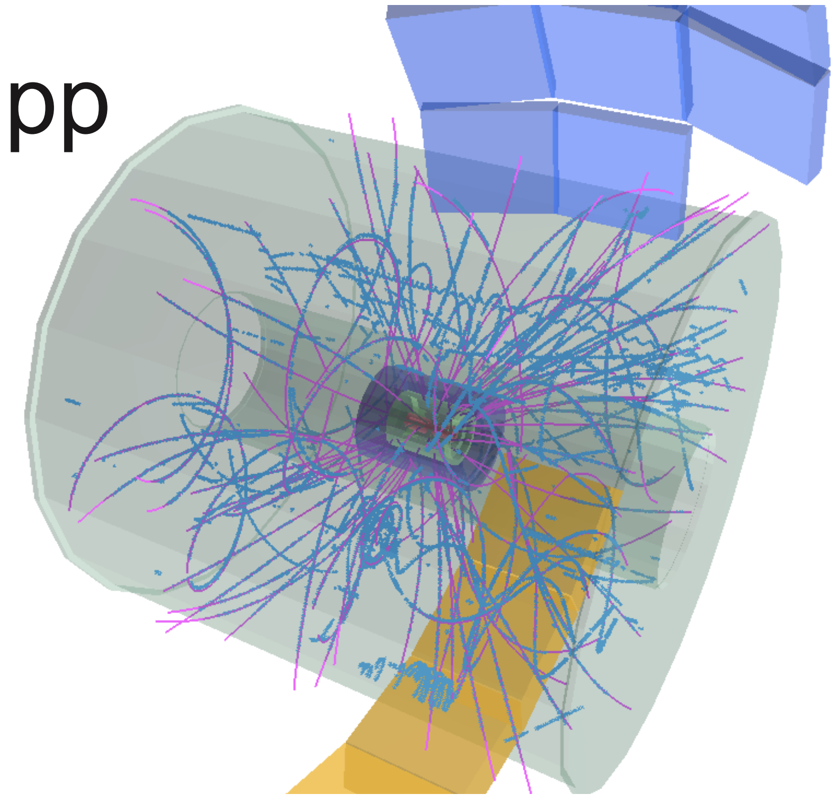

Pb-Pb

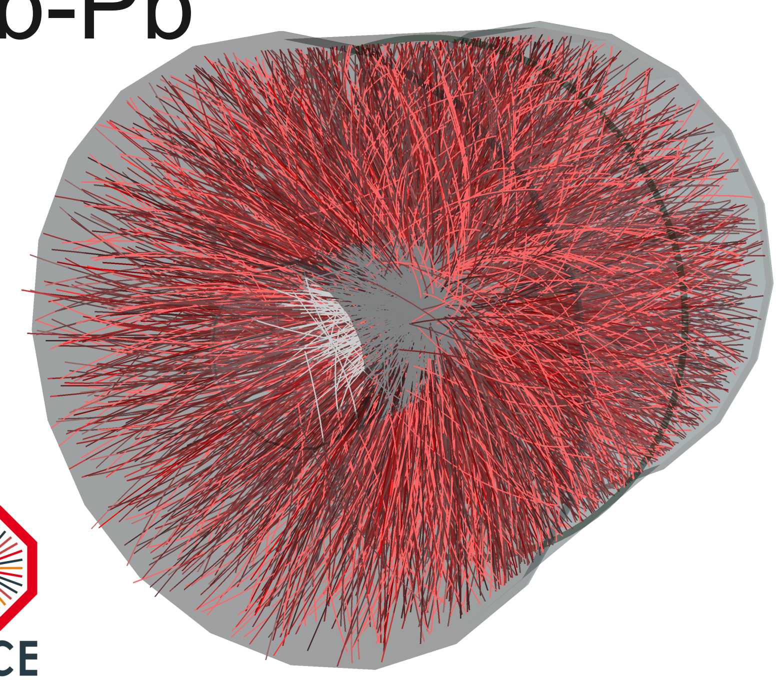

ALICE
A JOURNEY OF DISCOVERY

A fireball in thermal equilibrium

- It is important to distinguish between
  - a *system of individual particles* and
  - a *medium* in which individual degrees of freedom do not matter anymore and we can apply thermodynamic concepts.

- Thermodynamic concepts are typically used for systems with 10^5-10^{23} particles in *local thermal equilibrium*.
  - central Pb-Pb collision 2.76 TeV (LHC): $dN_{ch}/d\eta \approx 1600$
  - high mult. p-Pb collision (LHC): $dN_{ch}/d\eta \approx 60$
  - pp collision 7 TeV (LHC): $dN_{ch}/d\eta \approx 6$

- Lifetime of the system must be long enough so that equilibrium can be established by several (simulations indicate 5-6) interactions between its constituents.

pp

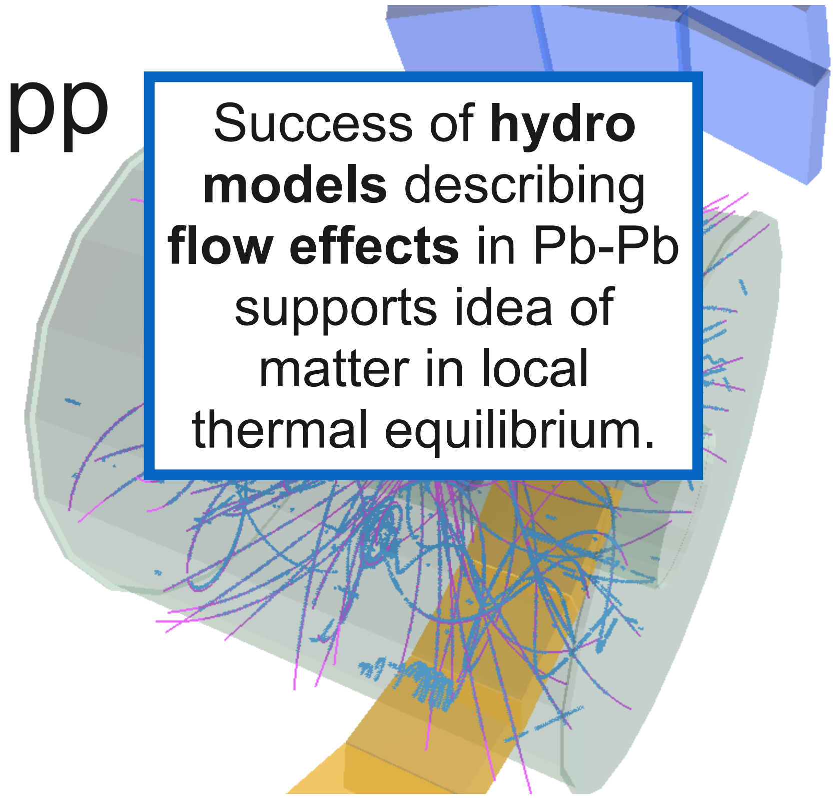

Success of **hydro models** describing **flow effects** in Pb-Pb supports idea of matter in local thermal equilibrium.

Pb-Pb

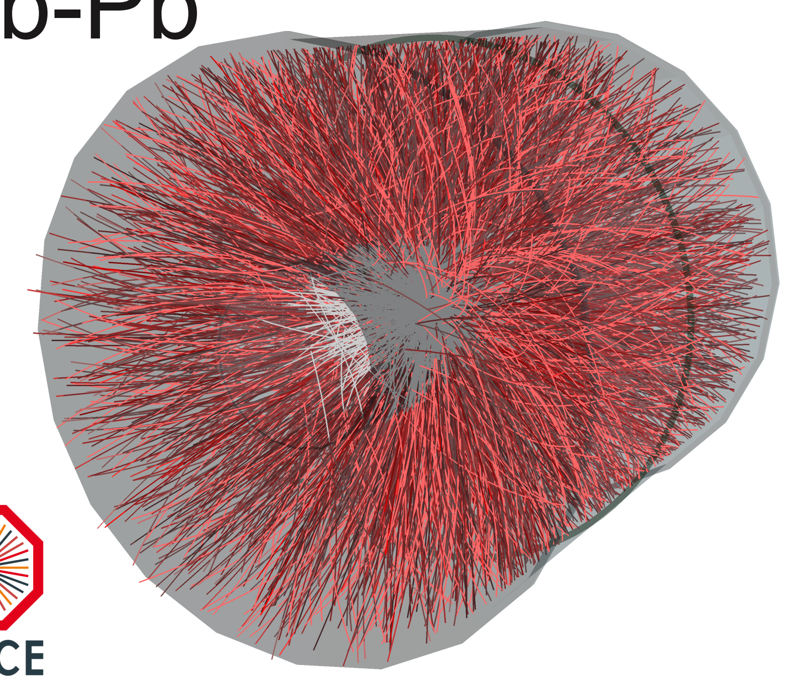

A fireball in thermal equilibrium

- It is important to distinguish between
  - a *system of individual particles* and
  - a *medium* in which individual degrees of freedom do not matter anymore and we can apply thermodynamic concepts.

- Thermodynamic concepts are typically used for systems with 10^5-10^{23} particles in *local thermal equilibrium*.
  - central Pb-Pb collision 2.76 TeV (LHC): $dN_{ch}/d\eta \approx 1600$
  - high mult. p-Pb collision (LHC): $dN_{ch}/d\eta \approx 60$
  - pp collision 7 TeV (LHC): $dN_{ch}/d\eta \approx 6$

- Lifetime of the system must be long enough so that equilibrium can be established by several (simulations indicate 5-6) interactions between its constituents.

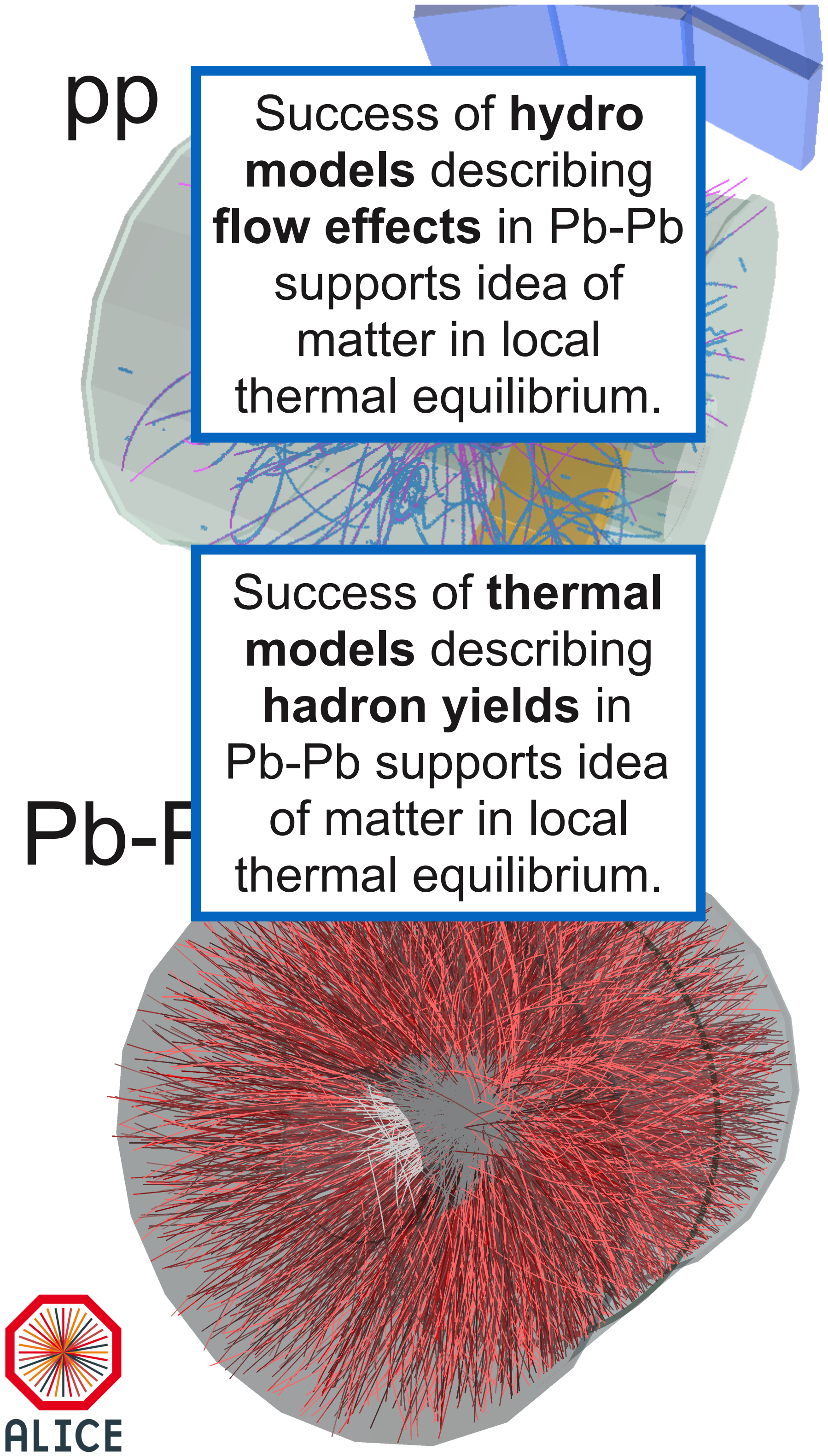

Success of **hydro models** describing **flow effects** in Pb-Pb supports idea of matter in local thermal equilibrium.

Success of **thermal models** describing **hadron yields** in Pb-Pb supports idea of matter in local thermal equilibrium.

ALICE

A fireball in thermal equilibrium

- It is important to distinguish between
  - a *system of individual particles* and
  - a *medium* in which individual degrees of freedom do not matter anymore and we can apply thermodynamic concepts.

- Thermodynamic concepts are typically used for systems with 10^5-10^{23} particles in *local thermal equilibrium*.
  - central Pb-Pb collision 2.76 TeV (LHC): $dN_{ch}/d\eta \approx 1600$
  - high mult. p-Pb collision (LHC): $dN_{ch}/d\eta \approx 60$
  - pp collision 7 TeV (LHC): $dN_{ch}/d\eta \approx 6$

- Lifetime of the system must be long enough so that equilibrium can be established by several (simulations indicate 5-6) interactions between its constituents.

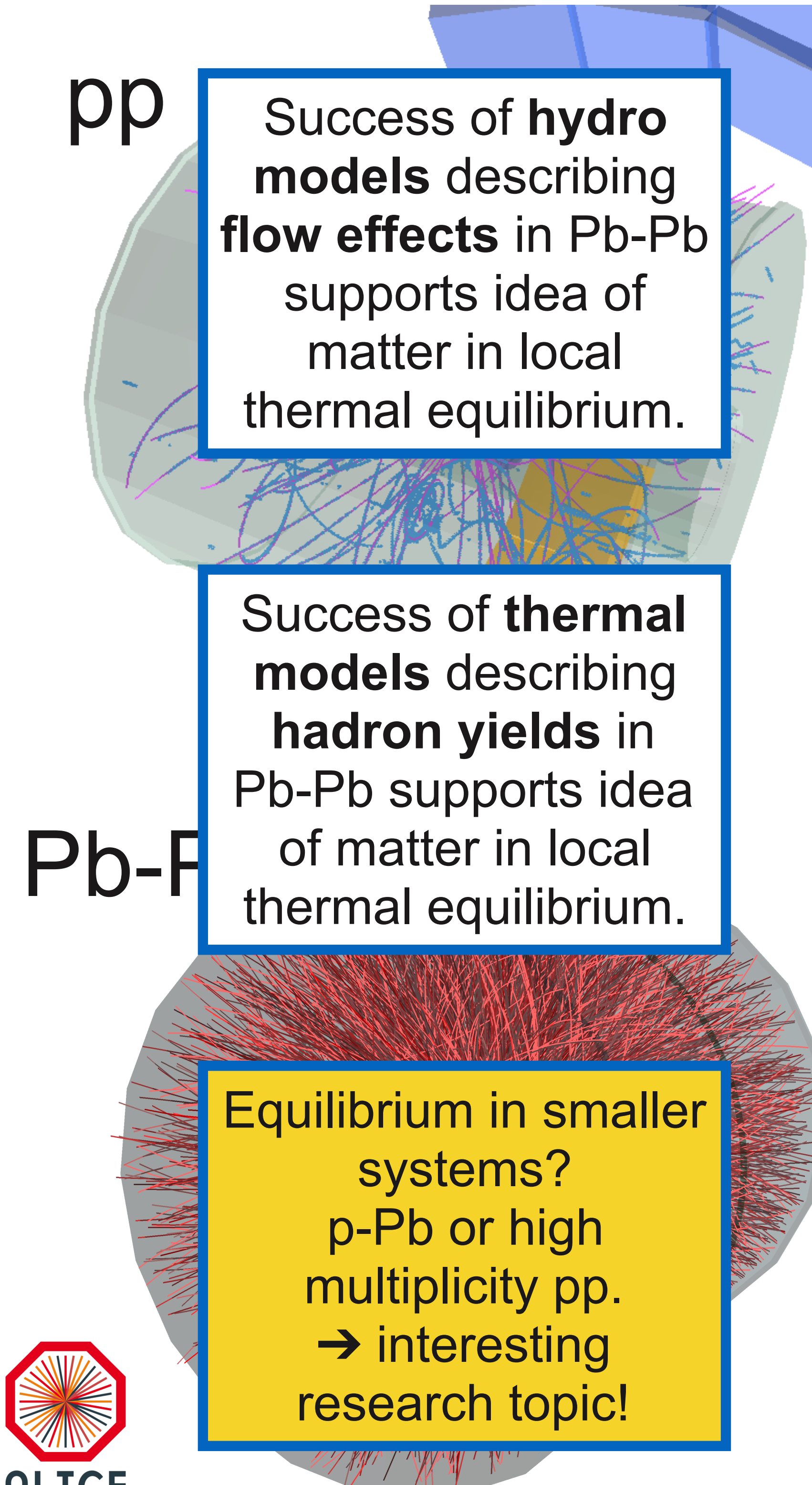

Success of **hydro models** describing **flow effects** in Pb-Pb supports idea of matter in local thermal equilibrium.

Success of **thermal models** describing **hadron yields** in Pb-Pb supports idea of matter in local thermal equilibrium.

Equilibrium in smaller systems?
p-Pb or high multiplicity pp.
➔ interesting research topic!

ALICE
A JOURNEY OF DISCOVERY

Radial and elliptic flow

ALICE

Isotropic radial flow

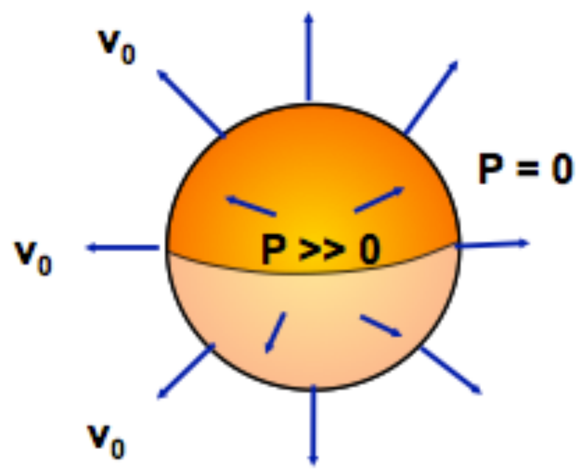

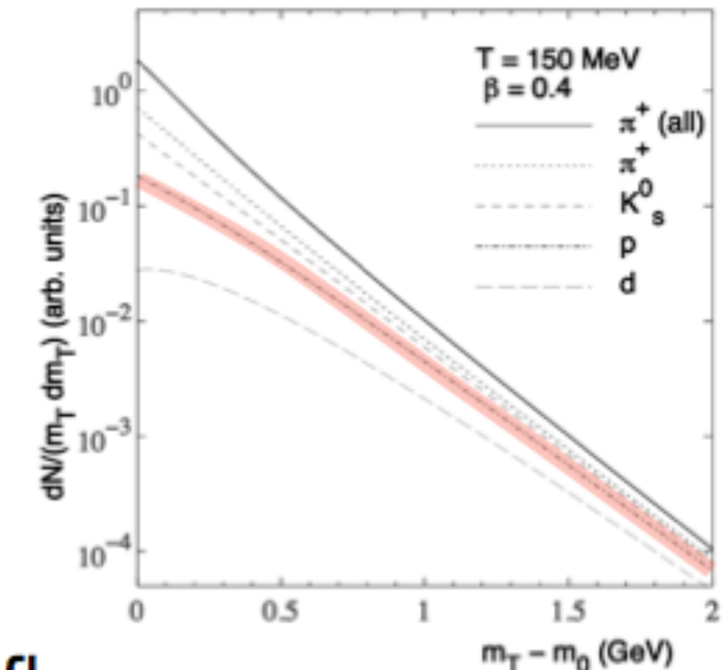

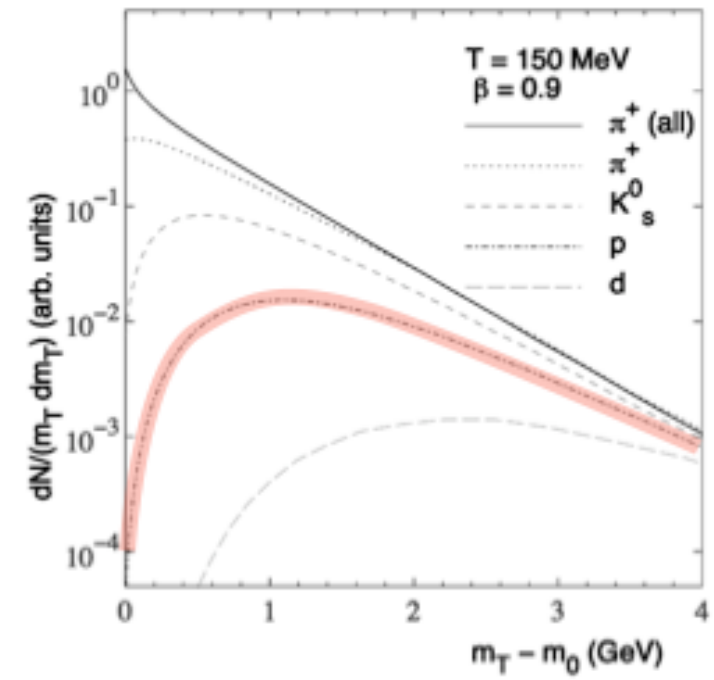

Anisotropic (elliptic) flow

Spatial deformation

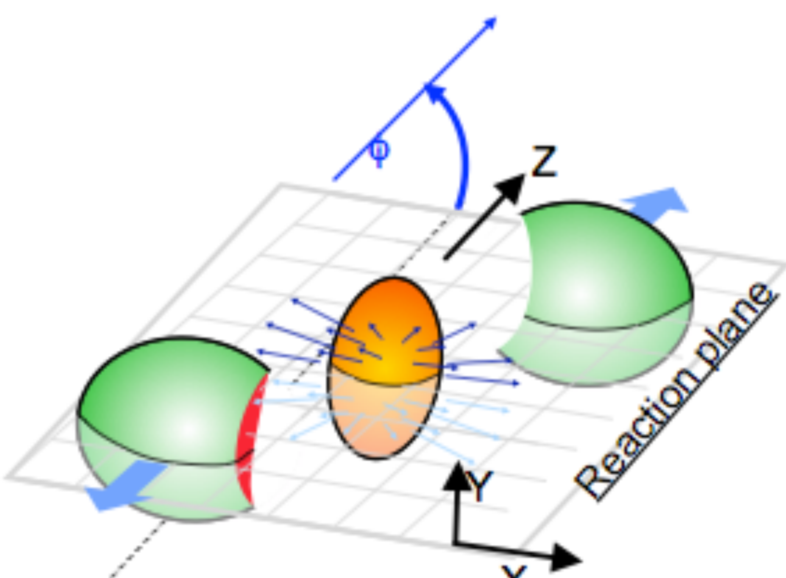

Azimuthal (φ) pressure gradients

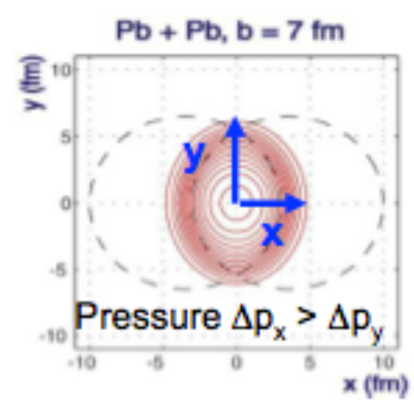

Anisotropic particle density

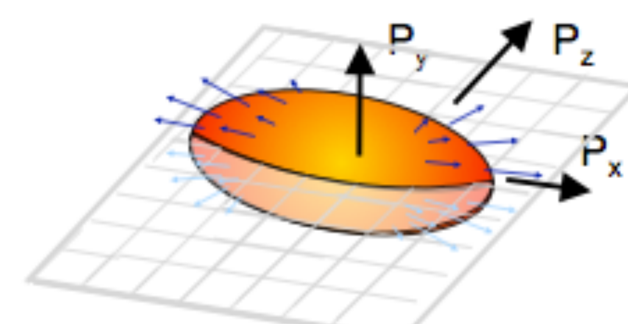

$$\frac{dN}{d\varphi} \propto 1 + 2v_1\cos[\varphi - \Psi_1] + 2v_2\cos[2(\varphi - \Psi_2)] + 2v_3\cos[3(\varphi - \Psi_3)] + \ldots$$

Collectivity and thermal equilibrium in Pb-Pb collisions

Anisotropic flow of identified particles

ALICE

- Clean mass ordering observed in the data.
- This is the expected behaviour from hydrodynamics: p = m · βγ.

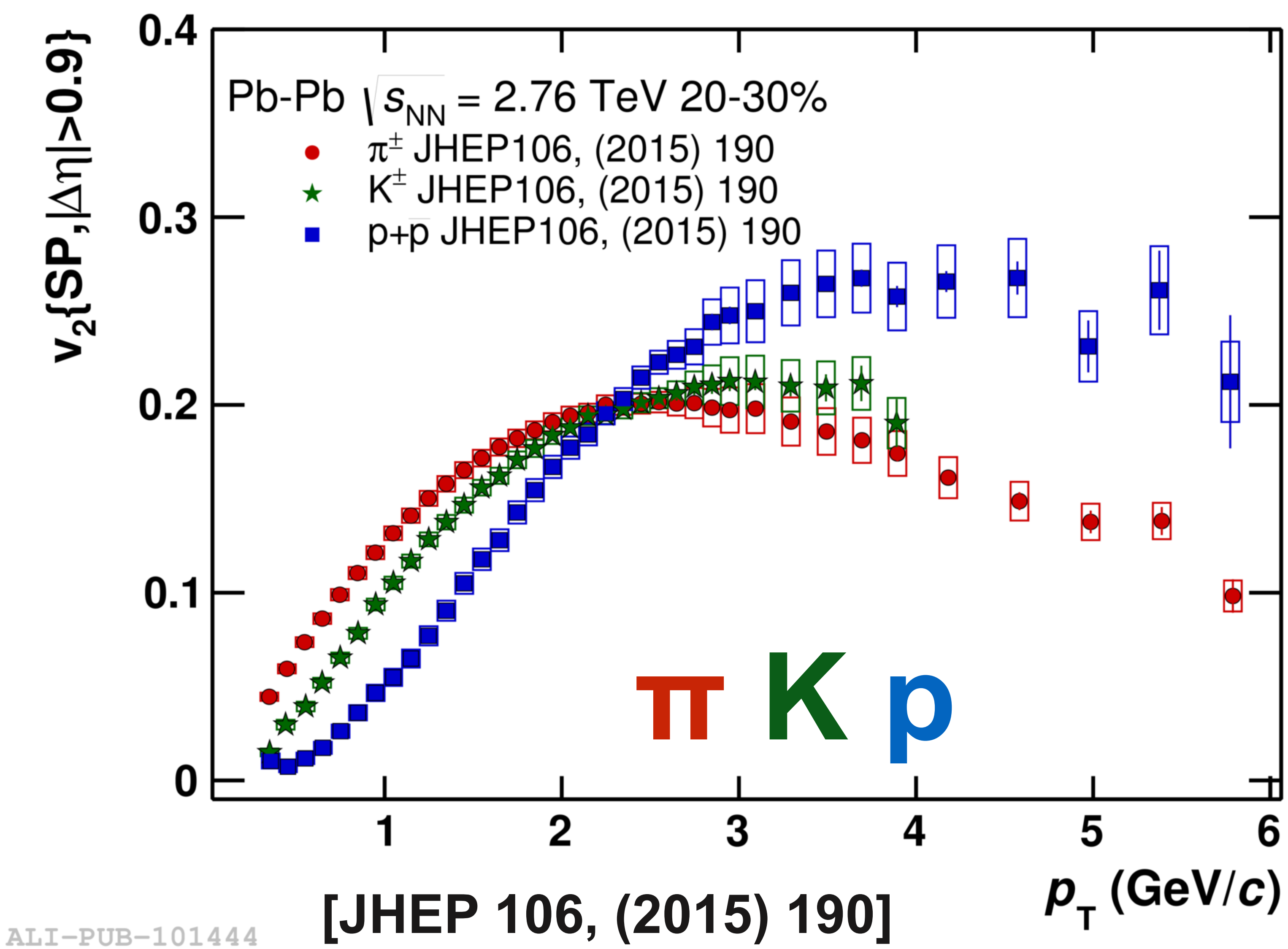

[JHEP 106, (2015) 190]

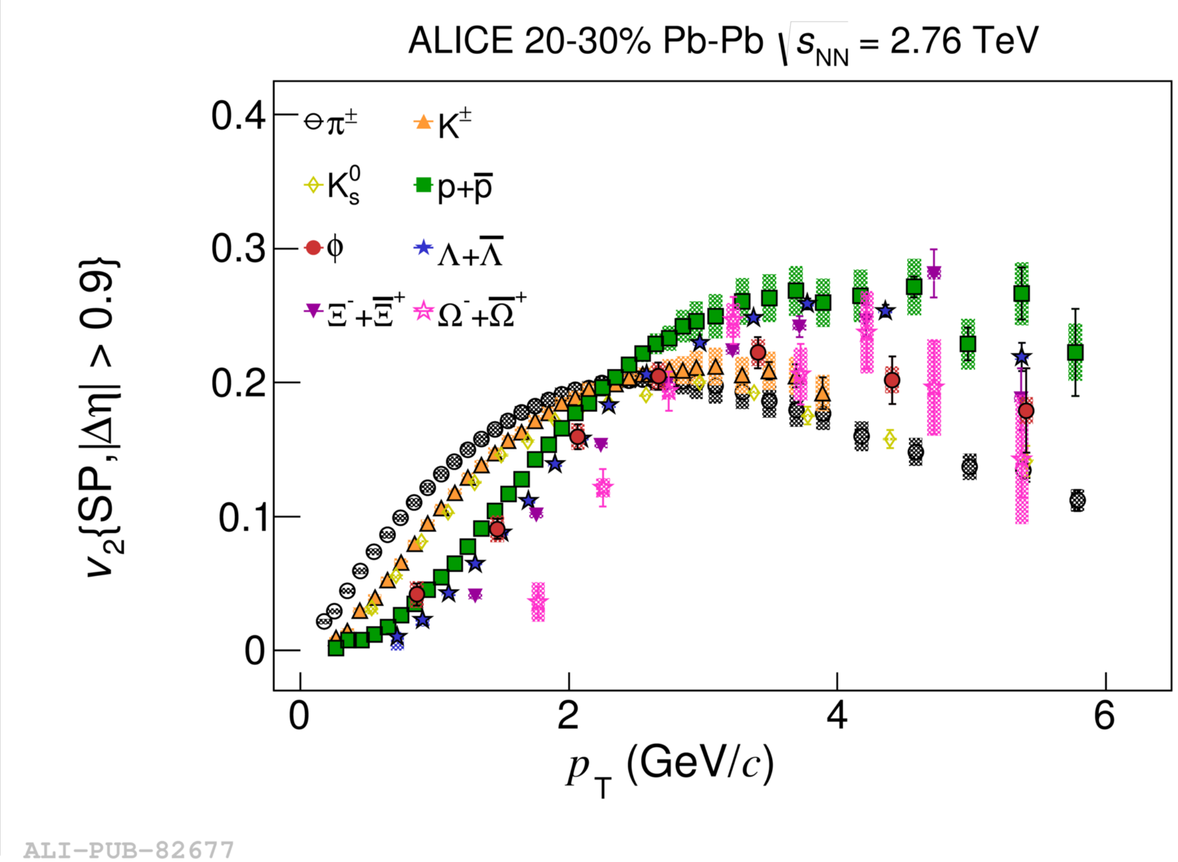

Radial flow in Pb-Pb

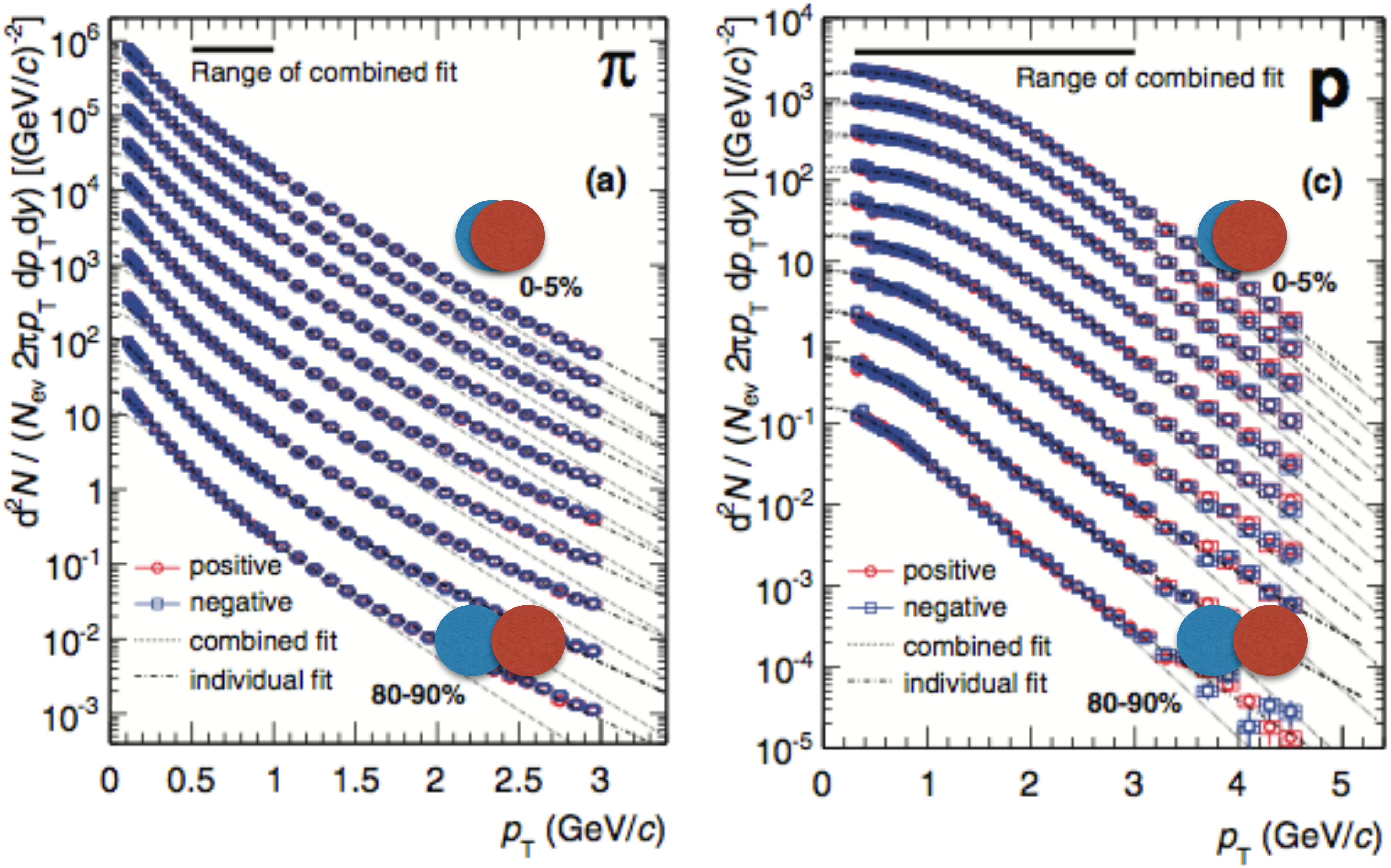

[Phys. Rev. C 88, 044910 (2013)]

Radial flow in Pb-Pb

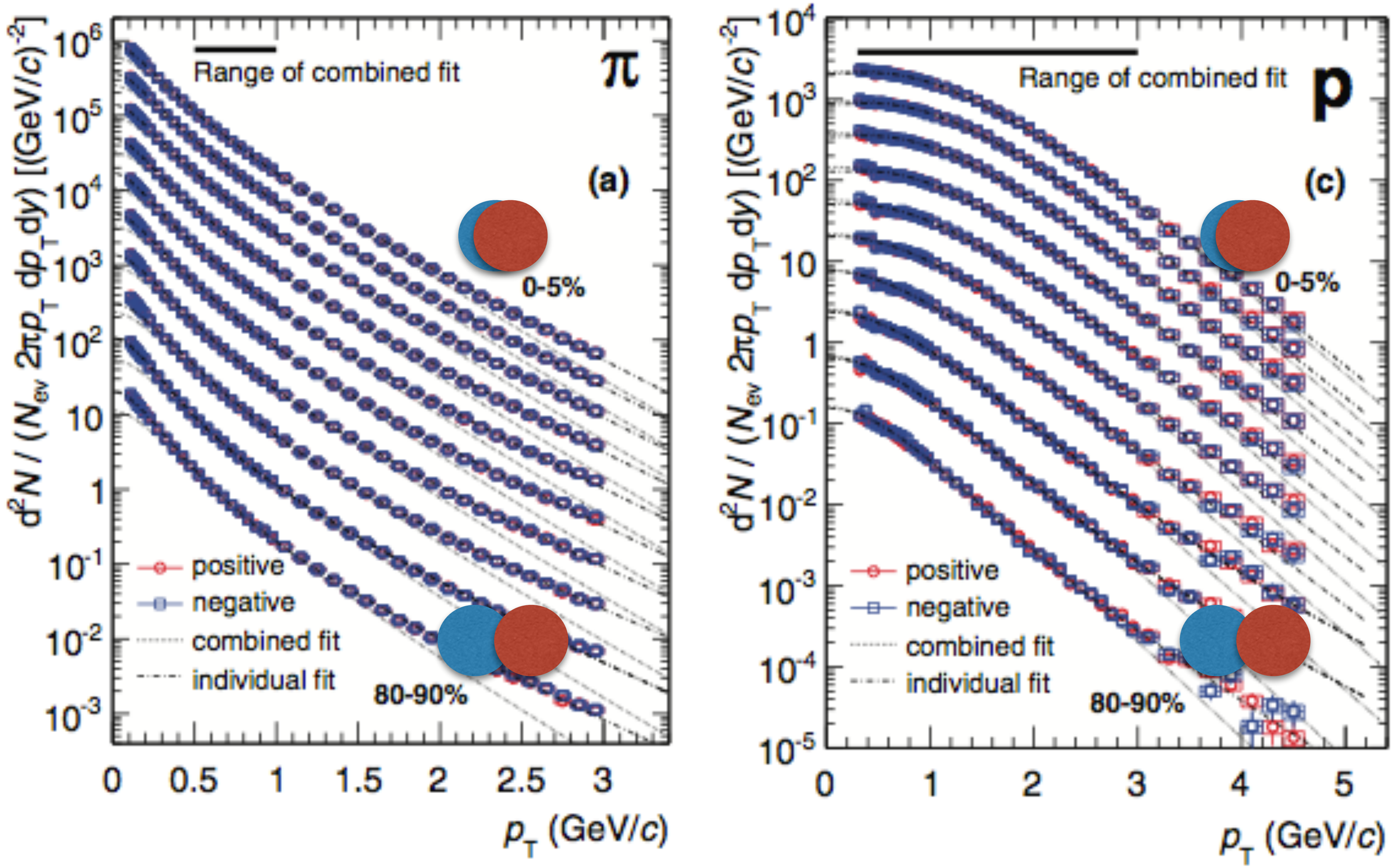

Characteristic hardening of the spectrum with increasing centrality. It is more pronounced for the heavier protons than for pions.
→ *Mass ordering* as expected from hydrodynamics.

[Phys. Rev. C 88, 044910 (2013)]

Radial flow in Pb-Pb

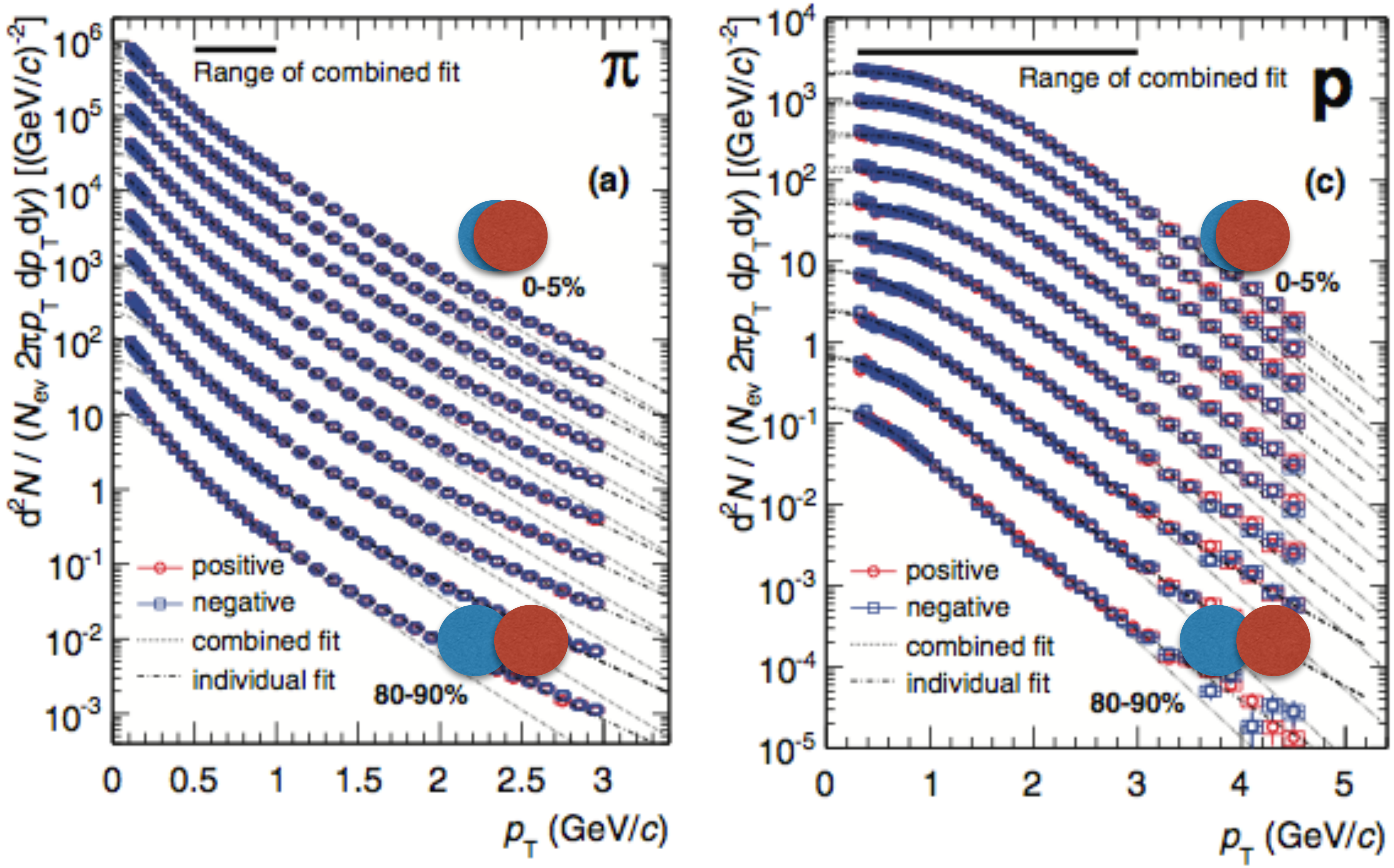

[Phys. Rev. C 88, 044910 (2013)]

Characteristic hardening of the spectrum with increasing centrality. It is more pronounced for the heavier protons than for pions.
→ *Mass ordering* as expected from hydrodynamics.

Very clean signature of radial flow in Pb-Pb collisions.

Radial flow in Pb-Pb

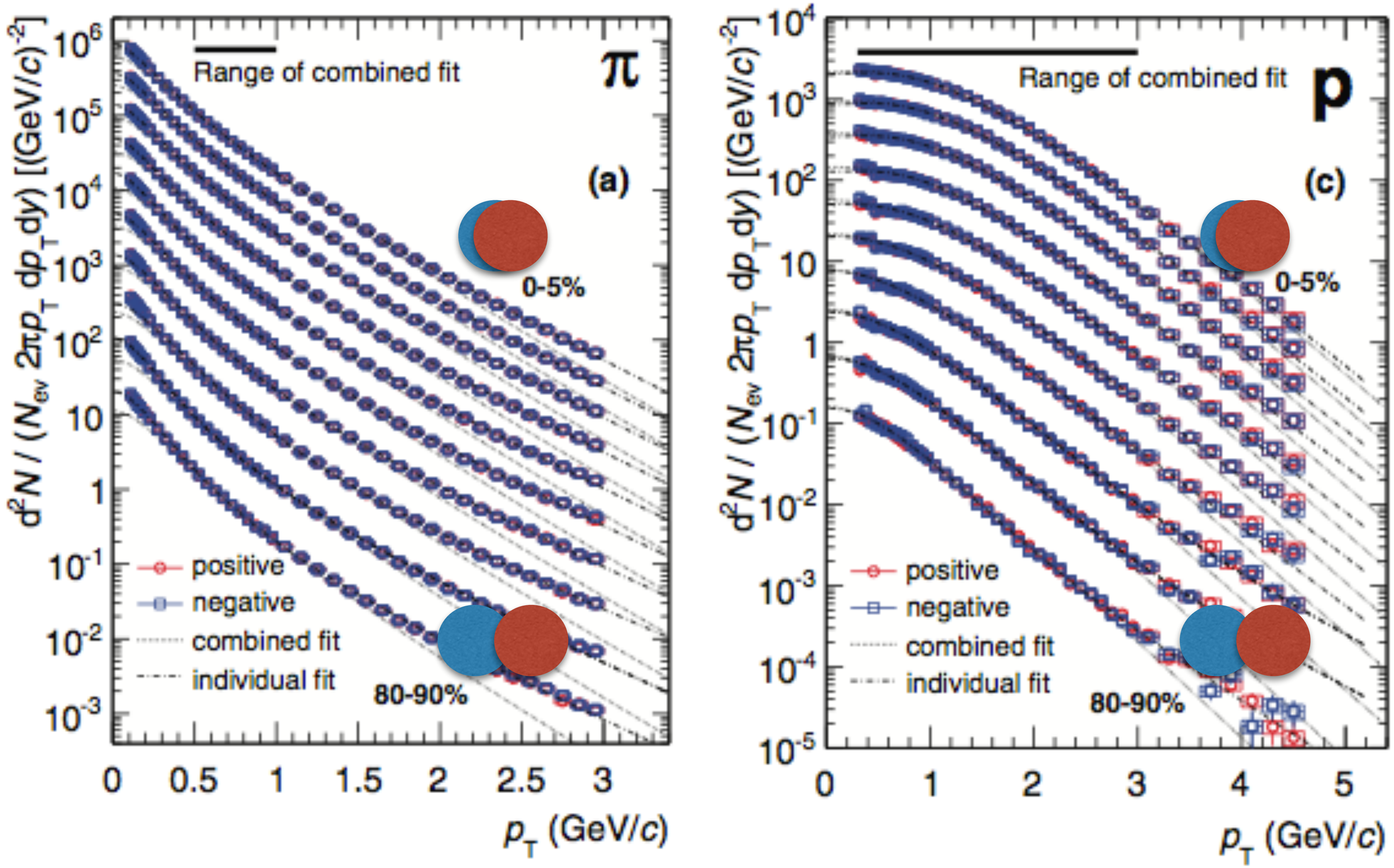

[Phys. Rev. C 88, 044910 (2013)]

Characteristic hardening of the spectrum with increasing centrality. It is more pronounced for the heavier protons than for pions. → *Mass ordering* as expected from hydrodynamics.

Very clean signature of radial flow in Pb-Pb collisions.

Full hydro models describe spectra fairly well.

Radial flow in Pb-Pb

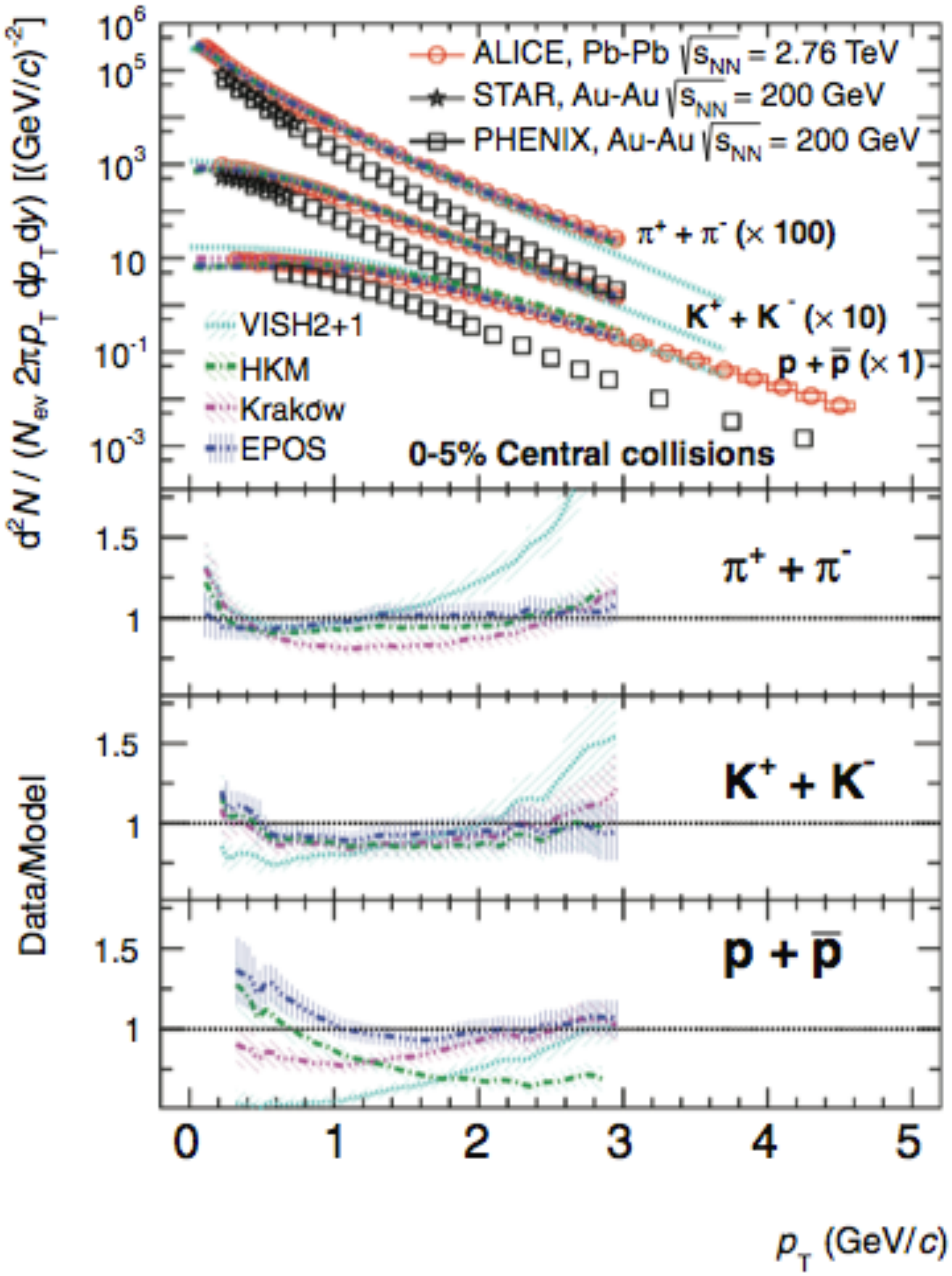

Characteristic hardening of the spectrum with increasing centrality. It is more pronounced for the heavier protons than for pions.
→ *Mass ordering* as expected from hydrodynamics.

Very clean signature of radial flow in Pb-Pb collisions.

Full hydro models describe spectra fairly well.

Radial flow in Pb-Pb

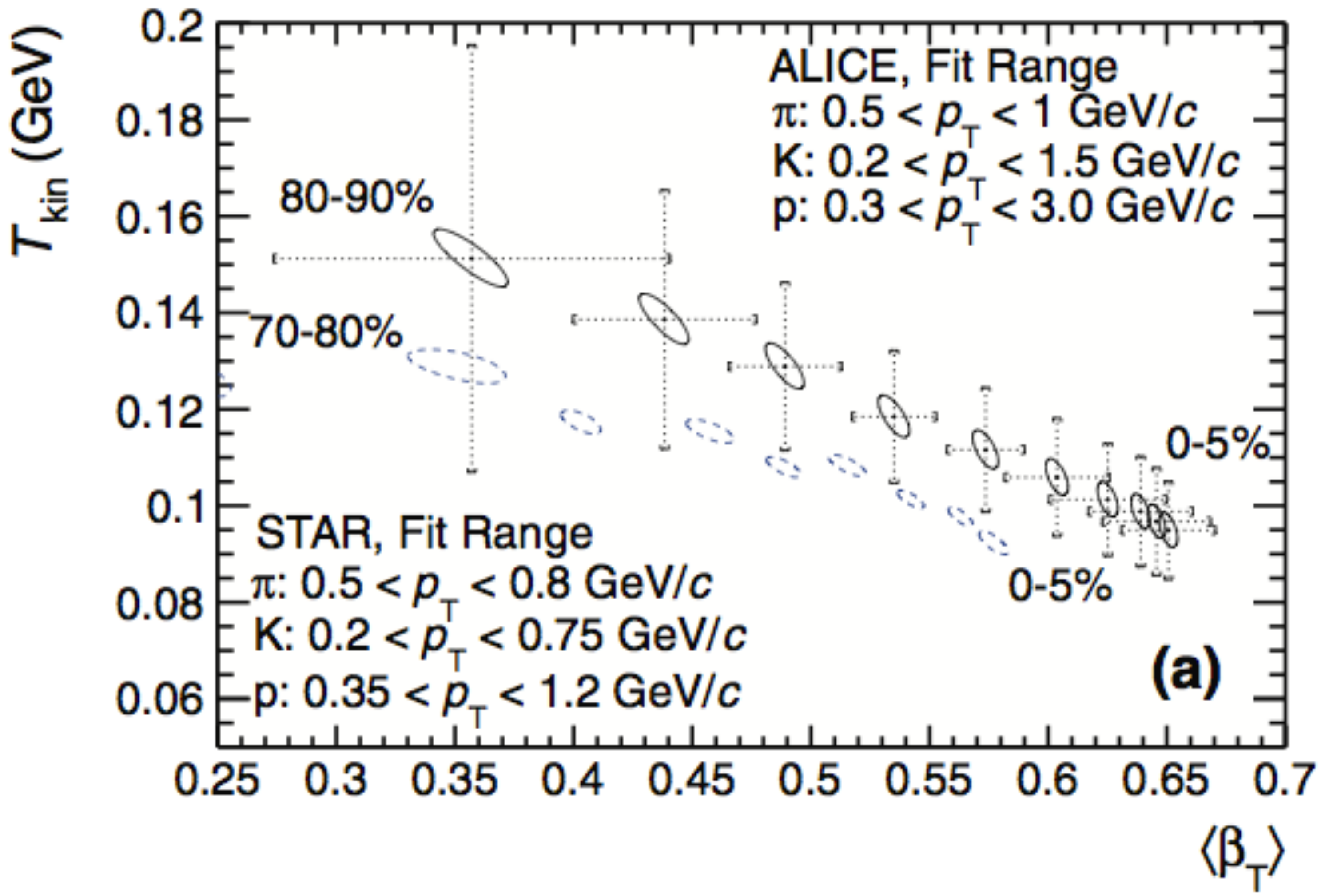

Characteristic hardening of the spectrum with increasing centrality. It is more pronounced for the heavier protons than for pions.
→ *Mass ordering* as expected from hydrodynamics.

Very clean signature of radial flow in Pb-Pb collisions.

Full hydro models describe spectra fairly well.

Radial flow in Pb-Pb

ALICE

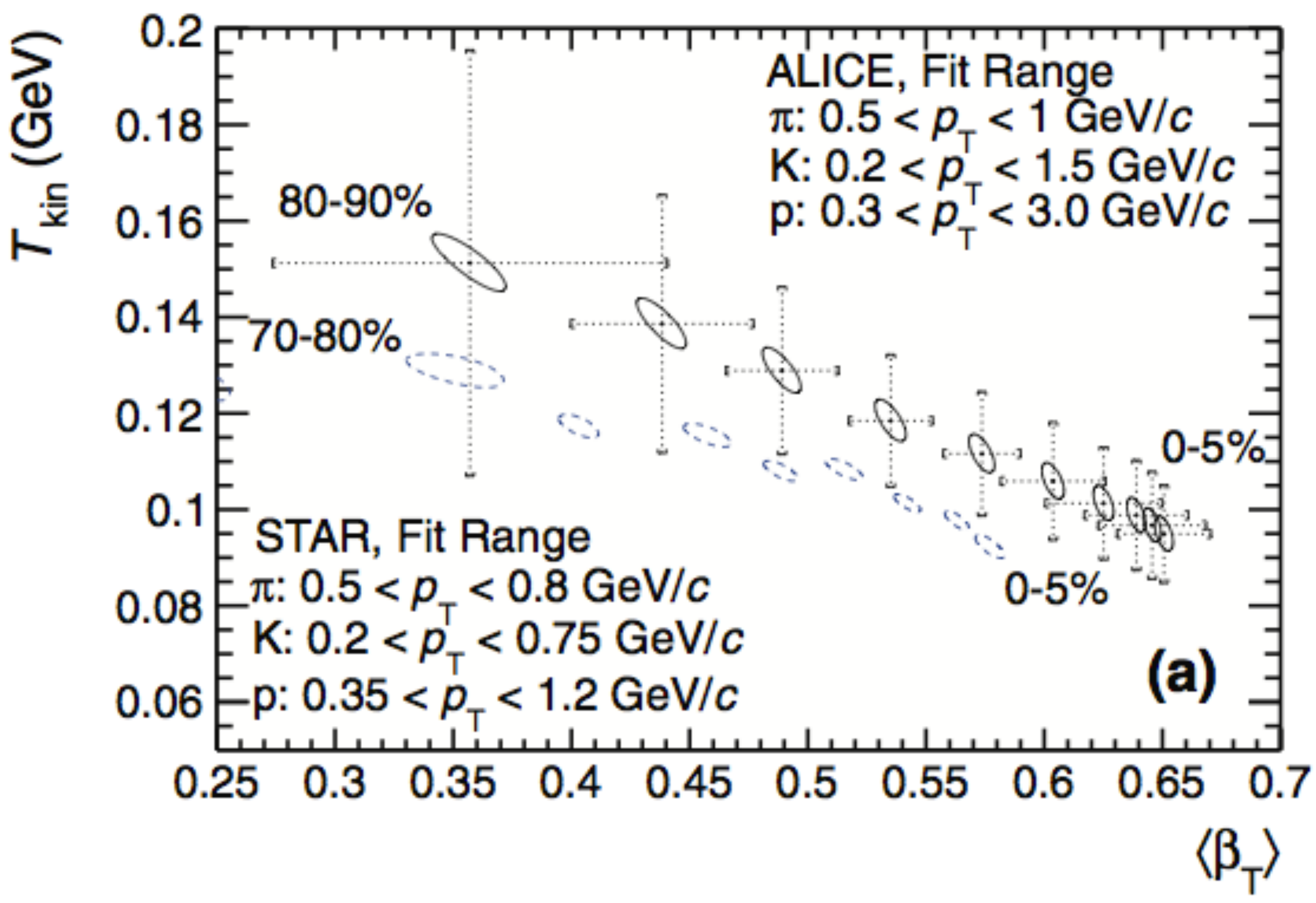

Characteristic hardening of the spectrum with increasing centrality. It is more pronounced for the heavier protons than for pions. → *Mass ordering* as expected from hydrodynamics.

Very clean signature of radial flow in Pb-Pb collisions.

Full hydro models describe spectra fairly well.

A combined blast-wave fit to the data (**simplified hydro model** → T_{kin}, β) gives also a reasonable description allowing a systematic study of the evolution of the spectral shape versus centrality.

Radial flow in Pb-Pb

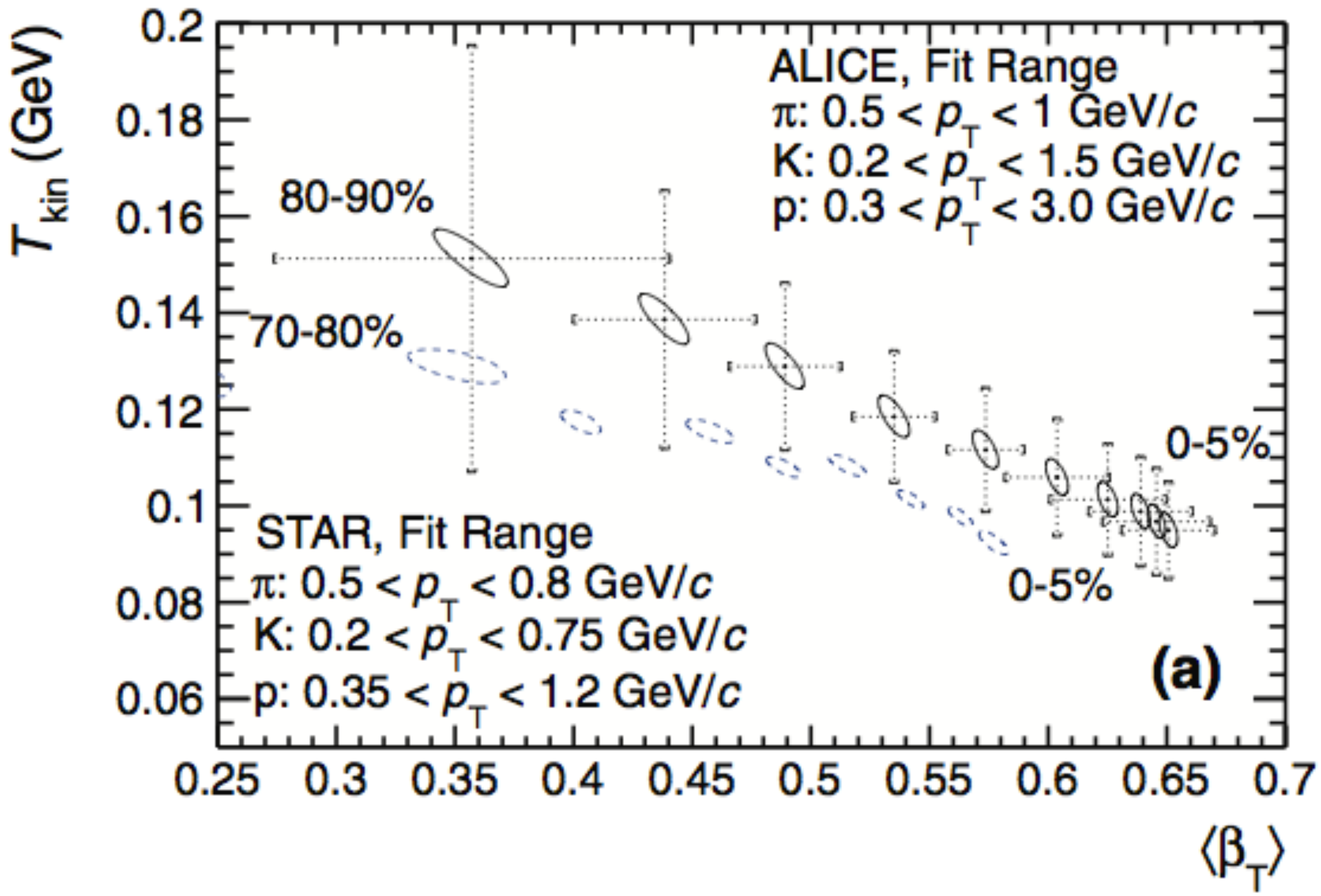

Within the severe limitations of the blast-wave model one finds: T_{kin} ≈ 100 MeV significantly smaller than T_{chem} ≈ 156 MeV and an average transverse expansion velocity around $<\beta_T>$ 0.65 for most central Pb-Pb collisions.

Characteristic hardening of the spectrum with increasing centrality. It is more pronounced for the heavier protons than for pions. → *Mass ordering* as expected from hydrodynamics.

Very clean signature of radial flow in Pb-Pb collisions.

Full hydro models describe spectra fairly well.

A combined blast-wave fit to the data (**simplified hydro model** → T_{kin}, β) gives also a reasonable description allowing a systematic study of the evolution of the spectral shape versus centrality.

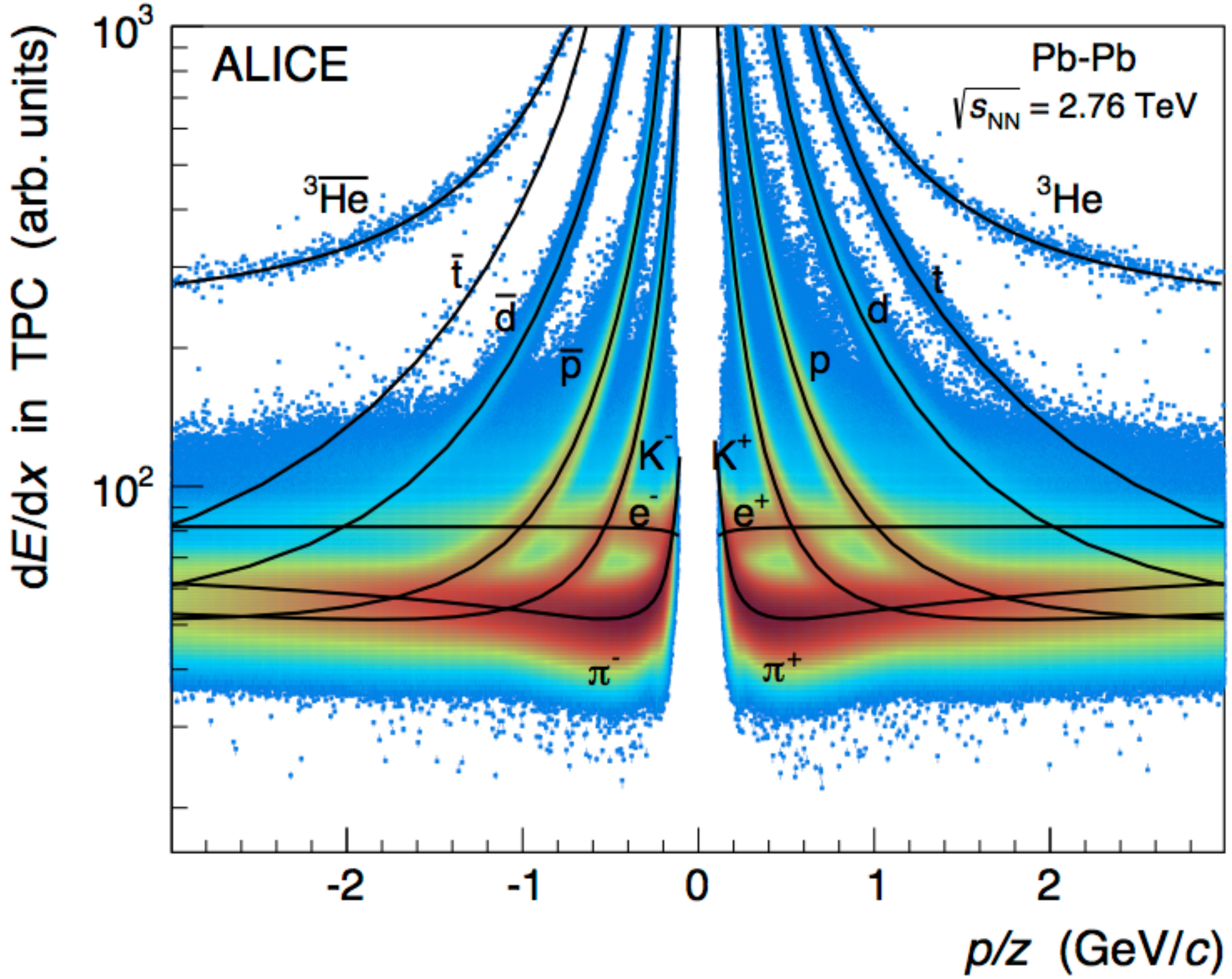

Collectivity and thermal equilibrium in Pb-Pb collisions with light (anti-)nuclei

Matter and anti-matter

Particle production in pp, p-Pb, and Pb-Pb collisions shows an equal abundance of matter and anti-matter in the central rapidity region: $\mu_B \approx 1$ MeV.

$$\frac{n_{\bar{p}}}{n_p} = e^{-(2\mu_B)/T} \qquad \frac{n_{^3\overline{He}}}{n_{^3He}} = e^{-(6\mu_B)/T}$$

[PRL 109, 252301 (2012)]

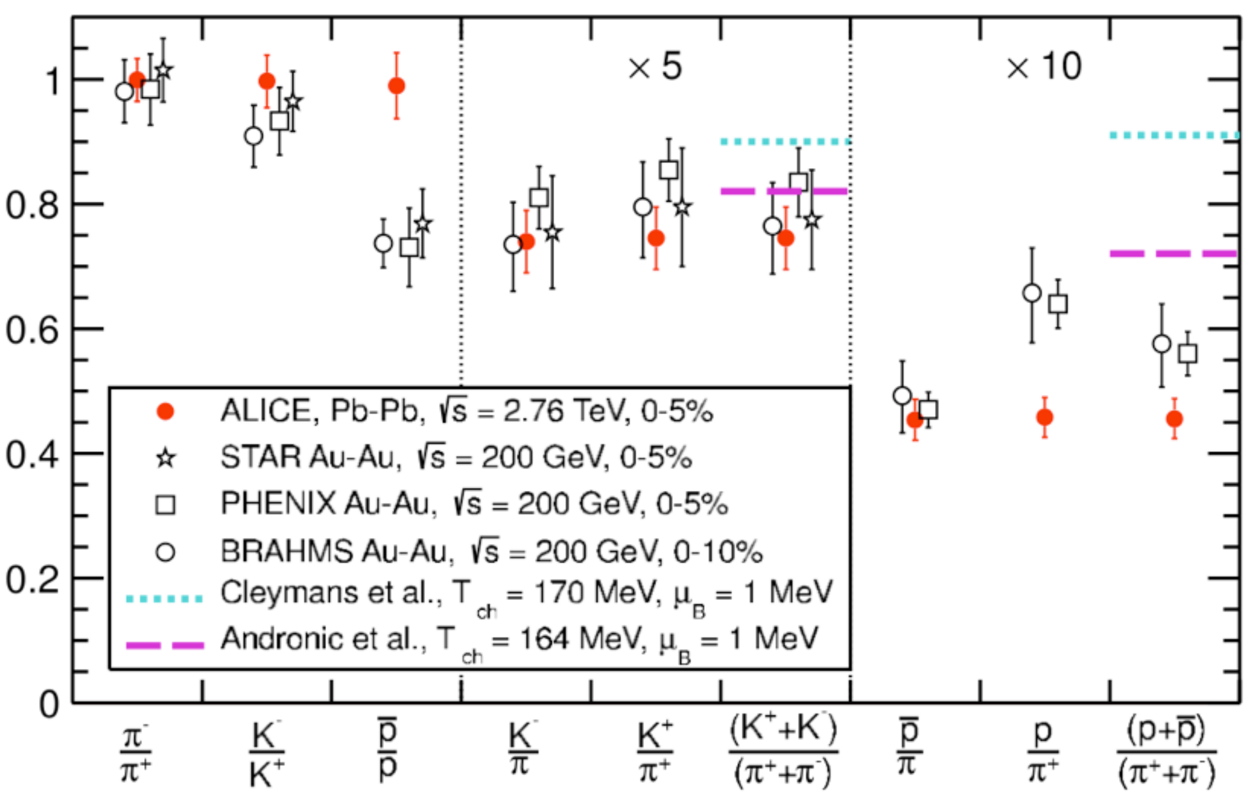

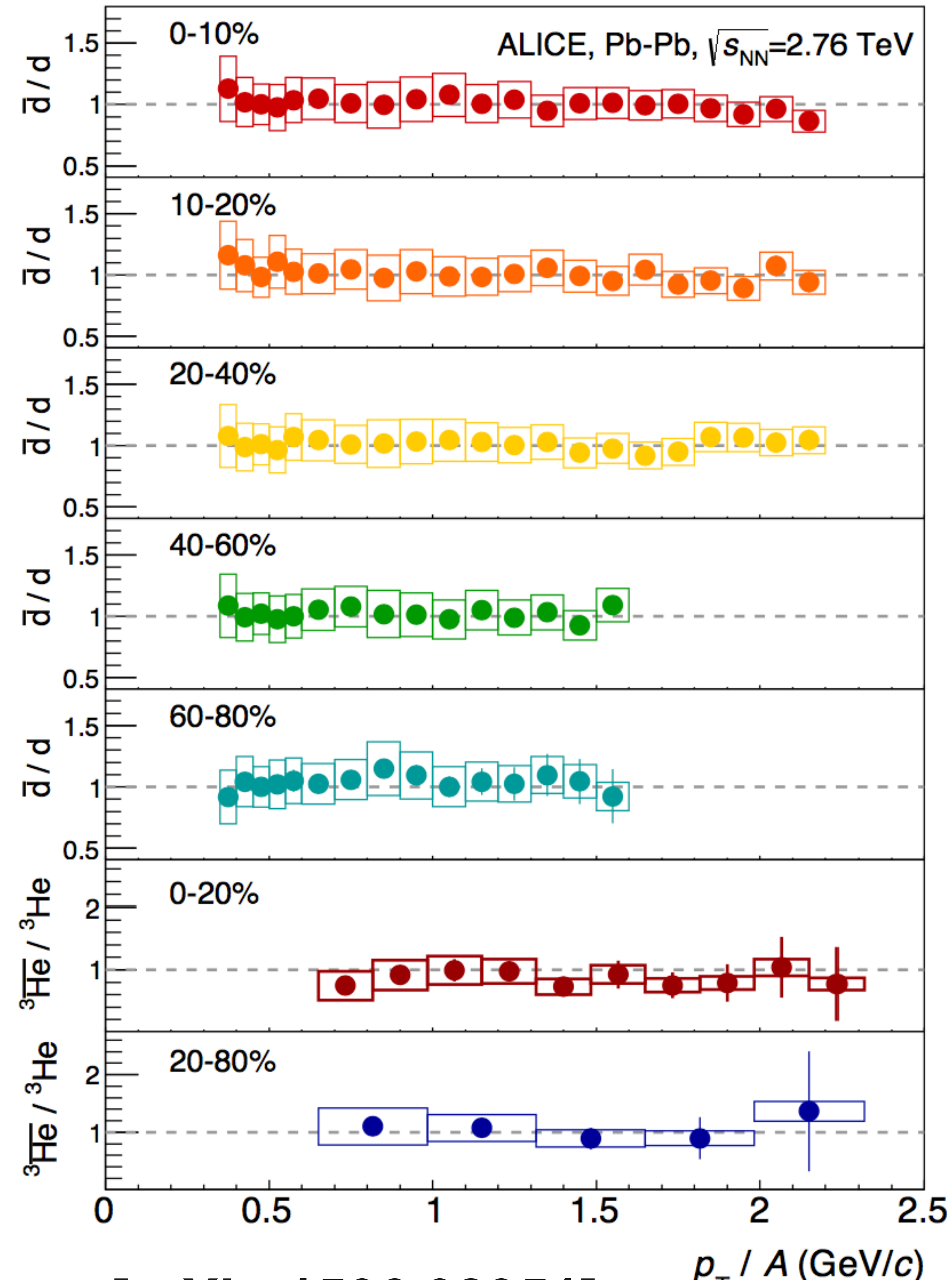

[arXiv:1506.08951]

Mass ordering

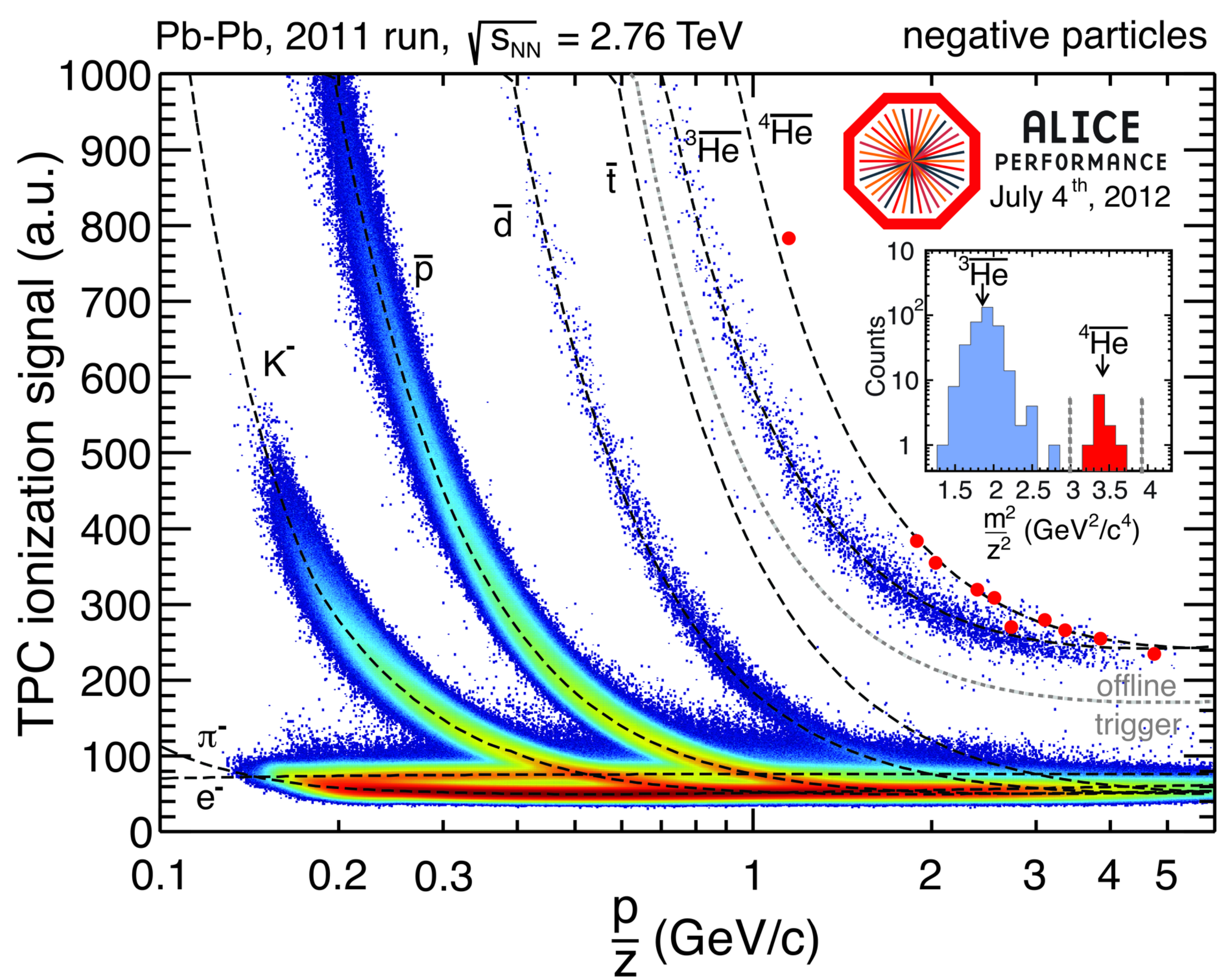

ALI-PERF-36713

Mass ordering

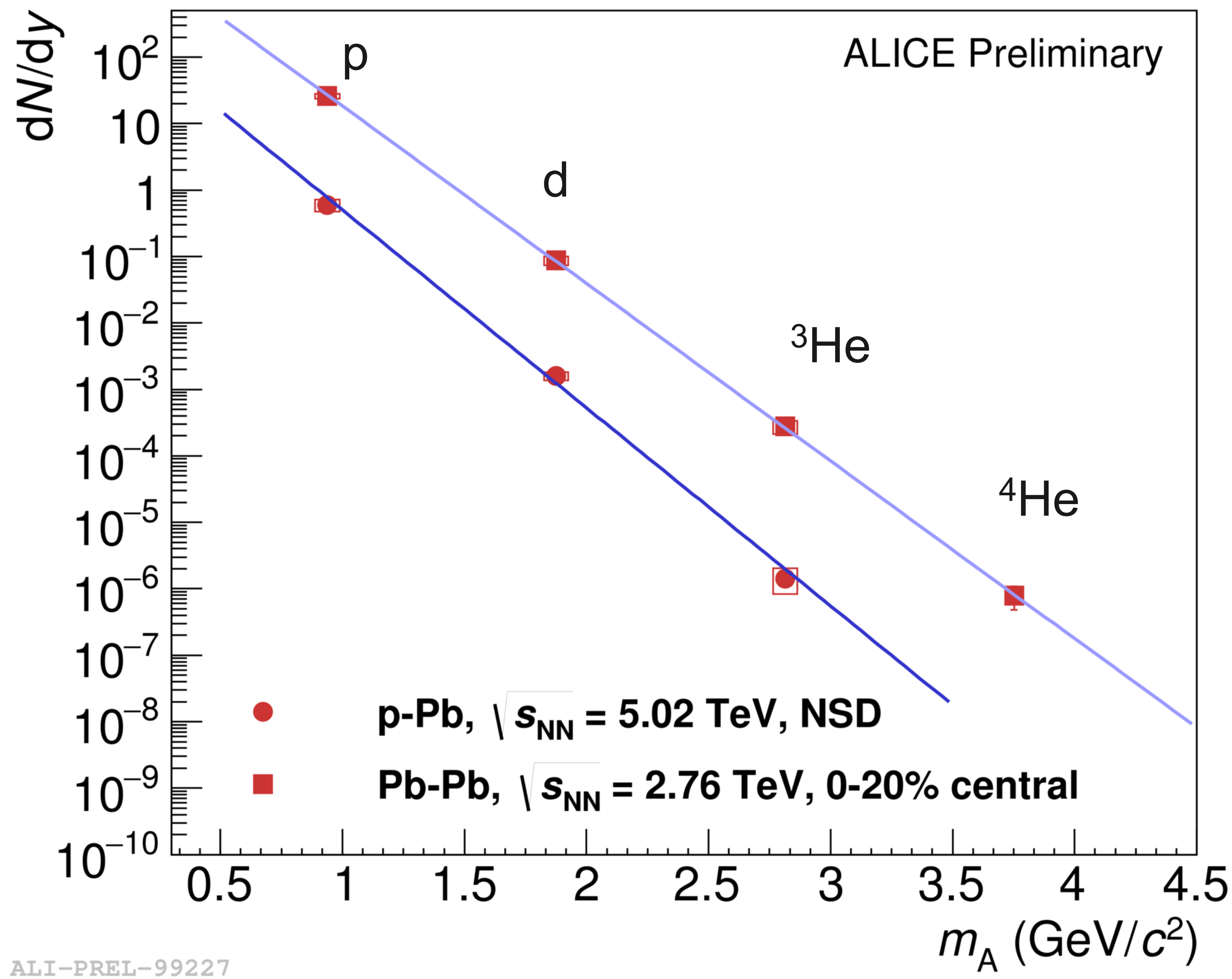

Mass ordering

For each additional nucleon the production yield decreases by a factor of about 300!

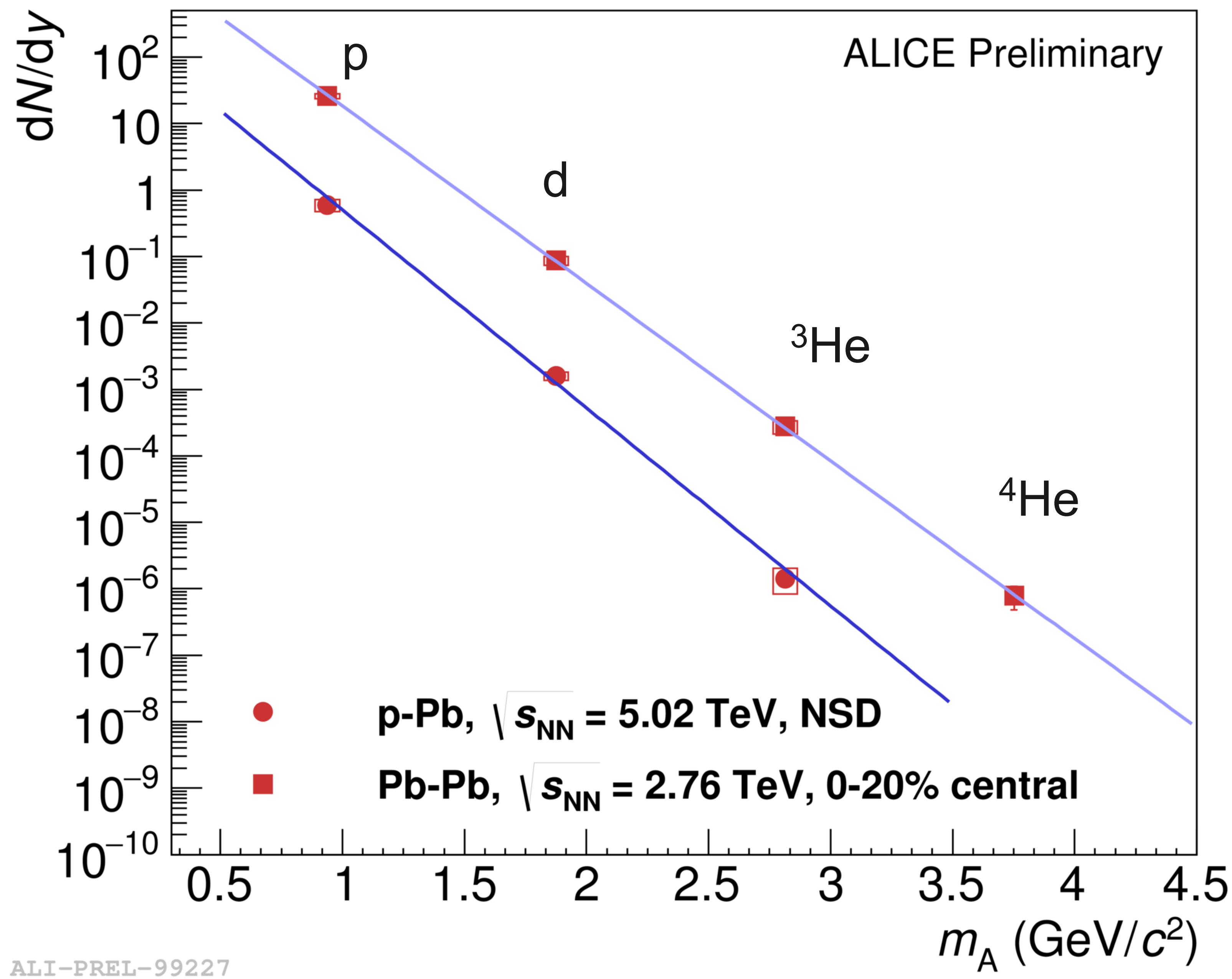

Mass ordering

For each additional nucleon the production yield decreases by a factor of about 300!

Such a behaviour can be directly derived from the thermal model which predicts in first order dN/dy ~ exp(-m/T)

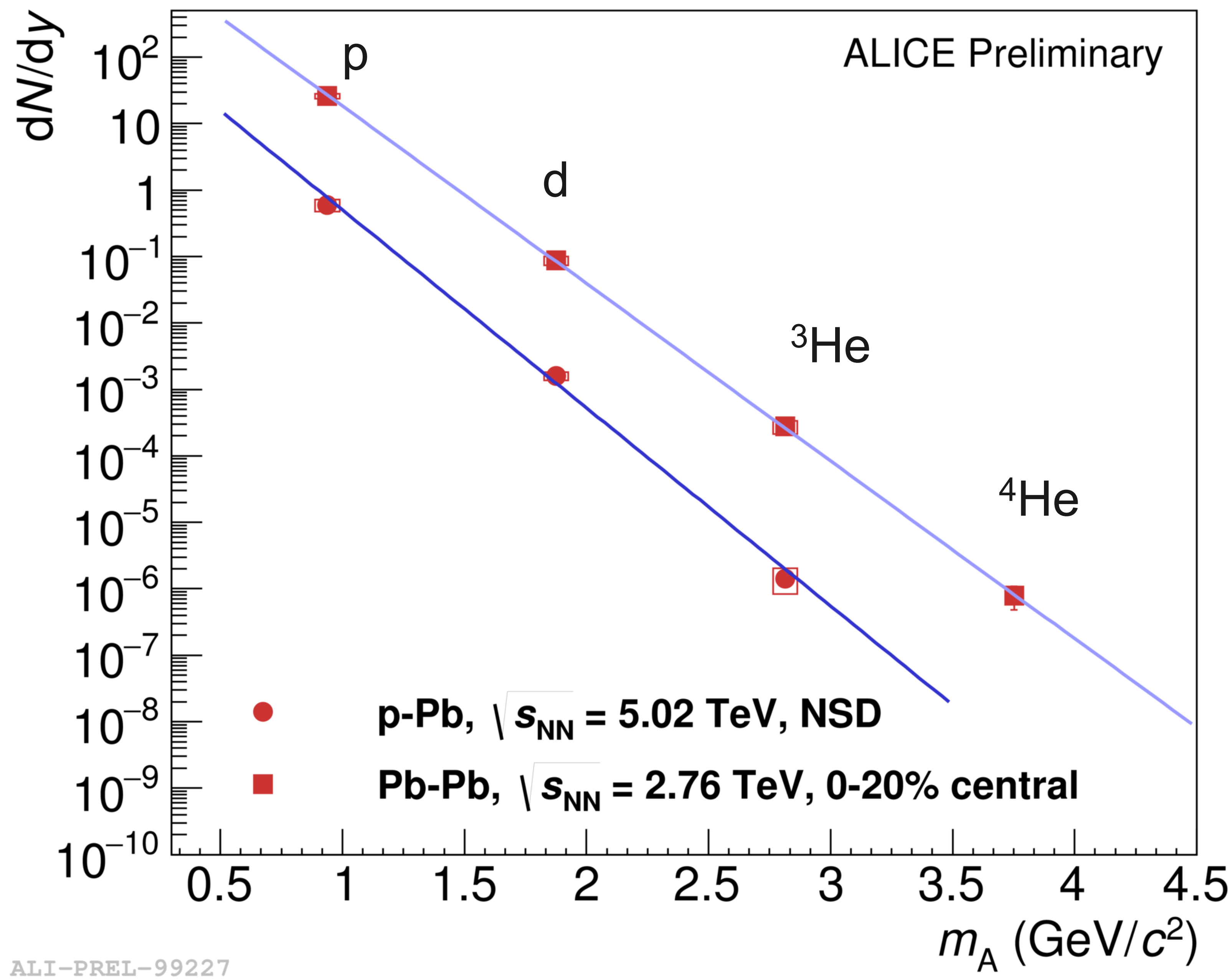

Side remark: CPT confirmation

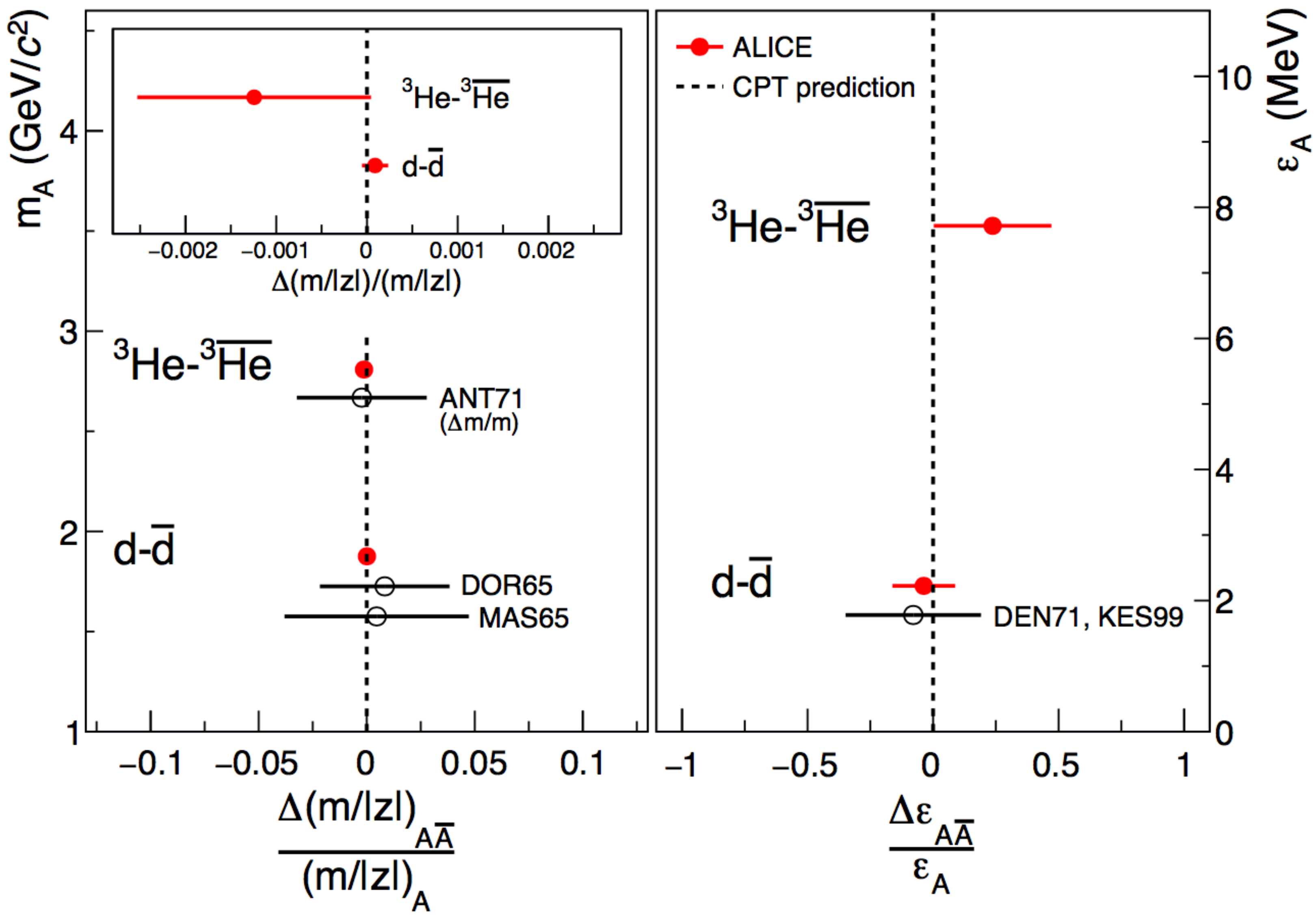

[Nature Physics 11 (2015) 811-814]

Side remark: CPT confirmation

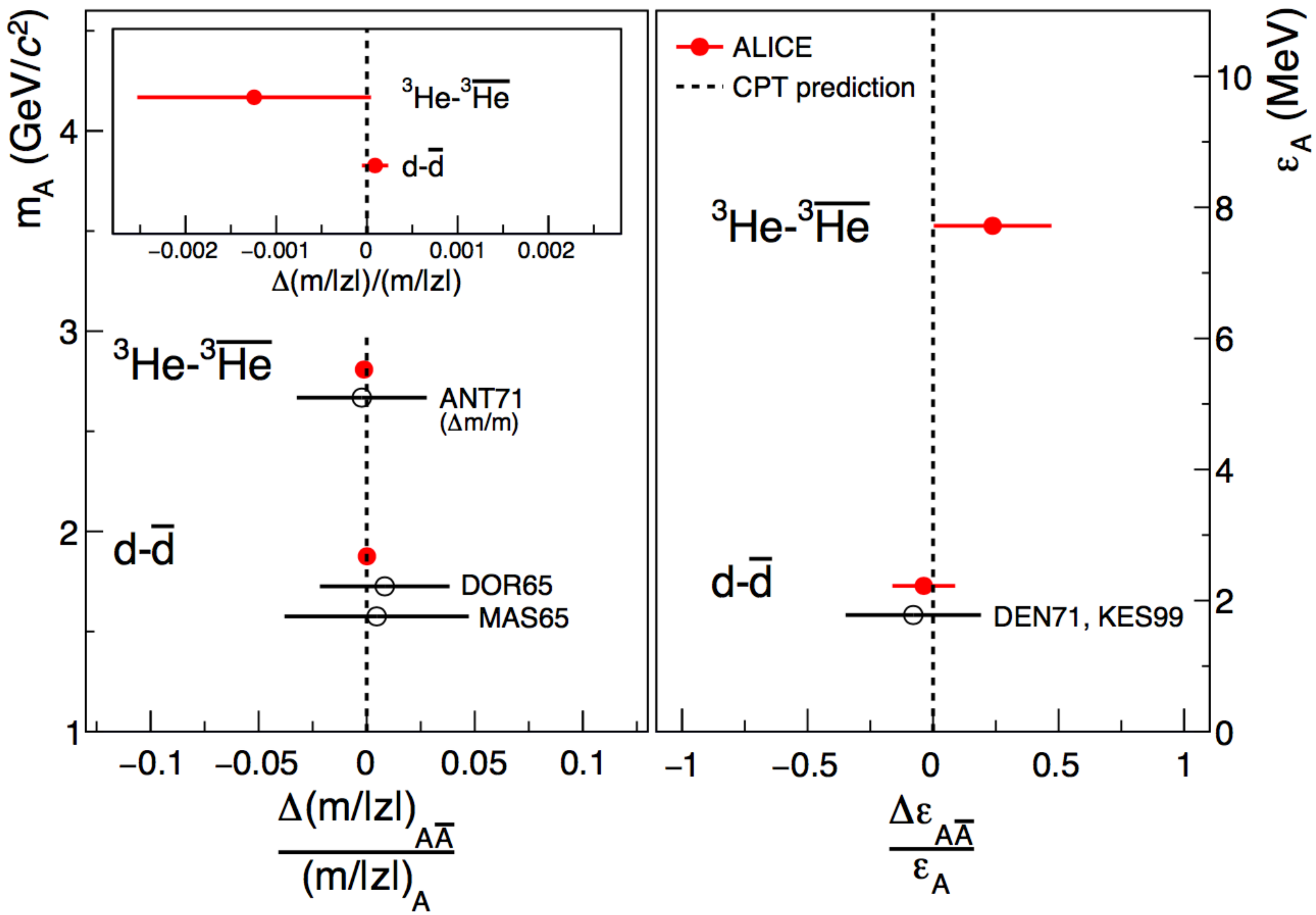

The ALICE collaboration performed a test of the CPT invariance looking at the mass difference between nuclei and anti-nuclei.

[Nature Physics 11 (2015) 811-814]

Side remark: CPT confirmation

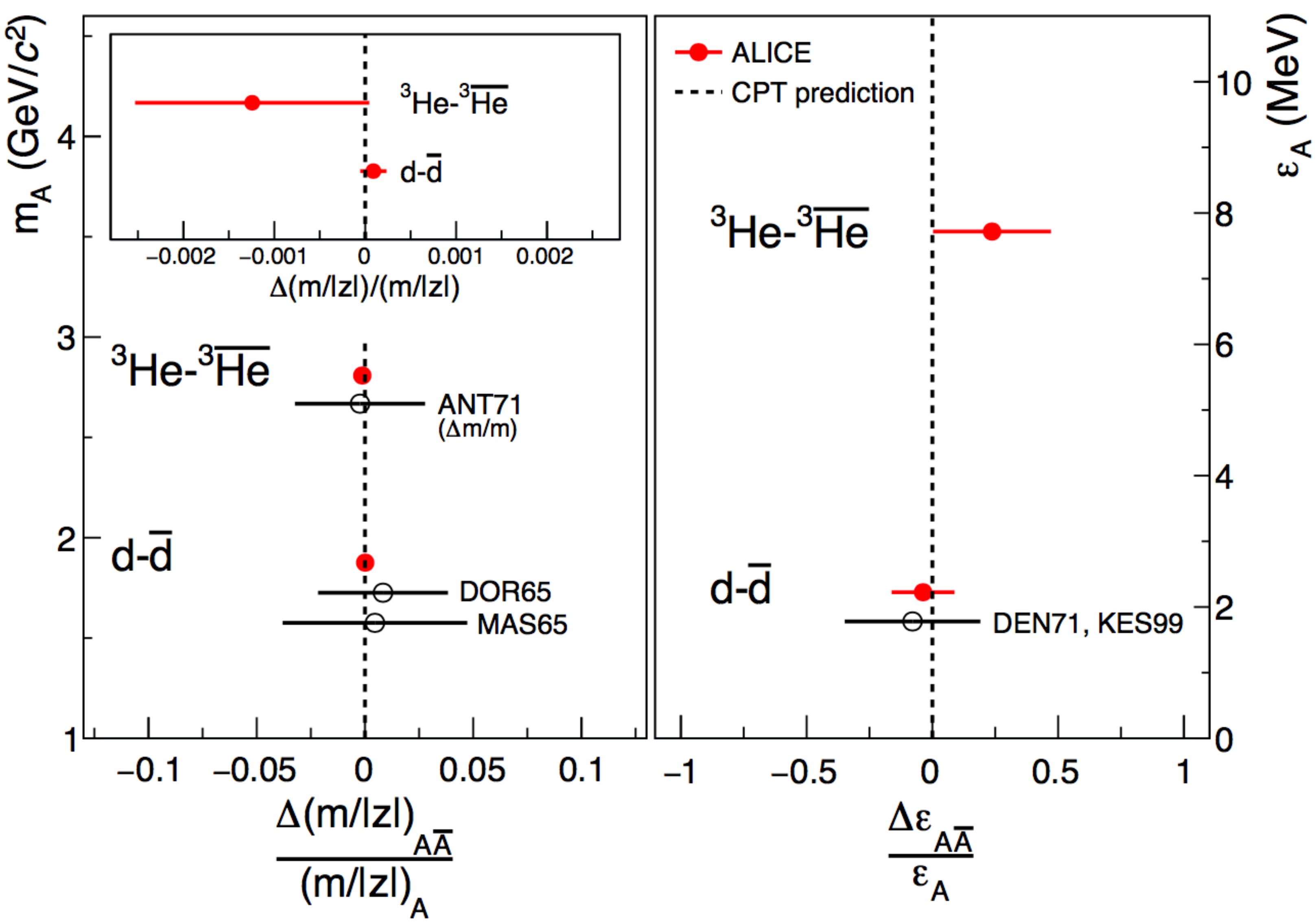

The ALICE collaboration performed a test of the CPT invariance looking at the mass difference between nuclei and anti-nuclei.

This test shows that the masses of nuclei and anti-nuclei are compatible within the uncertainties. The binding energies are compatible in nuclei and anti-nuclei as well.

[Nature Physics 11 (2015) 811-814]

Elliptic flow of (anti-)deuterons

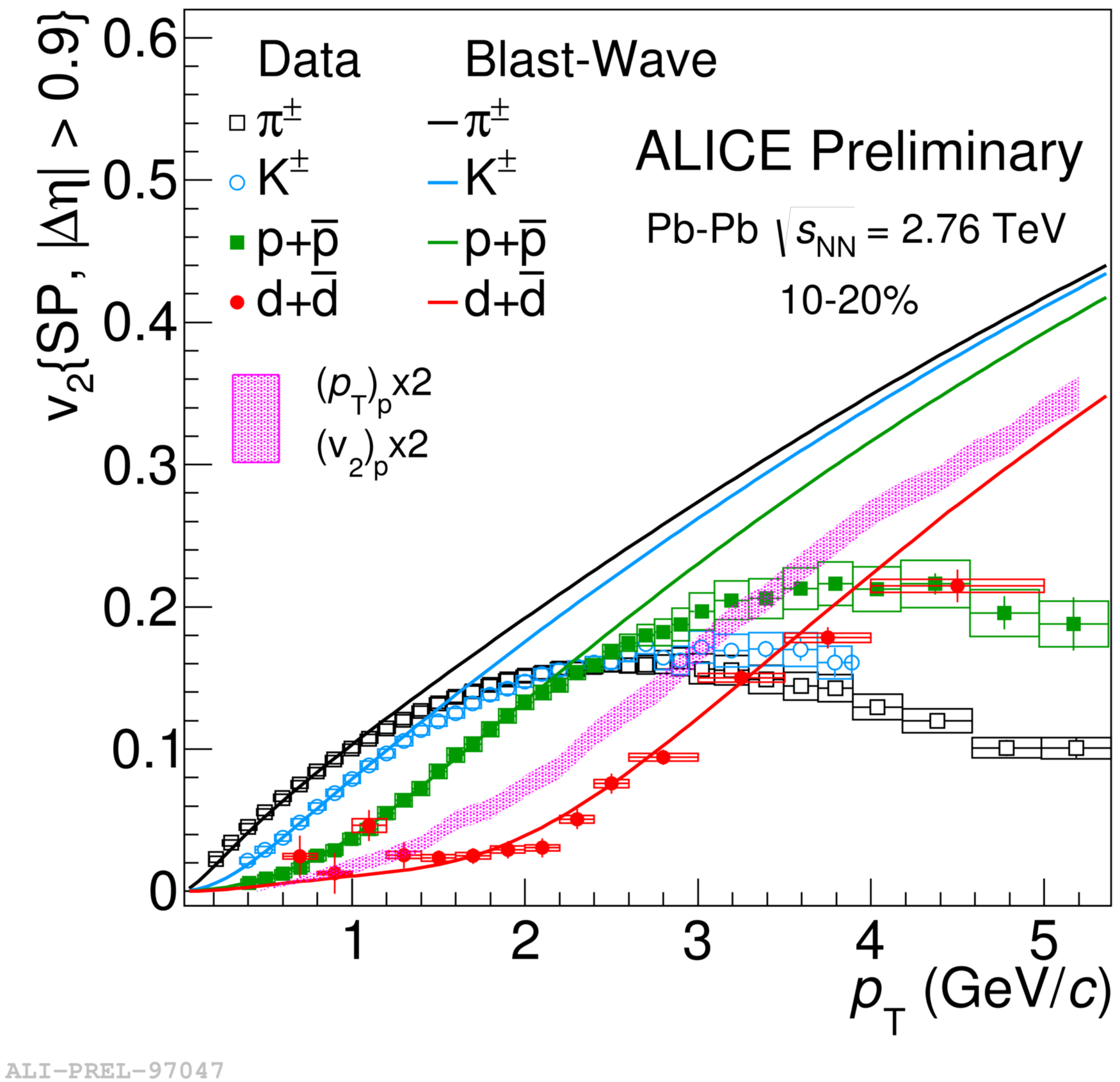

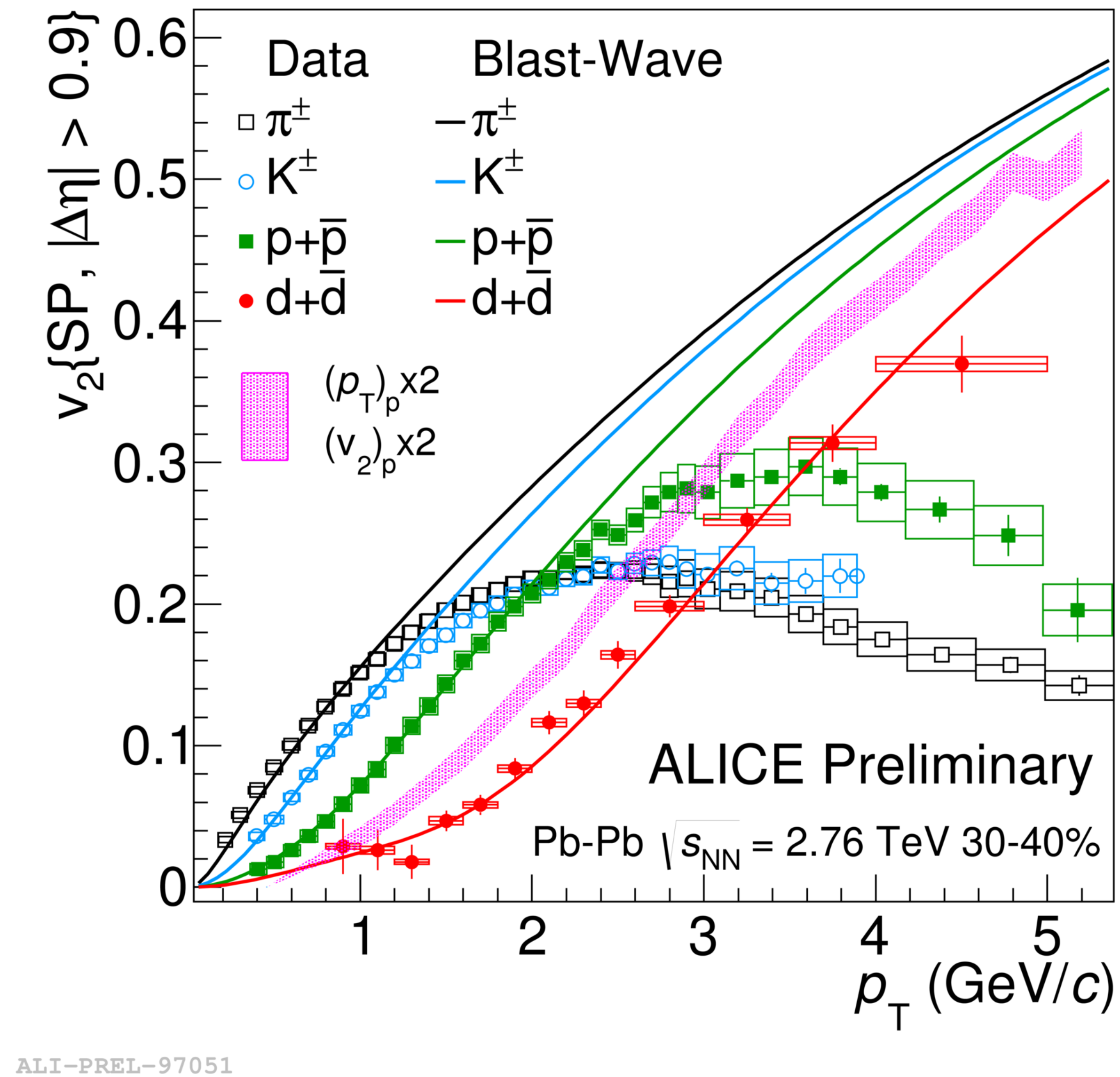

Elliptic flow of (anti-)deuterons

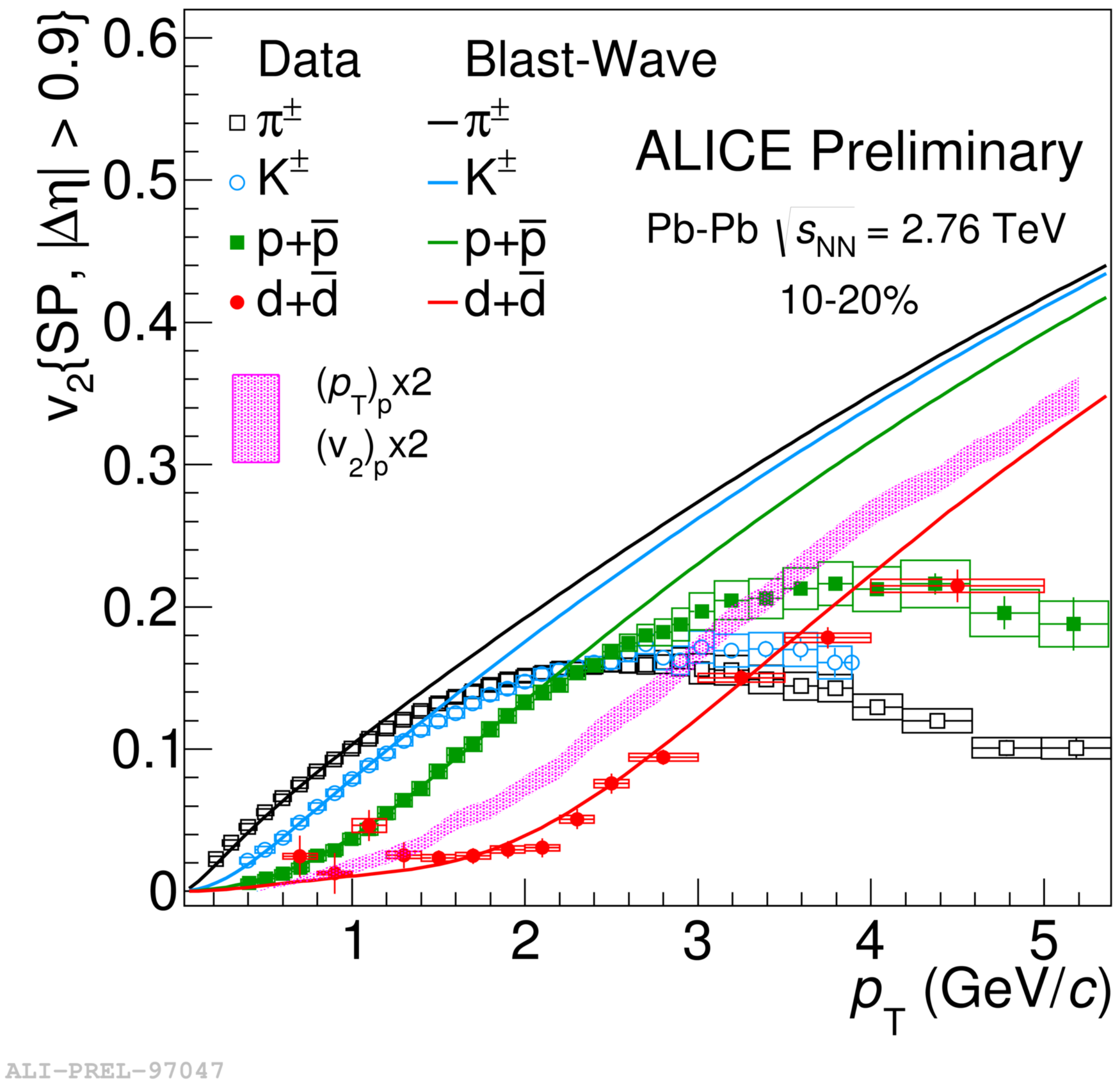

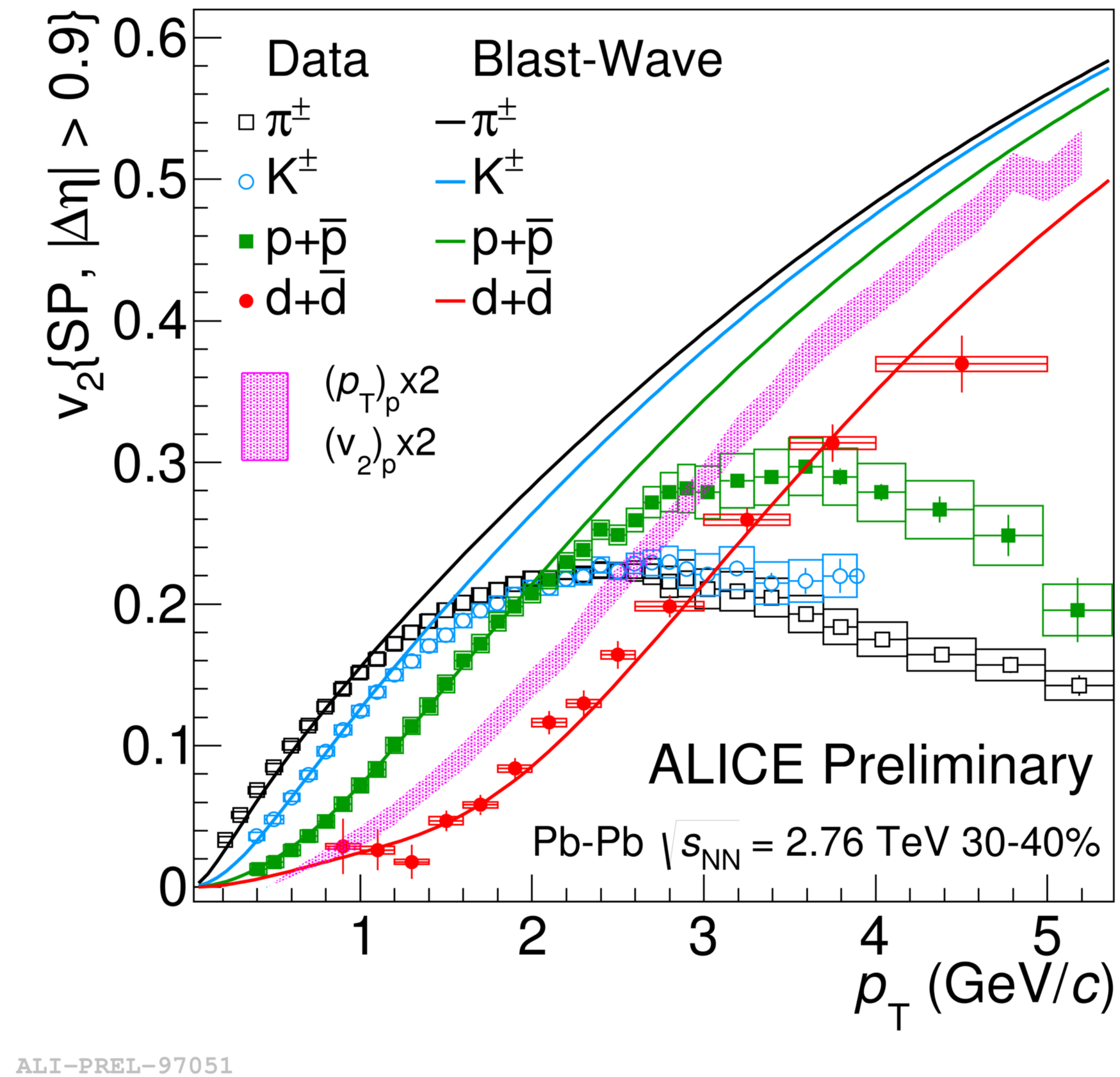

Deuteron v_2 is well described by the blast-wave fit which describes π, K, p.

Elliptic flow of (anti-)deuterons

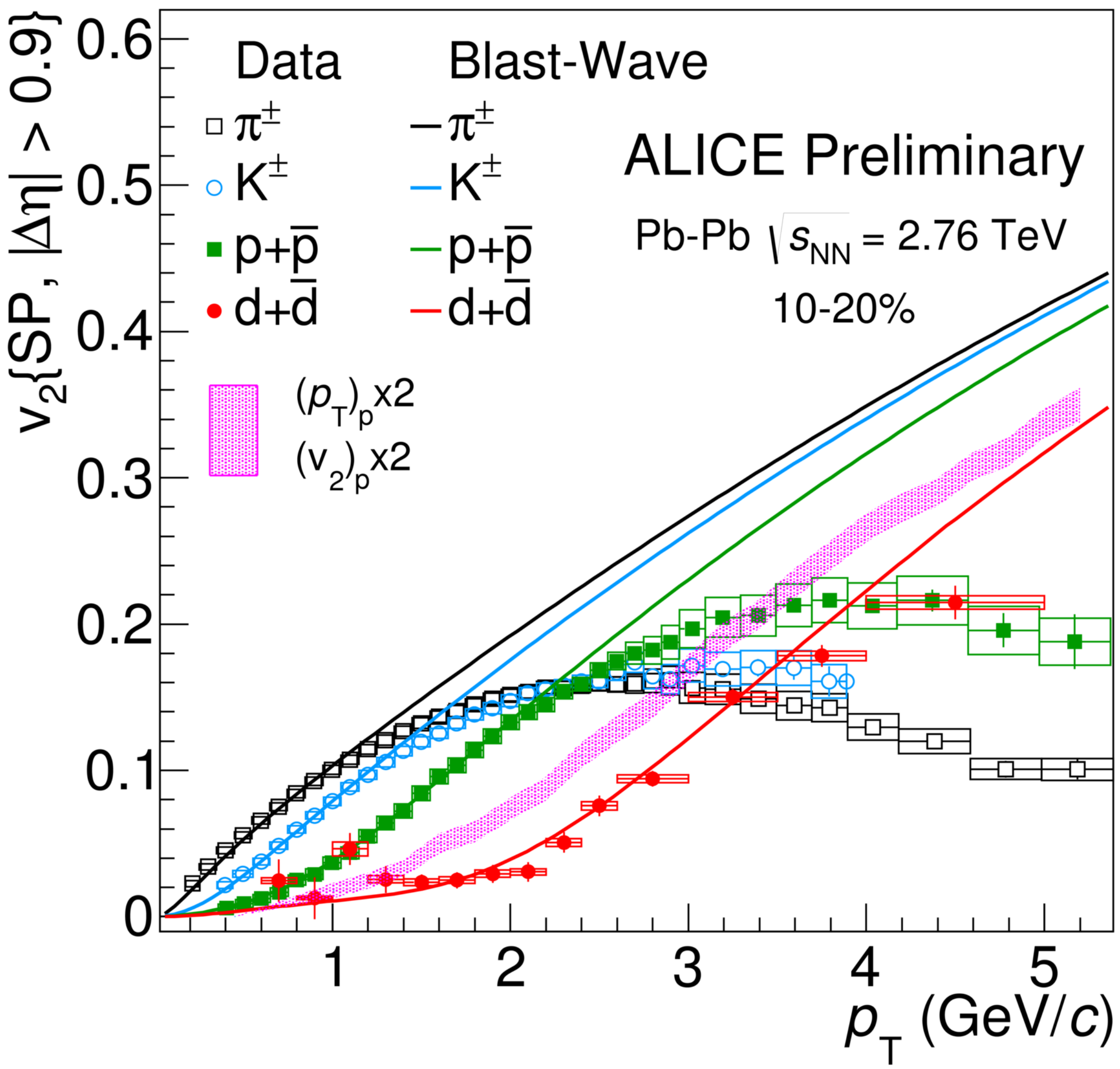

ALI-PREL-97047

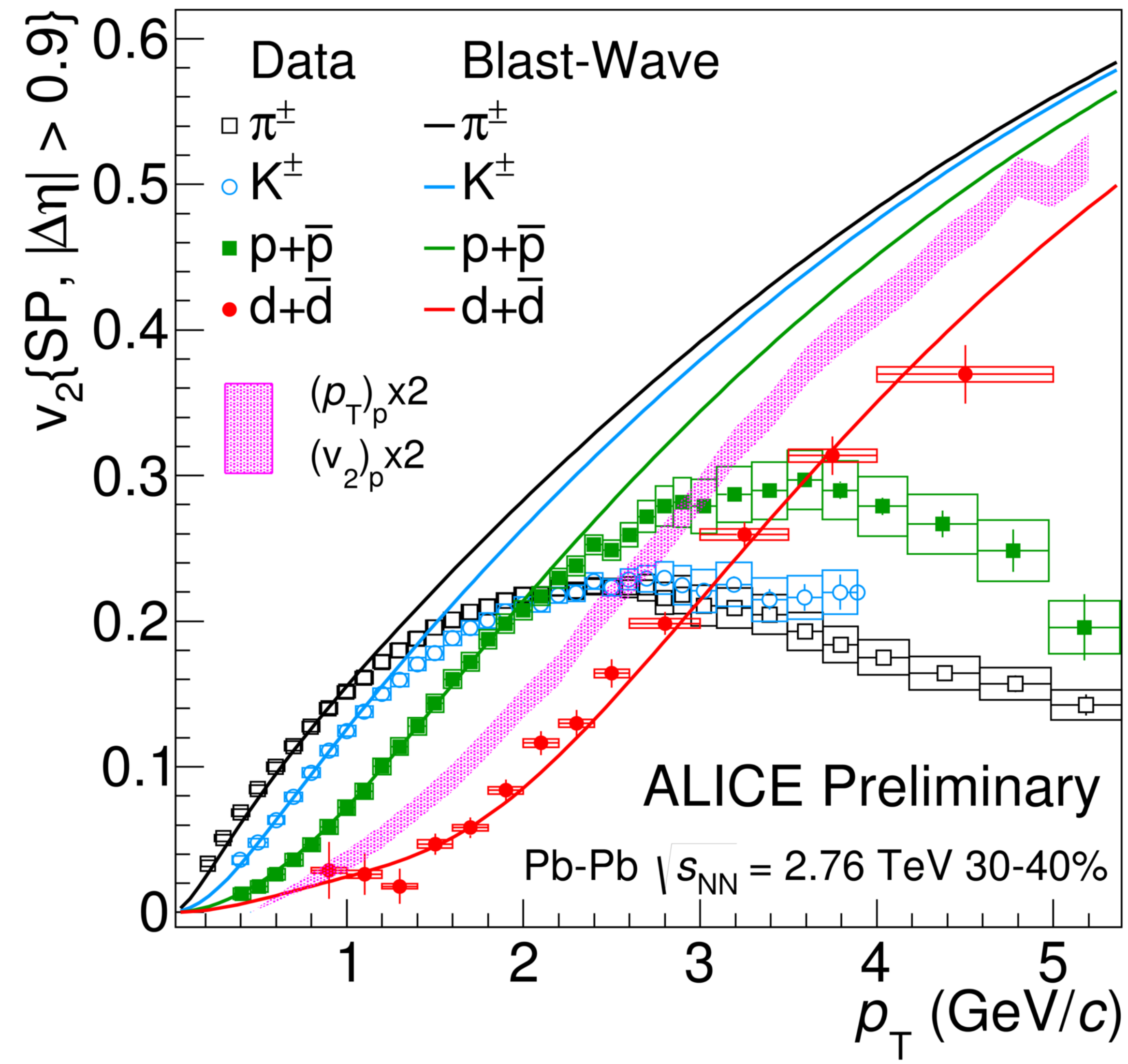

ALI-PREL-97051

Deuteron v_2 is well described by the blast-wave fit which describes π, K, p.

A simple coalescence approach estimated by the proton v_2 ($=2v_2(2p_T)$) does not describe the data.

Radial flow of (anti-)d and (anti-)^{3}He

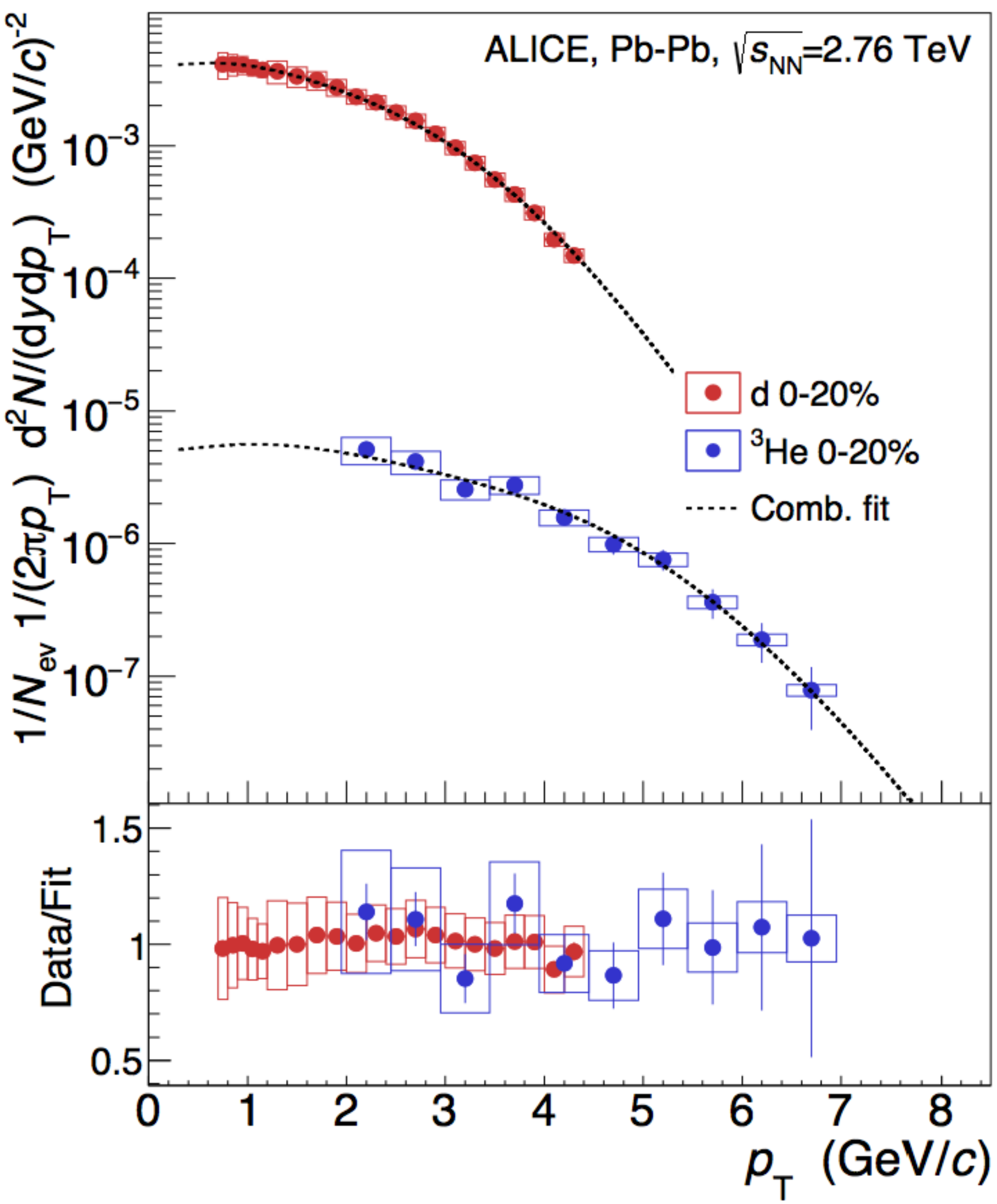

[arXiv:1506.08951]

Radial flow of (anti-)d and (anti-)^{3}He

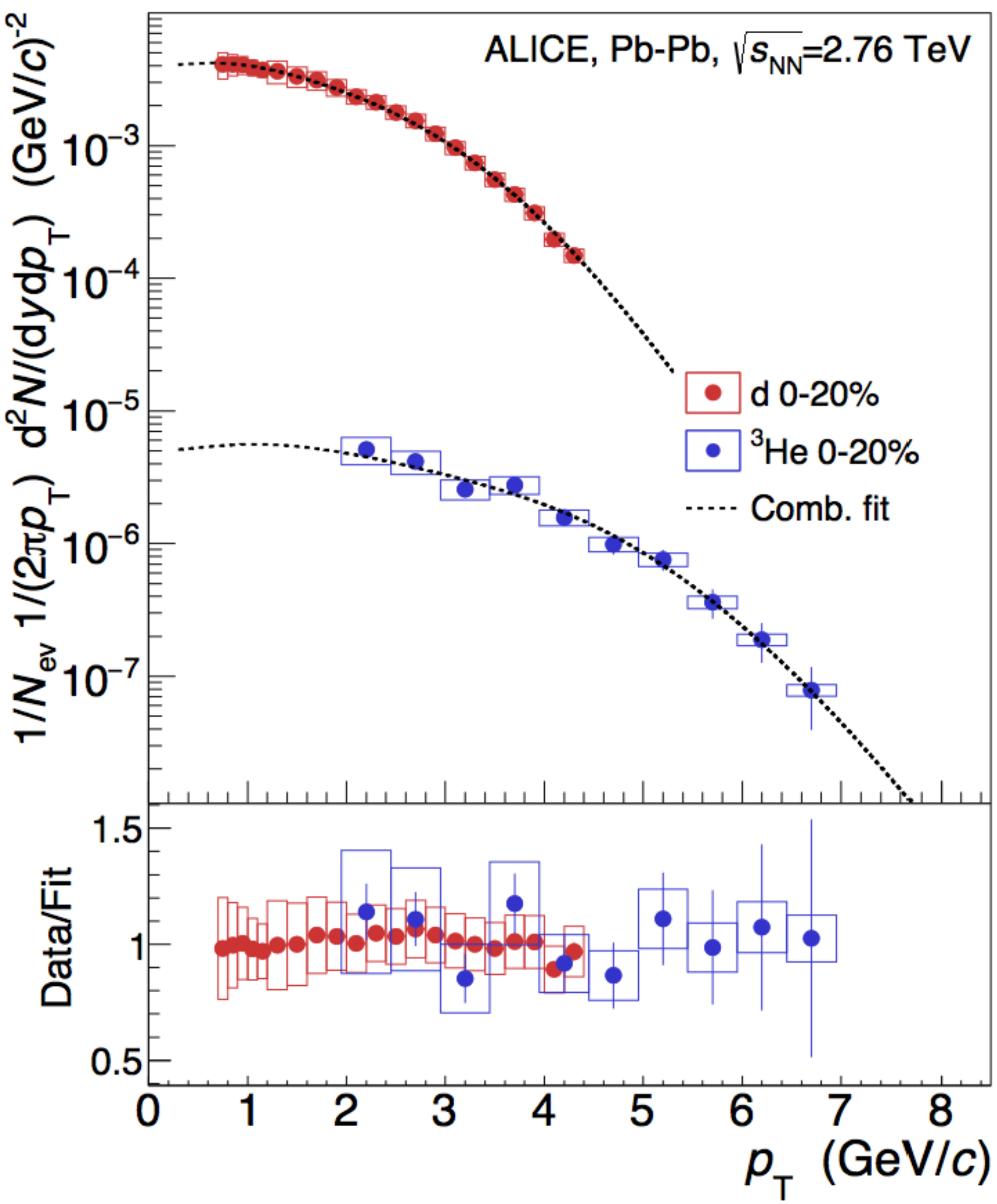

[arXiv:1506.08951]

Also the p_T-spectra of deuteron and ^{3}He are well described by the blast-wave fit which describes to π, K, p.

Radial flow of (anti-)d and (anti-)^{3}He

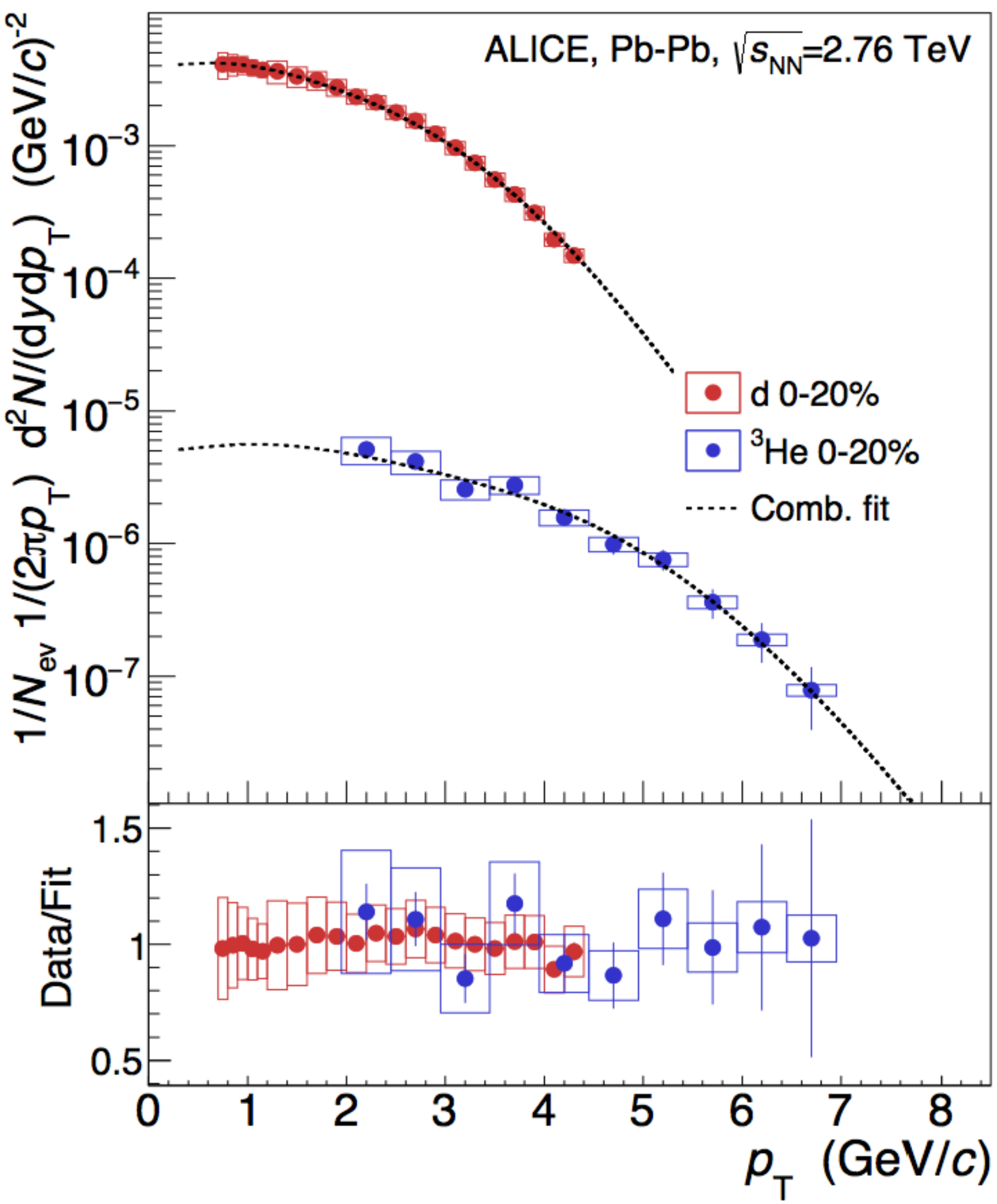

[arXiv:1506.08951]

Also the p_T-spectra of deuteron and ^{3}He are well described by the blast-wave fit which describes to π, K, p.

Also the p_T-integrated particle yields are described by the same thermal fit which describes all other light flavour hadrons.

Radial flow of (anti-)d and (anti-)^{3}He

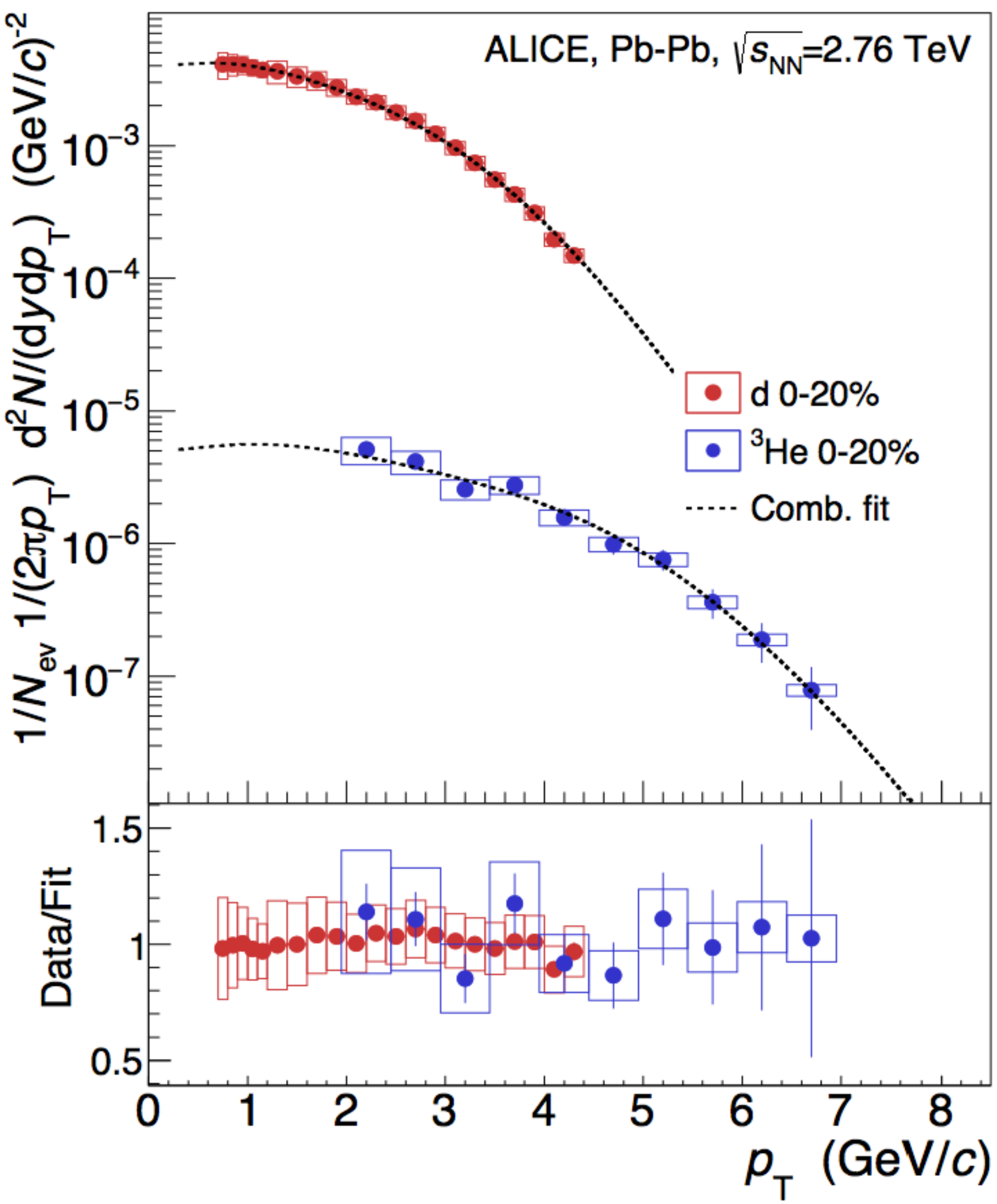

[arXiv:1506.08951]

Also the p_T-spectra of deuteron and ^{3}He are well described by the blast-wave fit which describes to π, K, p.

Also the p_T-integrated particle yields are described by the same thermal fit which describes all other light flavour hadrons.

Despite their low binding energy (E_B = 2.2 MeV << T_C = 156 MeV), light (anti-)nuclei behave like all other **non-composite** particles.

Chemical equilibrium

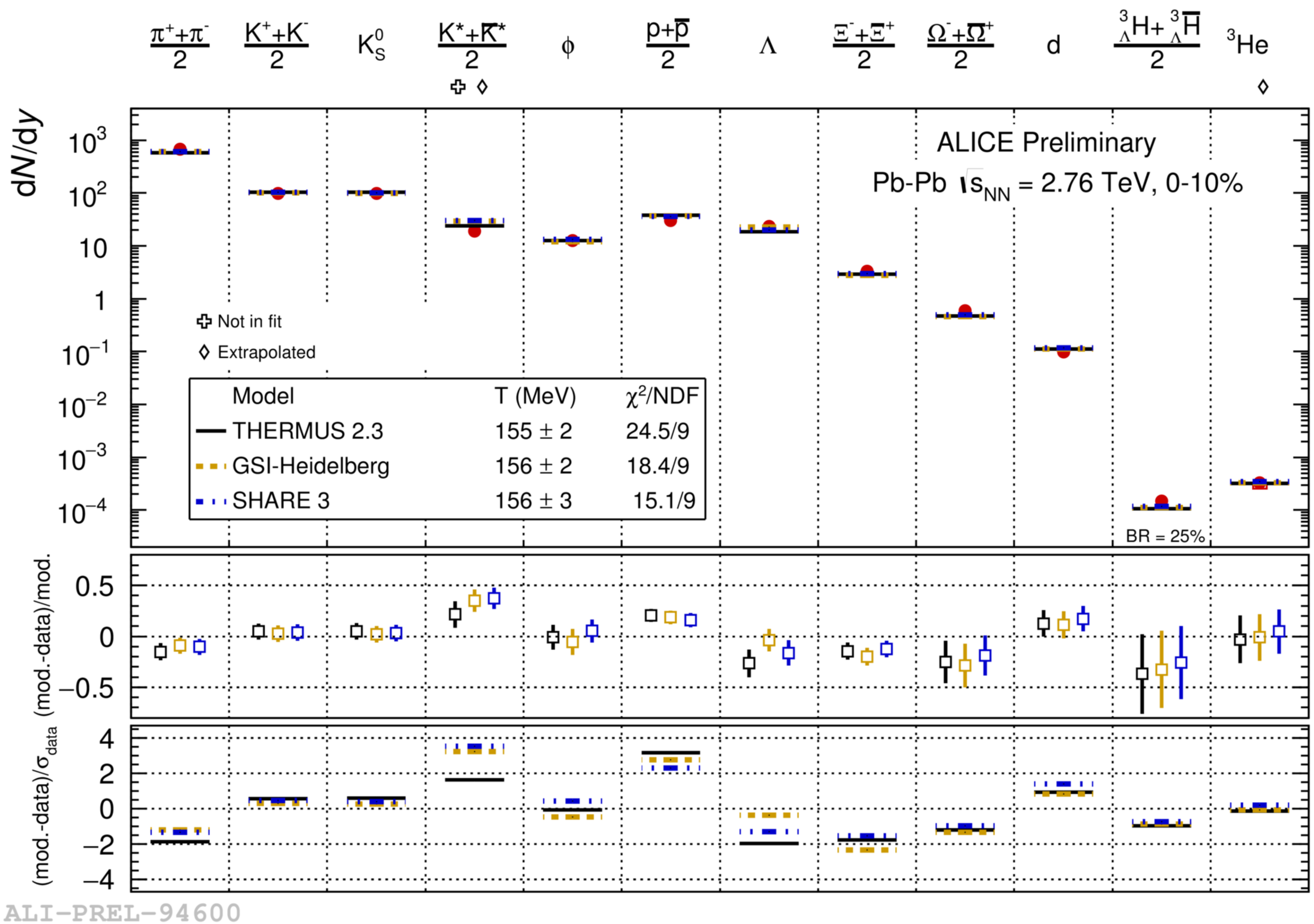

[Wheaton et al, Comput.Phys.Commun, 180 84]
[Petran et al, arXiv:1310.5108]
[Andronic et al, PLB 673 142]

Chemical equilibrium

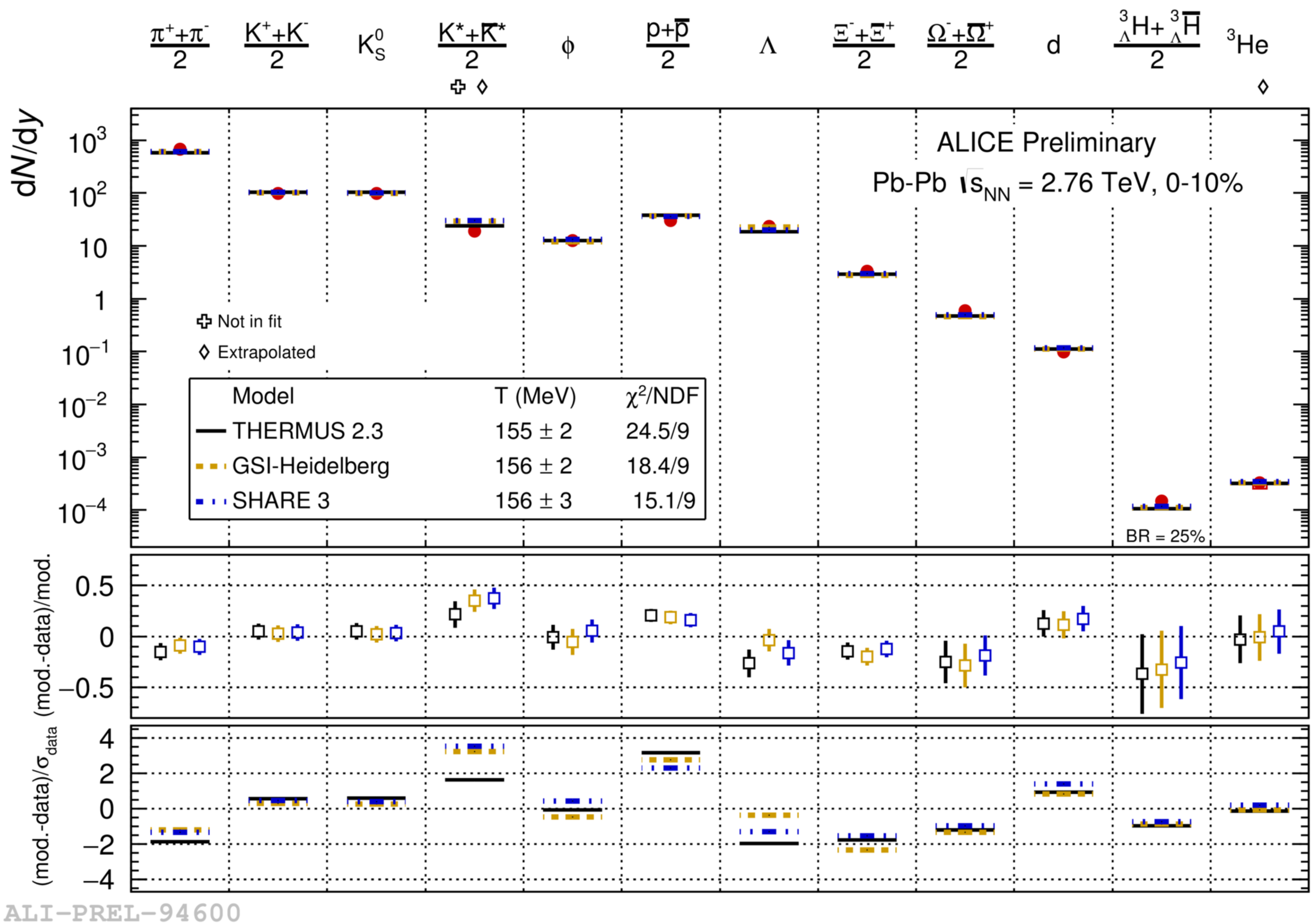

Particle yields of light flavor hadrons are described over 7 orders of magnitude within 20% (except K^{*0}) with a common chemical freeze-out temperature of $T_{ch} \approx 156$ MeV (prediction from RHIC extrapolation was ≈ 164 MeV).

[Wheaton et al, Comput.Phys.Commun, 180 84]
[Petran et al, arXiv:1310.5108]
[Andronic et al, PLB 673 142]

Chemical equilibrium

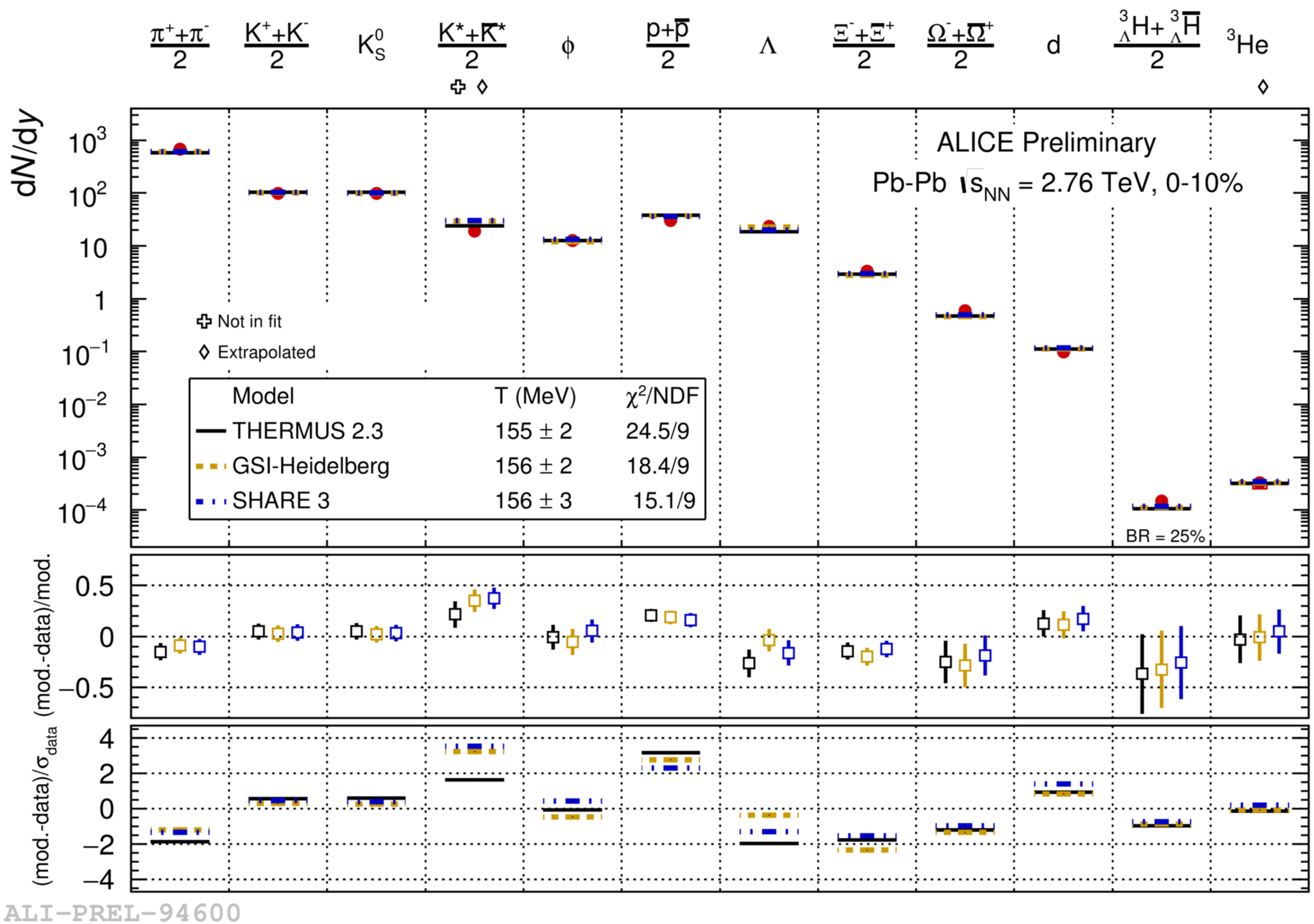

Particle yields of light flavor hadrons are described over 7 orders of magnitude within 20% (except K^{*0}) with a common chemical freeze-out temperature of $T_{ch} \approx 156$ MeV (prediction from RHIC extrapolation was ≈ 164 MeV).

Hadrons are produced in apparent chemical equilibrium in Pb-Pb collisions at LHC energies.

[Wheaton et al, Comput.Phys.Commun, 180 84]
[Petran et al, arXiv:1310.5108]
[Andronic et al, PLB 673 142]

Chemical equilibrium

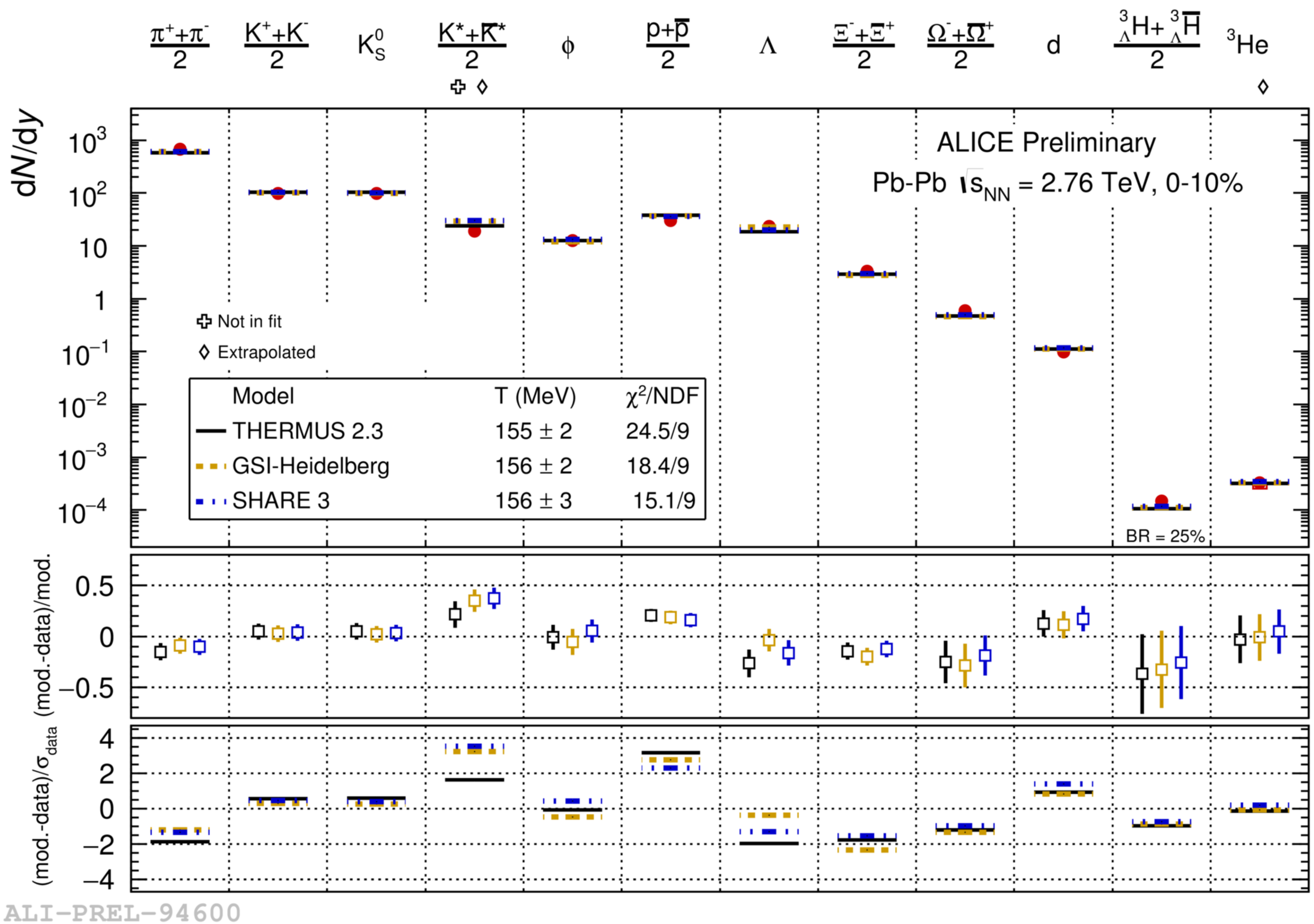

Particle yields of light flavor hadrons are described over 7 orders of magnitude within 20% (except K^{*0}) with a common chemical freeze-out temperature of T_{ch} ≈ 156 MeV (prediction from RHIC extrapolation was ≈ 164 MeV).

Hadrons are produced in apparent chemical equilibrium in Pb-Pb collisions at LHC energies.

Largest deviations observed for **protons** (incomplete hadron spectrum, baryon annihilation in hadronic phase,..?) and for $\mathbf{K^{*0}}$.

[Wheaton et al, Comput.Phys.Commun, 180 84]
[Petran et al, arXiv:1310.5108]
[Andronic et al, PLB 673 142]

Chemical equilibrium

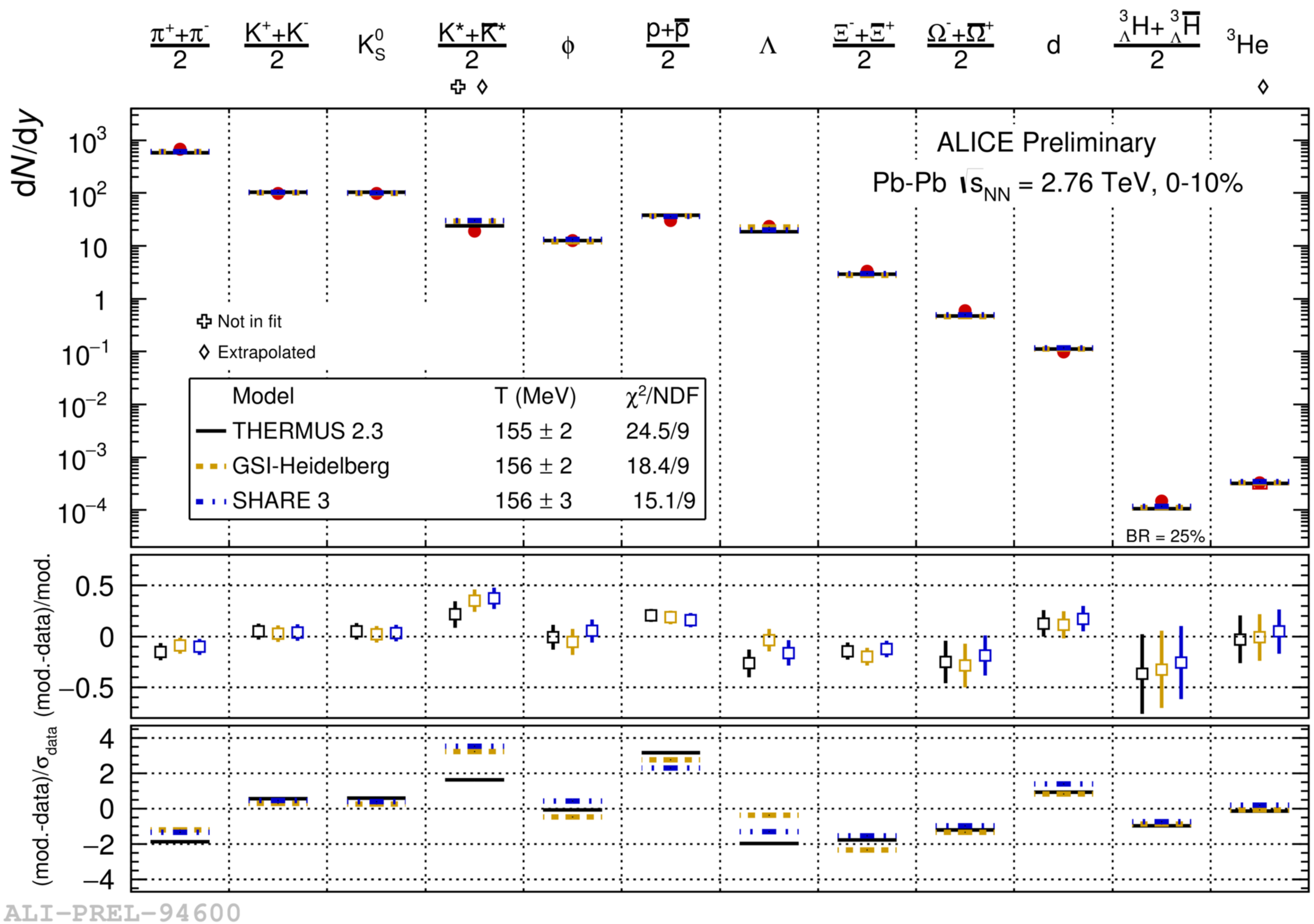

Particle yields of light flavor hadrons are described over 7 orders of magnitude within 20% (except K^{*0}) with a common chemical freeze-out temperature of $T_{ch} \approx$ 156 MeV (prediction from RHIC extrapolation was ≈ 164 MeV).

Hadrons are produced in apparent chemical equilibrium in Pb-Pb collisions at LHC energies.

Largest deviations observed for **protons** (incomplete hadron spectrum, baryon annihilation in hadronic phase,..?) and for $\mathbf{K^{*0}}$.

Three different versions of thermal model implementations give similar results.

[Wheaton et al, Comput.Phys.Commun, 180 84]
[Petran et al, arXiv:1310.5108]
[Andronic et al, PLB 673 142]

Net charge fluctuations

- Results are shown for 0-5% most central collisions.
- ALICE values significantly lower than the hadron gas expectation while RHIC measurements are still compatible.
- Strong dependence on rapidity window observed which seems to saturate above Δη ≈ 2.3 assuming diffusion functions. Initial fluctuations are diluted by final state interactions and limited experimental acceptance.

$$\nu_{(+-,dyn.)} = \frac{\langle N_+(N_+-1)\rangle}{\langle N_+\rangle^2} + \frac{\langle N_-(N_- -1)\rangle}{\langle N_-\rangle^2} - 2\frac{\langle N_+N_-\rangle}{\langle N_+\rangle\langle N_-\rangle}$$

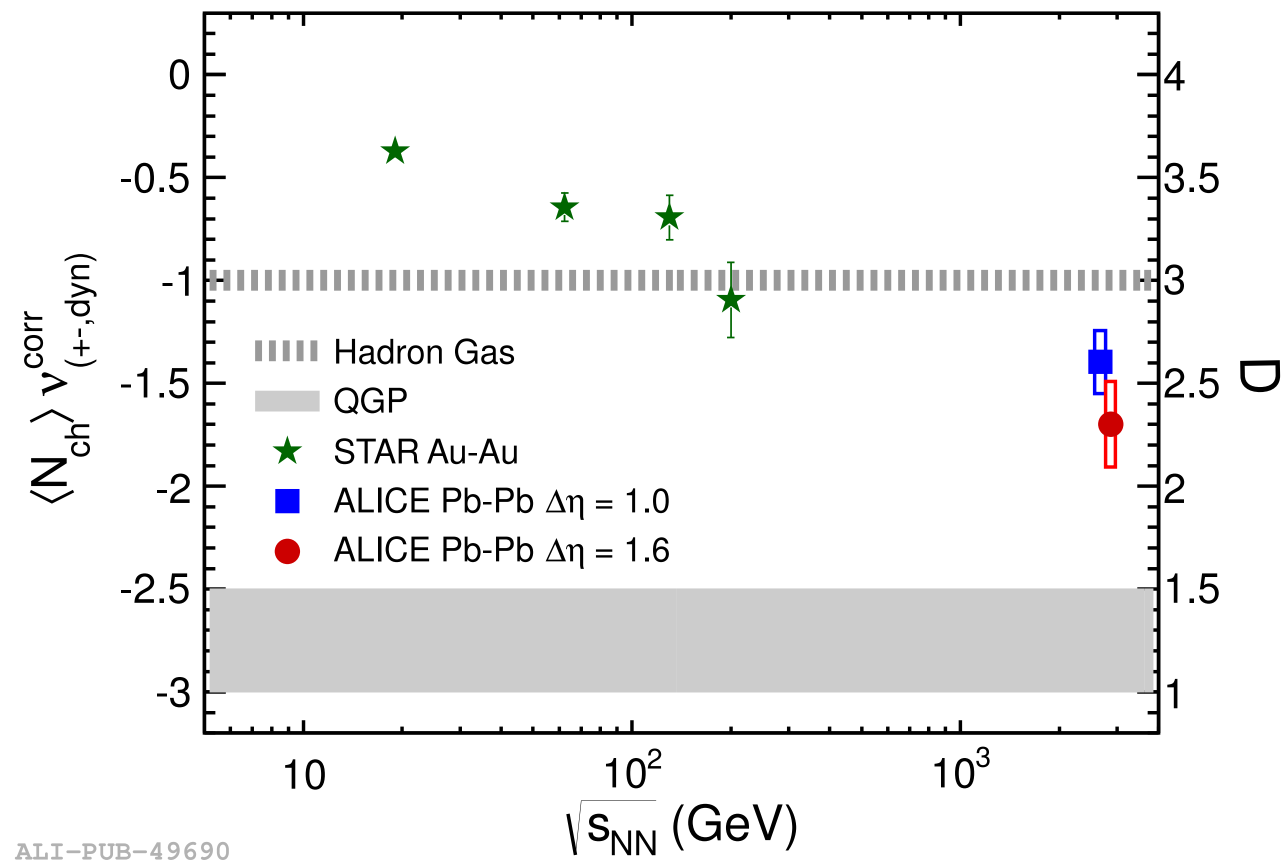

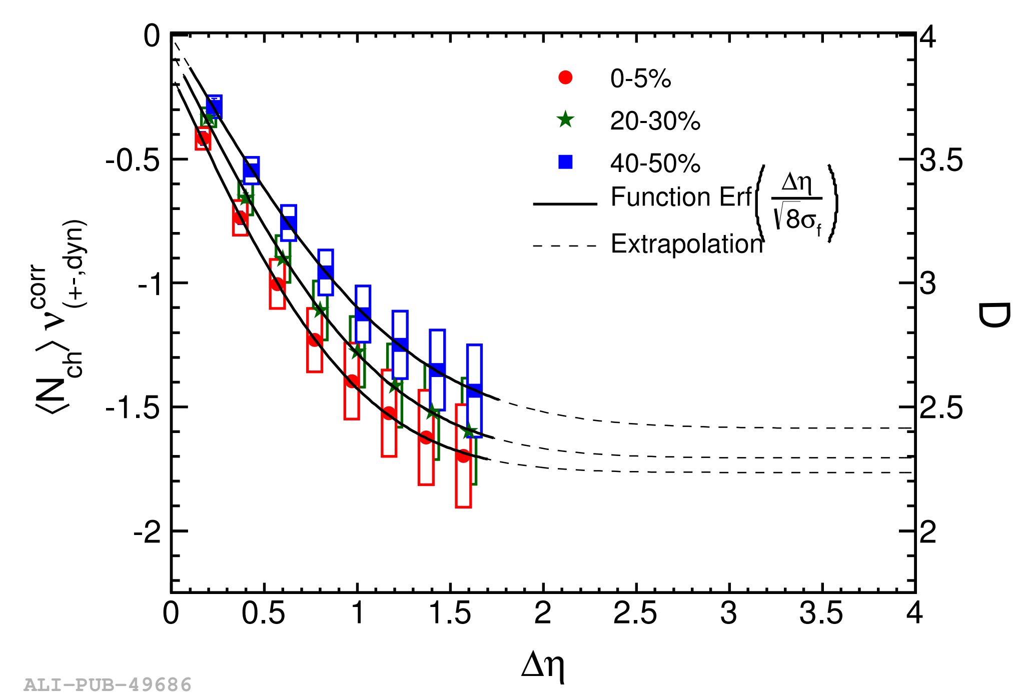

Collectivity and thermal equilibrium in **pp and p-Pb** collisions

Strange baryon production vs. dN_{ch}/dη (A)

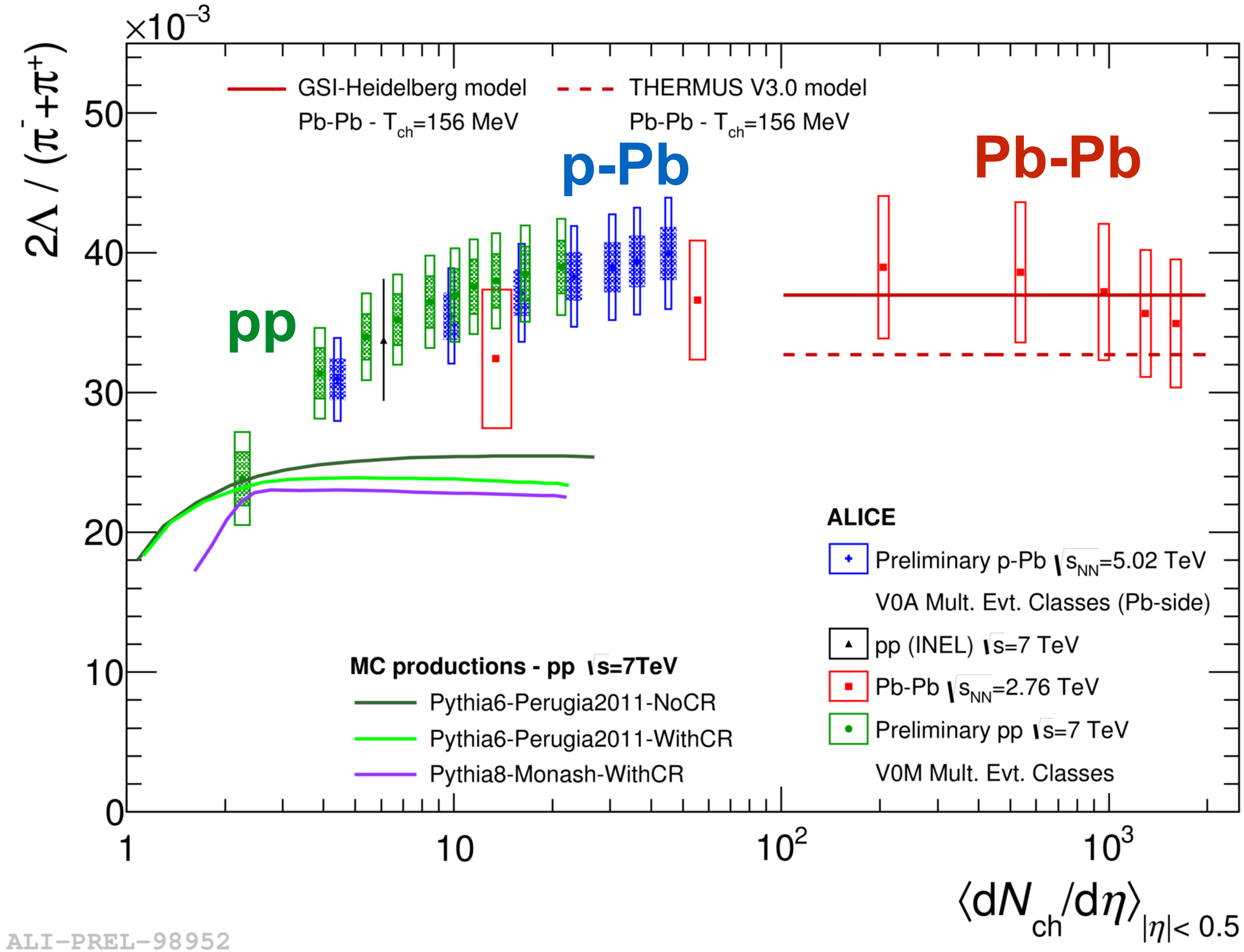

Strange baryon production vs. dN_{ch}/dη (A)

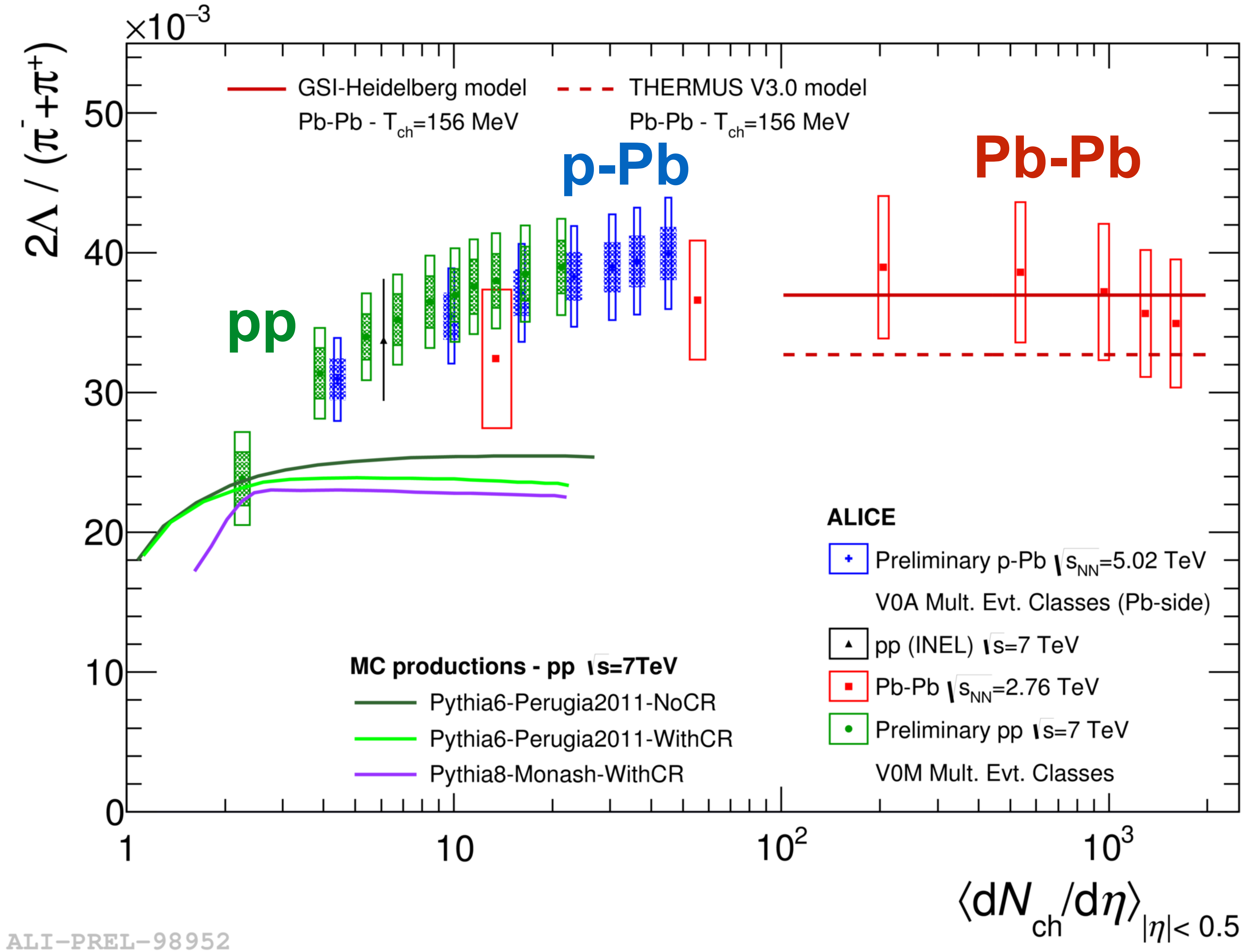

Strange baryon production is the most sensitive to the system size.

Strange baryon production vs. dN_{ch}/dη (A)

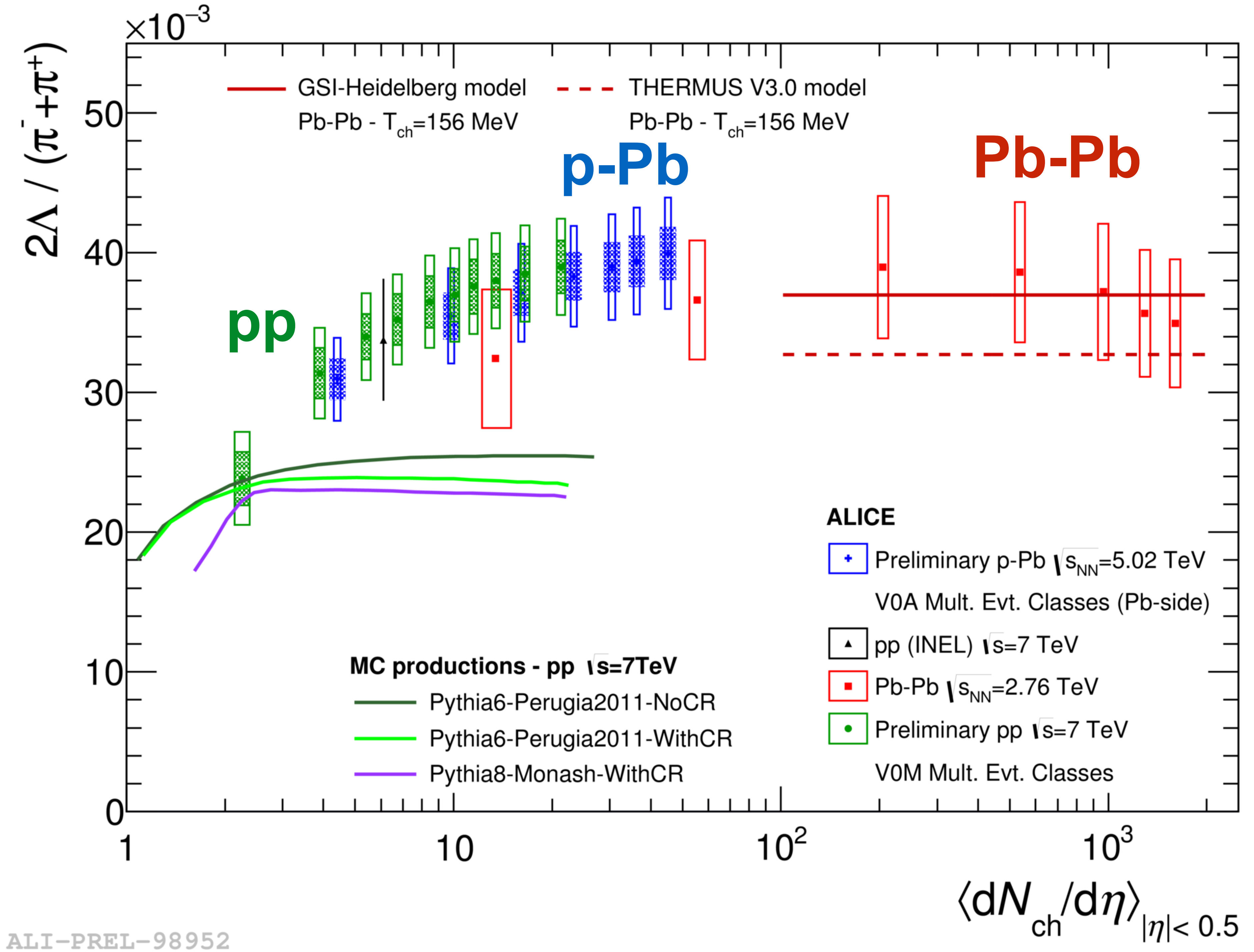

Strange baryon production is the most sensitive to the system size.

Λ/π ratio is at the grand-canonical limit in Pb-Pb collisions.

Strange baryon production vs. dN_{ch}/dη (A)

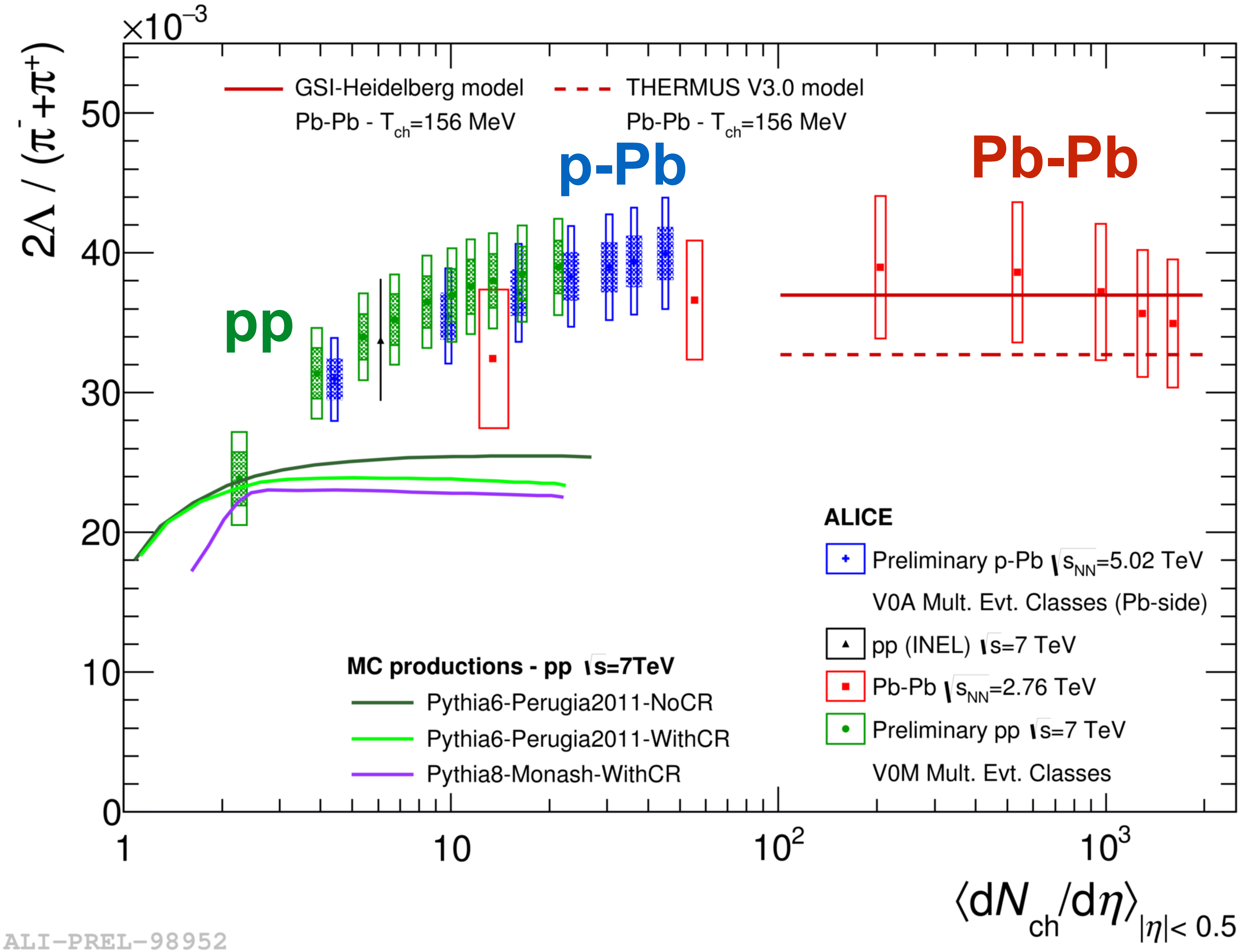

- Strange baryon production is the most sensitive to the system size.
- Λ/π ratio is at the grand-canonical limit in Pb-Pb collisions.
- Similar values are reached in highest multiplicity p-Pb collisions.

Strange baryon production vs. dN_{ch}/dη (A)

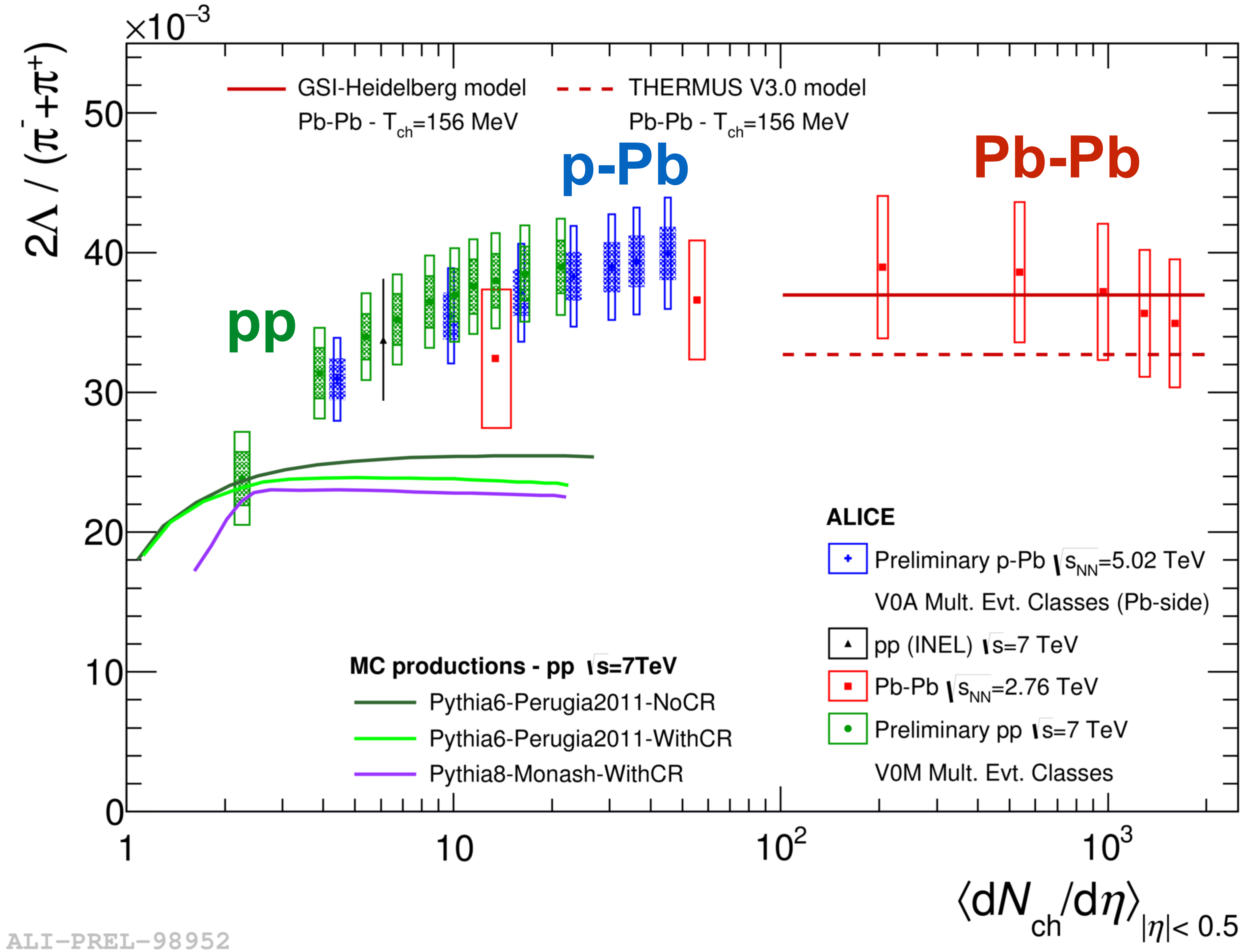

Strange baryon production is the most sensitive to the system size.

Λ/π ratio is at the grand-canonical limit in Pb-Pb collisions.

Similar values are reached in highest multiplicity p-Pb collisions.

Increase of strangeness production with increasing multiplicity.

Strange baryon production vs. dN_{ch}/dη (A)

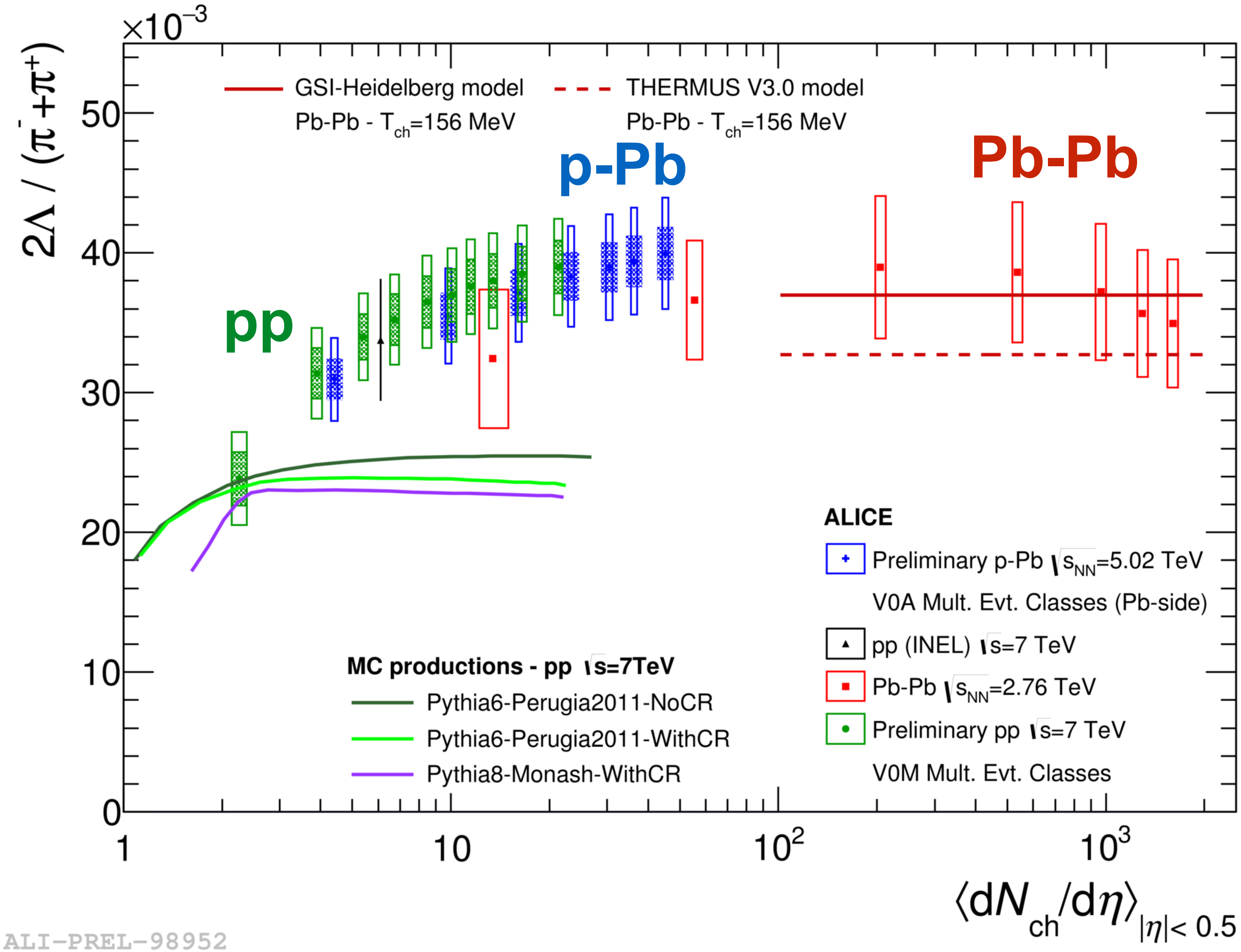

Strange baryon production is the most sensitive to the system size.

Λ/π ratio is at the grand-canonical limit in Pb-Pb collisions.

Similar values are reached in highest multiplicity p-Pb collisions.

Increase of strangeness production with increasing multiplicity.

Similar multiplicity dependence in pp and p-Pb.

Strange baryon production vs. dN_{ch}/dη (A)

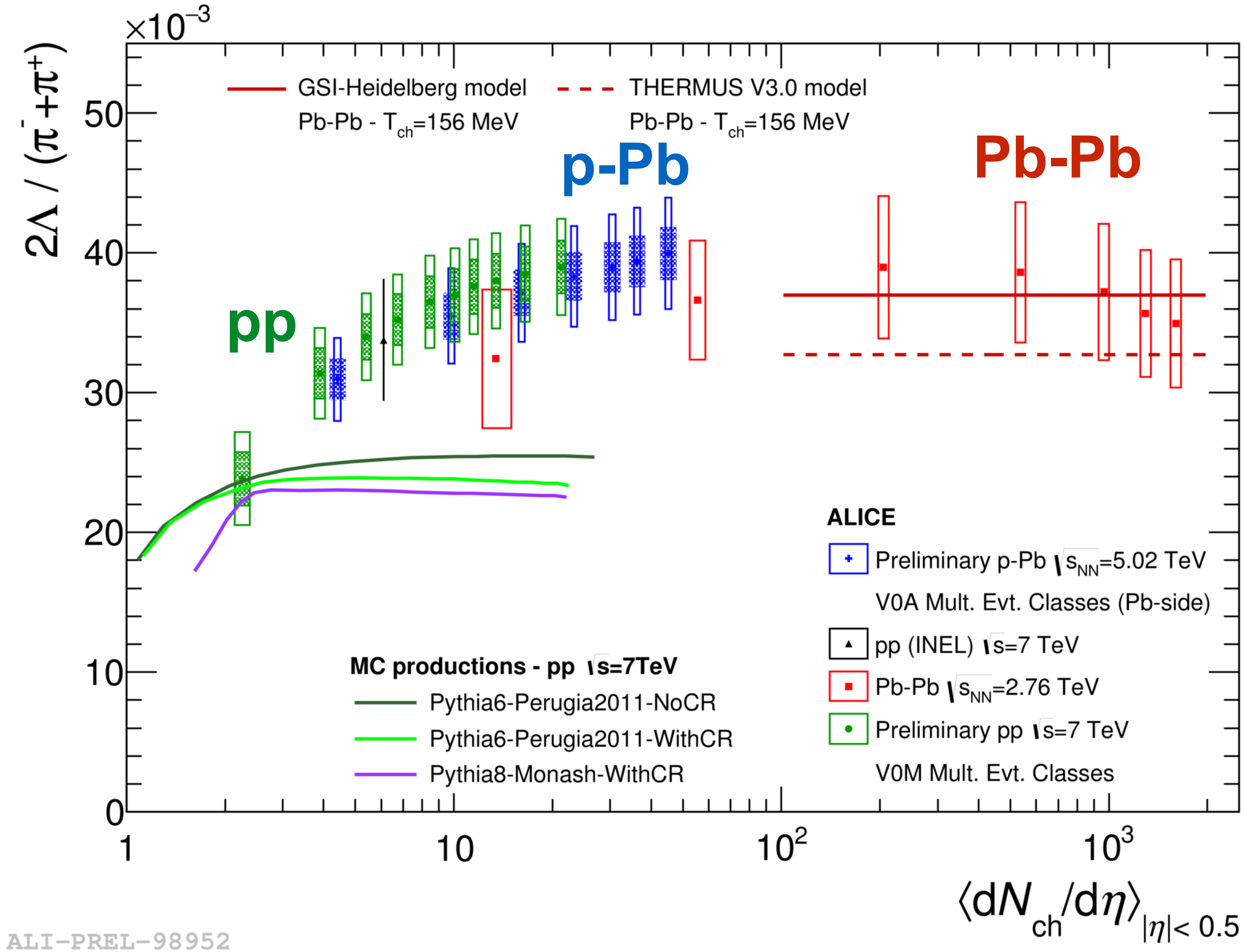

Strange baryon production is the most sensitive to the system size.

Λ/π ratio is at the grand-canonical limit in Pb-Pb collisions.

Similar values are reached in highest multiplicity p-Pb collisions.

Increase of strangeness production with increasing multiplicity.

Similar multiplicity dependence in pp and p-Pb.

pp data allows comparisons to the full machinery of QCD-inspired event generators.

Strange baryon production vs. dN_{ch}/dη (B)

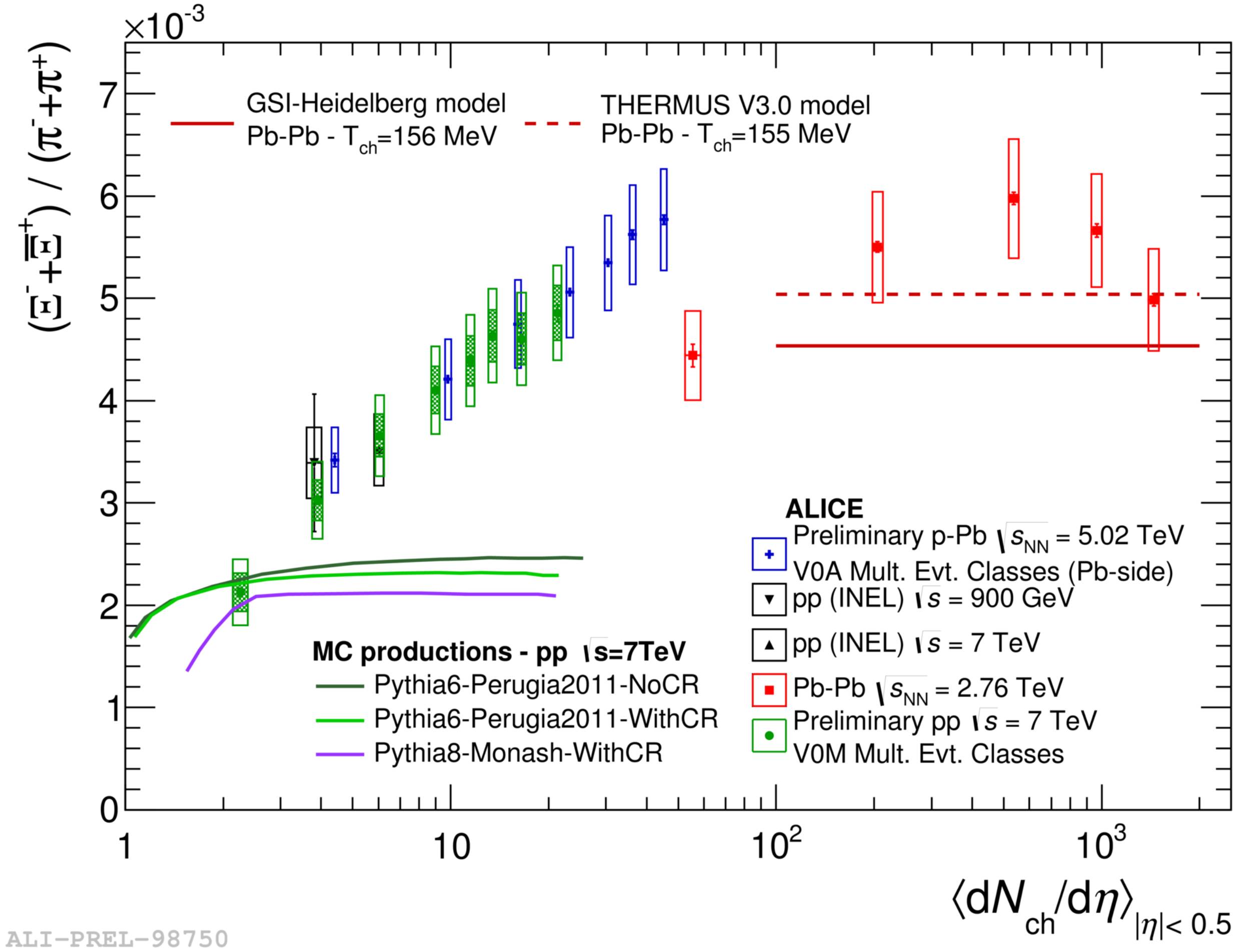

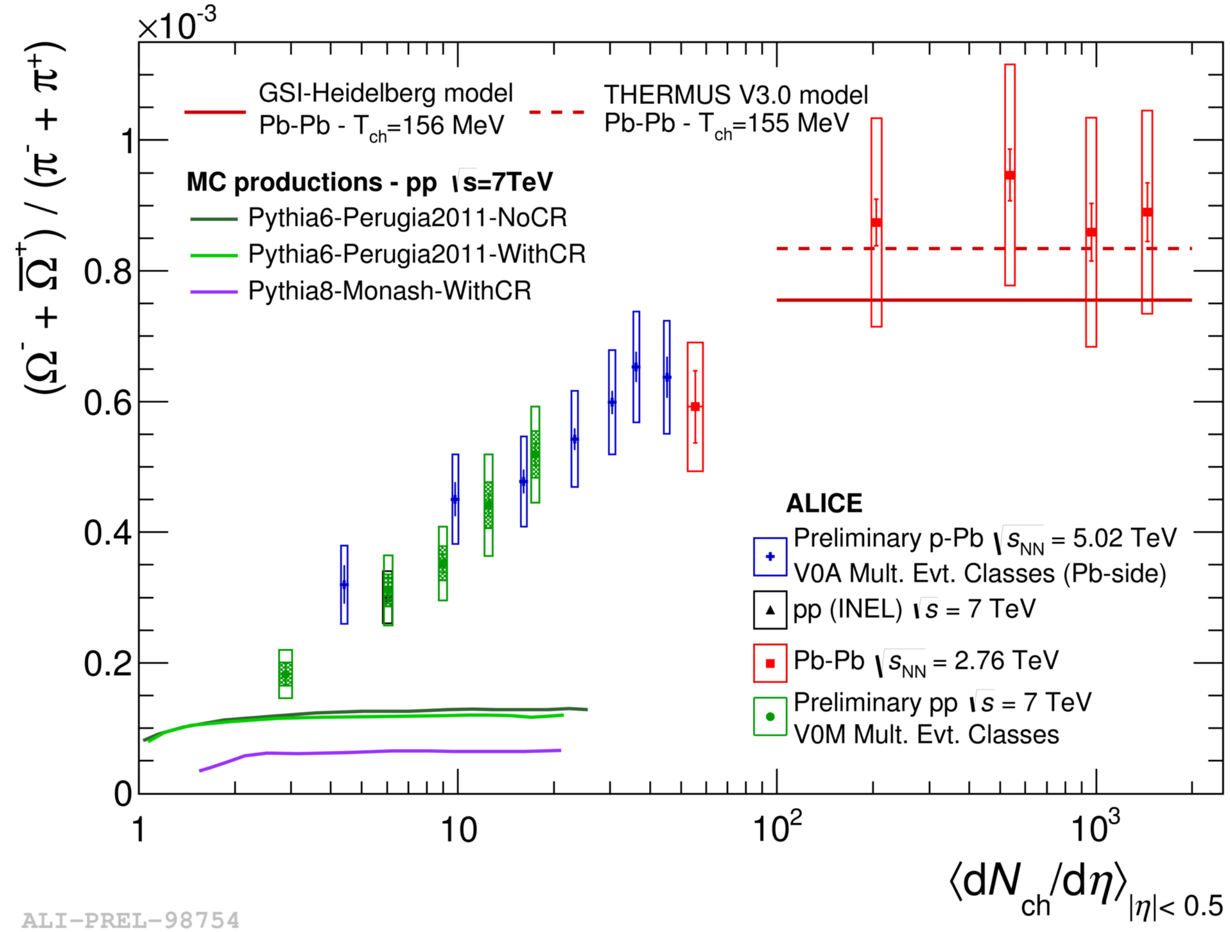

Strange baryon production vs. dN_{ch}/dη (B)

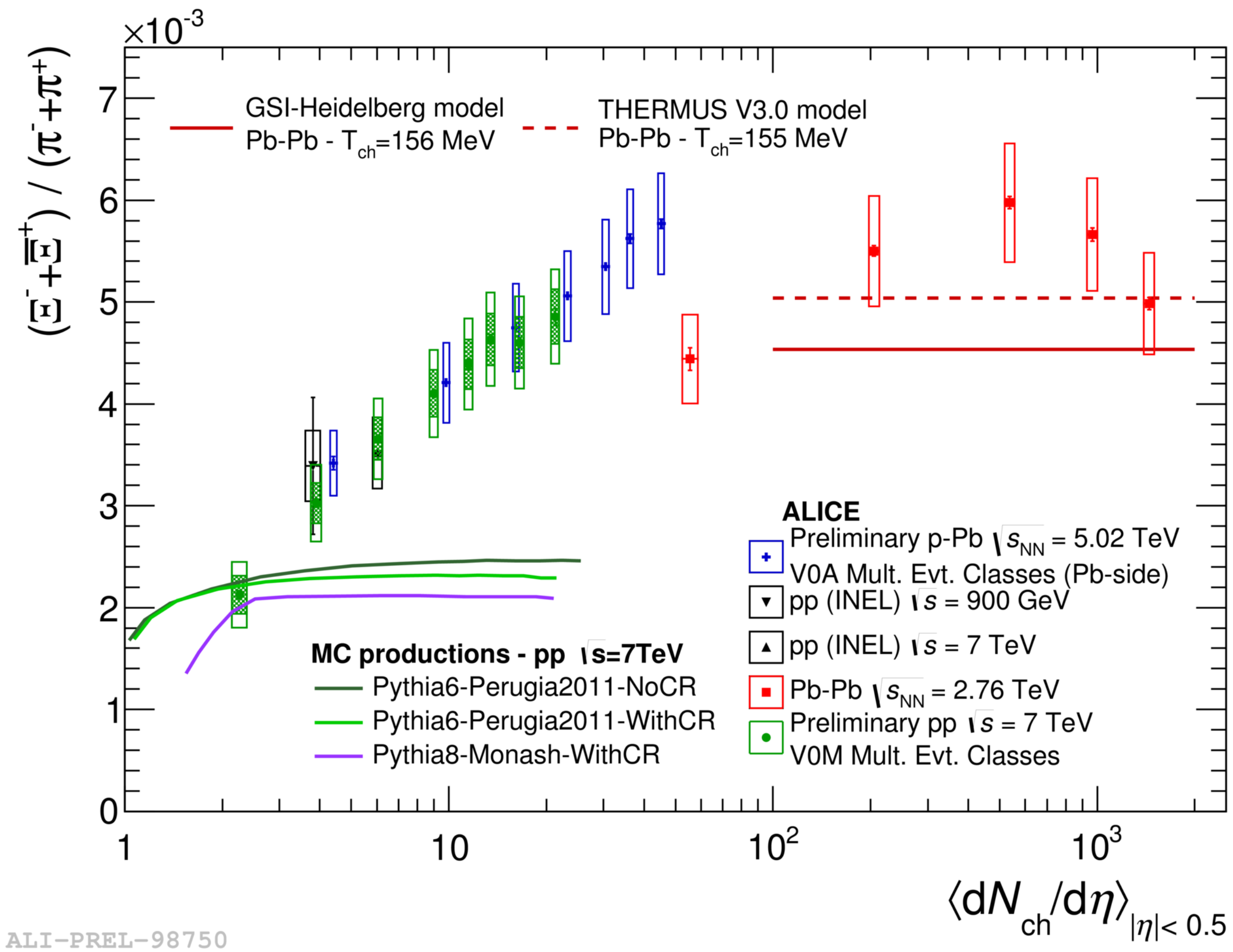

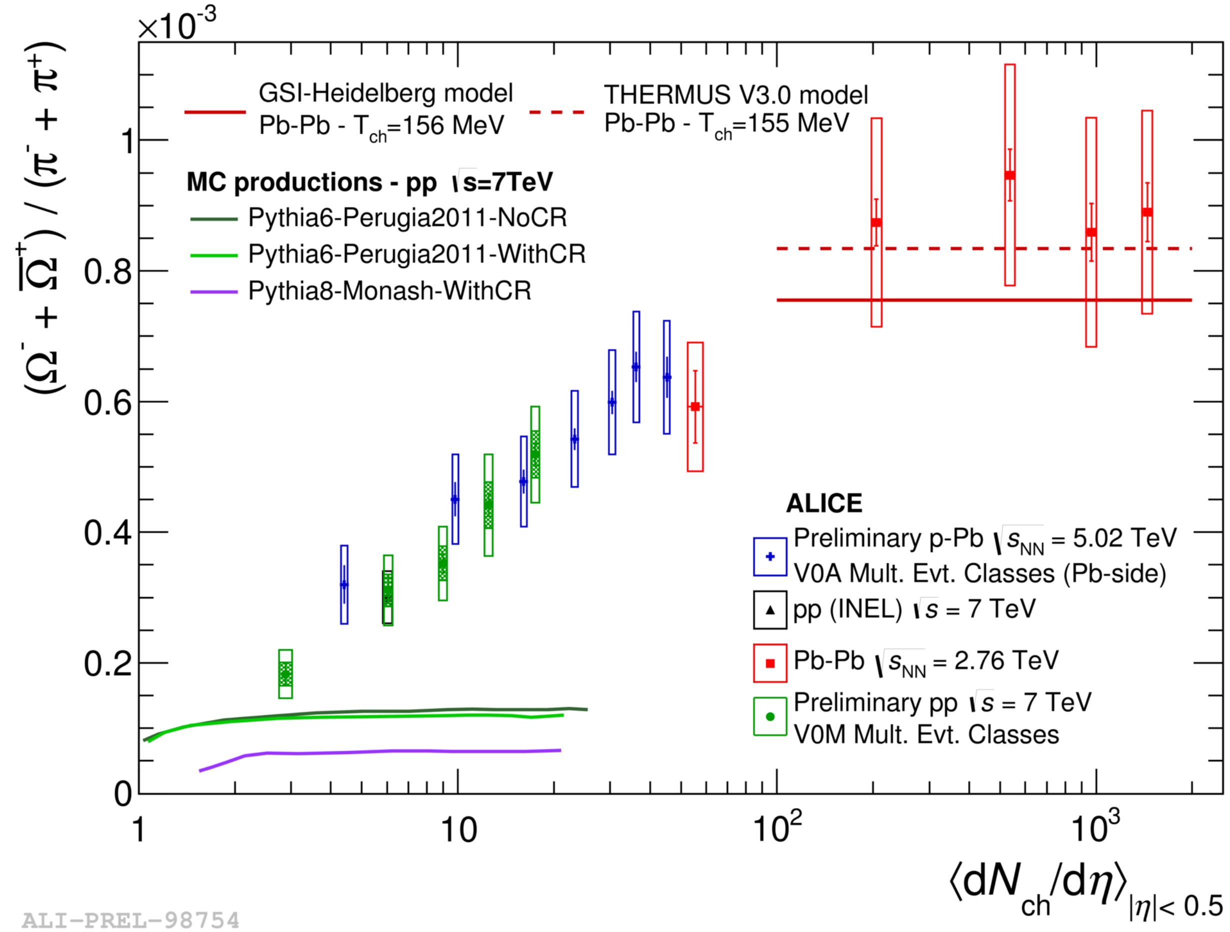

Increase of strangeness production with increasing multiplicity is even more pronounced for multi-strange particles.

Strange baryon production vs. dN_{ch}/dη (B)

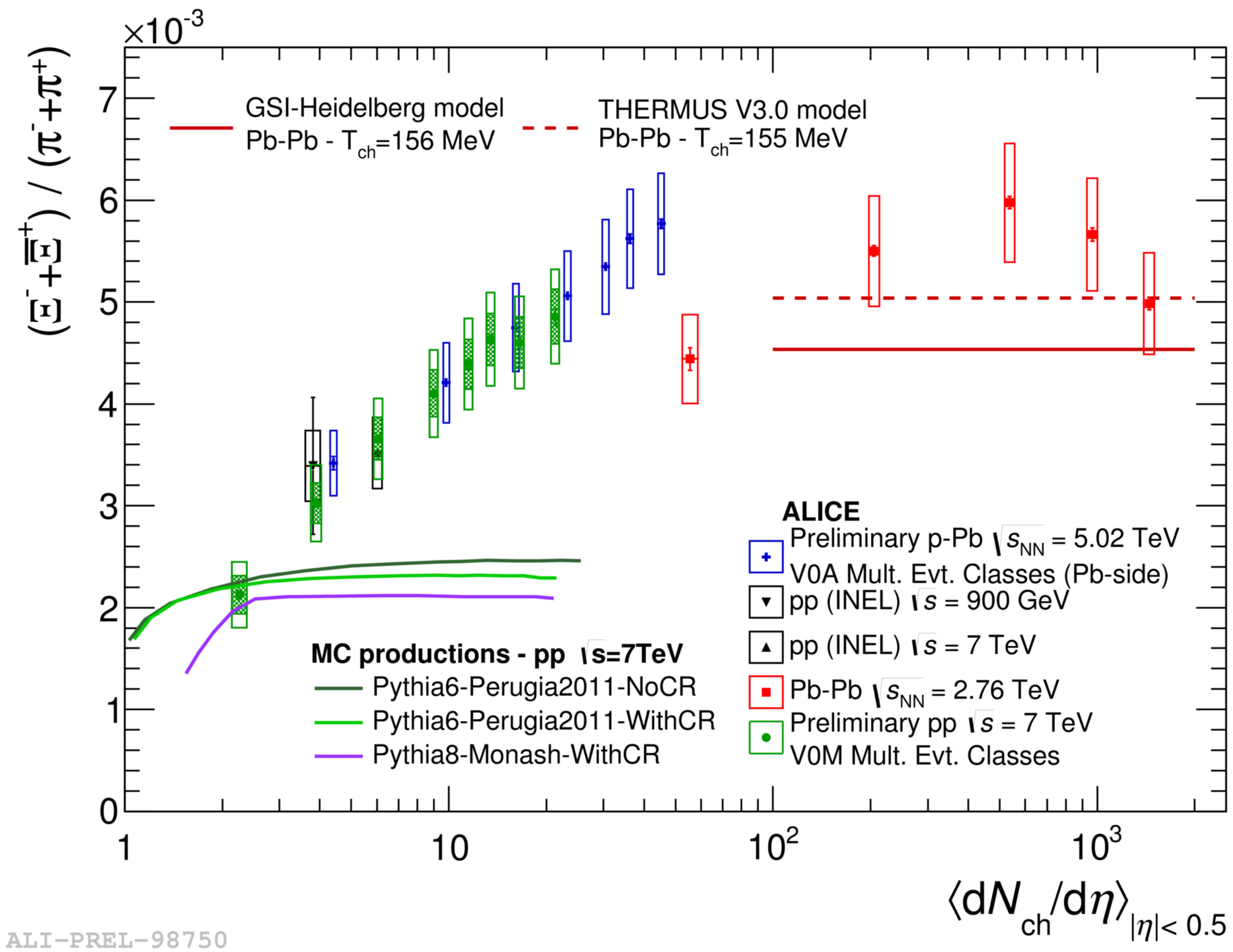

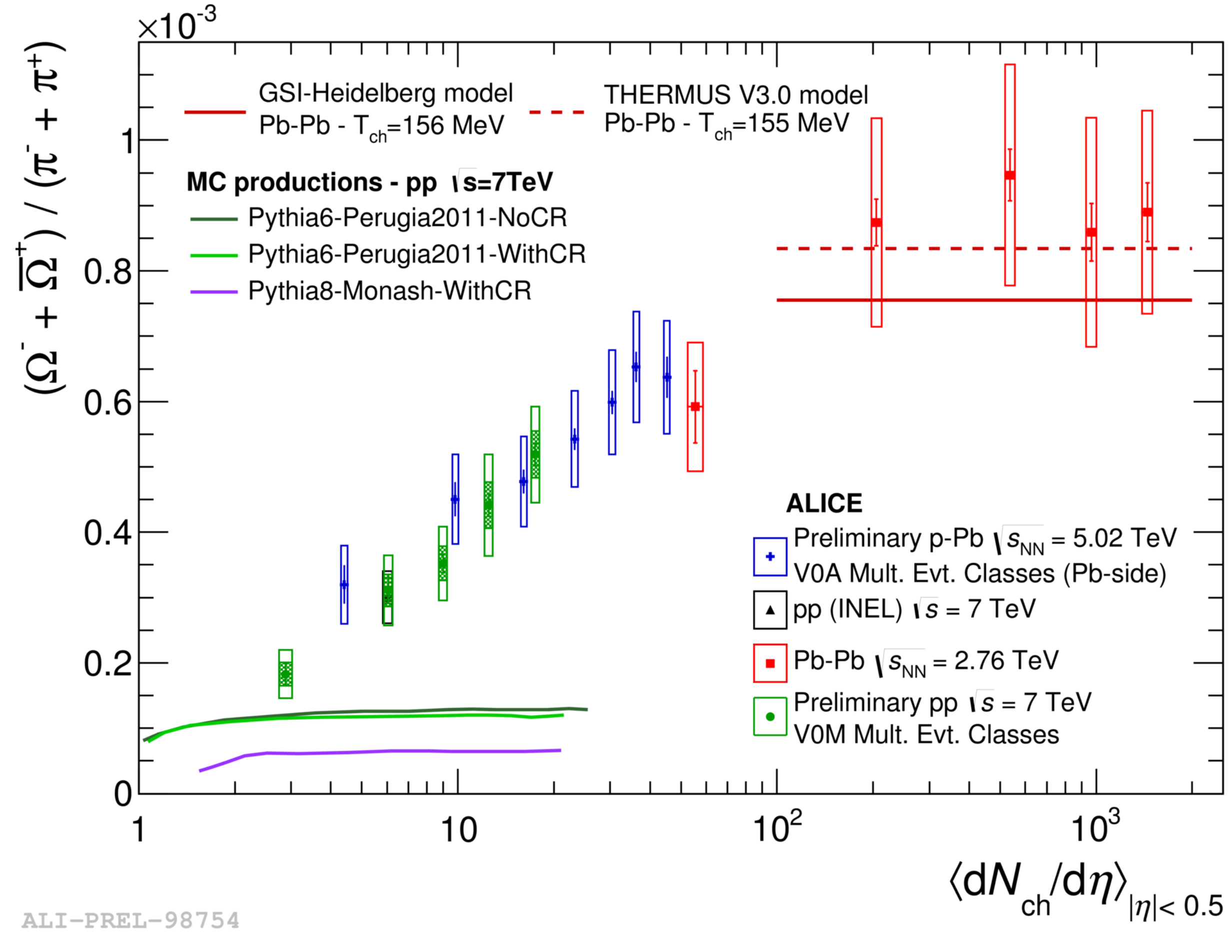

Increase of strangeness production with increasing multiplicity is even more pronounced for multi-strange particles.

Ξ/π reaches GC saturation value in highest multiplicity p-Pb collisions. Ω/π not quite.

Strange baryon production vs. dN_{ch}/dη (B)

ALICE

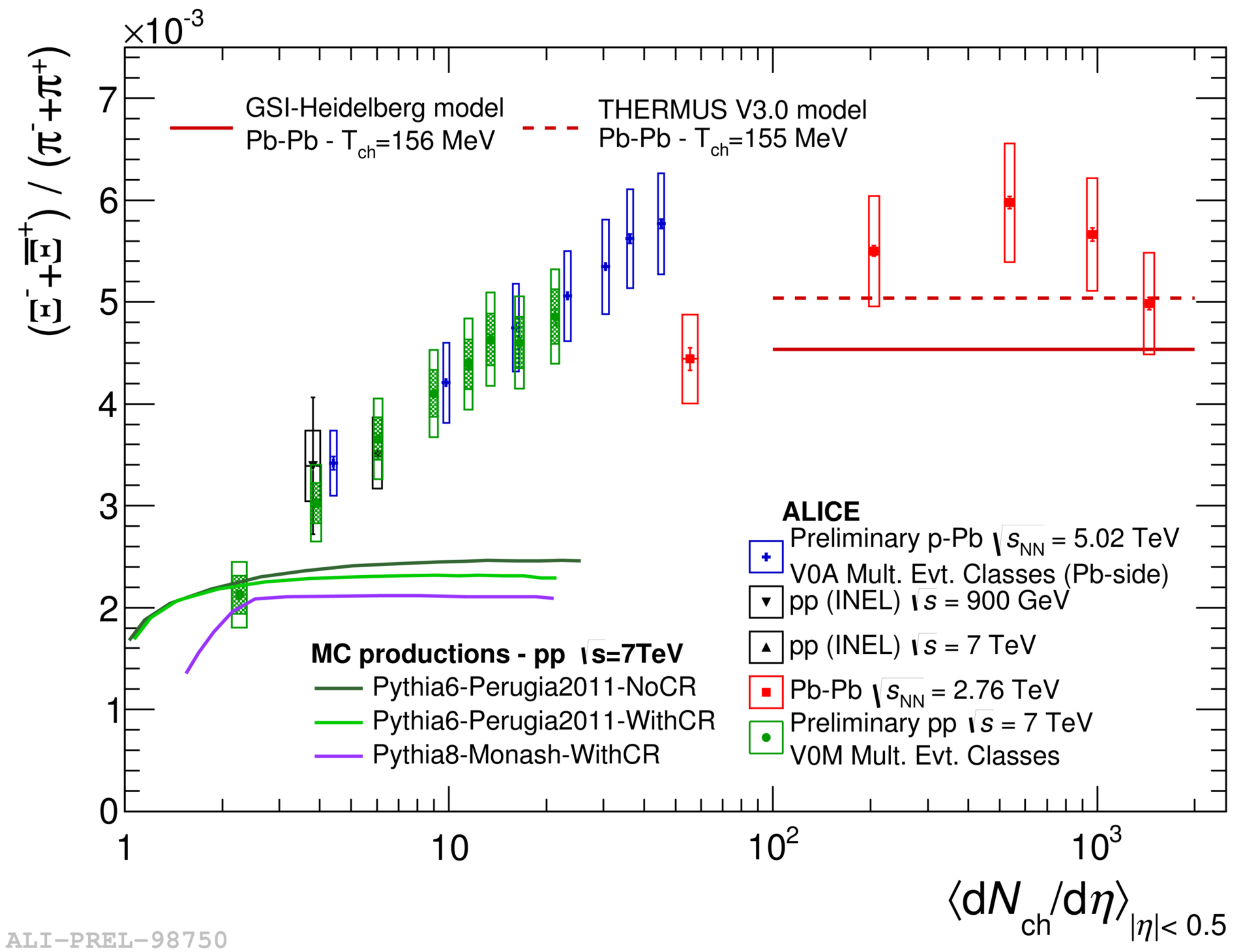

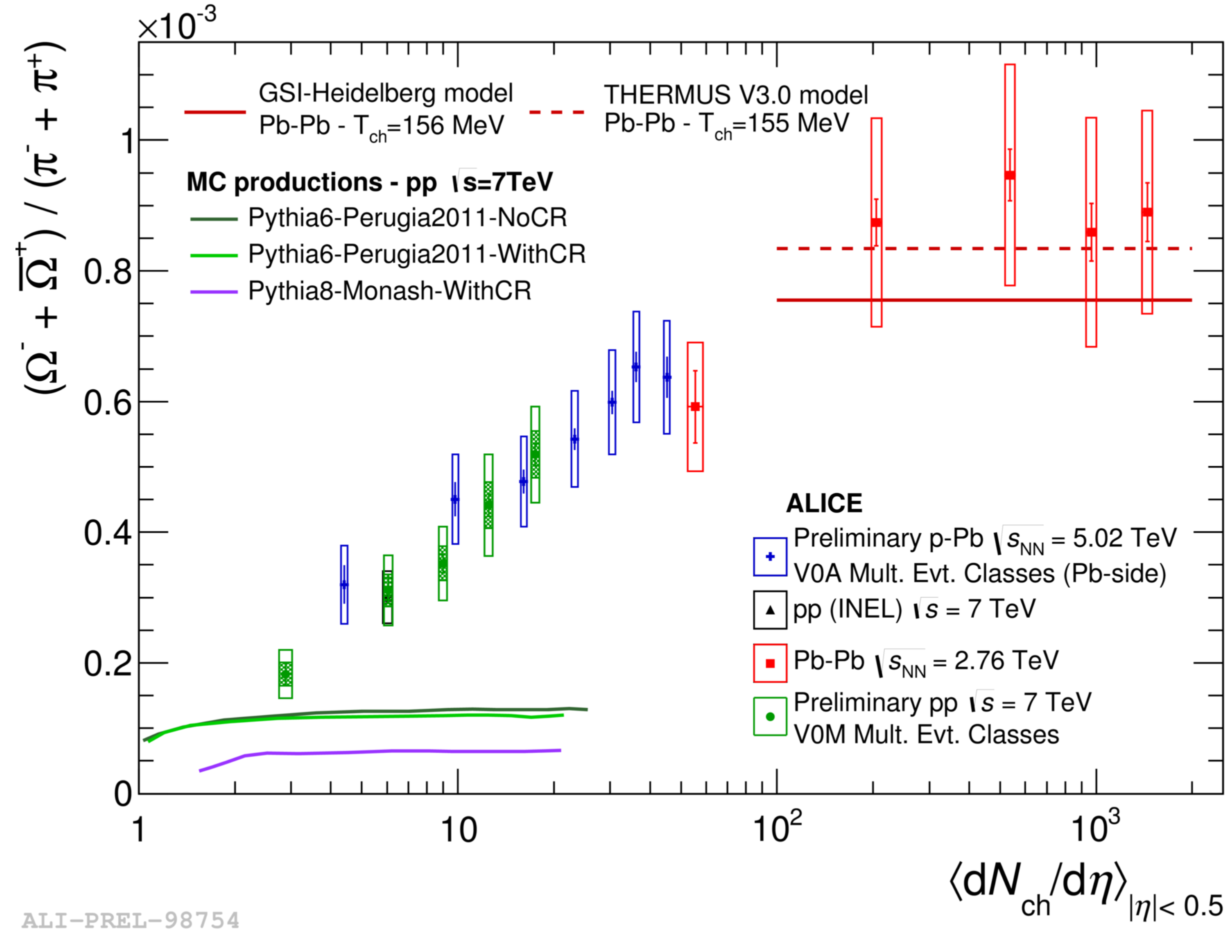

Increase of strangeness production with increasing multiplicity is even more pronounced for multi-strange particles.

Ξ/π reaches GC saturation value in highest multiplicity p-Pb collisions. Ω/π not quite.

Neither Pythia 6 nor 8 reproduces the data in any of the tunes tested.

Canonical suppression

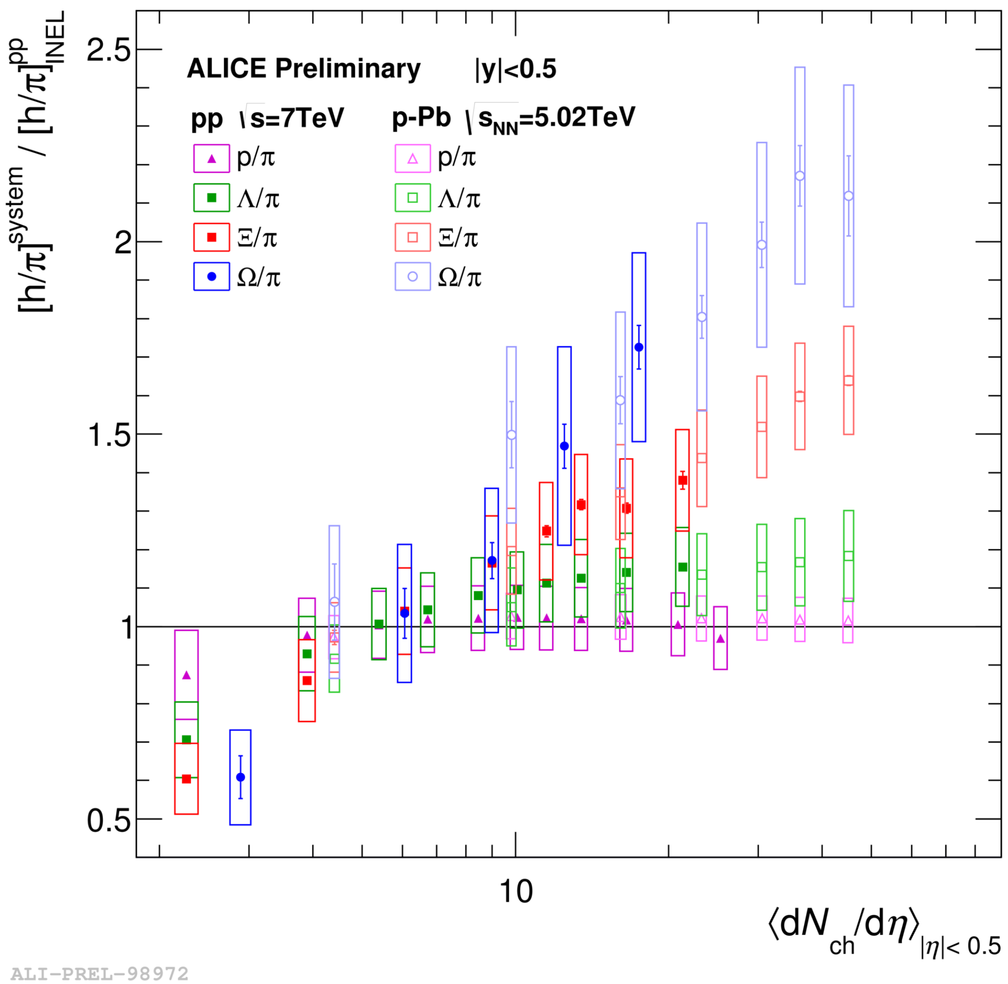

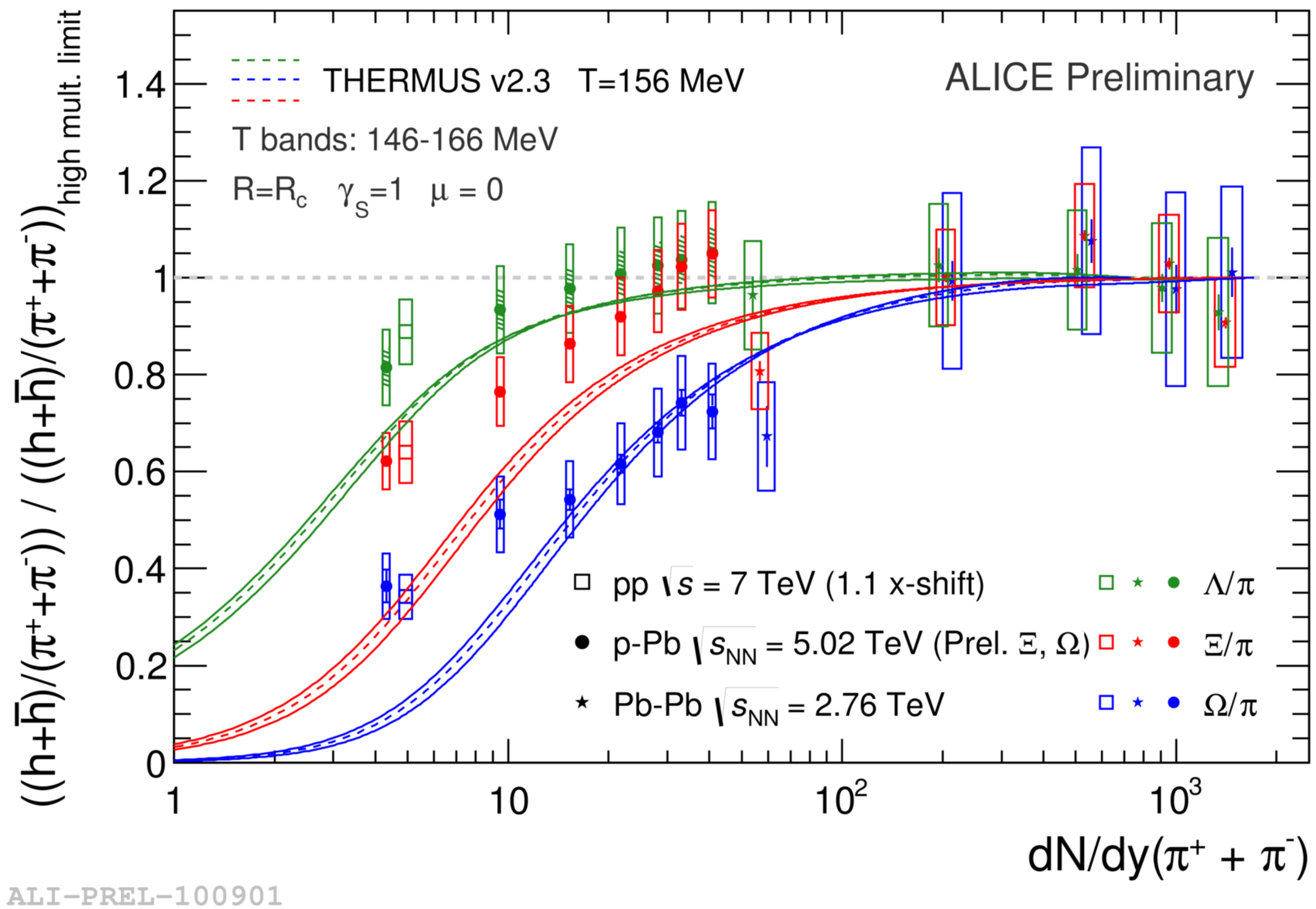

Canonical suppression

ALICE

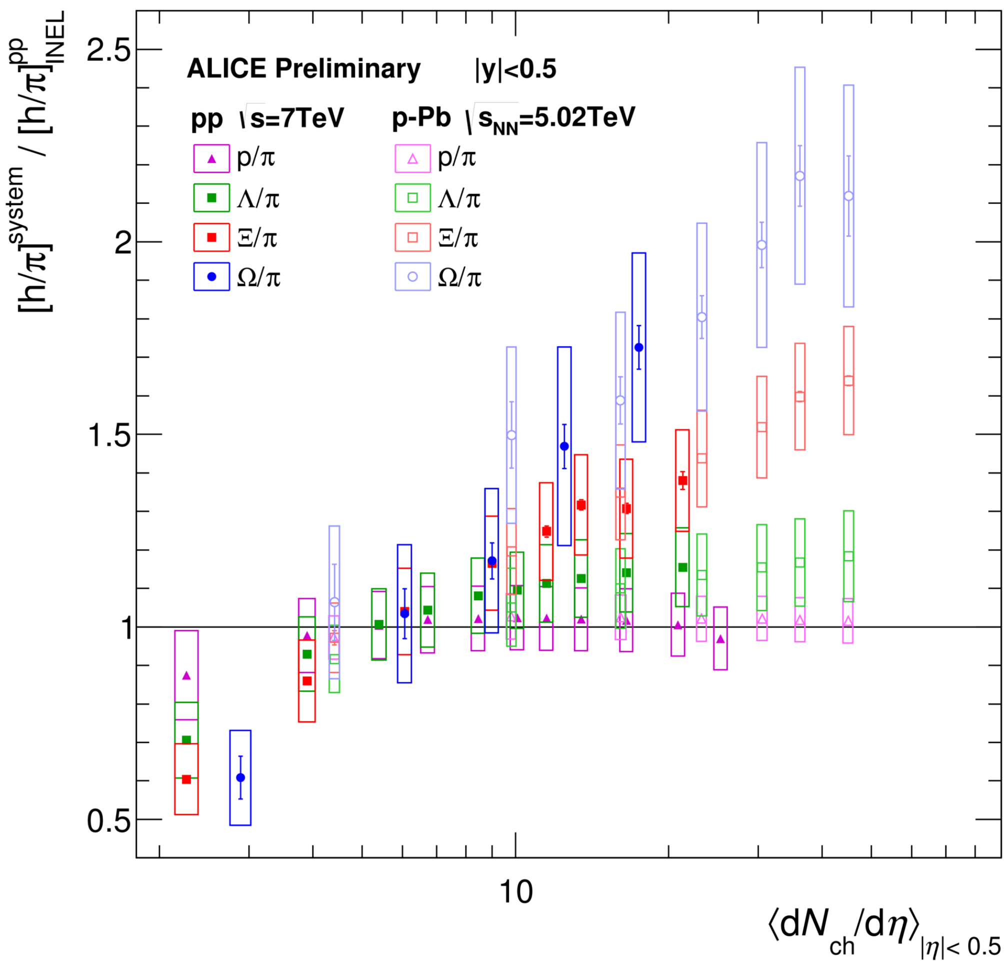

ALI-PREL-98972

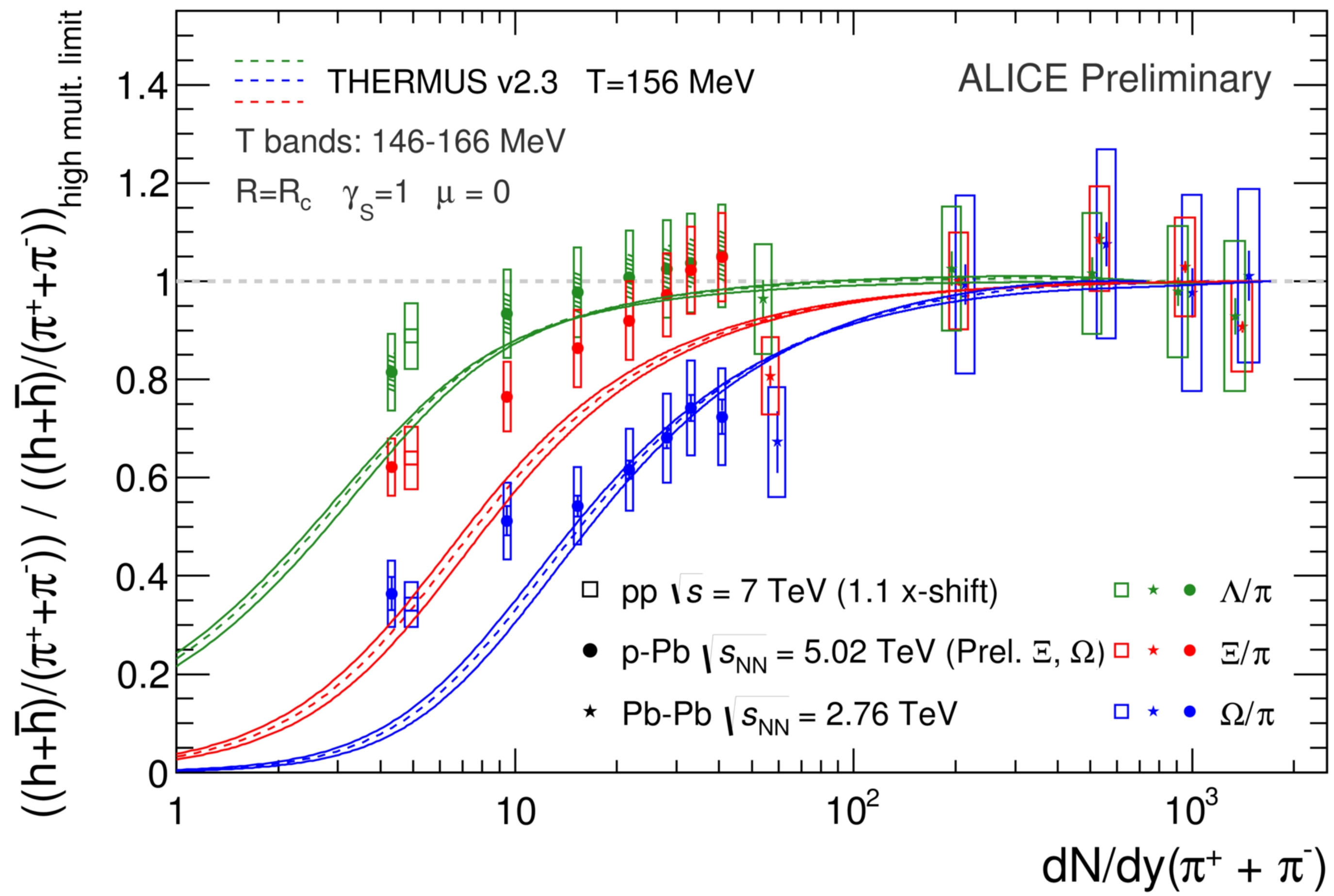

ALI-PREL-100901

p/π ratio does not change with multiplicity. Faster enhancement for Ω > Ξ > Λ.

Canonical suppression

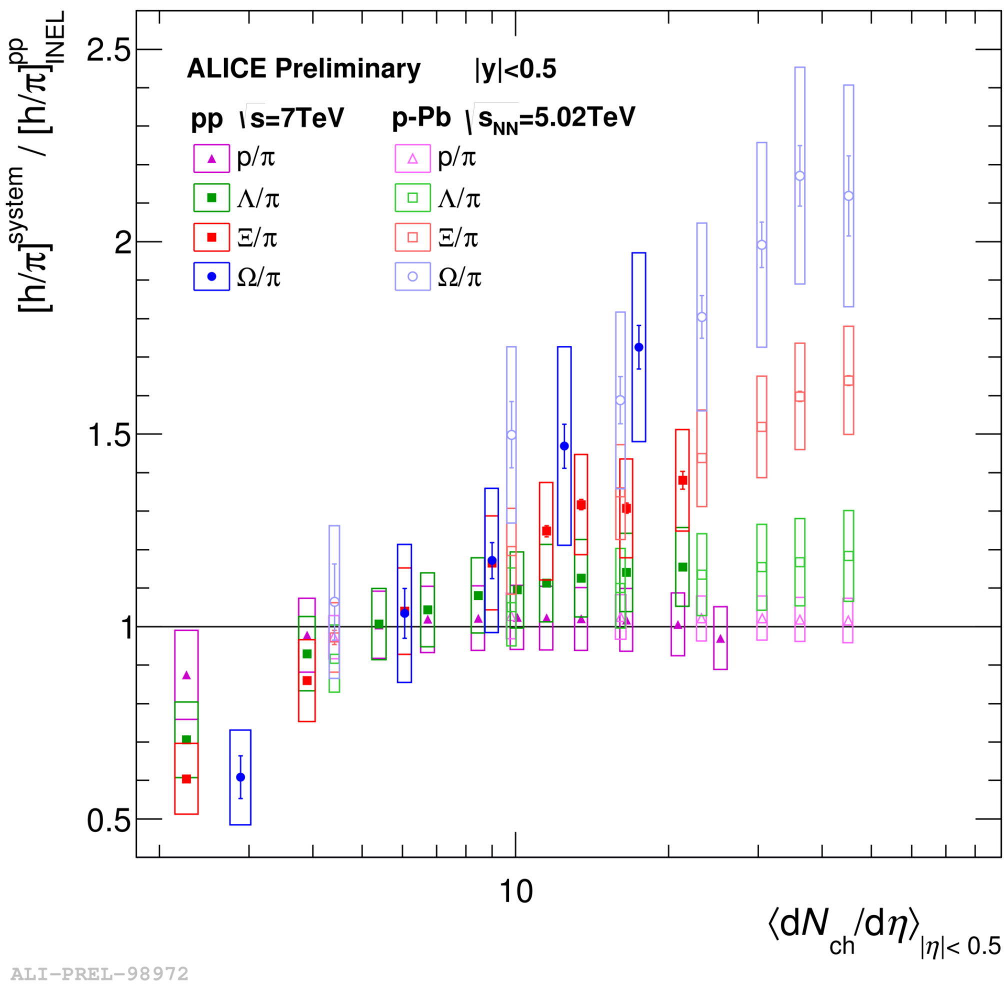

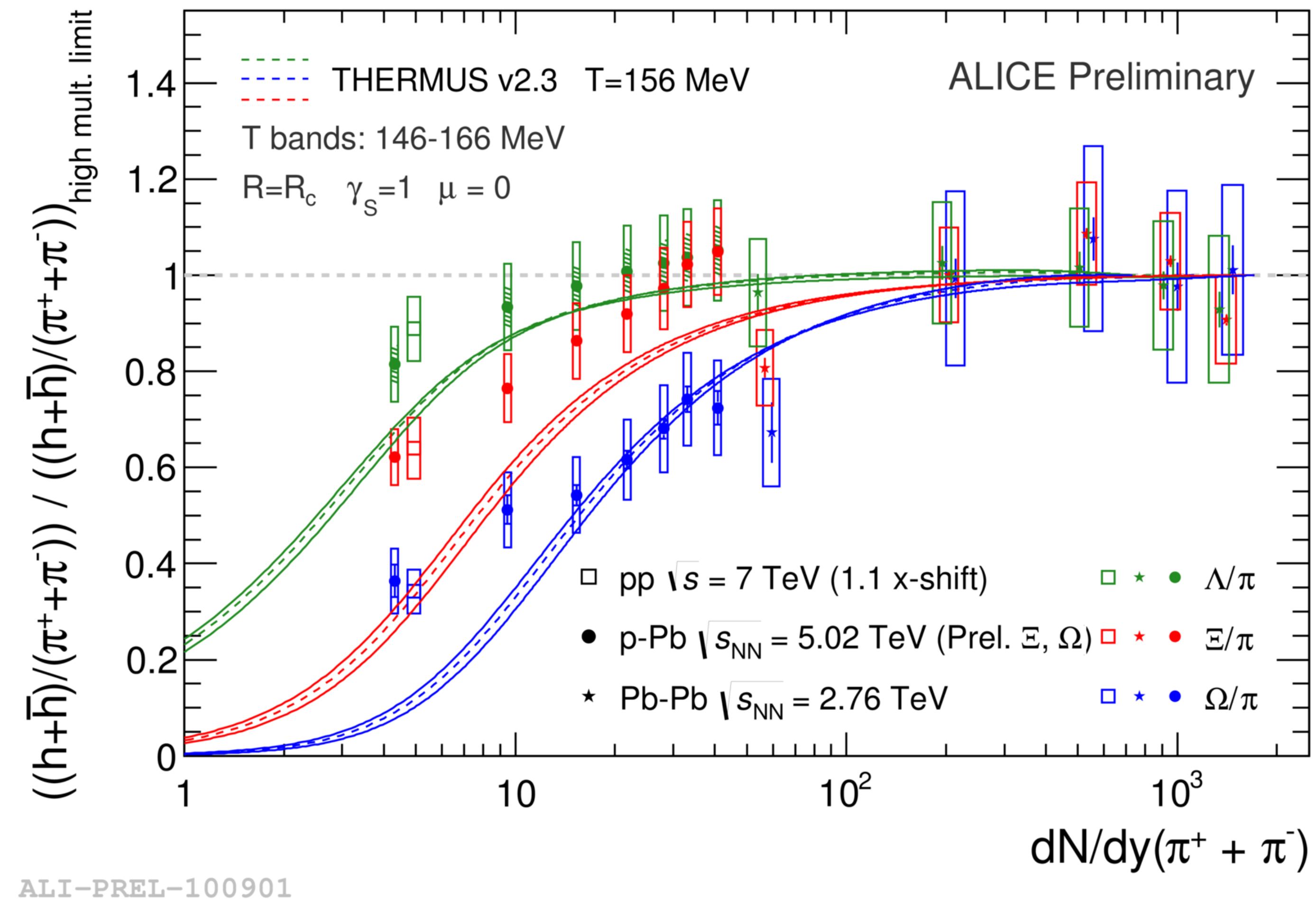

p/π ratio does not change with multiplicity. Faster enhancement for Ω > Ξ > Λ.

The effect is clearly strangeness and not baryon number related.

Canonical suppression

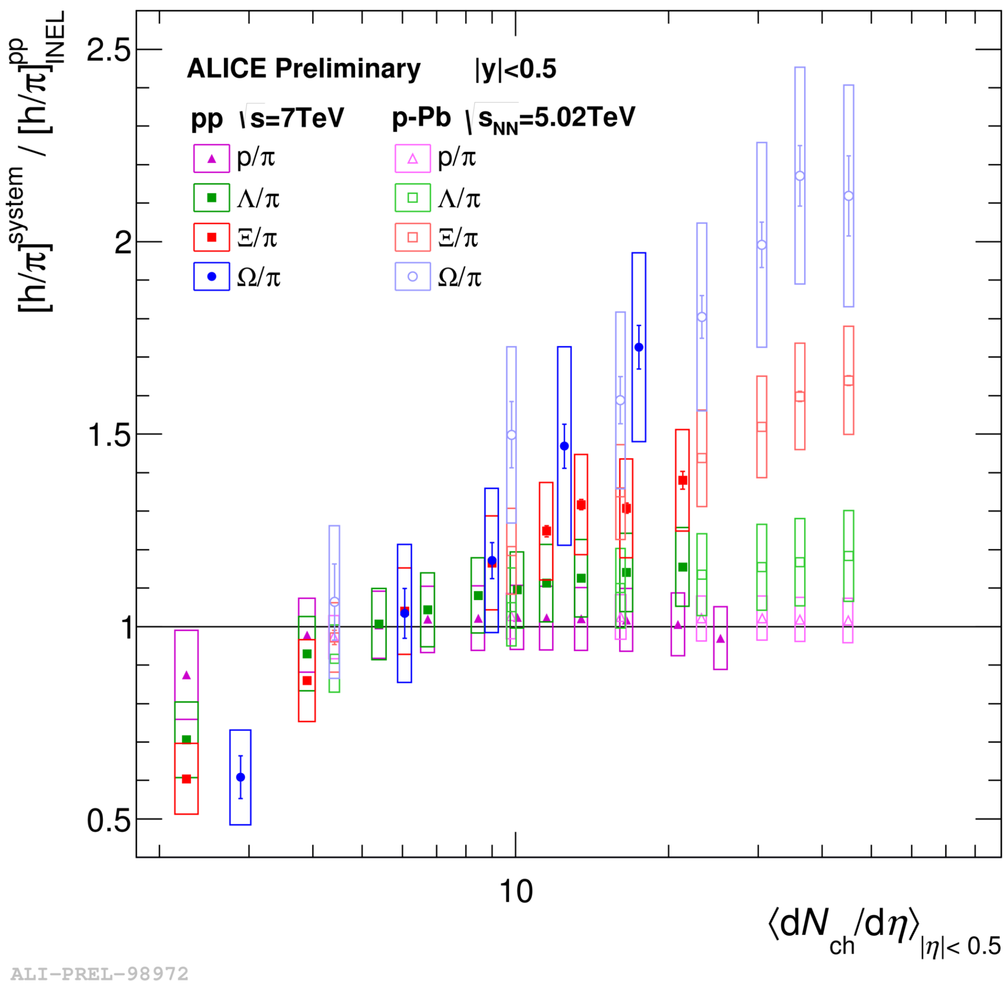

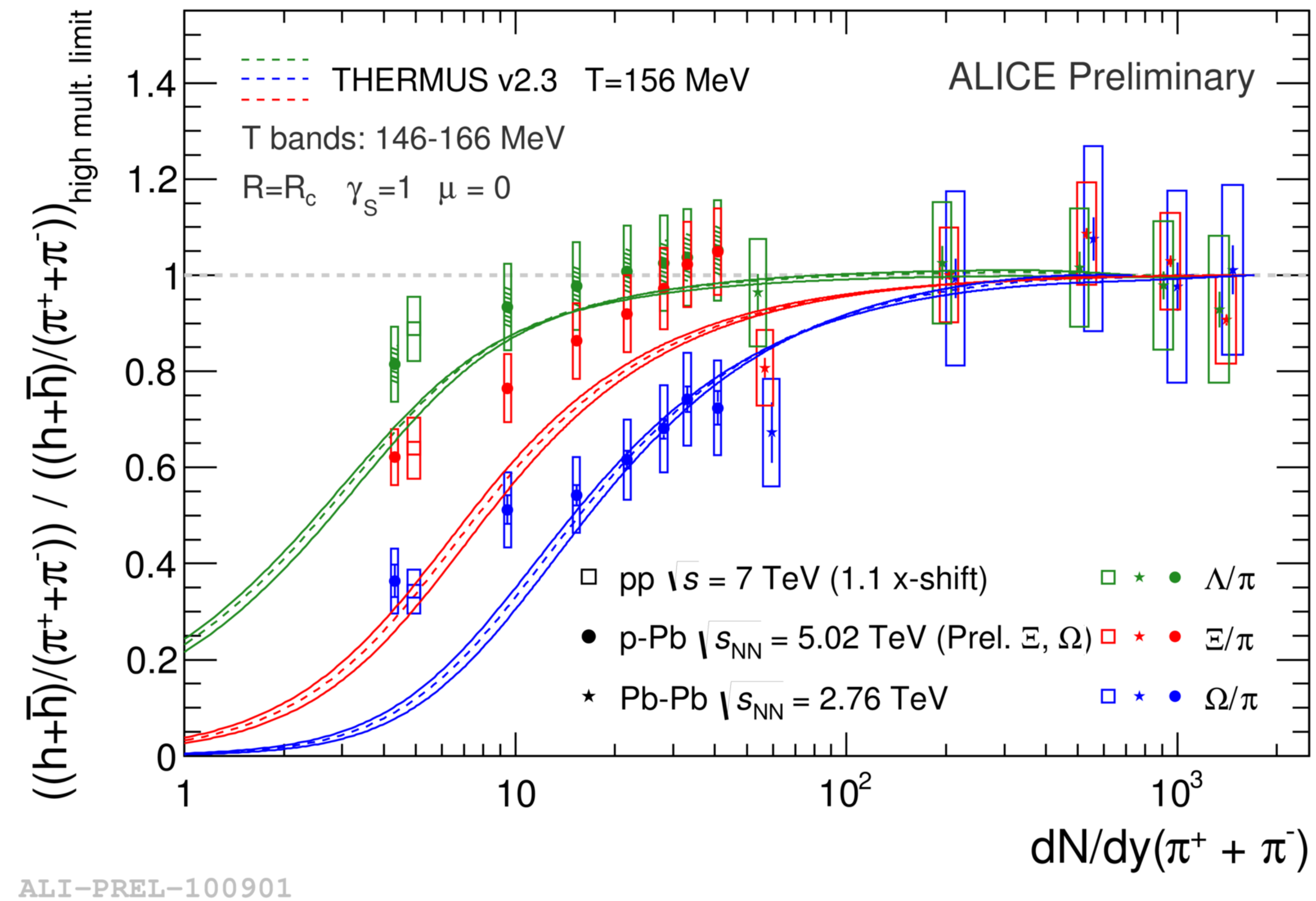

p/π ratio does not change with multiplicity. Faster enhancement for Ω > Ξ > Λ.

The effect is clearly strangeness and not baryon number related.

The behaviour can be qualitatively described by canonical suppression.

Blast-wave fits to p-Pb data

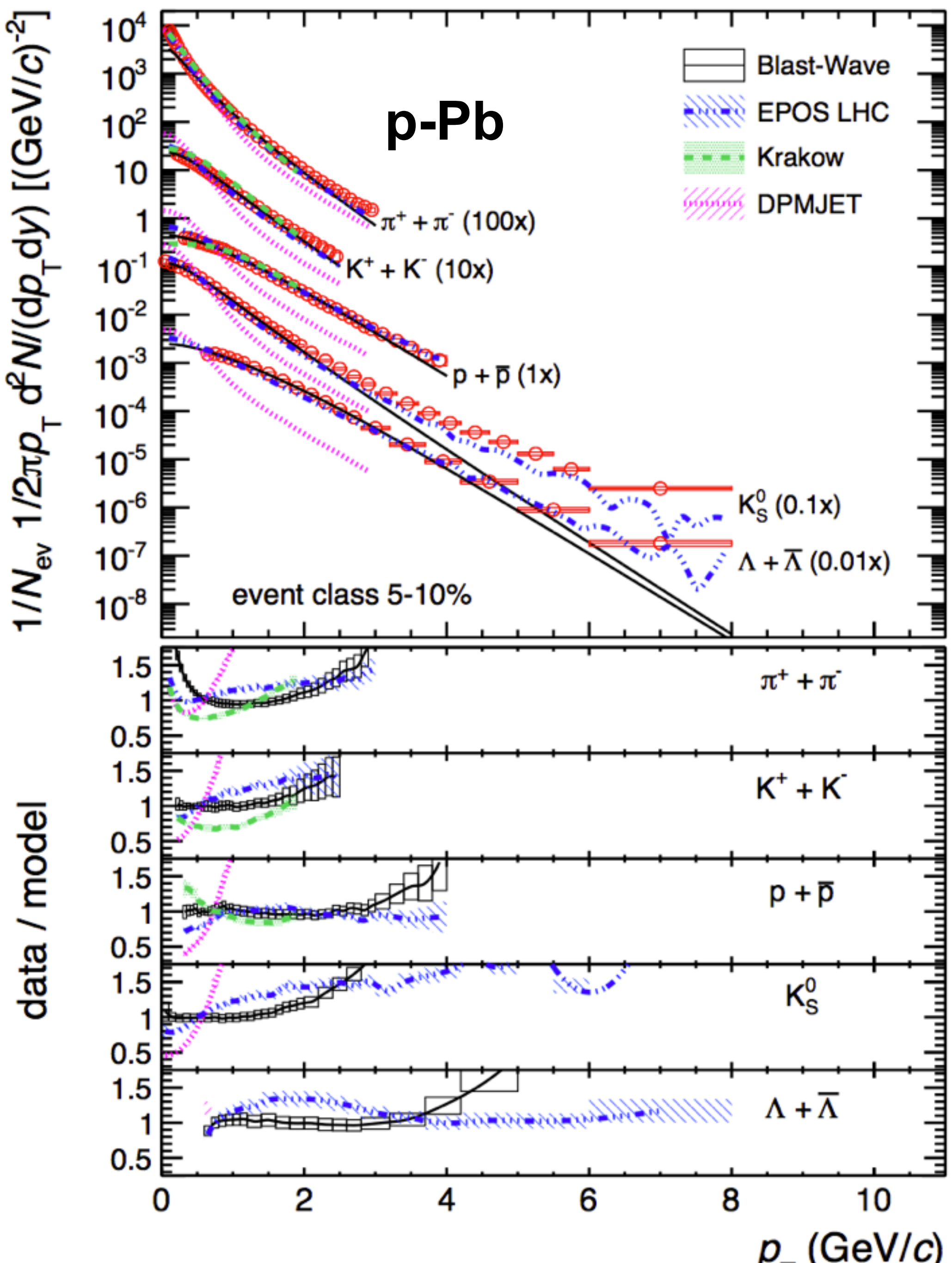

[Phys. Lett. B 728 (2014) 25-38]

Blast-wave fits to p-Pb data

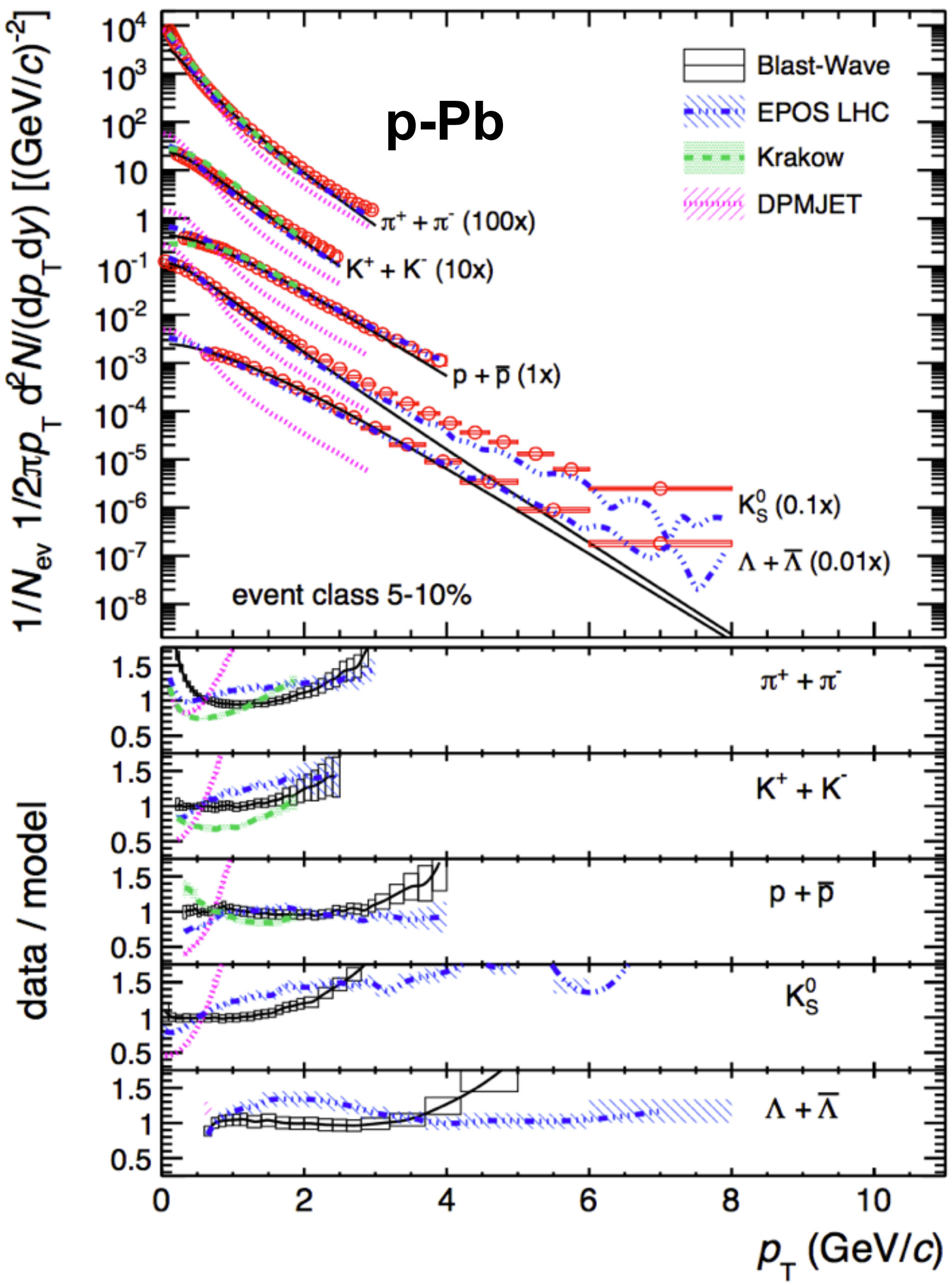

[Phys. Lett. B 728 (2014) 25-38]

Hydrodynamic models (EPOS, Krakow) show a better agreement than QCD inspired models (DPMJET).

Blast-wave fits to p-Pb data

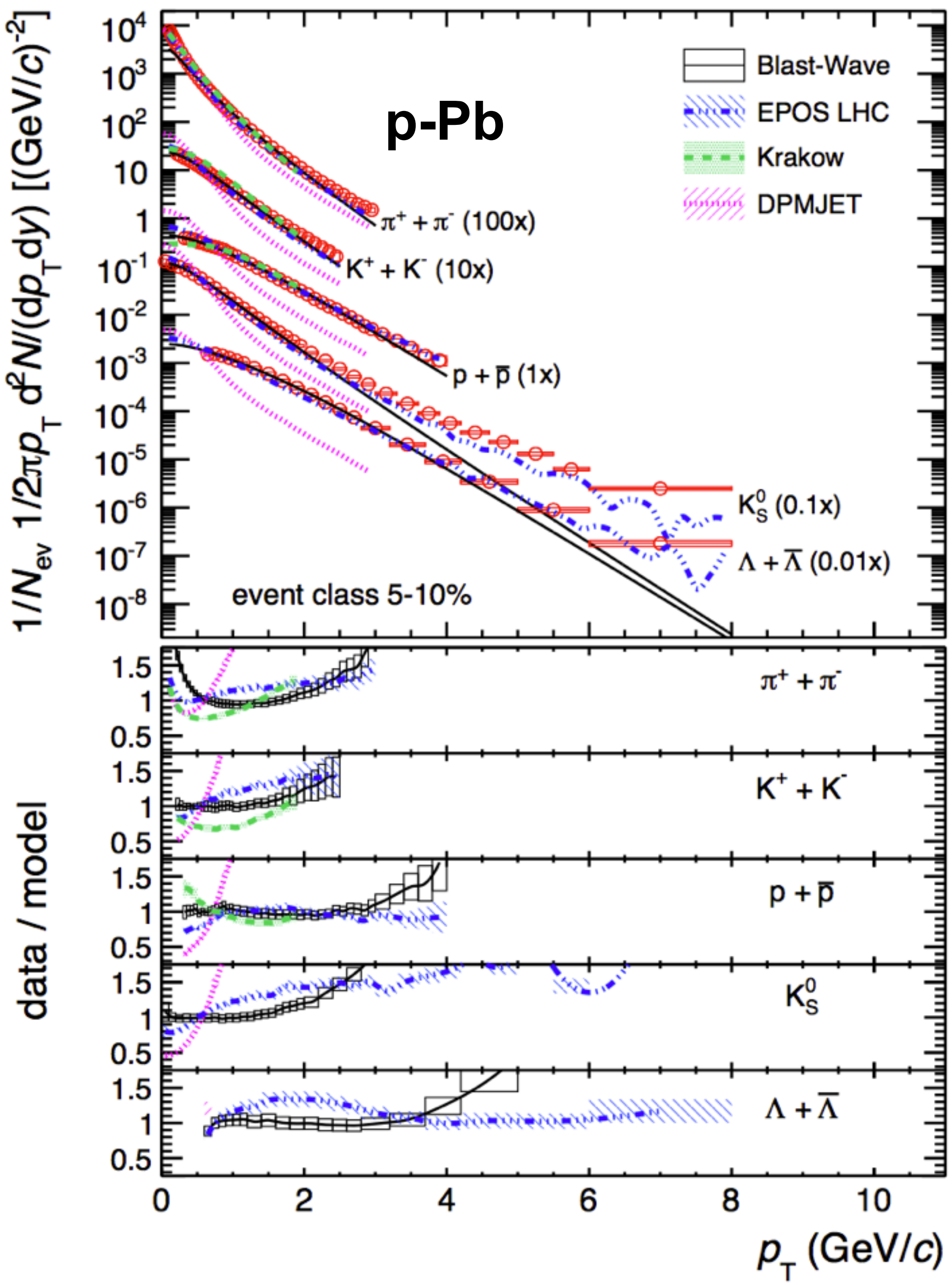

[Phys. Lett. B 728 (2014) 25-38]

Hydrodynamic models (EPOS, Krakow) show a better agreement than QCD inspired models (DPMJET).

A combined blast-wave fit to the data gives a reasonable description also here.

Blast-wave fits to p-Pb data

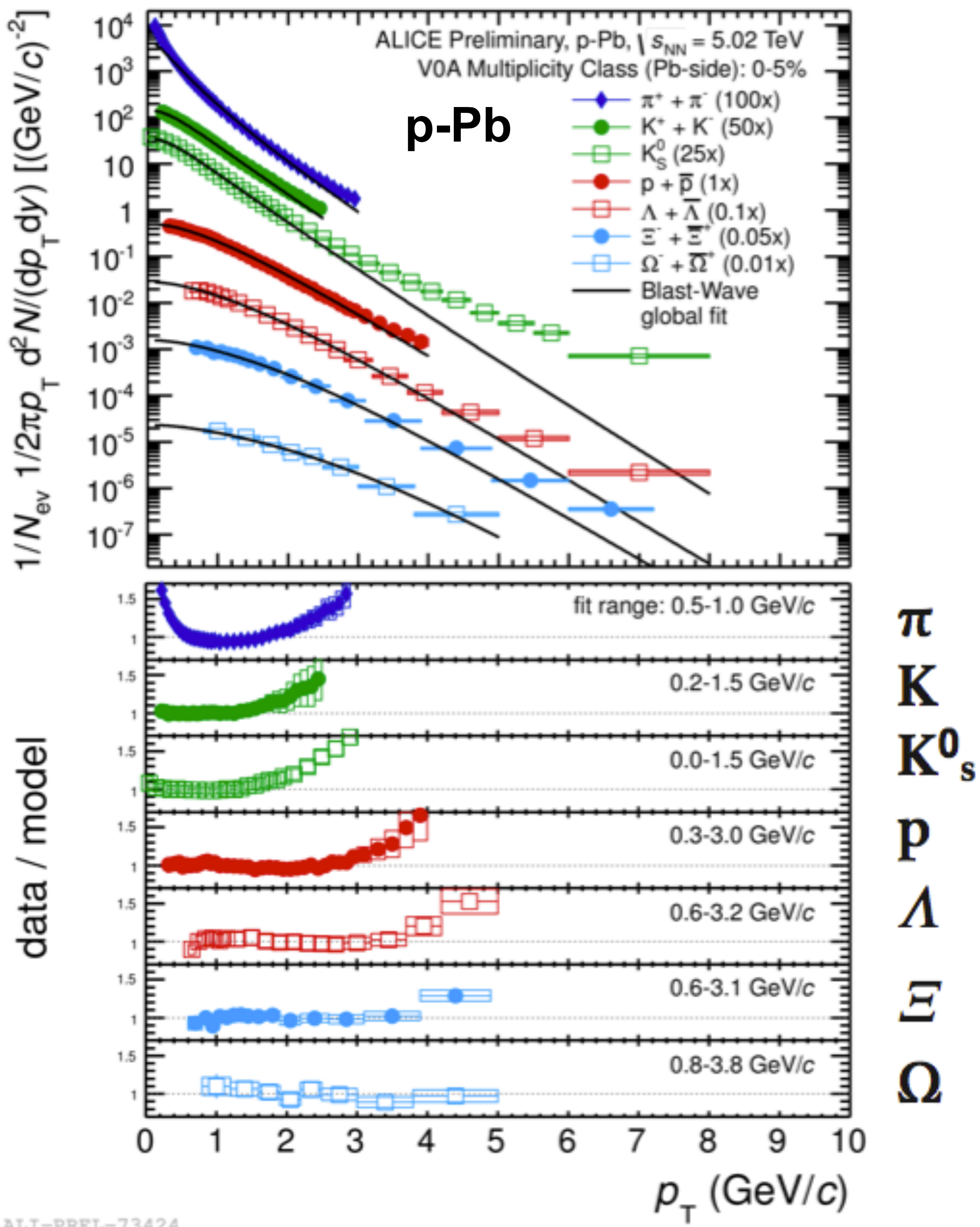

Hydrodynamic models (EPOS, Krakow) show a better agreement than QCD inspired models (DPMJET).

A combined blast-wave fit to the data gives a reasonable description also here.

Blast-wave fits to p-Pb data

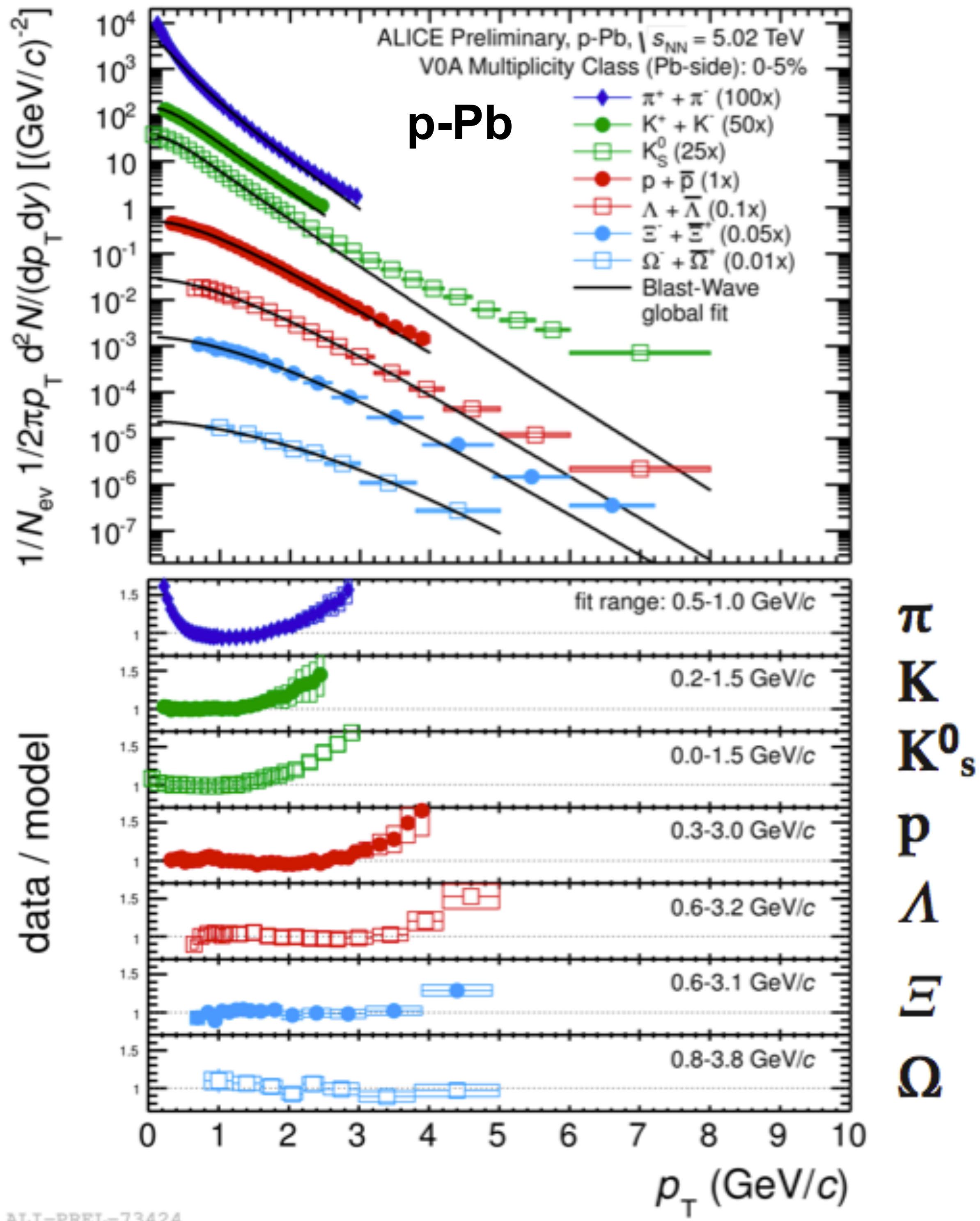

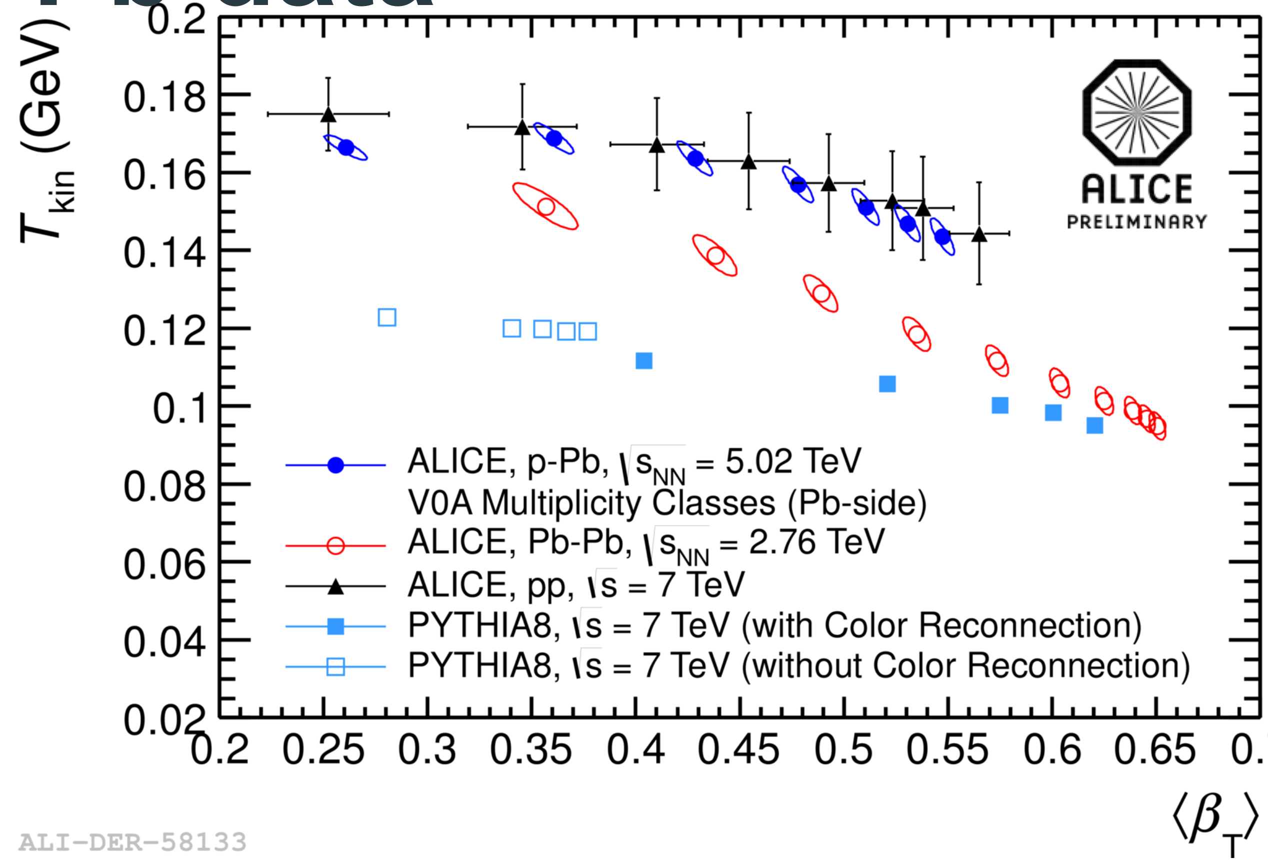

Hydrodynamic models (EPOS, Krakow) show a better agreement than QCD inspired models (DPMJET).

A combined blast-wave fit to the data gives a reasonable description also here.

Blast-wave fits to p-Pb data

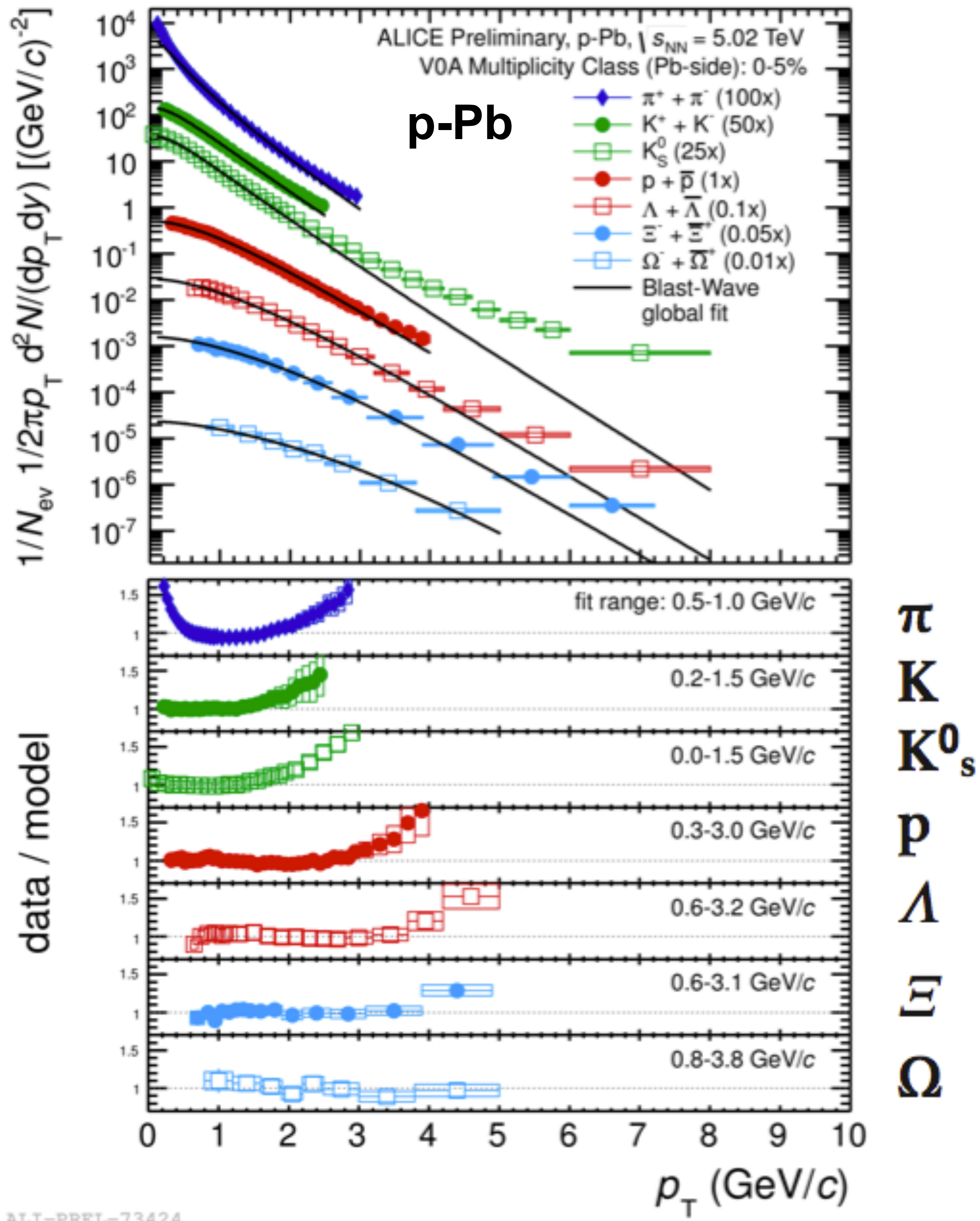

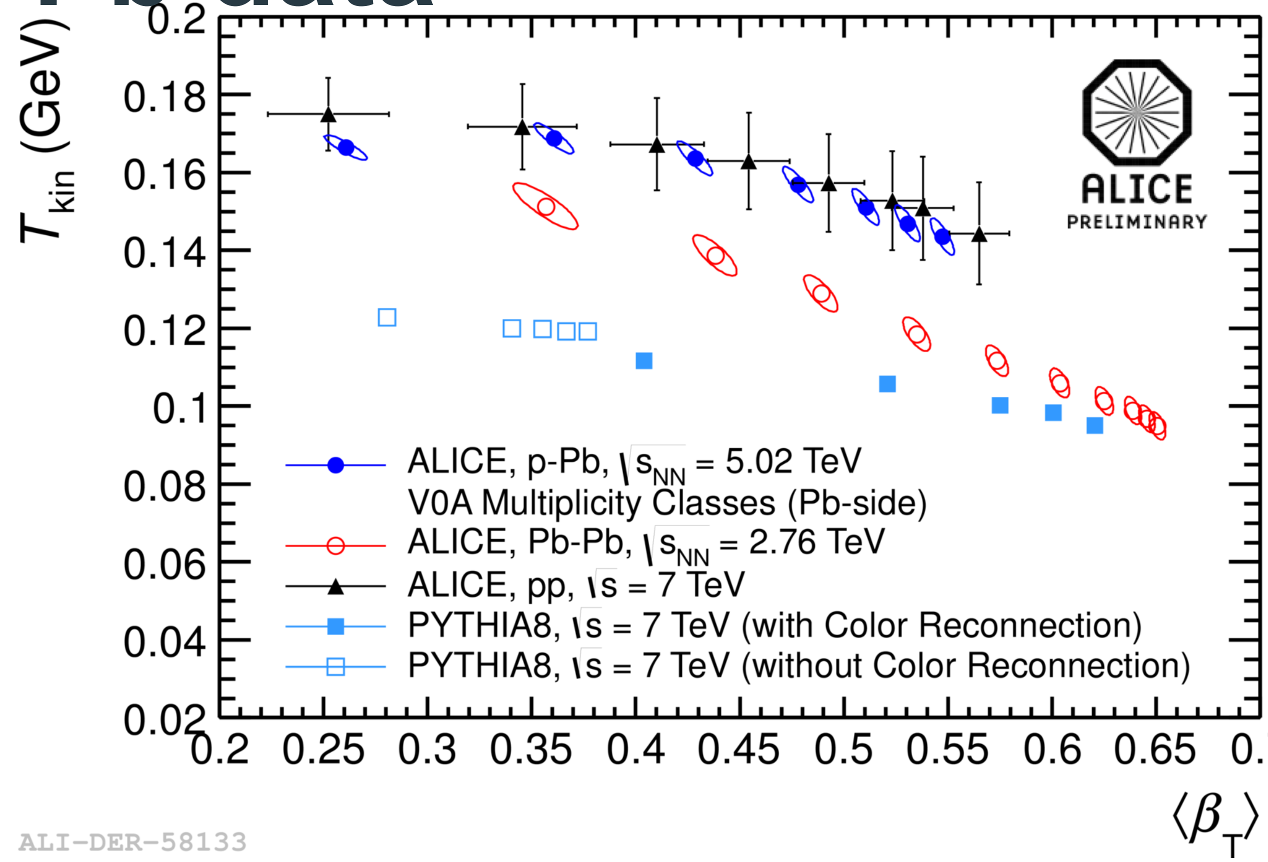

Hydrodynamic models (EPOS, Krakow) show a better agreement than QCD inspired models (DPMJET).

A combined blast-wave fit to the data gives a reasonable description also here.

p-Pb and Pb-Pb data follow the same trend → consistent with a collective expansion.

Blast-wave fits to p-Pb data

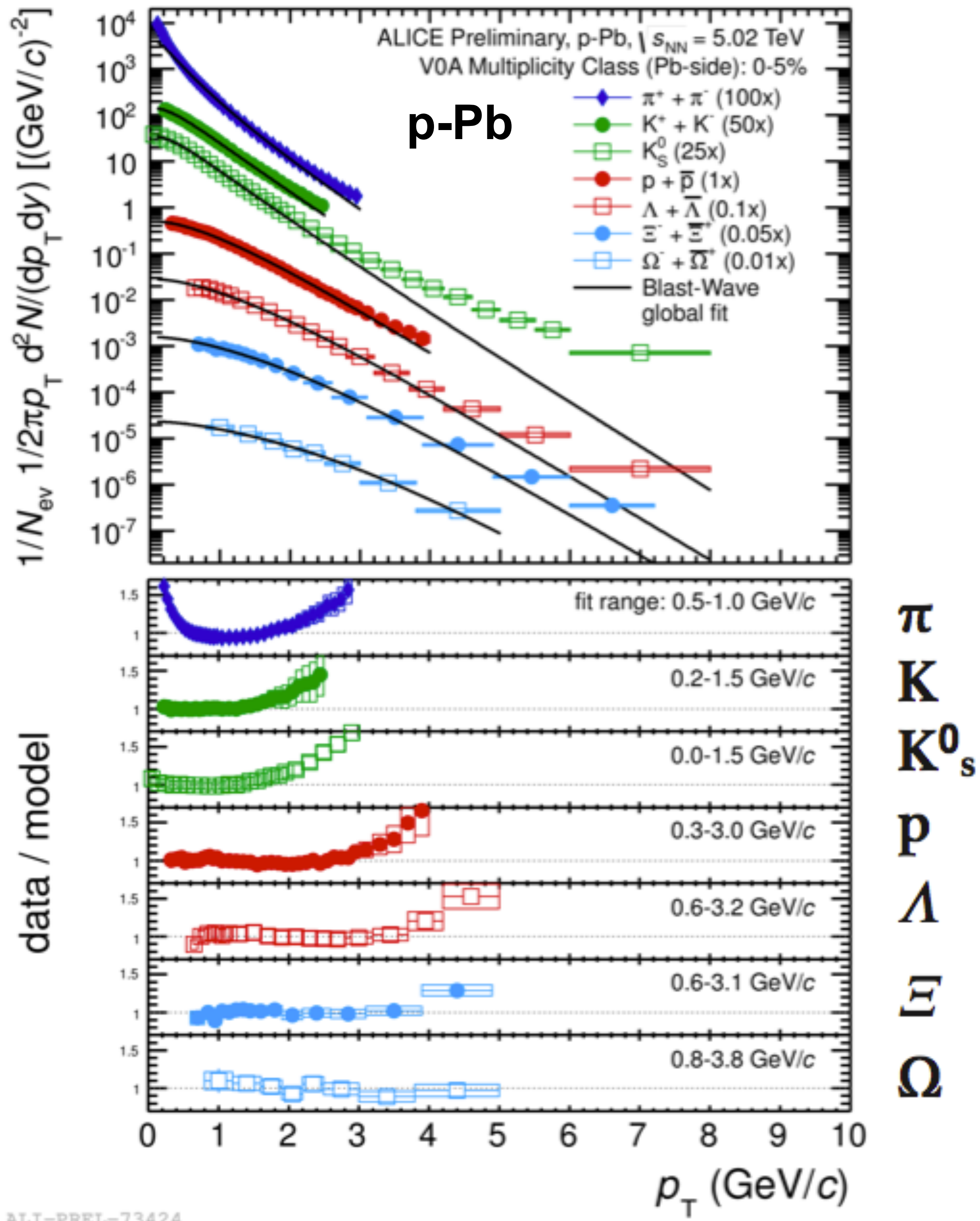

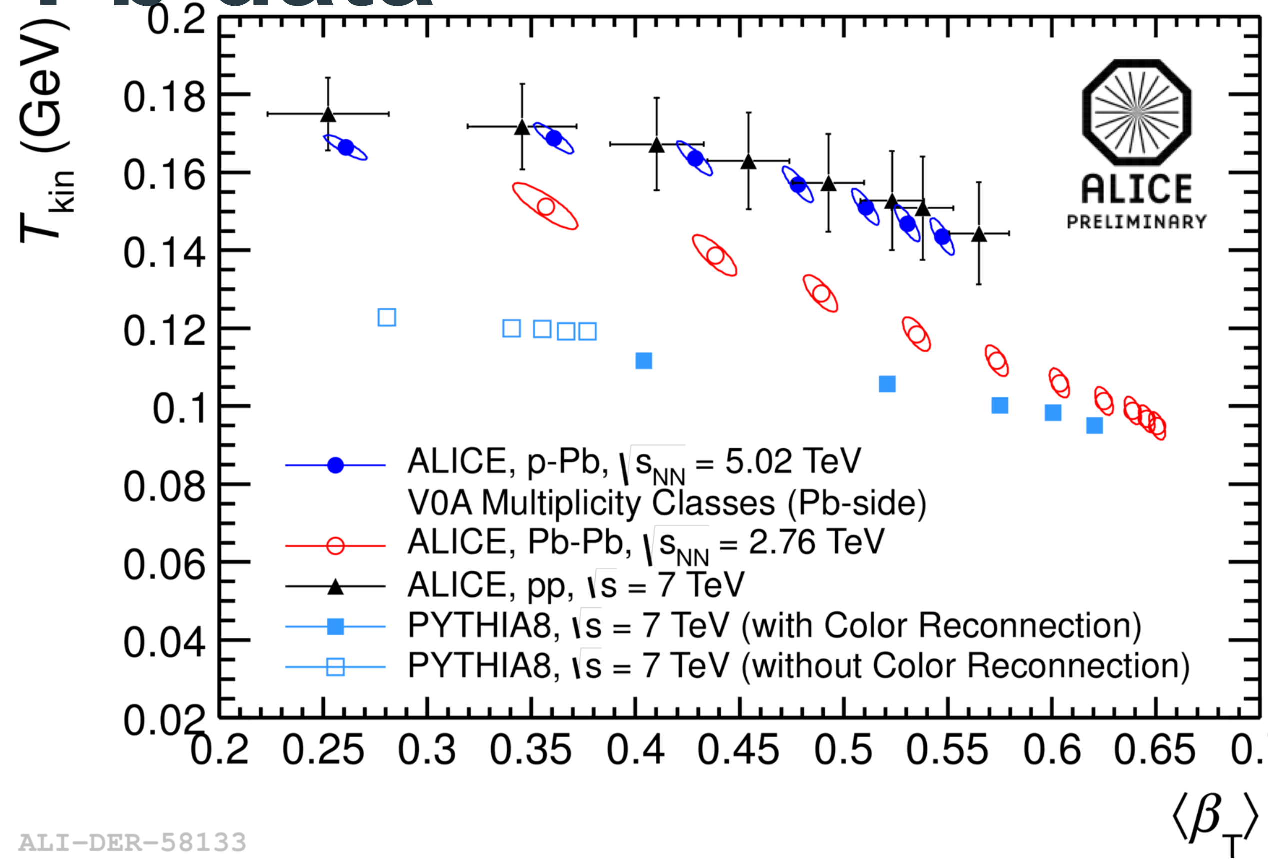

Hydrodynamic models (EPOS, Krakow) show a better agreement than QCD inspired models (DPMJET).

A combined blast-wave fit to the data gives a reasonable description also here.

p-Pb and Pb-Pb data follow the same trend → consistent with a collective expansion.

PYTHIA 8 with color reconnection shows a similar trend (without hydrodynamic flow).

Blast-wave fits to p-Pb data

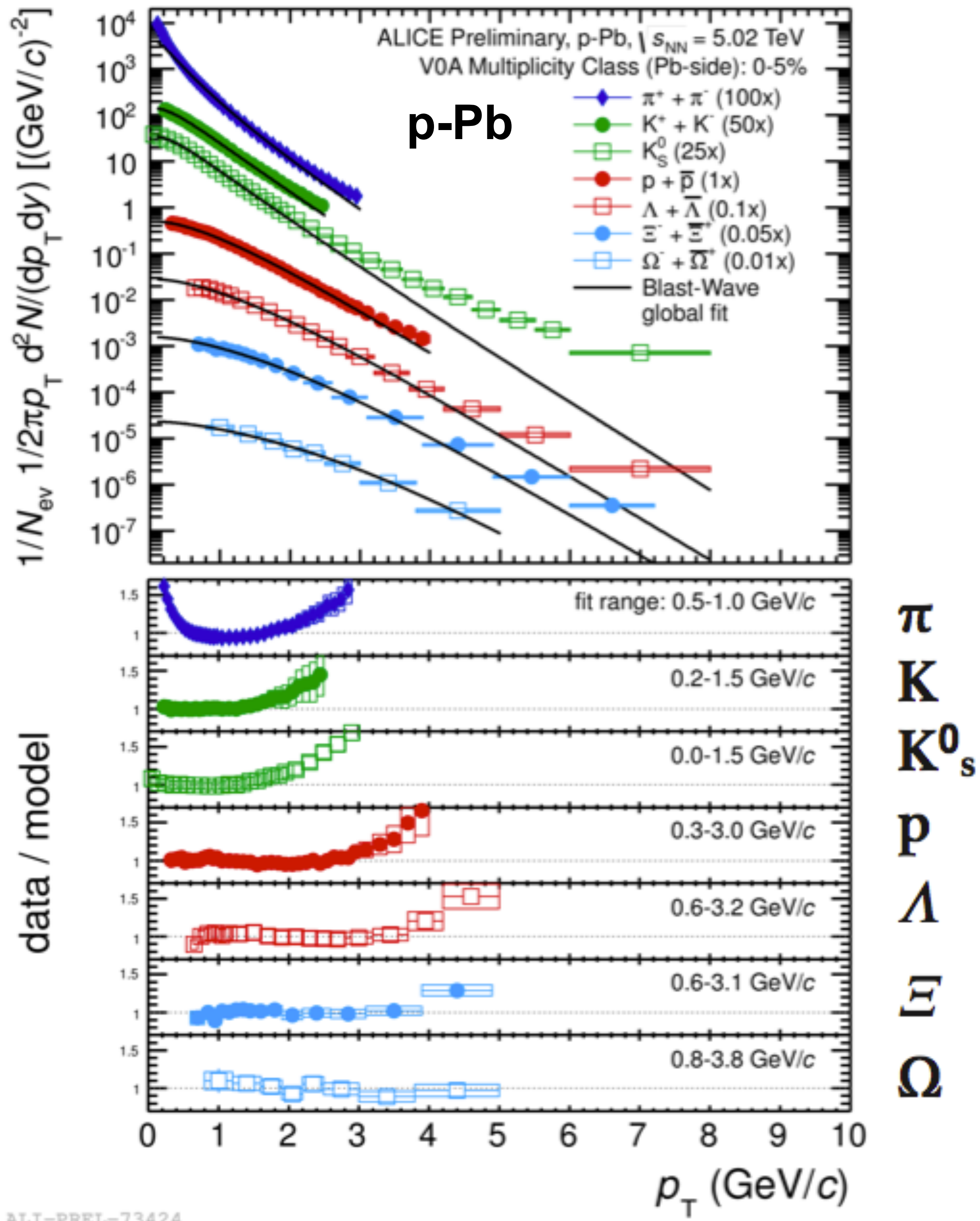

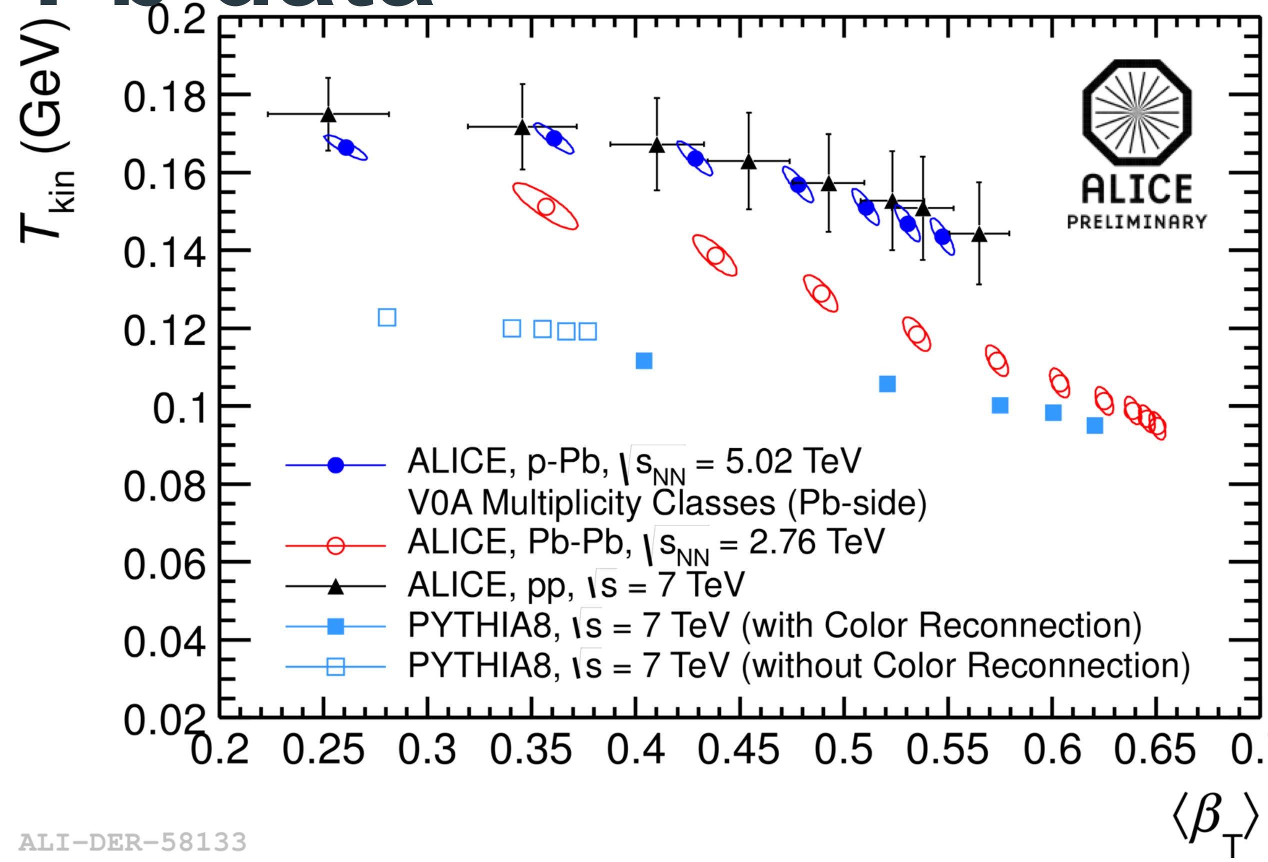

Hydrodynamic models (EPOS, Krakow) show a better agreement than QCD inspired models (DPMJET).

A combined blast-wave fit to the data gives a reasonable description also here.

p-Pb and Pb-Pb data follow the same trend → consistent with a collective expansion.

PYTHIA 8 with color reconnection shows a similar trend (without hydrodynamic flow).

Other effects can mimic flow-like patterns! And also pp data shows a similar trend..

Direct photons and hard probes

Direct photons in Pb-Pb

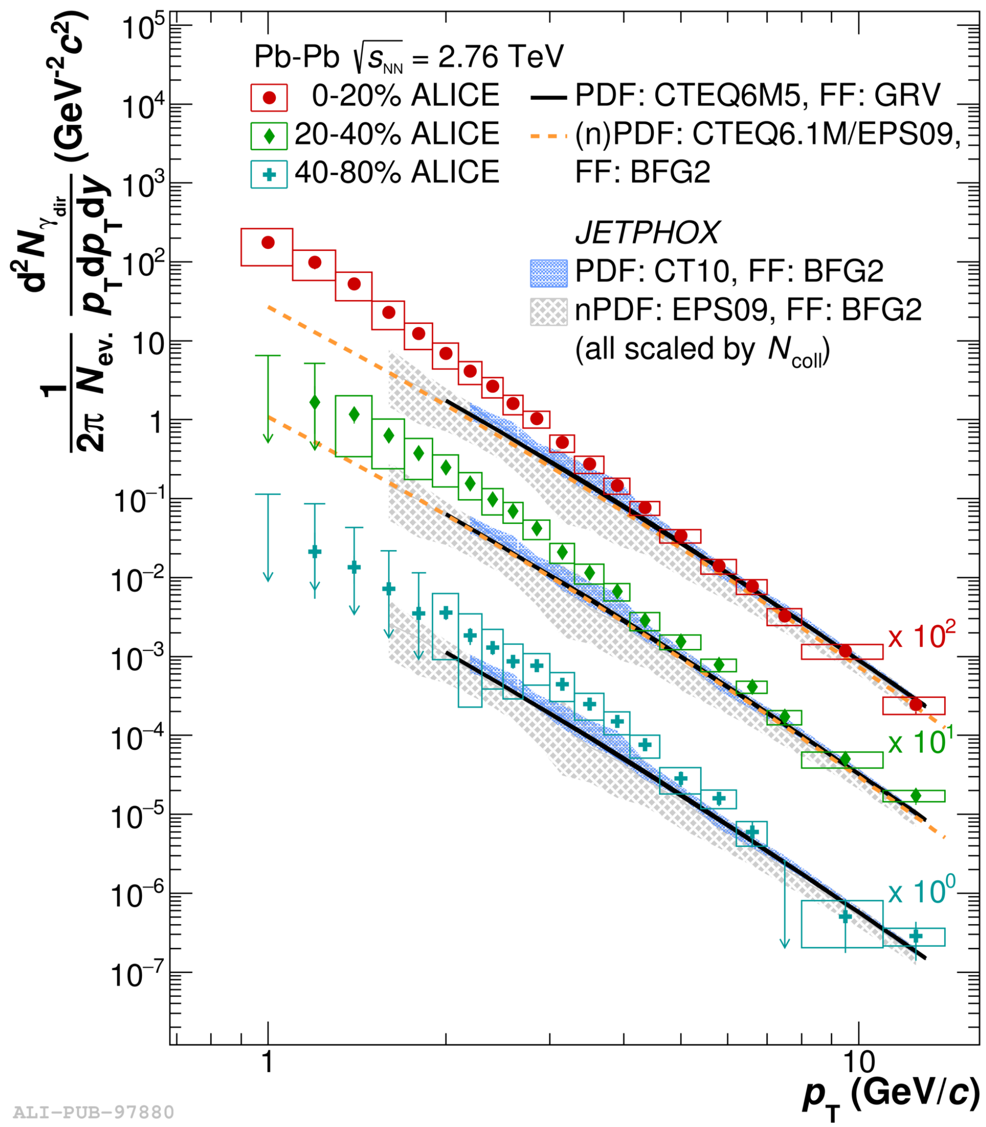

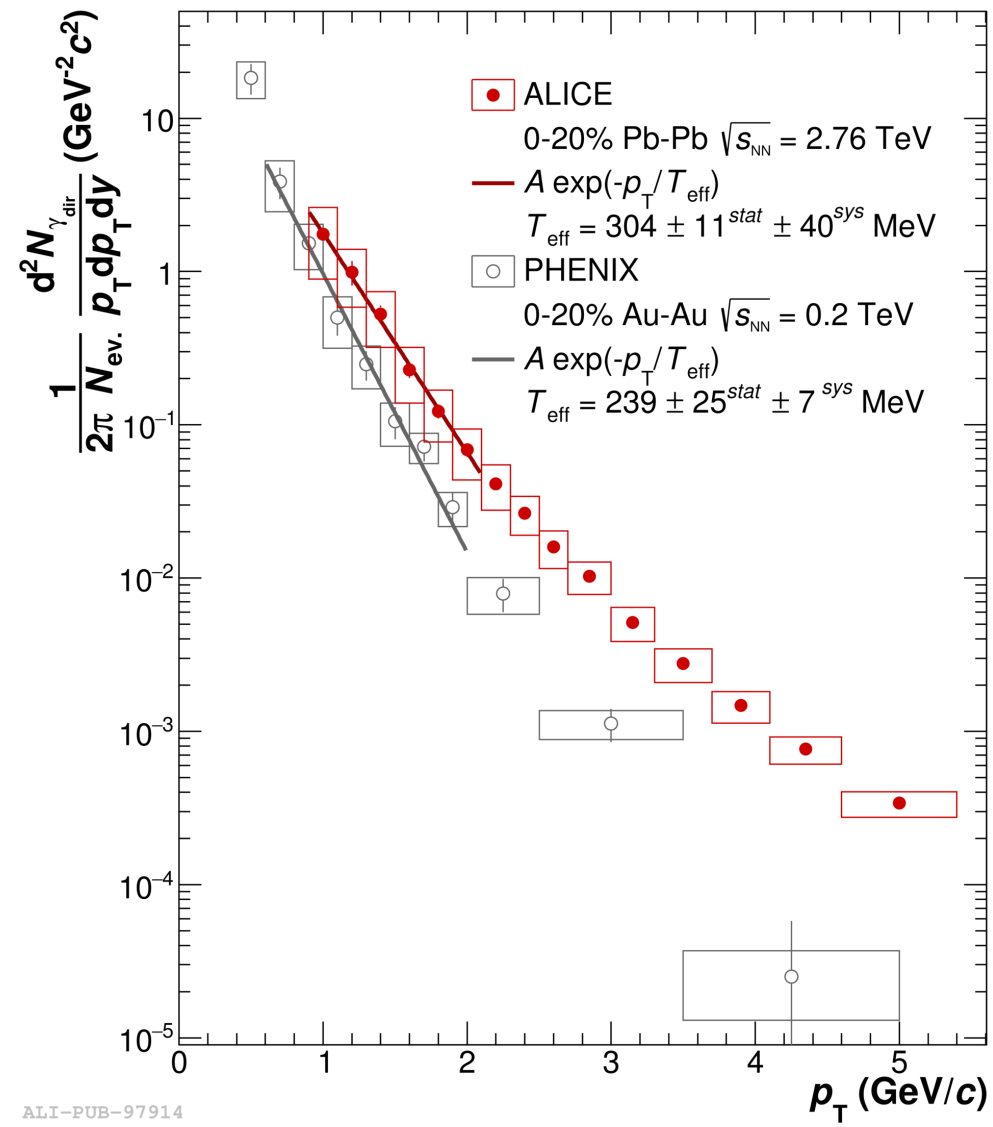

[arXiv:1509.07324]

Direct photons in Pb-Pb

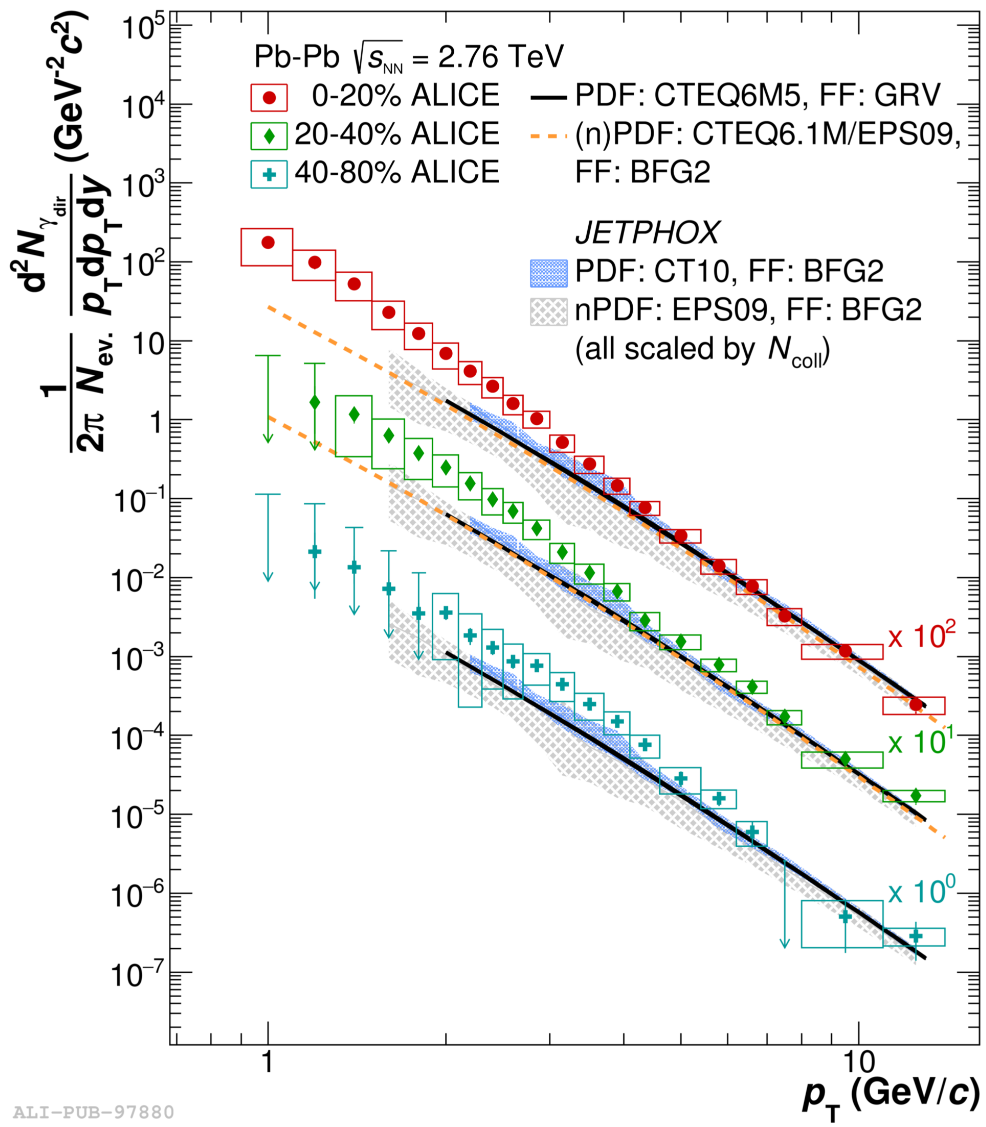

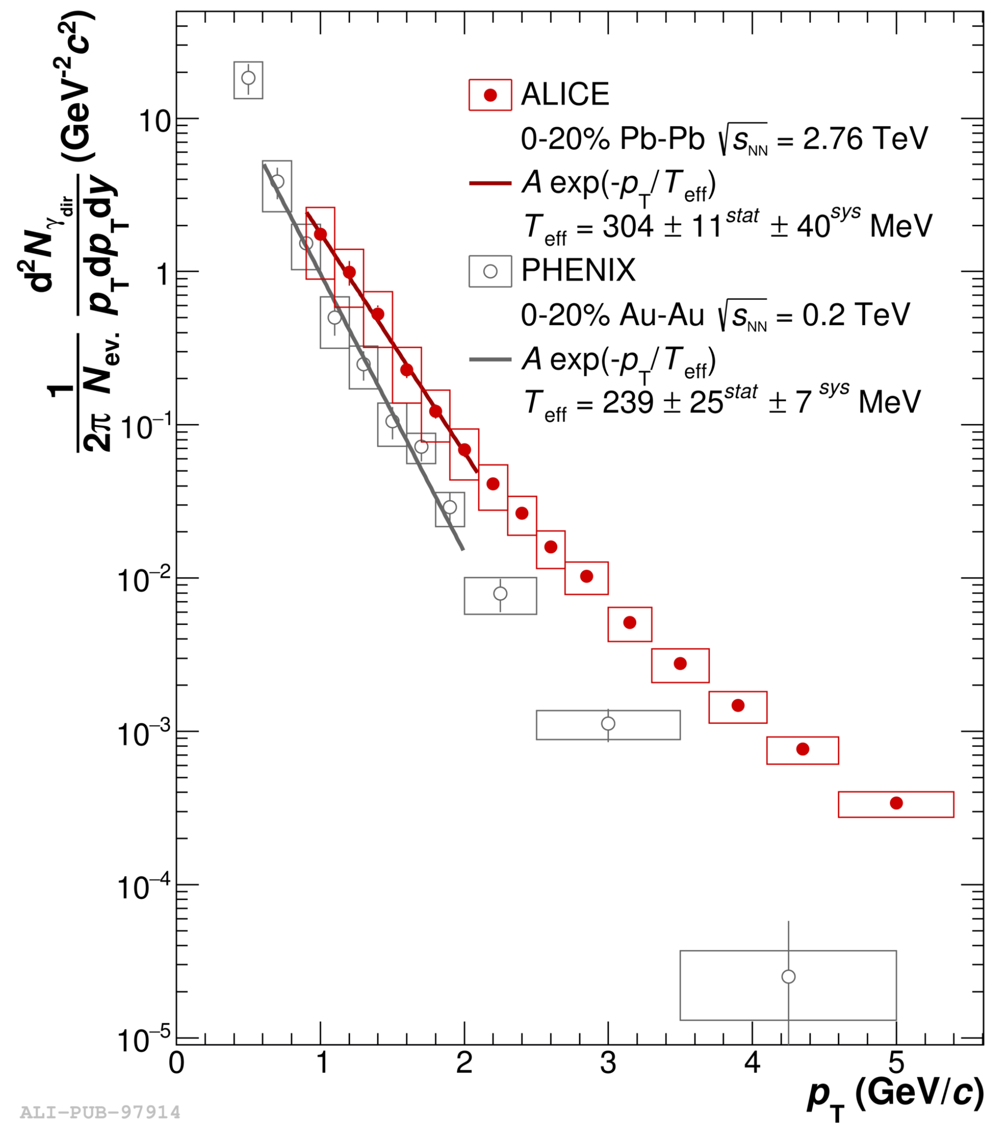

2.6σ excess at low p_T in 0-20% most central collisions.

[arXiv:1509.07324]

Direct photons in Pb-Pb

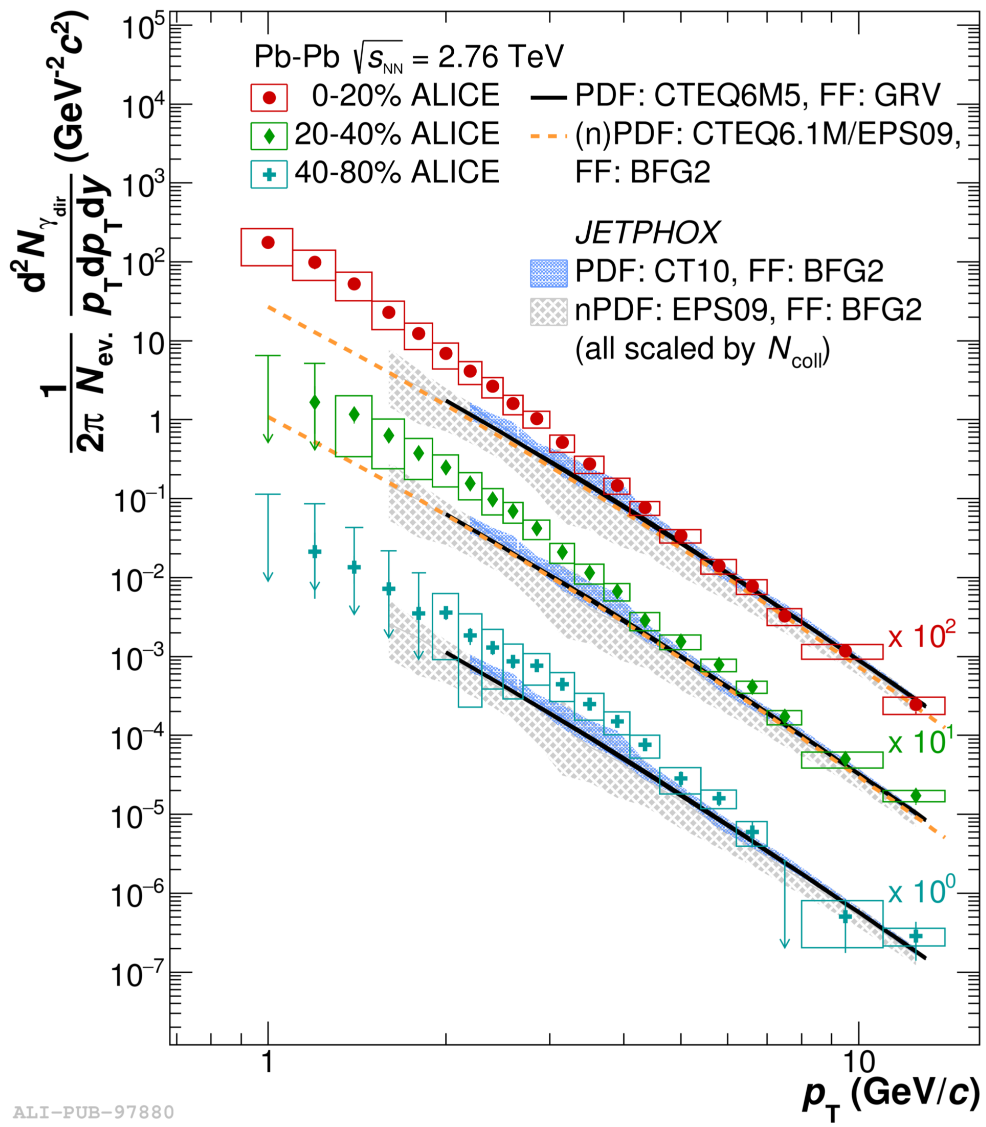

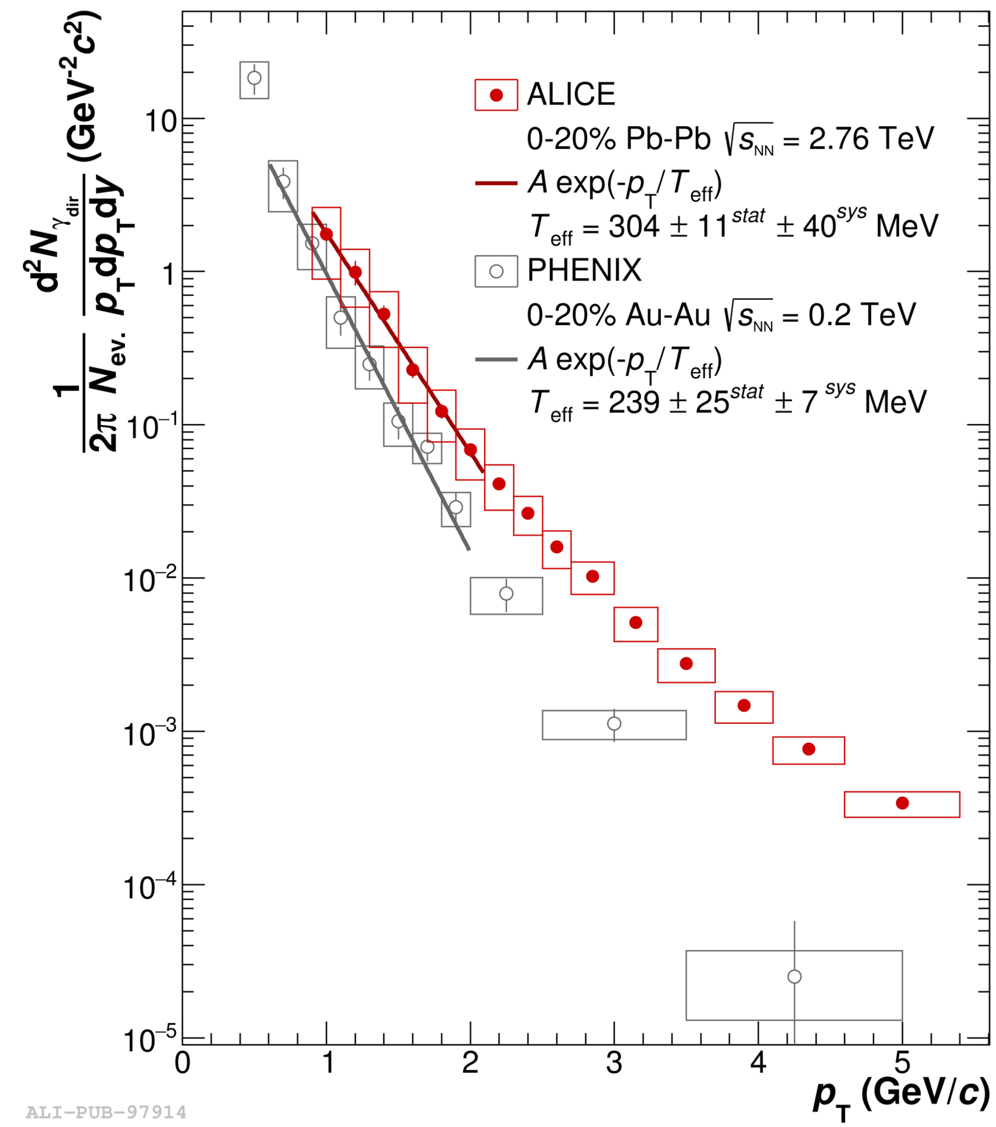

2.6σ excess at low p_T in 0-20% most central collisions.

T_{eff} = 304 ± 11 ± 40 MeV
Higher initial temperature and larger blue shift by stronger radial flow.

[arXiv:1509.07324]

Jet shapes

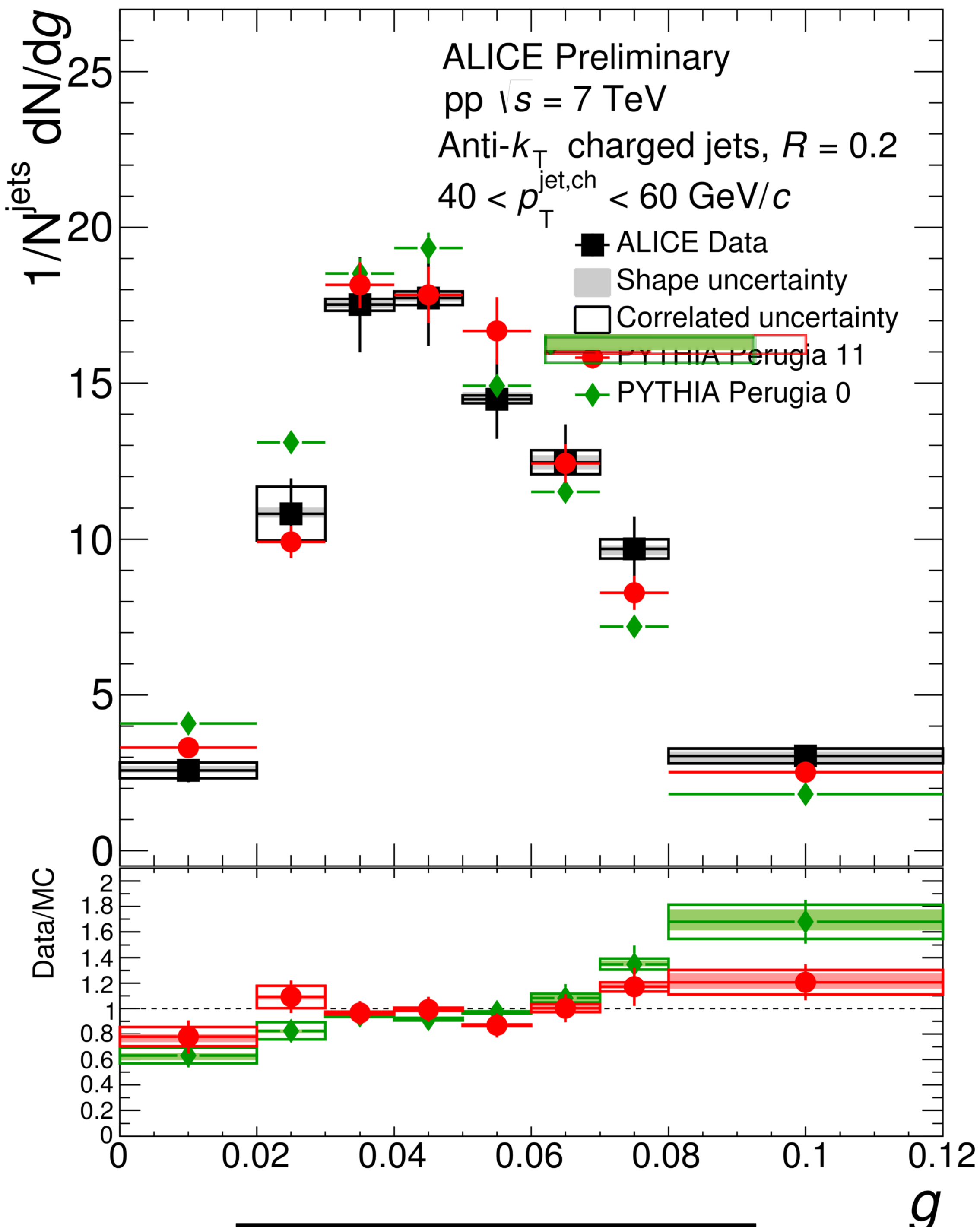

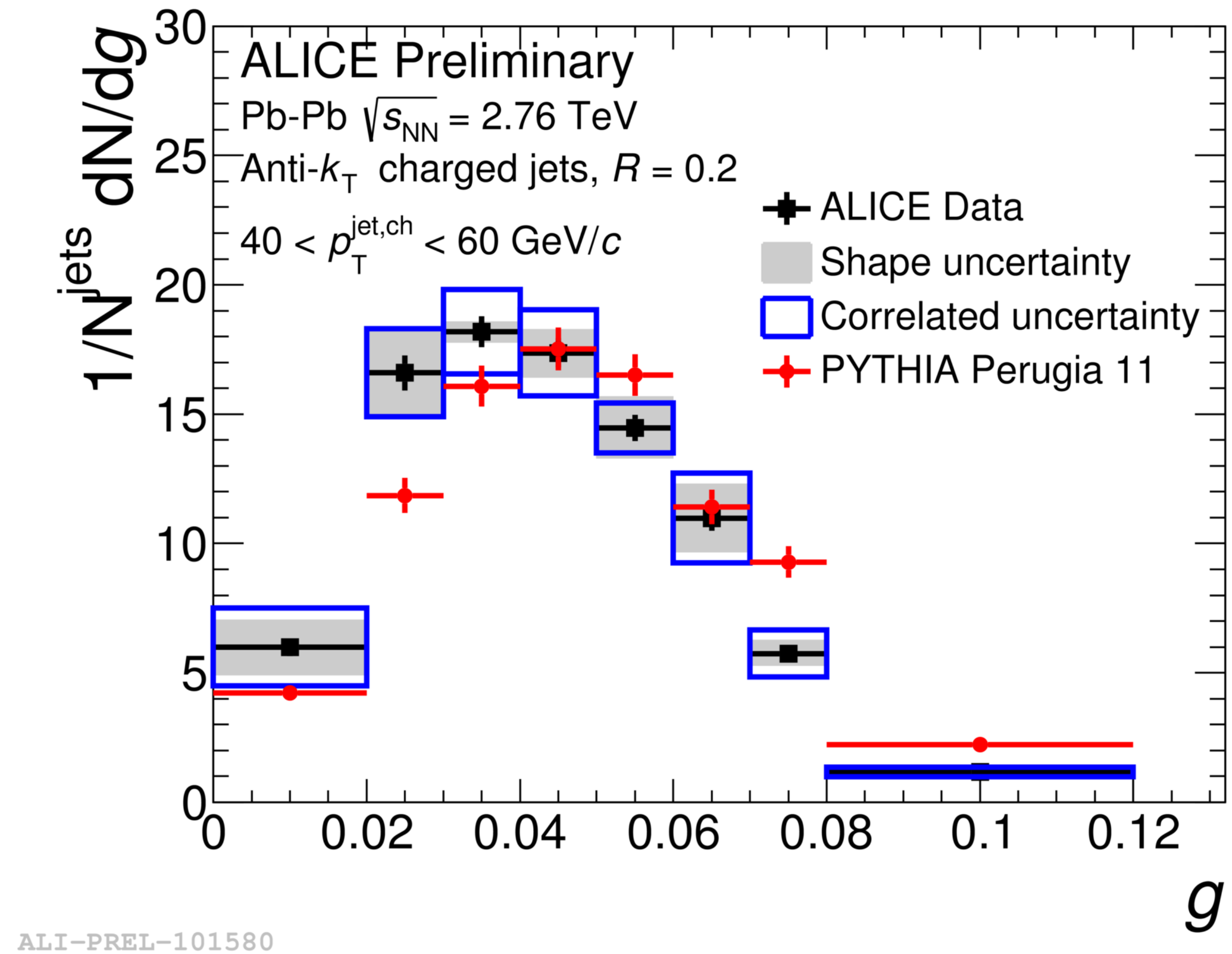

$$g = \sum_{i \in jet} \frac{p_T^i}{p_{T,jet}} |\Delta R_{ijet}|$$

Jet shapes

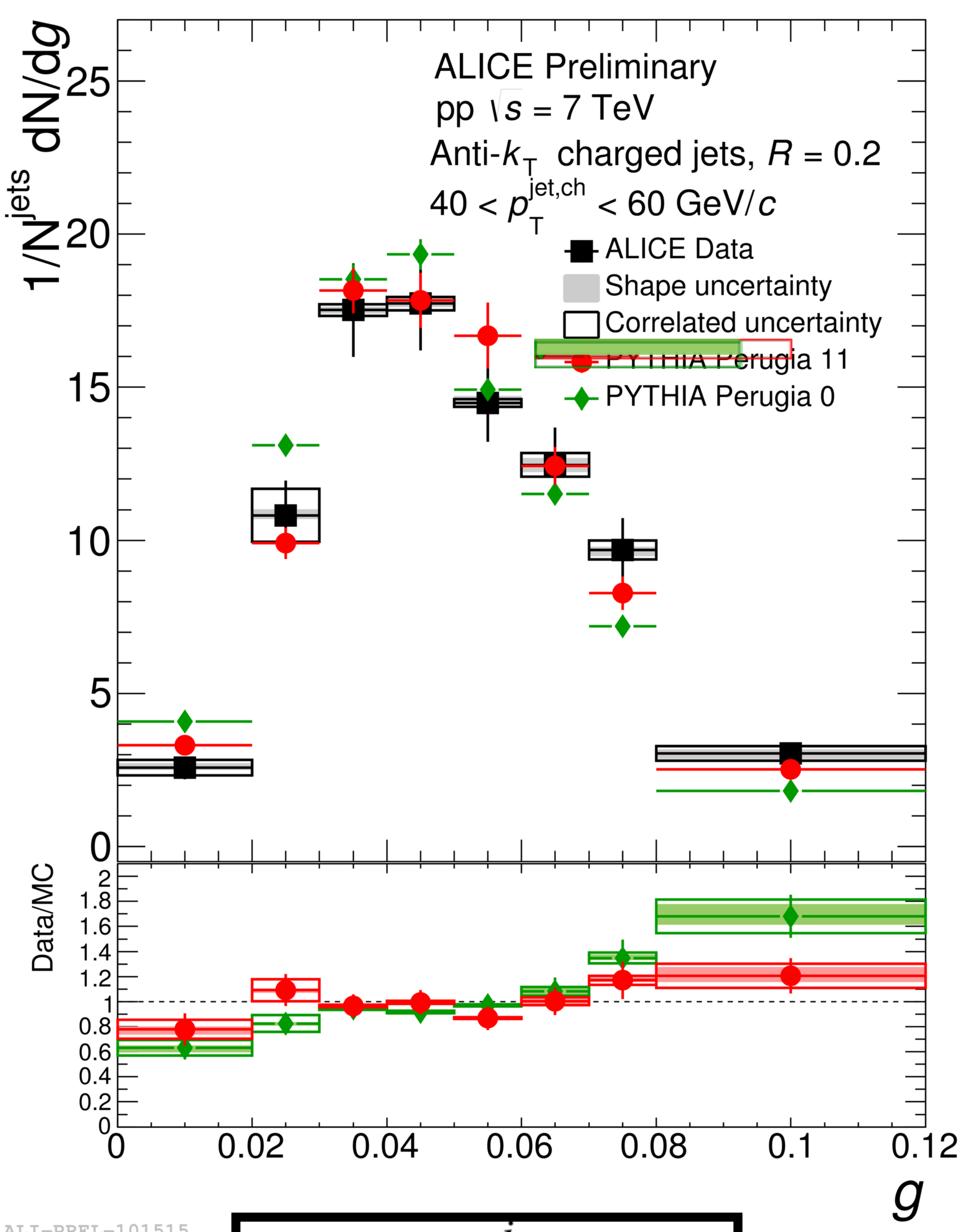

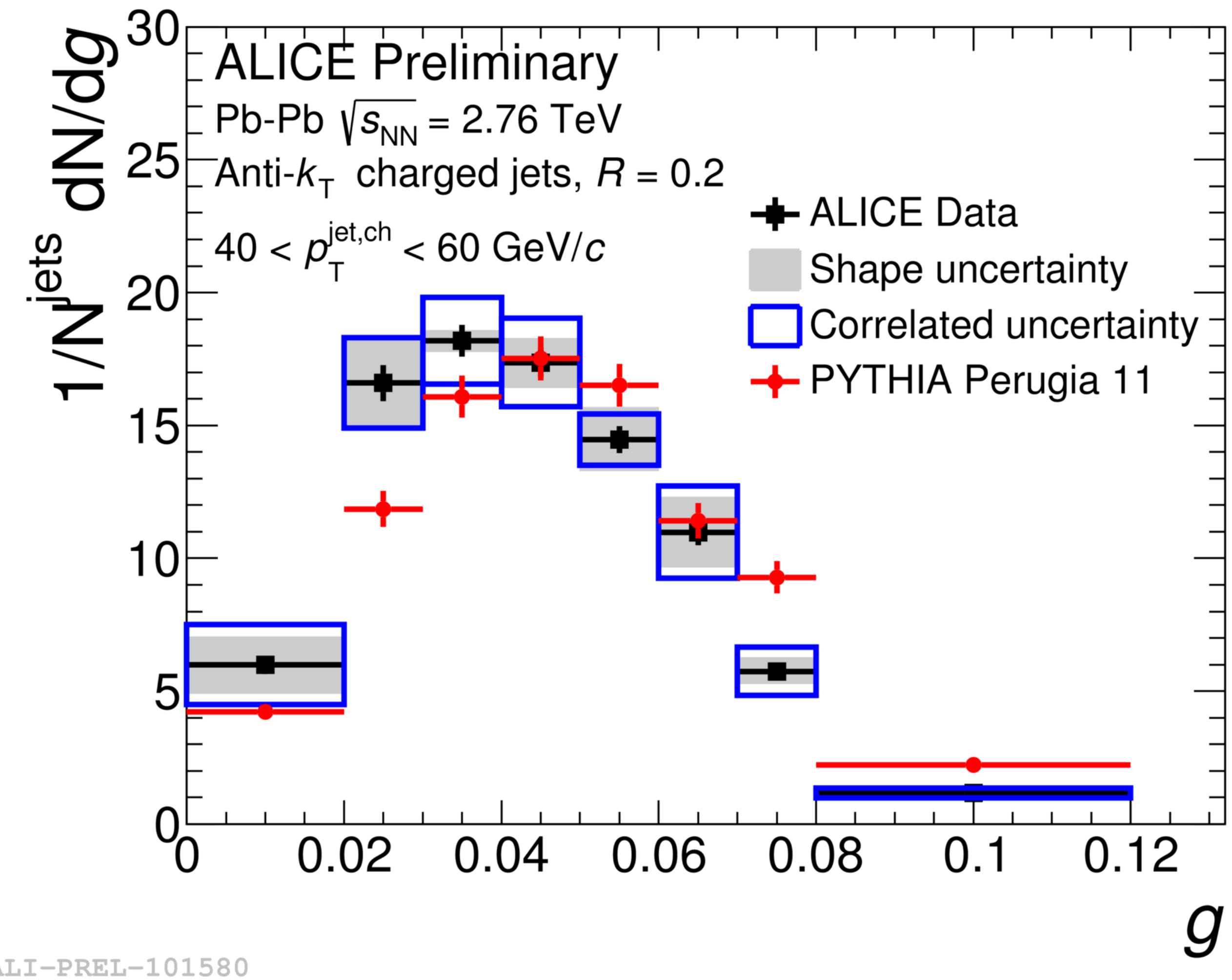

New variables to characterise jet core shapes (constituents in R < 0.2): Radial moment (g), Dispersion in p_T, leading/sub-leading p_T.

$$g = \sum_{i \in jet} \frac{p_T^i}{p_{T,jet}} |\Delta R_{i\,jet}|$$

Jet shapes

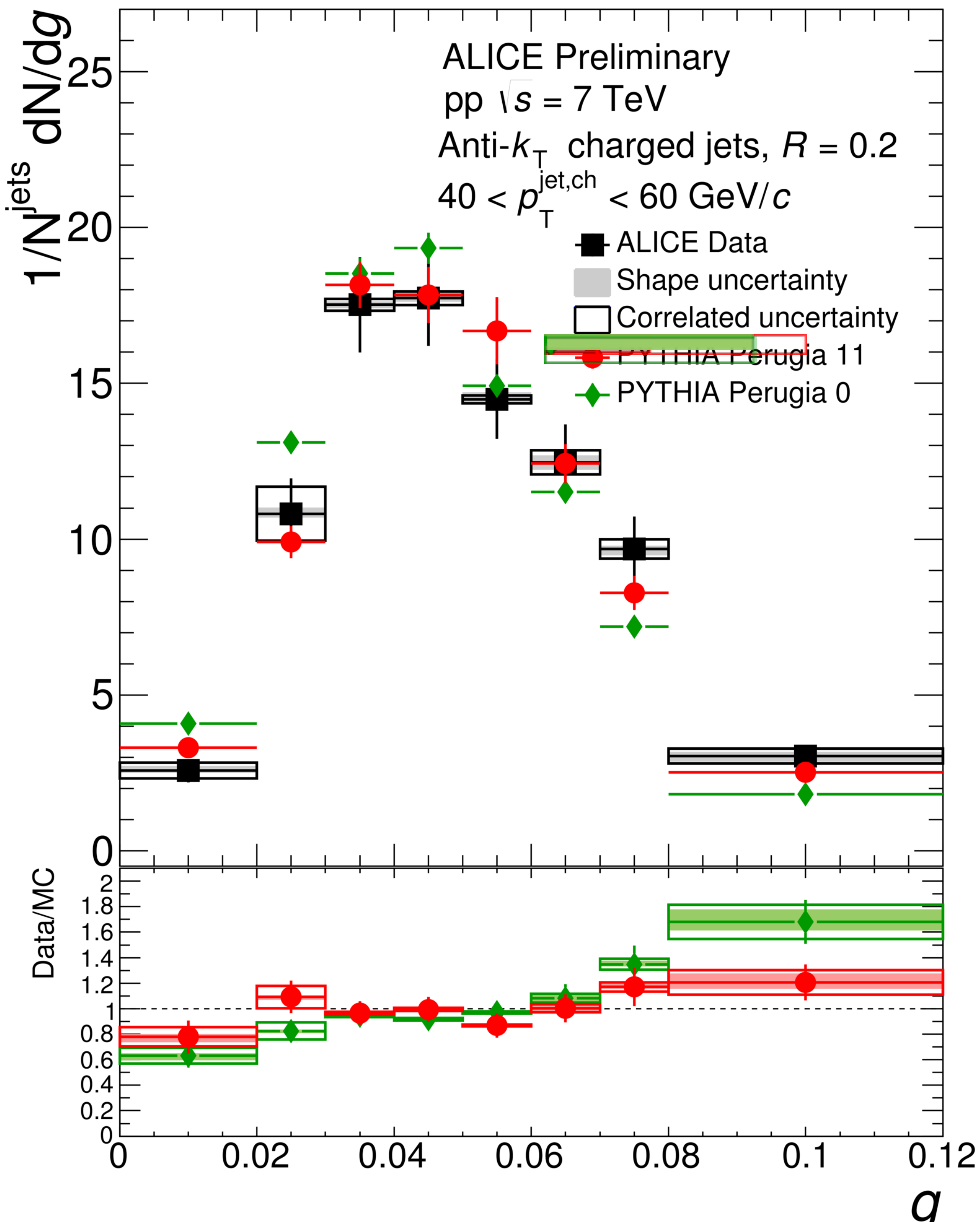

ALI-PREL-101515

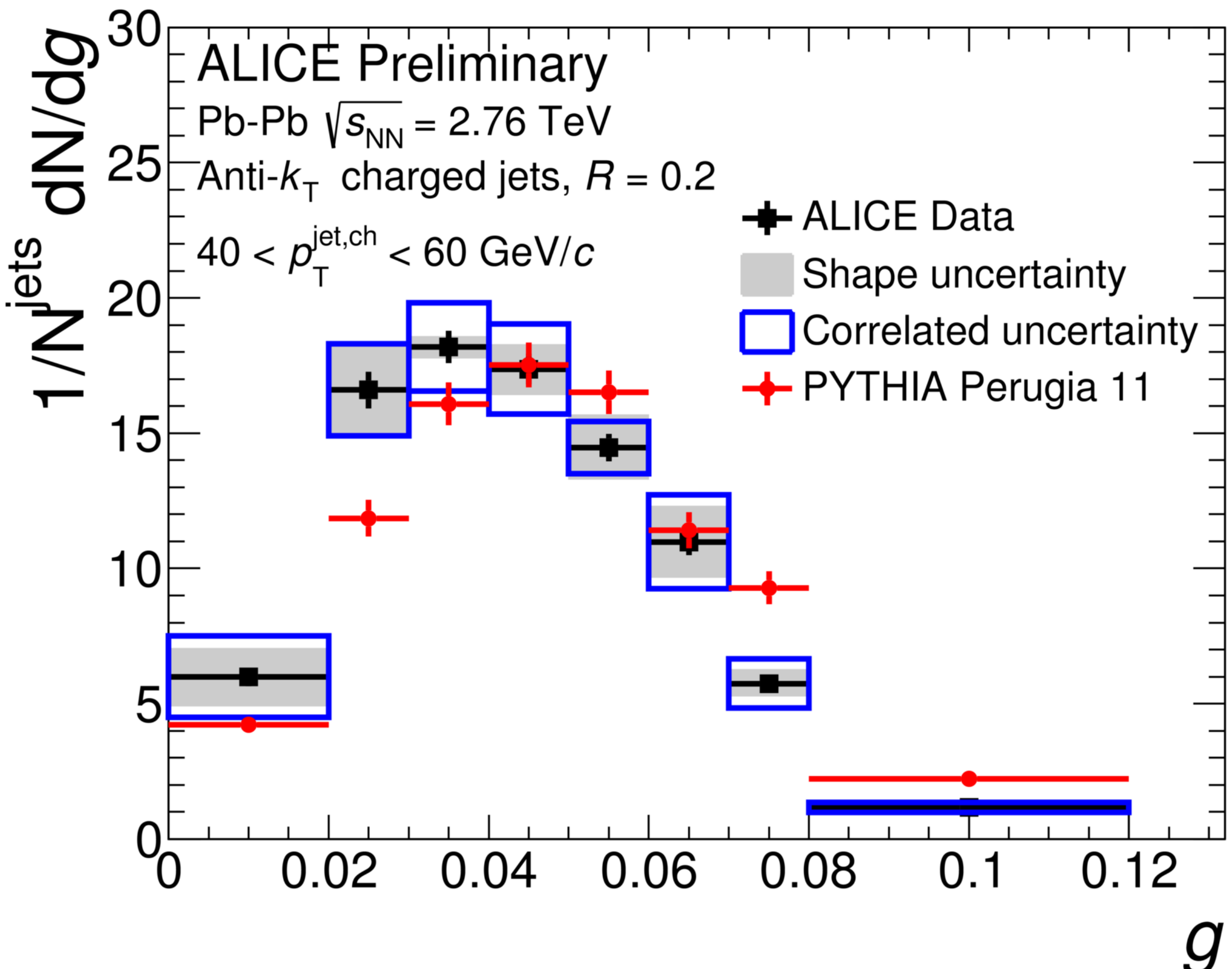

ALI-PREL-101580

$$g = \sum_{i \in jet} \frac{p_T^i}{p_{T,jet}} |\Delta R_{i\,jet}|$$

New variables to characterise jet core shapes (constituents in R < 0.2): Radial moment (g), Dispersion in p_T, leading/sub-leading p_T.

Core of jets in Pb-Pb appears to more collimated than in pp collisions.

J/ψ (re-)generation

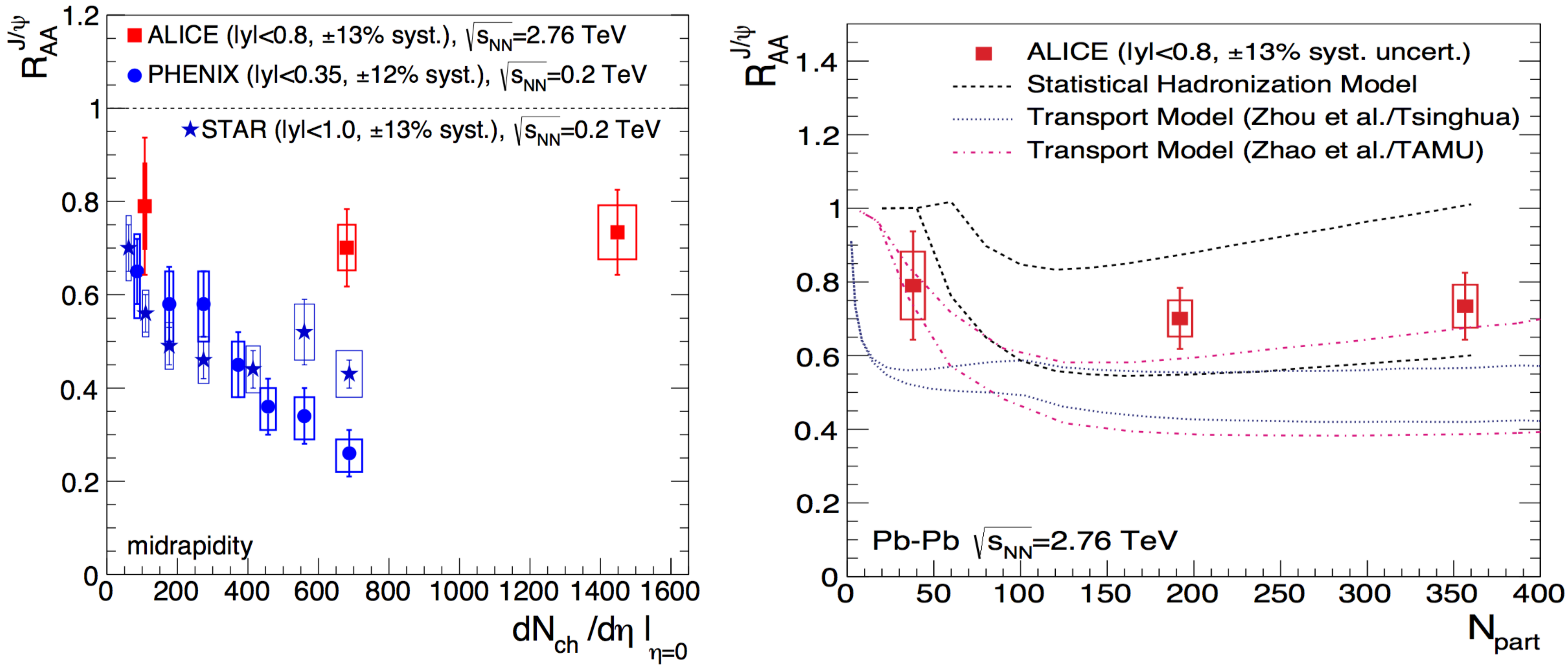

[PLB 743, 314 (2014)]

J/ψ (re-)generation

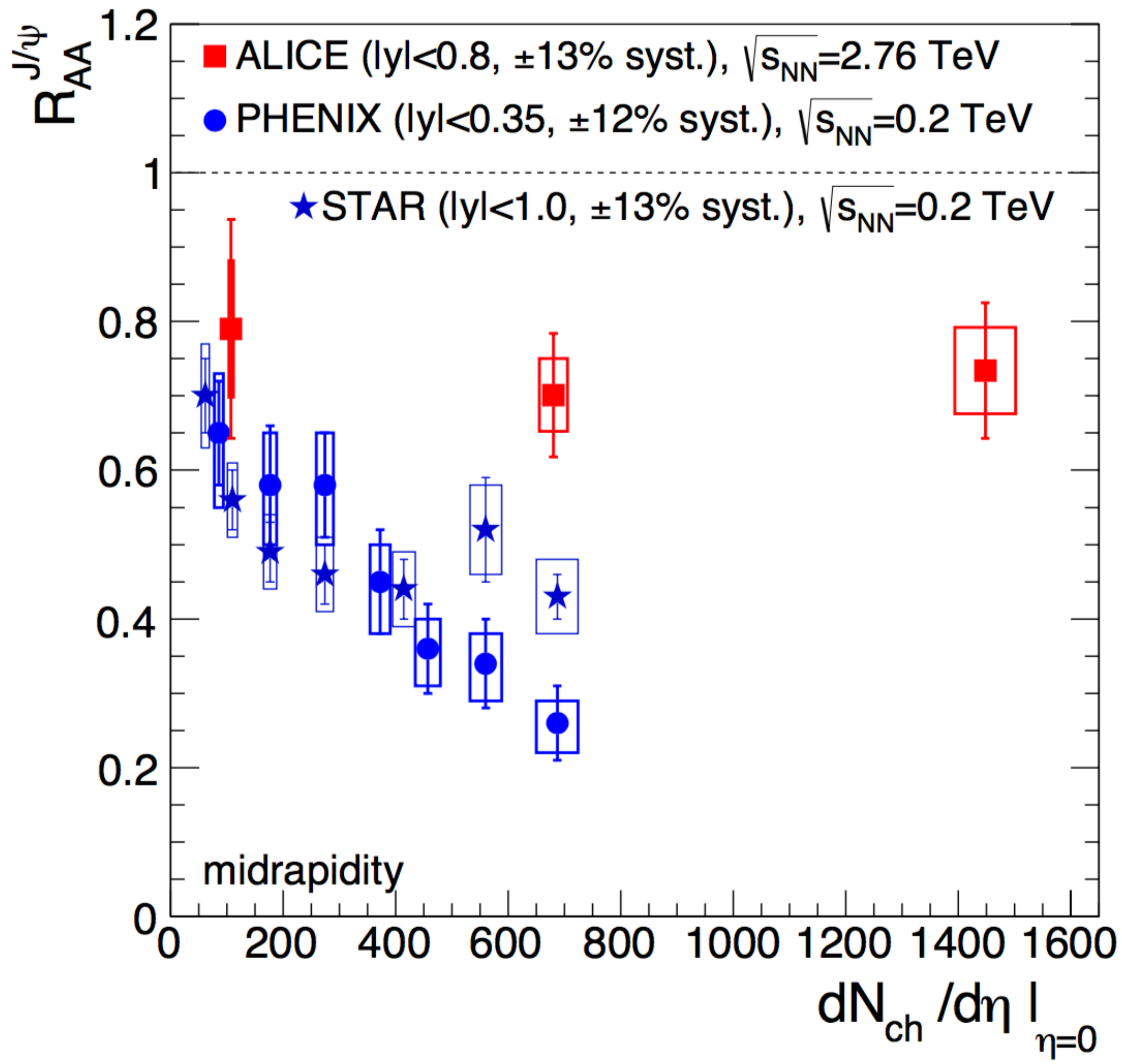

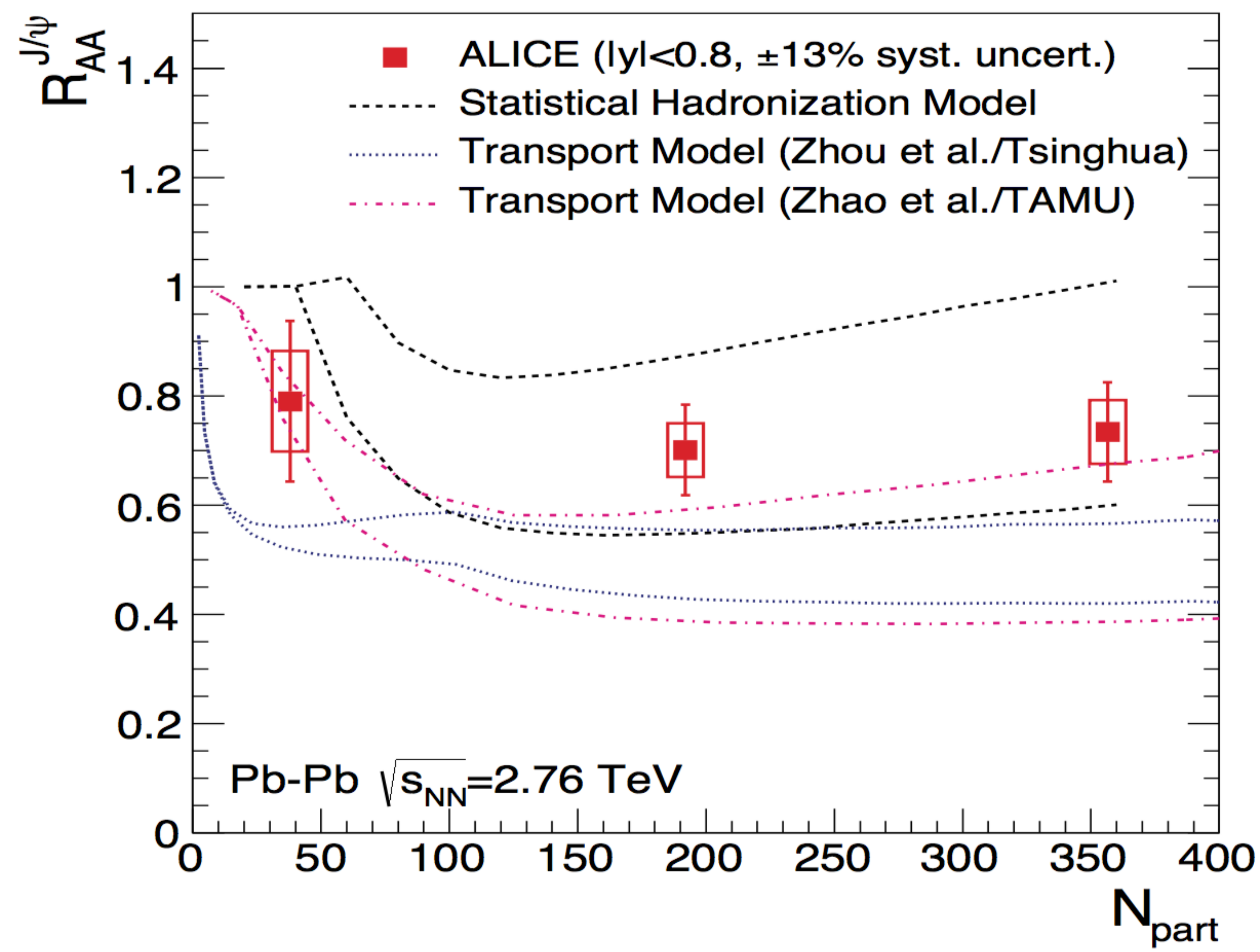

R$_{AA}$ is significantly larger at LHC energies with respect to RHIC (dominantly at low p_T).

[PLB 743, 314 (2014)]

J/ψ (re-)generation

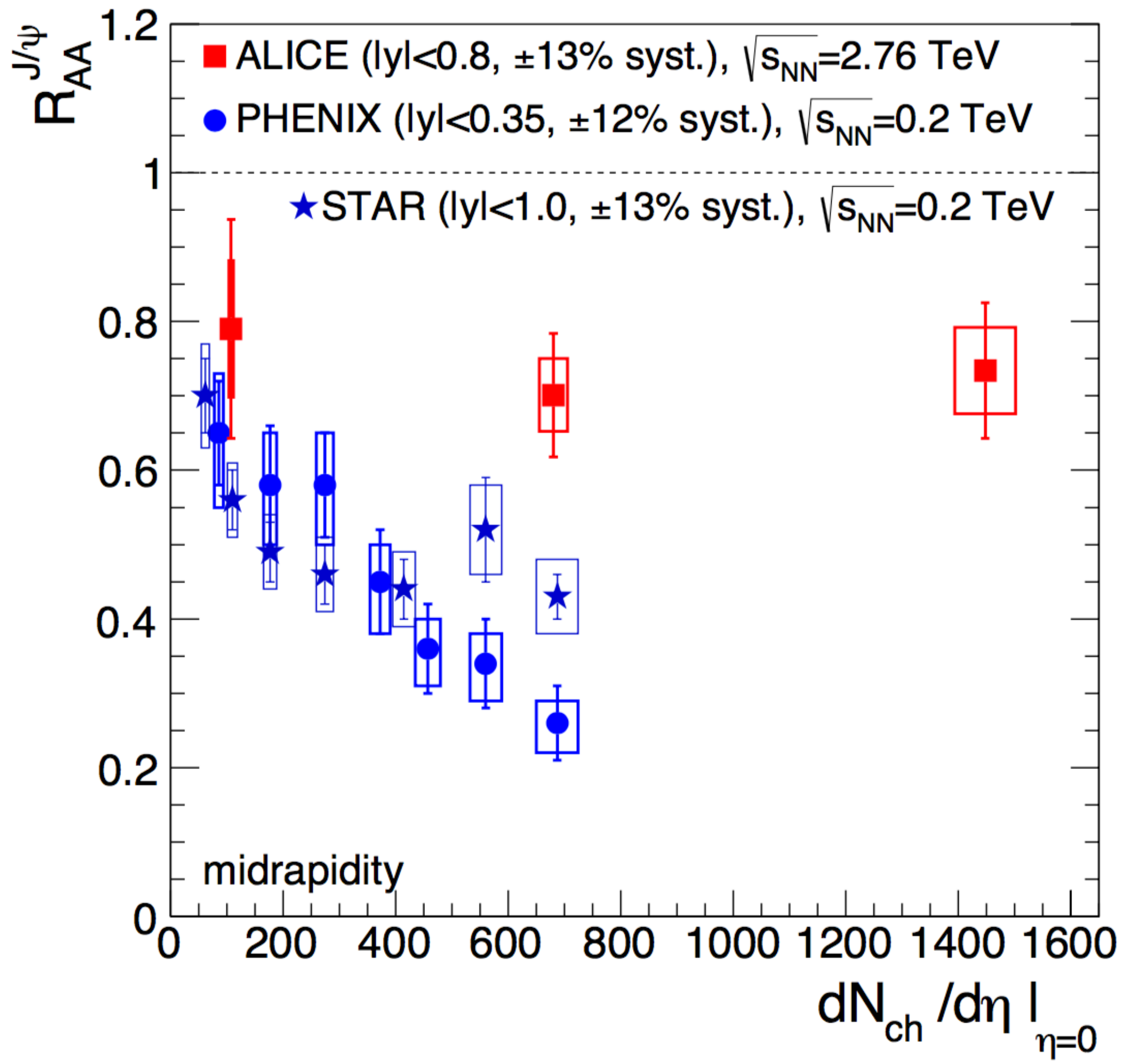

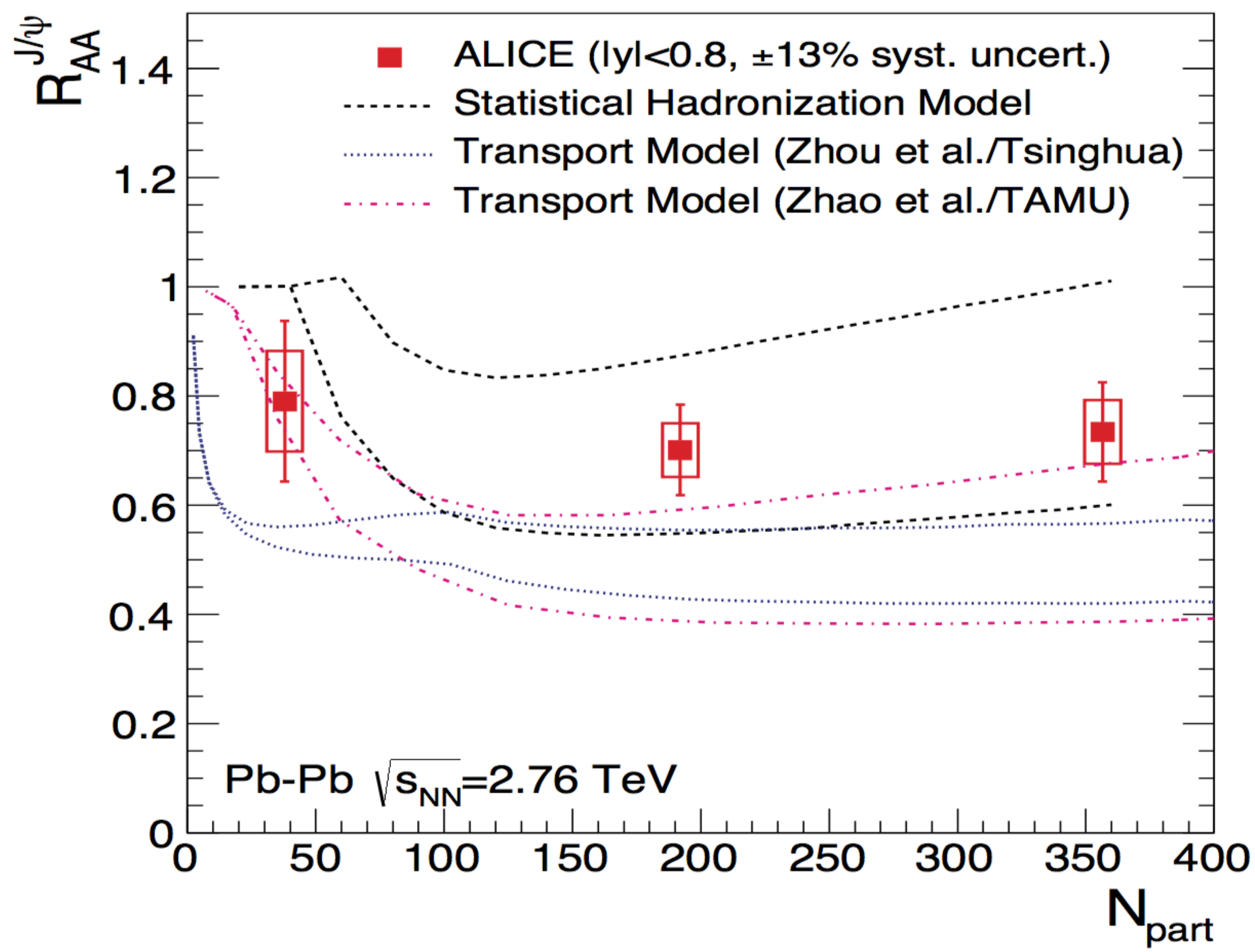

R_{AA} is significantly larger at LHC energies with respect to RHIC (dominantly at low p_T).

Evidence for a new production mechanism.

[PLB 743, 314 (2014)]

Run 3

ALICE upgrade for Run 3

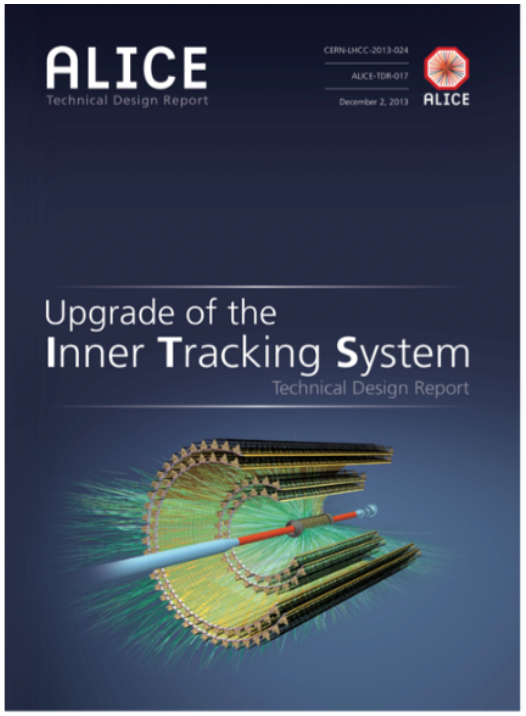

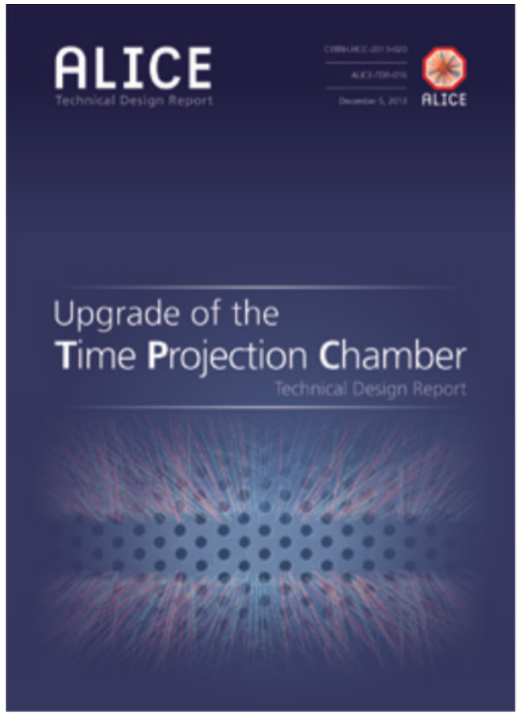

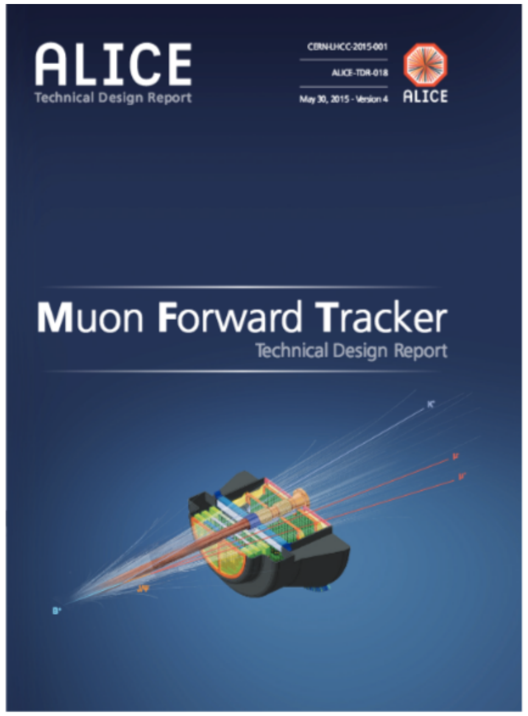

- Major ALICE detector/sytem upgrade:
  - –Read-out Pb-Pb MB collisions at 50 kHz.
- Unique physics program with 100x larger statistics.
  - – Dileptons, Quarkonia, HF, jets, (anti-)nuclei
- Many activities are ongoing

Particle	Yield
Anti-alpha $^4\overline{\mathrm{He}}$	3.0×10^4
Anti-hypertriton $^3_{\bar{\Lambda}}\overline{\mathrm{H}}$ $(\bar{\Lambda}\bar{p}\bar{n})$	3.0×10^5
$^4_{\bar{\Lambda}}\overline{\mathrm{H}}$ $(\bar{\Lambda}\bar{p}\bar{n}\bar{n})$	8.0×10^2
$^5_{\bar{\Lambda}}\overline{\mathrm{H}}$ $(\bar{\Lambda}\bar{p}\bar{n}\bar{n}\bar{n})$	3.0
$^4_{\bar{\Lambda}\bar{\Lambda}}\overline{\mathrm{H}}$ $(\bar{\Lambda}\bar{\Lambda}\bar{p}\bar{n})$	3.4×10^1
$^5_{\bar{\Lambda}\bar{\Lambda}}\overline{\mathrm{H}}$ $(\bar{\Lambda}\bar{\Lambda}\bar{p}\bar{n}\bar{n})$	0.2

Particle yields (including reconstruction efficiency) for 10^{10} central Pb-Pb collisions from ALICE upgrade LOI.

Summary

Summary

- The complete data set of pp, p-Pb, and Pb-Pb collisions has been analysed and allows excellent systematic studies to be performed.
- ALICE took very high quality in LHC Run 1, continues to do so in LHC Run 2 and has ambitious plans for LHC Run 3.
- Clear support for the creation of a fireball in local thermodynamics equilibrium in Pb-Pb collisions.
- Light (anti-)nuclei appear to behave like non-composite hadrons in this fireball.
- Medium created at the LHC appears to be hotter in the initial phase than the medium at RHIC.
- New jet shape variables characterise medium modifications.

Supporting slides

Jet shapes (B)

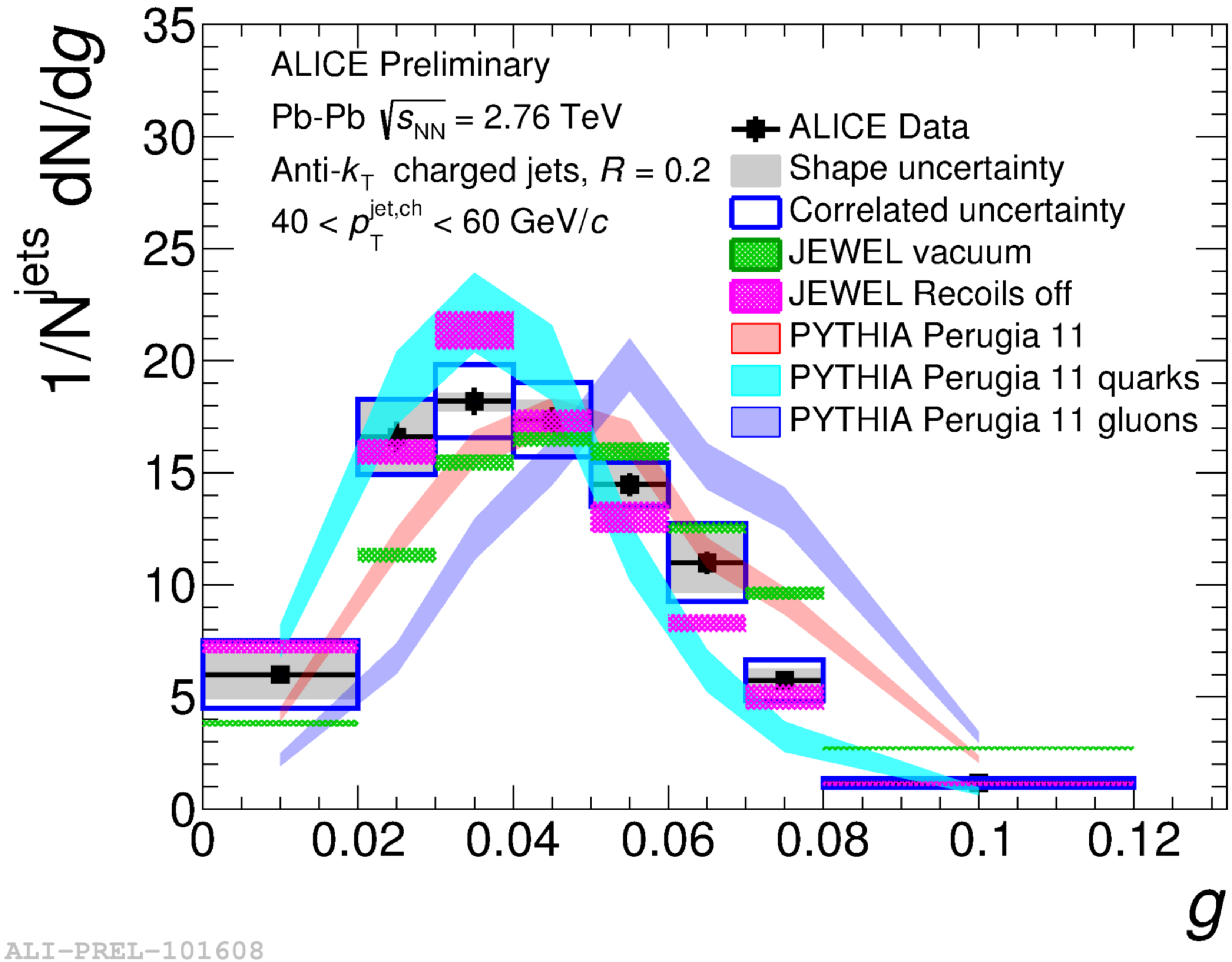
ALICE Preliminary
Pb-Pb $\sqrt{s_{NN}}$ = 2.76 TeV
Anti-k_T charged jets, R = 0.2
40 < $p_T^{jet,ch}$ < 60 GeV/c
ALICE Data
Shape uncertainty
Correlated uncertainty
JEWEL vacuum
JEWEL Recoils off
PYTHIA Perugia 11
PYTHIA Perugia 11 quarks
PYTHIA Perugia 11 gluons
$1/N^{jets}$ dN/dg
g
0
5
10
15
20
25
30
35
0.02
0.04
0.06
0.08
0.1
0.12
ALI-PREL-101608

Jet shapes (B)

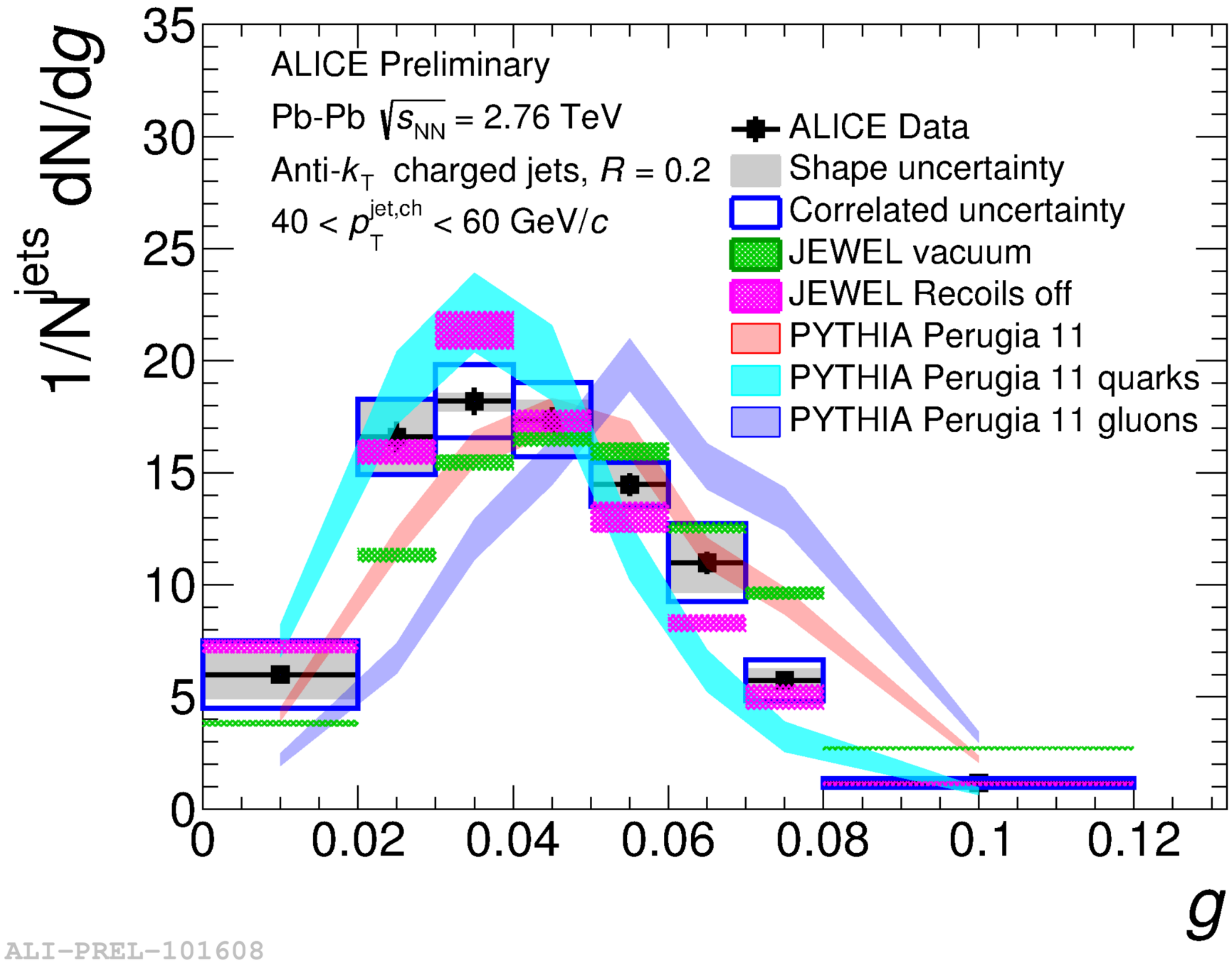

Quark jets are more collimated than gluon jets according to PYTHIA.

Jet shapes (B)

ALICE

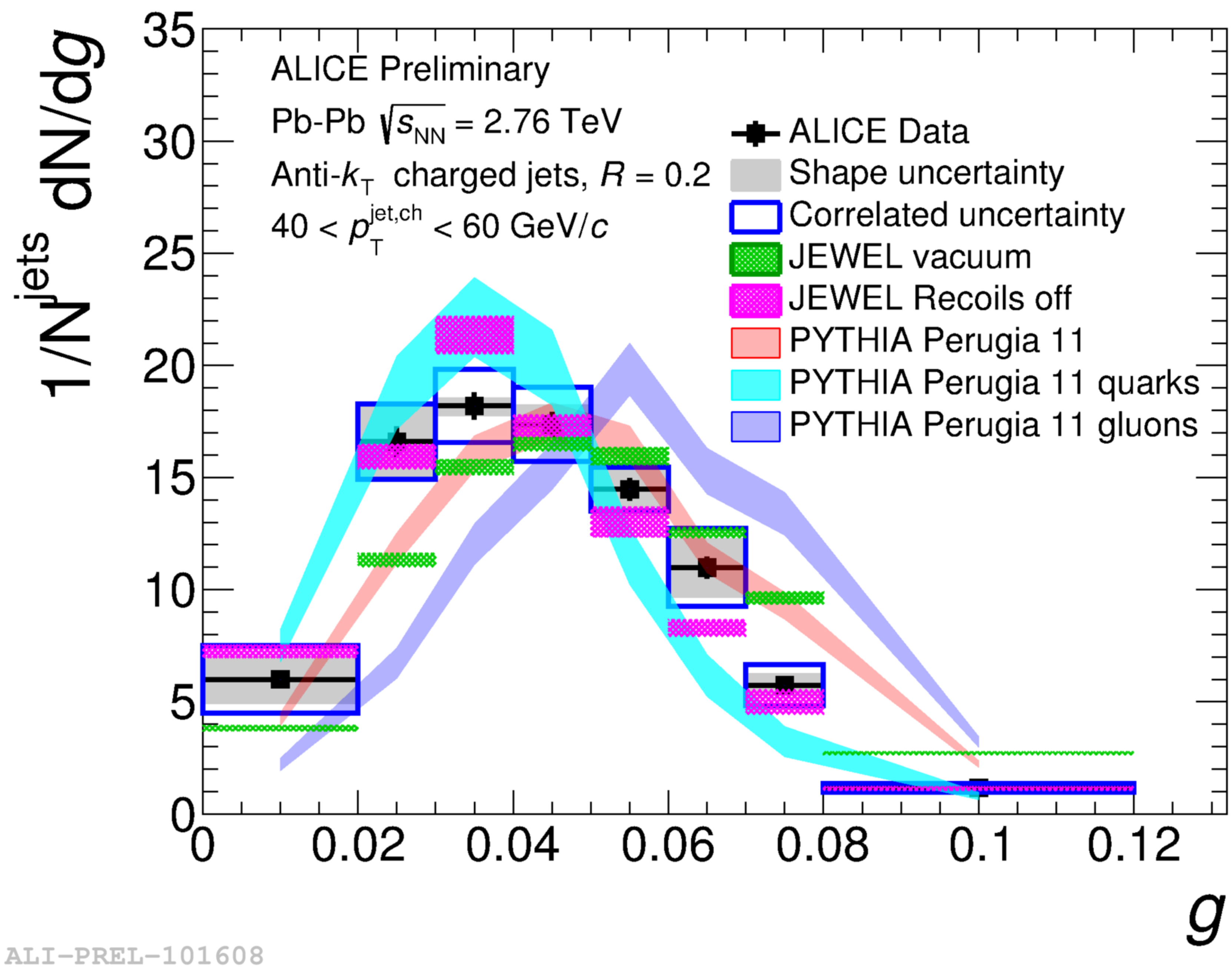

Quark jets are more collimated than gluon jets according to PYTHIA.

JEWEL is in qualitative agreement with the data.

Jet shapes (B)

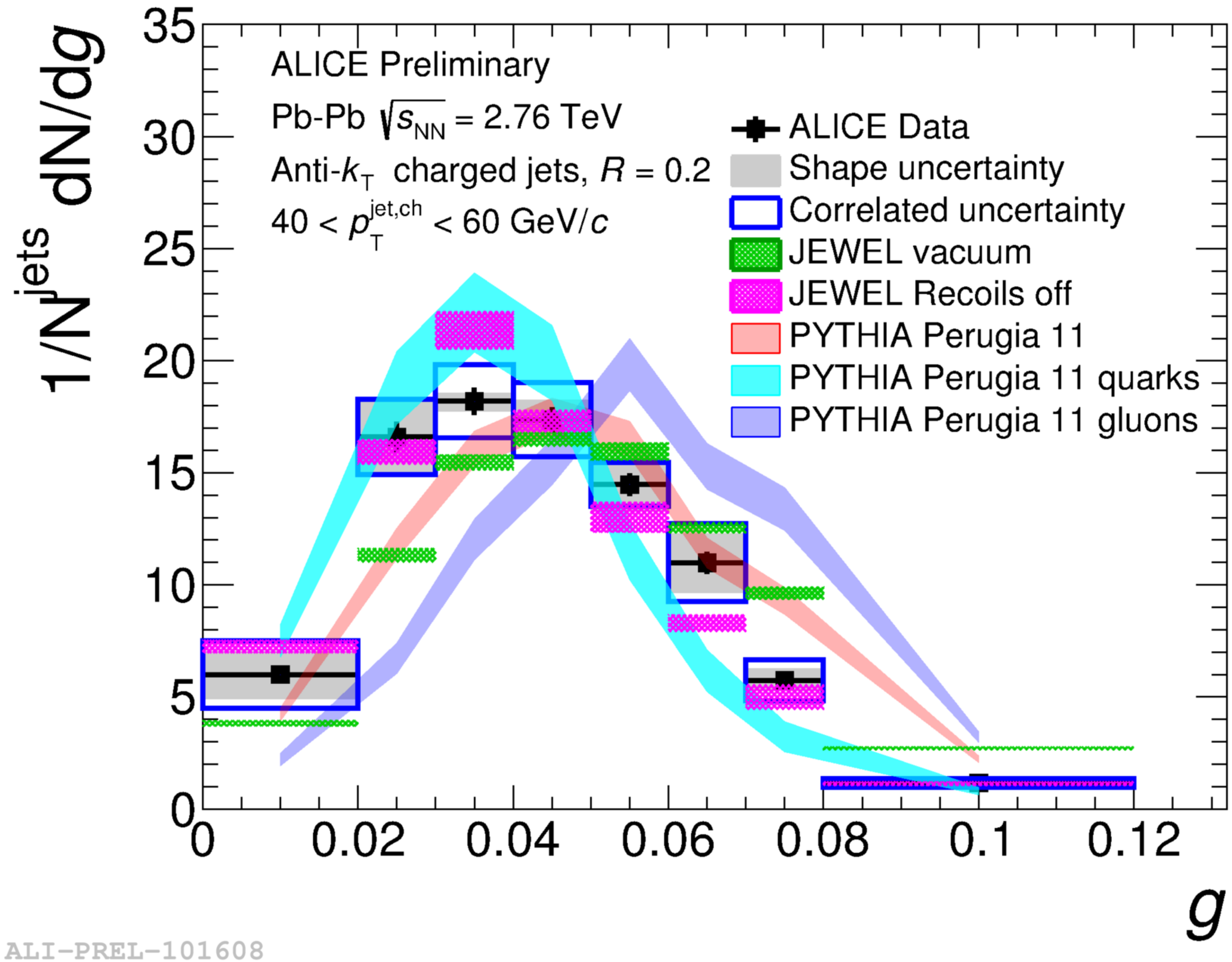

Quark jets are more collimated than gluon jets according to PYTHIA.

JEWEL is in qualitative agreement with the data.

Hint of jet core modifications in Pb-Pb.

Precision of CPT tests

$$\Delta\mu_{\mathrm{d\bar{d}}} = (1.7 \pm 0.9(\mathrm{stat.}) \pm 2.6(\mathrm{syst.})) \times 10^{-4}\ \mathrm{GeV}/c^2 \quad (1)$$

$$\Delta\mu_{^3\mathrm{He}^3\overline{\mathrm{He}}} = (-1.7 \pm 1.2(\mathrm{stat.}) \pm 1.4(\mathrm{syst.})) \times 10^{-3}\ \mathrm{GeV}/c^2 \quad (2)$$

corresponding to

$$\frac{\Delta\mu_{\mathrm{d\bar{d}}}}{\mu_{\mathrm{d}}} = (0.9 \pm 0.5(\mathrm{stat.}) \pm 1.4(\mathrm{syst.})) \times 10^{-4}$$

$$\frac{\Delta\mu_{^3\mathrm{He}^3\overline{\mathrm{He}}}}{\mu_{^3\mathrm{He}}} = (-1.2 \pm 0.9(\mathrm{stat.}) \pm 1.0(\mathrm{syst.})) \times 10^{-3}$$

Coalescence parameter B2

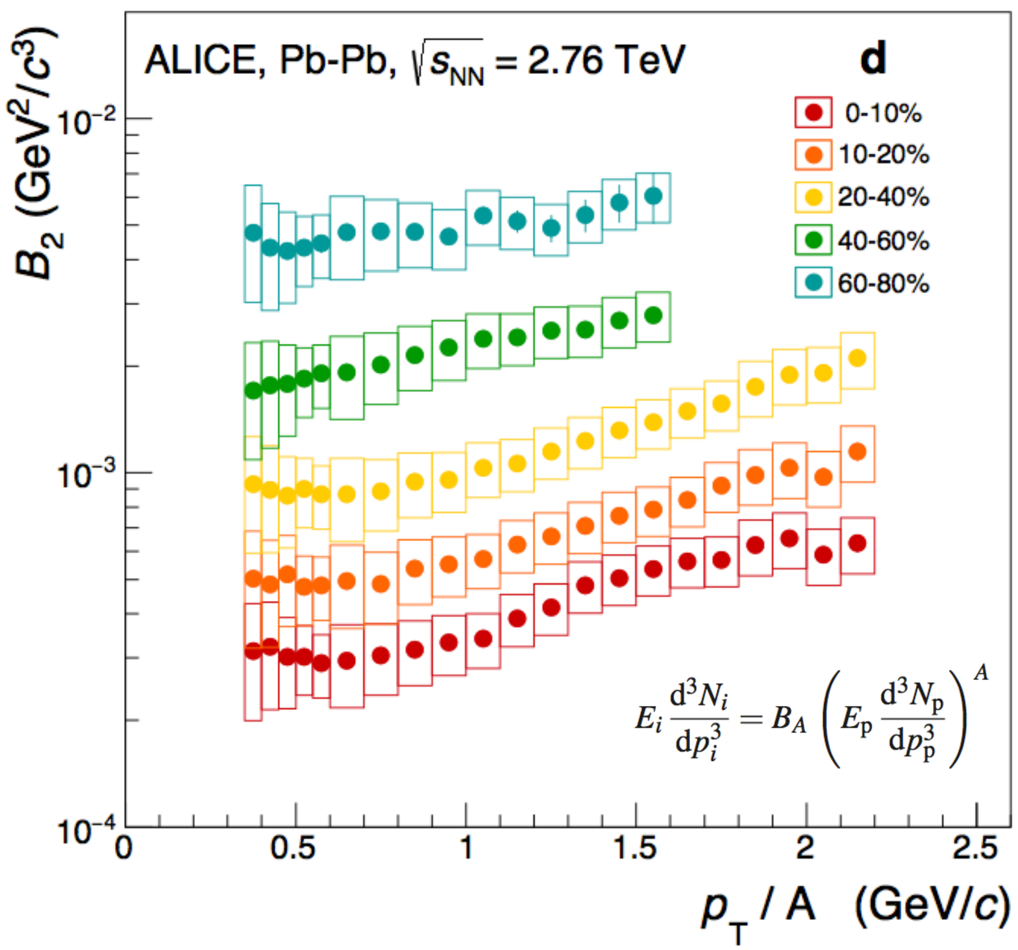

[arXiv:1506.08951]

Coalescence parameter B2 decreases with increasing centrality indicating an increase in the size of the emitting source.

Knock-out nuclei from material

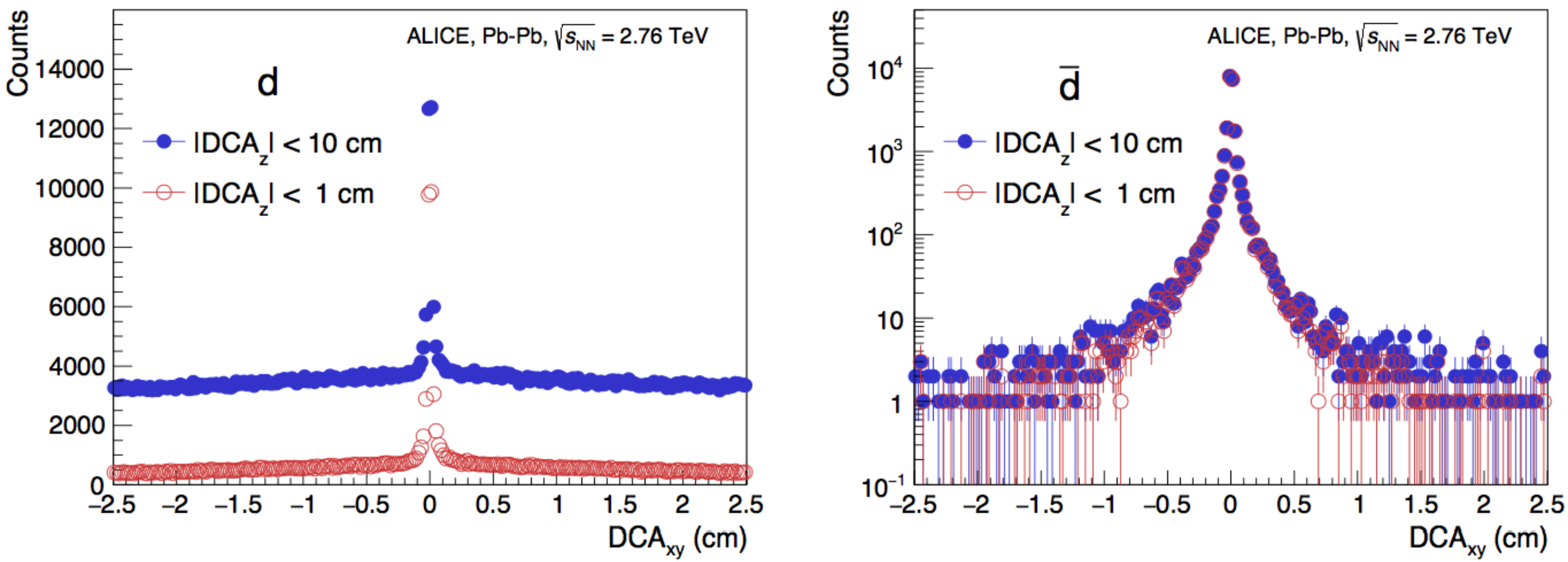

[arXiv:1506.08951]

- Raw nuclei yield is contaminated by knock-out particles from the detector material which needs to be carefully subtracted.
- The ratio of primarily produced nuclei to those from knock-out decreases with increasing mass number.

The observation of light nuclei at ALICE and the $X(3872)$ conundrum

A. Esposito,[1] A.L. Guerrieri,[2] L. Maiani,[3] F. Piccinini,[4] A. Pilloni,[3] A.D. Polosa,[3] and V. Riquer[3]
[1] *Department of Physics, 538W 120th Street, Columbia University, New York, NY, 10027, USA*
[2] *Dipartimento di Fisica and INFN, Università di Roma 'Tor Vergata' Via della Ricerca Scientifica 1, I-00133 Roma, Italy*
[3] *Dipartimento di Fisica and INFN, 'Sapienza' Università di Roma P.le Aldo Moro 5, I-00185 Roma, Italy*
[4] *INFN Pavia, Via A. Bassi 6, I-27100 Pavia, Italy*

The new data reported by ALICE on the production of light nuclei with $p_\perp \lesssim 10$ GeV in Pb-Pb collisions at $\sqrt{s_{NN}} = 2.76$ TeV are used to compute an order-of-magnitude estimate of the expected production cross sections of light nuclei in proton-proton collisions at high transverse momenta. We compare the hypertriton, helium-3 and deuteron production cross sections to that of $X(3872)$, measured in prompt pp collisions by CMS. The results we find suggest a different production mechanism for the $X(3872)$, making questionable any loosely bound molecule interpretation.

PACS numbers: 12.38.Mh, 14.40.Rt, 25.75.-q
Keywords: Hadron molecules, Nuclei production, Heavy ion collisions

THE X(3872) SOME SORT OF DD* DEUTERON?

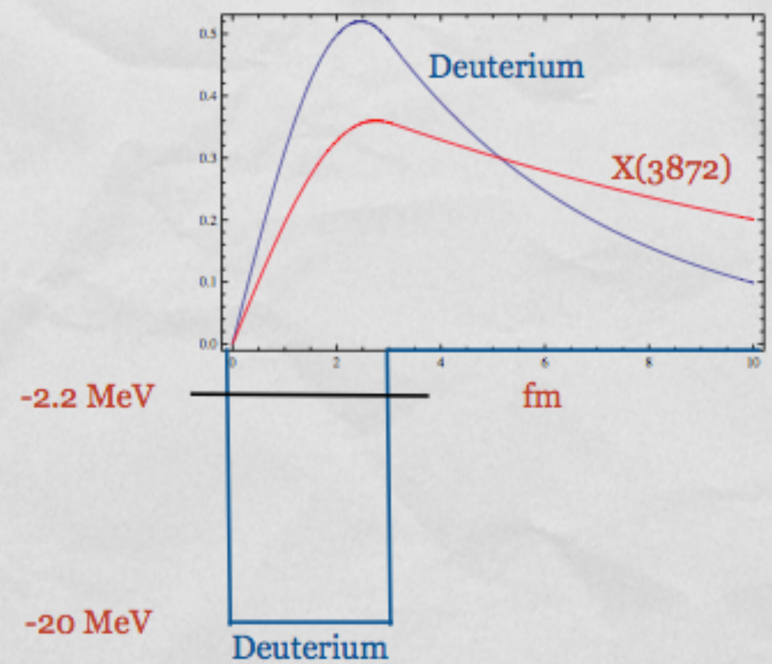

$$k_{\rm rel} = \sqrt{2\mu\langle T\rangle_\psi^2} \approx \begin{cases} 80 \text{ MeV} & \text{for deuterium} \\ 50 \text{ MeV} & \text{for } X;\ \ U_0 \approx -7 \text{ MeV} \quad \mathcal{E}_b \approx -0.14 \text{ MeV} \end{cases}$$

$$\frac{\hbar^2}{2\mu r_0^2} - \frac{g^2}{4\pi}\frac{e^{-\frac{m_\pi c}{\hbar} r_0}}{r_0} = \mathcal{E}_b = 0.14 \text{ MeV} \Rightarrow r_0 \approx 12 \text{ fm}$$

Dark matter searches

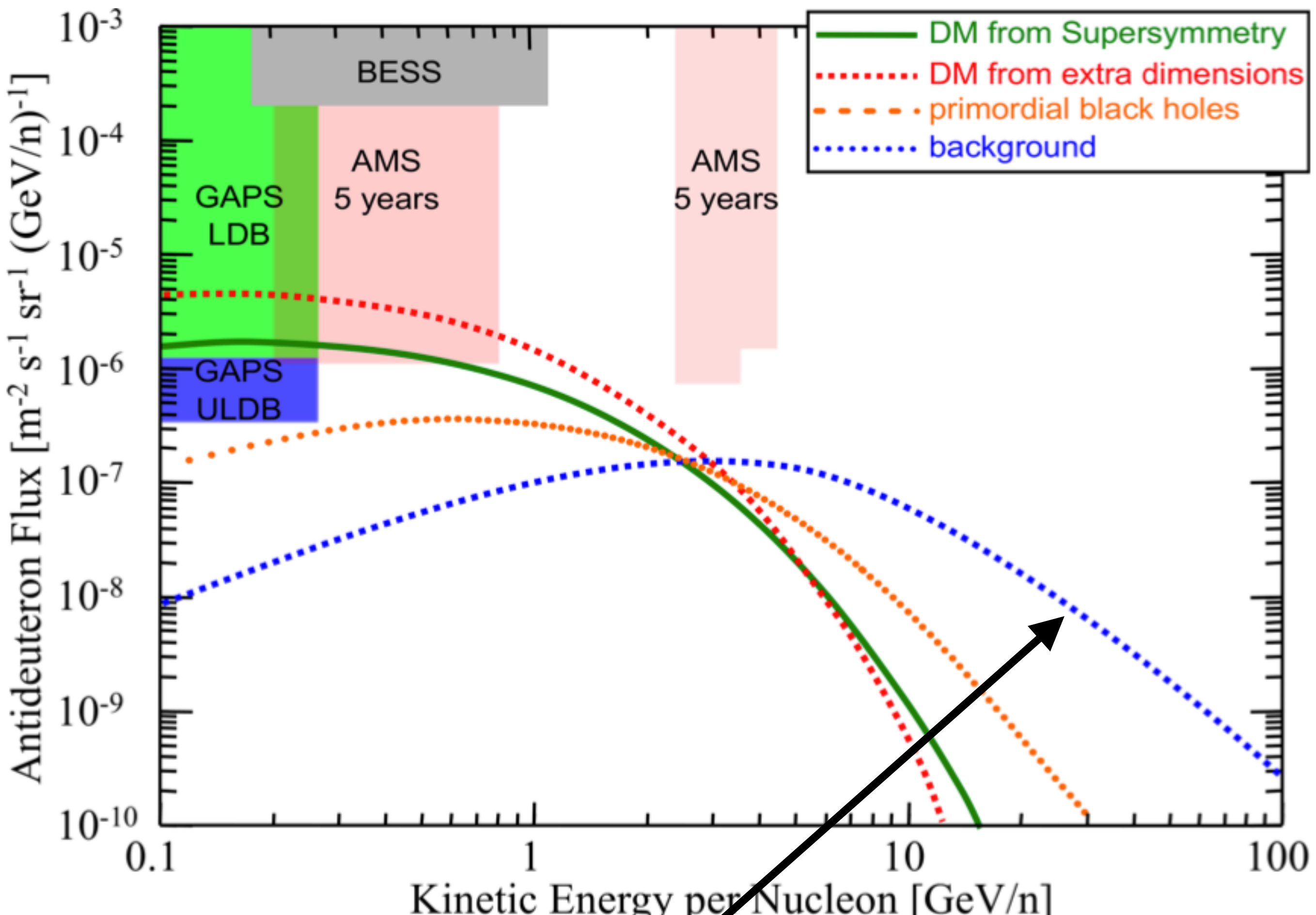

Calculated in based on lower energy data

[1303.1615]

[astro-ph/0503544v1]

Dark matter searches

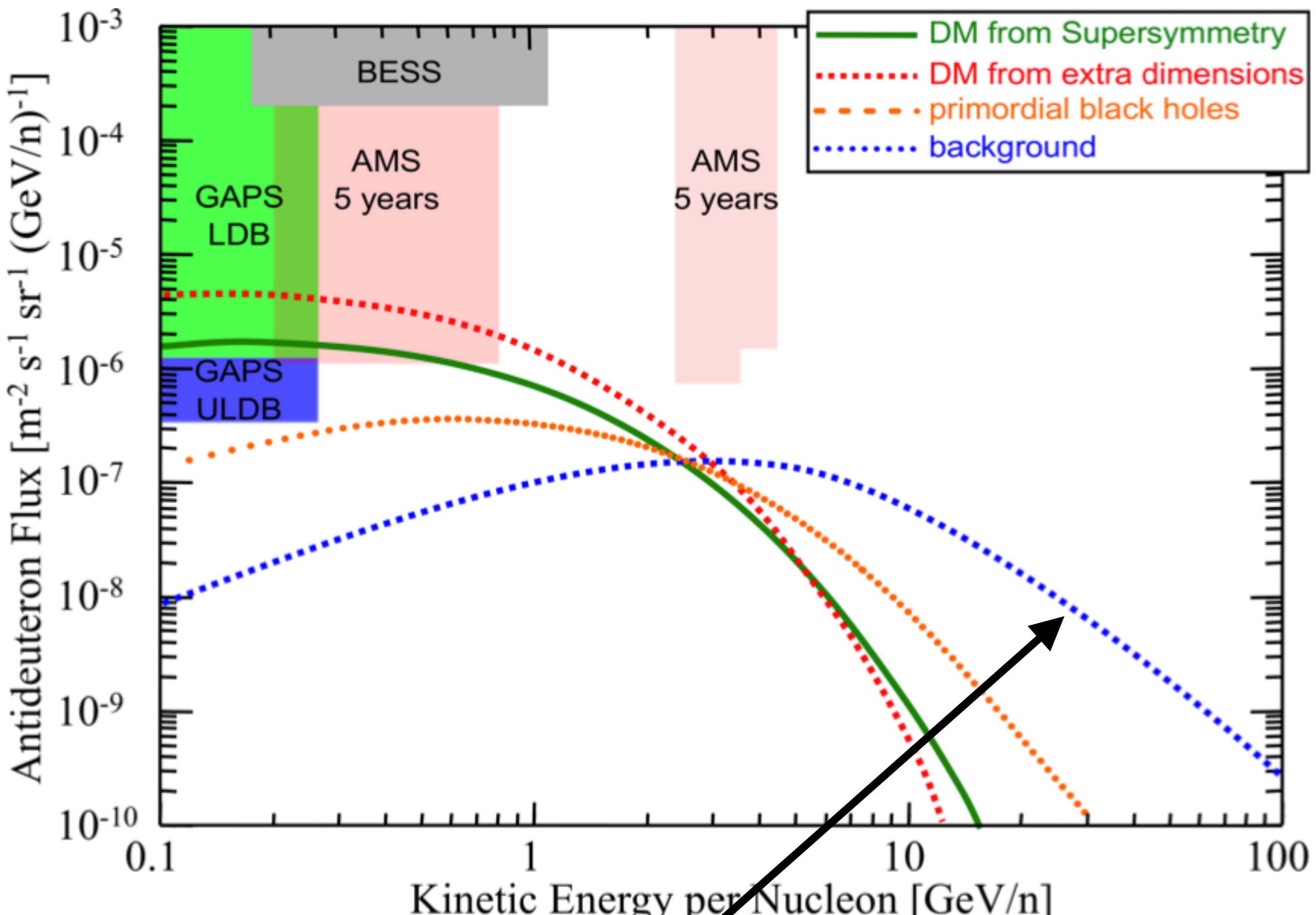

Some DM theories predict weakly interacting massive particles (WIMPs), such as the Lightest Supersymmetric Particle (LSP).

Calculated in based on lower energy data

[1303.1615]

[astro-ph/0503544v1]

Dark matter searches

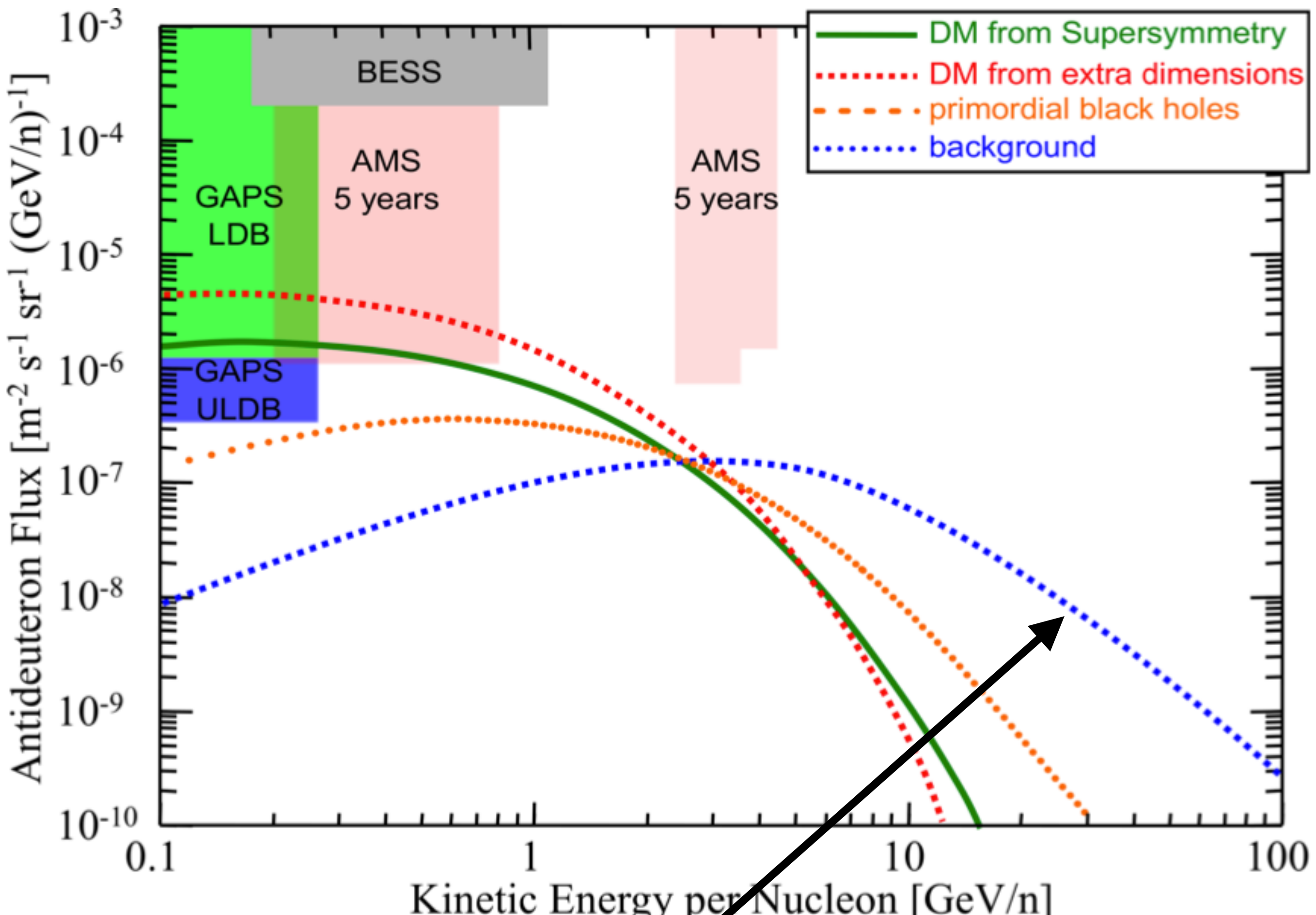

Some DM theories predict weakly interacting massive particles (WIMPs), such as the Lightest Supersymmetric Particle (LSP).

WIMPs would have no charge, so self-annihilation products should be equally split between matter and anti-matter.

Calculated in based on lower energy data

[1303.1615]
[astro-ph/0503544v1]

Dark matter searches

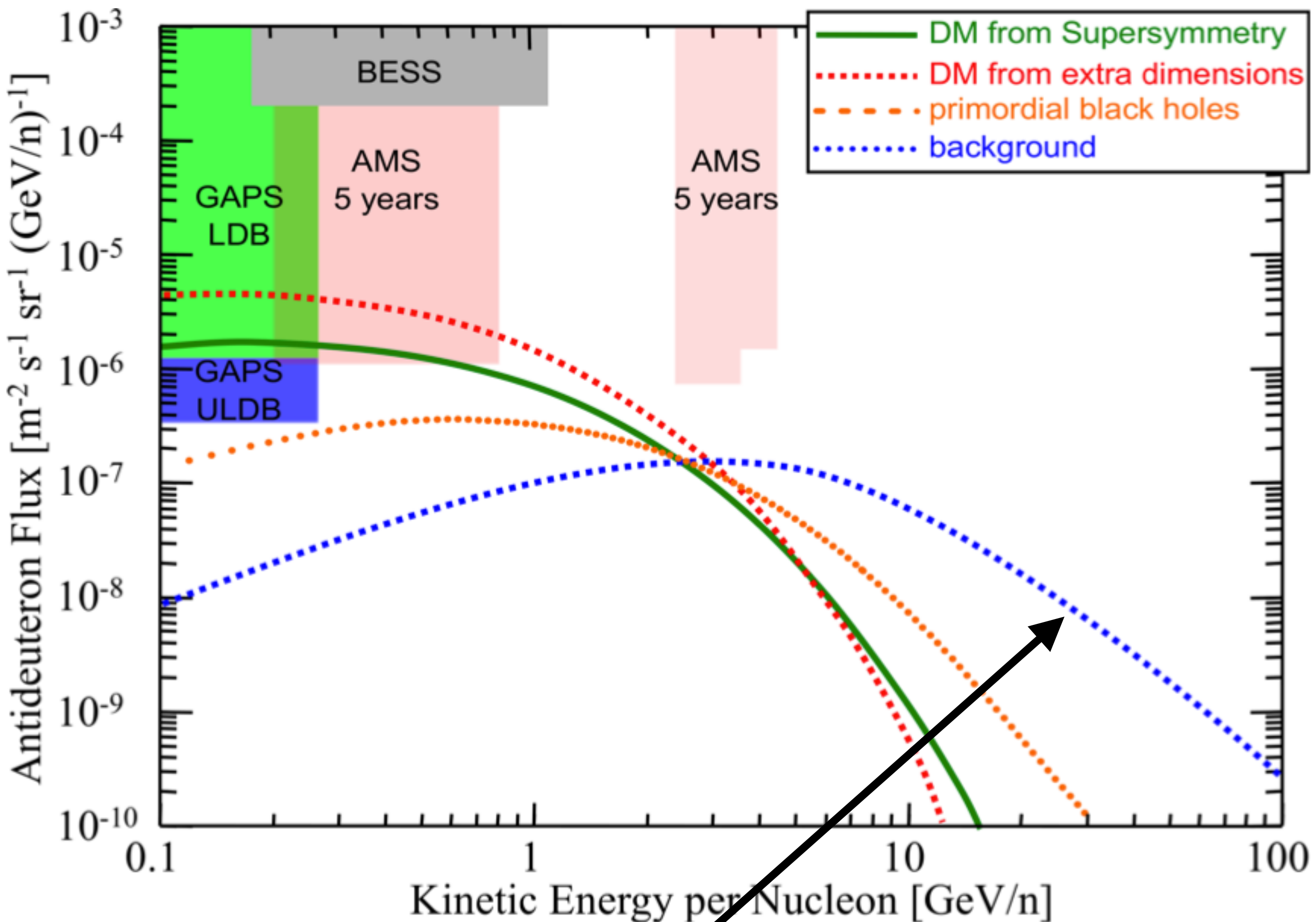

Some DM theories predict weakly interacting massive particles (WIMPs), such as the Lightest Supersymmetric Particle (LSP).

WIMPs would have no charge, so self-annihilation products should be equally split between matter and anti-matter.

Anti-deuterons are comparatively rare in cosmic rays (believed to be entirely of secondary and tertiary origin).

Calculated in based on lower energy data

[1303.1615]

[astro-ph/0503544v1]

Dark matter searches

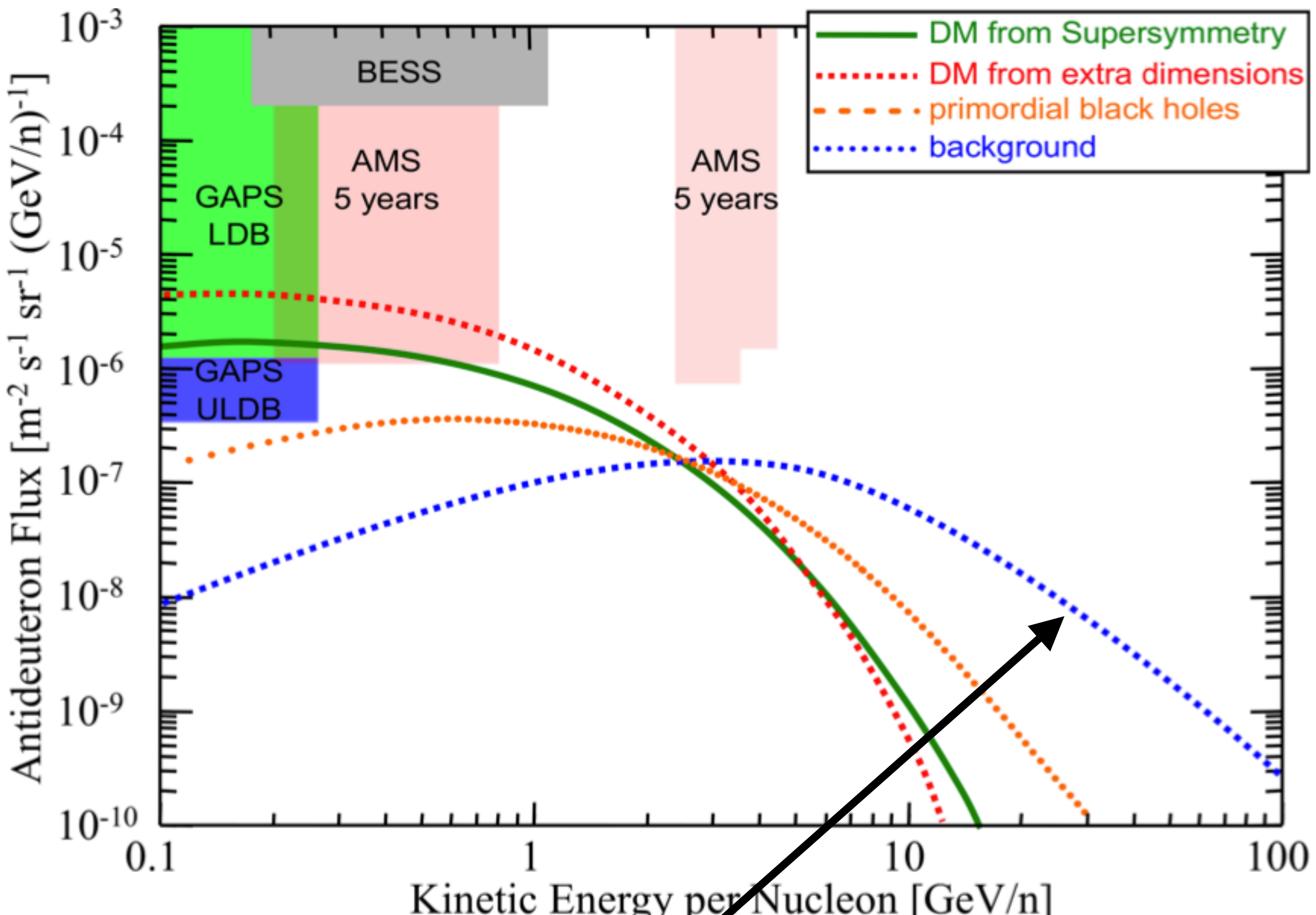

Calculated in based on lower energy data

[1303.1615]
[astro-ph/0503544v1]

Some DM theories predict weakly interacting massive particles (WIMPs), such as the Lightest Supersymmetric Particle (LSP).

WIMPs would have no charge, so self-annihilation products should be equally split between matter and anti-matter.

Anti-deuterons are comparatively rare in cosmic rays (believed to be entirely of secondary and tertiary origin).

Therefore, a clear excess in anti-deuterons above the flux expected from secondary/tertiary productions would be strongly suggestive of dark matter.